LEABHARLANN CHOLÁISTE NA TRÍONÓIDE, BAILE ÁTHA CLIATH | TRINITY COLLEGE LIBRARY DUBLIN
Ollscoil Átha Cliath | The University of Dublin

Terms and Conditions of Use of Digitised Theses from Trinity College Library Dublin

Copyright statement

All material supplied by Trinity College Library is protected by copyright (under the Copyright and Related Rights Act, 2000 as amended) and other relevant Intellectual Property Rights. By accessing and using a Digitised Thesis from Trinity College Library you acknowledge that all Intellectual Property Rights in any Works supplied are the sole and exclusive property of the copyright and/or other IPR holder. Specific copyright holders may not be explicitly identified. Use of materials from other sources within a thesis should not be construed as a claim over them.

A non-exclusive, non-transferable licence is hereby granted to those using or reproducing, in whole or in part, the material for valid purposes, providing the copyright owners are acknowledged using the normal conventions. Where specific permission to use material is required, this is identified and such permission must be sought from the copyright holder or agency cited.

Liability statement

By using a Digitised Thesis, I accept that Trinity College Dublin bears no legal responsibility for the accuracy, legality or comprehensiveness of materials contained within the thesis, and that Trinity College Dublin accepts no liability for indirect, consequential, or incidental, damages or losses arising from use of the thesis for whatever reason. Information located in a thesis may be subject to specific use constraints, details of which may not be explicitly described. It is the responsibility of potential and actual users to be aware of such constraints and to abide by them. By making use of material from a digitised thesis, you accept these copyright and disclaimer provisions. Where it is brought to the attention of Trinity College Library that there may be a breach of copyright or other restraint, it is the policy to withdraw or take down access to a thesis while the issue is being resolved.

Access Agreement

By using a Digitised Thesis from Trinity College Library you are bound by the following Terms & Conditions. Please read them carefully.

I have read and I understand the following statement: All material supplied via a Digitised Thesis from Trinity College Library is protected by copyright and other intellectual property rights, and duplication or sale of all or part of any of a thesis is not permitted, except that material may be duplicated by you for your research use or for educational purposes in electronic or print form providing the copyright owners are acknowledged using the normal conventions. You must obtain permission for any other use. Electronic or print copies may not be offered, whether for sale or otherwise to anyone. This copy has been supplied on the understanding that it is copyright material and that no quotation from the thesis may be published without proper acknowledgement.

StpA and the Regulation of OmpF Porin Expression in *Escherichia coli*

A dissertation presented for the degree of Doctor of Philosophy, in the Faculty of Science, University of Dublin, Trinity College

by

Padraig Deighan

Department of Microbiology
Moyne Institute of Preventive Medicine
University of Dublin, Trinity College

August 2001

DECLARATIONS

I, Padraig Deighan, am the sole author of this thesis. The work presented herein represents my own work except where duly acknowledged in the text, and has not been previously presented for a higher degree at this or any other University. Some parts of this work have been published in the following papers:

Deighan, P., A. Free, and C. J. Dorman. (2000) A role for the *Escherichia coli* H-NS-like protein StpA in OmpF porin expression through modulation of *micF* RNA stability. *Mol. Microbiol.* **38**:126-139

Free, A., M. E. Porter, P. Deighan, and C. J. Dorman. (2001) Requirement for the molecular adapter function of StpA at the *Escherichia coli bgl* promoter depends upon the level of truncated H-NS protein. *Mol. Microbiol.* In Press

I agree that the Library of Trinity College, Dublin, may lend or copy this thesis upon request.

Padraig Deighan.

Padraig Deighan

SUMMARY

When the proteomic profile of a wild-type strain of *Escherichia coli* and its *stpA hns* mutant derivative were compared by two-dimensional gel electrophoresis, the levels of expression of several proteins were altered. One of these, which was strongly down-regulated in the absence of the regulatory proteins StpA and H-NS, was identified as the outer membrane porin protein, OmpF. In this study, the molecular details of how StpA and H-NS control OmpF porin expression were examined.

Measurements of *ompF* promoter activity, and *ompF* mRNA and proteins levels, showed that both StpA and H-NS controlled OmpF expression at a post-transcriptional level, by affecting the stability of the *ompF* message. This was primarily mediated by an indirect effect requiring the *micF* locus. The product of the *micF* gene, MicF antisense RNA, represses *ompF* expression by interacting with the *ompF* mRNA, thereby interfering with its translation. Both StpA and H-NS prevented the accumulation of MicF RNA, but intriguingly, this was achieved by distinct mechanisms in the case of each protein. Whereas H-NS repressed *micF* transcription, the StpA protein was shown to destabilise the MicF RNA, demonstrating a novel facet of OmpF regulation. Experiments with purified StpA showed that it could directly associate with both the MicF and *ompF* RNAs. Moreover, the RNA-binding protein, StpA, was shown to interfere with formation of the MicF RNA–*ompF* mRNA complex *in vitro*, consistent with the deduced role of the protein *in vivo*.

The cellular content of StpA was shown to be growth phase regulated and induced by several environmental conditions that do not affect H-NS protein levels. Furthermore, a role for StpA in the regulation of the stationary phase sigma factor (σ^S) was identified, and this effect also operates at a post-transcriptional level. Taken together, this work shows that StpA has a unique role to play in gene regulation, independent from its paralogue H-NS.

For my parents,

With love

ACKNOWLEDGEMENTS

For me this is the most important page of this thesis. There is no way I could have achieved this goal without the invaluable help and guidance from many people. During my undergrad days Cyril and Tim were instrumental in swaying me down this path, and for the last few years allied with Peter as my thesis committee, they have helped keep this project on track and on time. However, the mastermind behind it all was my supervisor, Charles. It is a fantastic experience working with him. He is an inspirational source of enthusiasm, ideas and advice, and seems to know every figure, in every journal – ever! He also got me 'in with' the Wellcome Trust and their support in every way is greatly appreciated.

Andrew Free, from whom I took over the 'Center for StpA Research' has always been available for e-mailed questions and comments regarding this work. His prompt and detailed replies and 'intriguing' discussions are greatly appreciated. Stephen has been a massive influence on this project and his guidance and expertise have shortened it by several months. He was also a huge influence on many projects and experiments (Pegs?) outside the lab. Ronan's slaggin's (founder of the part-time scheme) means there is never a dull moment and I am grateful for the library runs (and WWF updates). Thanks lads for the all the craic, lunches, pints and 'stings' over the years. Christophe is *h*always approachable for millions of questions and *h*always has an answer 'when it is him I am looking for'. Your patience, help and 'calm' were fantastic. You 'are like a real father to me'! Thanks also to Orla, Sorcha, Matt and Denise for making the lab a brilliant place to work every day, and to Connie for always smiling and sorting out any catastrophes. The help of past members of the lab - Susan, Jim, Dave, Brian, Lesley, Niamh and Ruth, who all contributed in some way is greatly appreciated. The chats and laughs with Gus and Adrian, Louise, SB and Schgeg, and everyone else in the Moyne over the years has made it a great place to work and a very enjoyable, quick few years. Thanks also to the prep room staff - Henry, Dave, Paddy, Joe, Fionnuala, Ronan and Margaret, for ensuring that everything ran smoothly each and every day.

My housemates, Beltz, Clowndog, Ryan and D have always provided an important escape from science, and often it's too easy to switch off and forget about the bugs!

A very very special Thank You to my parents and family. Thanks for all your fantastic support and encouragement, and especially to my Mum and Dad for getting me back on my feet and for always being there.

Finally, and most importantly, Tara, a truly amazing friend who has patiently taken every step with me. Thank You for everything.

CONTENTS

Title		I
Declaration		II
Summary		III
Dedication		IV
Acknowledgements		V
Table of Contents		VI
List of Figures		XI
List of Tables		XIII
Chapter 1:	**General Introduction**	**1**
1.1	*Escherichia coli*	2
1.2	Outer membrane	3
1.2.1	Outer membrane lipids	3
1.2.2	Outer membrane proteins	4
1.3	OmpF and OmpC	7
1.4	Regulation of porin gene expression	9
1.4.1	EnvZ-OmpR	10
1.4.2	MicF antisense RNA	12
1.5	Non-coding RNAs	14
1.6	The nucleoid	16
1.6.1	Structure of DNA in the nucleoid	17
1.6.2	Nucleoid proteins	19
1.7	H-NS	22
1.7.1	Control of gene expression by H-NS	23
1.7.2	Regulation of *hns*	26
1.7.3	Structure of H-NS	27
1.8	H-NS-like proteins	28
1.9	StpA	30
1.10	The stress sigma factor	33
1.11	Overview	35

Chapter 2: Materials and Methods 36

2.1 Chemicals and growth media 37
2.1.1 Chemicals, reagents and radionucleotides 37
2.1.2 Growth media 37
2.2 Bacterial strains and culture conditions 40
2.2.1 Bacterial strains 40
2.2.2 Bacterial culture conditions 40
2.3 Plasmids and oligonucleotides 41
2.3.1 Plasmids 41
2.3.2 Oligonucleotides 41
2.4 Transduction with bacteriophage P1 41
2.4.1 Preparation of a high titre P1 *cml* lysate 42
2.4.2 Transduction with P1 *cml* 43
2.5 Transformation of *E. coli* with plasmid DNA 44
2.5.1 Preparation of calcium chloride-competent cells 44
2.5.2 Transformation of calcium chloride-competent cells 44
2.5.3 Preparation of electrocompetent cells 45
2.5.4 Transformation of electrocompetent cells 45
2.6 Assays based on spectrophotometry 46
2.6.1 Monitoring bacterial growth 46
2.6.2 Assessing quantity and purity of RNA 46
2.6.3 Determination of protein concentration by the Bradford assay 47
2.6.4 Assay of β-galactosidase activity 47
2.7 Preparation of plasmid and chromosomal DNA 48
2.7.1 Small-scale isolation of plasmid DNA 48
2.7.2 Small-scale isolation of high purity plasmid DNA 49
2.7.3 Large-scale preparation of high purity plasmid DNA 50
2.7.4 Purification of chromosomal DNA 50
2.8 Manipulation of DNA *in vitro* 50
2.8.1 Restriction endonuclease cleavage of DNA 50
2.8.2 Phosphatase treatment of restriction endonuclease-cleaved DNA 51
2.8.3 Purification of linear DNA 51
2.8.4 Ligation of DNA molecules 52
2.8.5 Phenol extraction and ethanol precipitation of DNA or RNA 52

2.9	Polymerase Chain Reaction	53
2.9.1	Amplification of DNA	53
2.10	Southern blotting	55
2.11	DNA sequencing	56
2.11.1	Denaturing polyacrylamide gel electrophoresis	56
2.12	Autoradiography	57
2.13	Isolation of RNA	58
2.14	Northern blotting	58
2.14.1	Denaturing electrophoresis of RNA	59
2.14.2	Transfer of RNA or DNA to nylon membrane	60
2.14.3	*In vitro* transcription of riboprobes	60
2.14.4	Hybridisation and detection of probe bound to immobilised targets	61
2.15	Primer Extension	61
2.15.1	5′-end labelling of DNA using [γ^{32}P]ATP	62
2.15.2	Primer-RNA annealing and cDNA synthesis	62
2.16	Gel mobility shift analysis of RNA–protein interactions	63
2.16.1	*In vitro* synthesis of labelled RNA	63
2.16.2	Formation and separation of RNA–protein complexes	64
2.17	Formation of the MicF–*ompF* duplex	65
2.18	Effect of StpA on MicF–*ompF-213* RNA duplex formation	66
2.19	Gel mobility shift analysis of DNA–protein interactions	66
2.20	Purification of StpA	67
2.21	SDS-PAGE	68
2.21.1	Staining of proteins	69
2.22	Preparation and analysis of outer membrane fractions	69
2.23	StpA antiserum	70
2.24	Western immunoblot analysis	71
2.24.1	Preparation of total cellular extracts	71
2.24.2	Transfer of proteins to nitrocellulose membrane	72
2.24.3	Detection of bound antigens	72
2.25	Protein–protein crosslinking	72
2.26	Analysis of DNA curvature	73

Chapter 3: Defining the role of StpA in OmpF porin expression 74

3.1 Introduction 75
3.1.1 Proteomic profile for *stpA* and *hns* mutants 75
3.1.2 H-NS regulates OmpF porin expression 77
3.2 Results 78
3.2.1 Construction and characterisation of strains 78
3.2.2 Effect of StpA and H-NS on OmpF porin expression 78
3.2.3 Effect of *stpA* and *hns* mutations on the *ompF* promoter 80
3.2.4 StpA and H-NS regulate *ompF* post-transcriptionally 80
3.2.5 Effect of *stpA* and *hns* mutations on stability of the *ompF* message 82
3.2.6 The promoter choice for *micF* transcription initiation is independent of StpA and H-NS 83
3.2.7 Interaction of StpA with the curved *micF–ompC* promoter region 84
3.2.8 Control of *micF* transcription 85
3.2.9 Control of MicF RNA 88
3.2.10 MicF RNA stability 88
3.3 Discussion 90

Chapter 4: StpA negatively affects MicF RNA–*ompF* m*RNA* duplex formation *in vitro* 96

4.1 Introduction 97
4.1.1 RNA structure 97
4.1.2 MicF RNA and *ompF-213* mRNA structures 97
4.1.3 MicF RNA–*ompF* mRNA interaction 98
4.2 Results 101
4.2.1 Purification of StpA 101
4.2.2 Oligomerisation of StpA 101
4.2.3 Recombinant StpA is functional *in vivo* 102
4.2.4 StpA-nucleic acid interactions *in vitro* 103
4.2.5 Interactions of StpA and H-NS with MicF RNA 104
4.2.6 Interactions of StpA and H-NS with *ompF-213* mRNA 105
4.2.7 Interactions of StpA and H-NS with *ompC-268* mRNA 105
4.2.8 Formation of a MicF RNA–*ompF* mRNA duplex 106

4.2.9 Effect of StpA on the MicF RNA–*ompF* mRNA duplex 107
4.3 Discussion 109

Chapter 5: StpA expression and regulation of σ^s 113

5.1 Introduction 114
5.1.1 *In vivo*-induced genes 114
5.2 Results 116
5.2.1 StpA antiserum 116
5.2.2 Growth-phase-dependent StpA levels in LB medium 117
5.2.3 Growth-phase-dependent StpA levels in M9 minimal medium 118
5.2.4 Comparison of StpA levels in rich and minimal media 118
5.2.5 Cellular content of H-NS 119
5.2.6 Cellular content of σ^s and control by StpA 120
5.2.7 Similar and disparate effects of StpA and H-NS on σ^s 121
5.2.8 Control of *rpoS* transcript levels 122
5.2.9 Effect of ethanol shock on the cellular content of σ^s and StpA 124
5.2.10 Thermal Shock and StpA levels 125
5.2.11 Osmotic shock and StpA levels 126
5.2.12 Induction of StpA and H-NS in macrophage-engulfed *Salmonella typhimurium* 127
5.3 Discussion 129
5.3.1 Growth-phase regulation of StpA 129
5.3.2 Influence of environmental stress conditions on StpA levels 132
5.3.3 StpA modulates σ^s expression 135

Chapter 6: General Discussion 138

Bibliography 147

FIGURES

1.1	Folding pattern of the OmpF porin	7
1.2	OmpR-mediated regulation of *ompF* and *ompC* porin gene expression	11
1.3	Effectors of *ompF* porin gene expression	13
1.4	Bipartite organisation of H-NS and StpA	27
1.5	Cladogram of H-NS- and StpA-like proteins	29
3.1	Proteomic profiles for wild-type *E. coli* GM37 and its *stpA hns* double mutant derivative	75
3.2	Genetic confirmation of *stpA* mutants	78
3.3	Genetic confirmation of *hns* mutants	78
3.4	Growth curves of wild-type and mutant strains in LB broth	78
3.5	Urea–SDS-PAGE of outer membrane porins	79
3.6	Effects of *stpA, hns* and *micF* mutations on *ompF* mRNA level	80
3.7	Complementation of down-regulated OmpF porin levels	82
3.8	*ompF* mRNA stability	83
3.9	Effects of StpA and H-NS on *micF* promoters	84
3.10	The *micF–ompC* promoter region is curved	84
3.11	StpA interacts with the *micF–ompC* promoter region	85
3.12	StpA specifically interacts with the *micF–ompC* promoter region	85
3.13	pMicF	86
3.14	Effect of *stpA* and *hns* mutations on expression of a *micF–lacZ* transcriptional fusion	87
3.15	Effect of StpA and H-NS on MicF RNA level	88
3.16	MicF RNA stability	88
3.17	Model summarising StpA and H-NS-dependent post-transcripional regulation of OmpF expression	95
4.1	RNA secondary structures	98
4.2	Purification of StpA	101
4.3	Oligomerisation of StpA	102
4.4	Recombinant StpAH6 is functional *in vivo*	103
4.5	StpA–RNA interactions *in vitro*	103
4.6	Interactions of StpA and H-NS with MicF RNA	104
4.7	Interactions of StpA and H-NS with *ompF-213* mRNA	105

4.8	Interactions of StpA and H-NS with *ompC-268* mRNA	106
4.9	Formation of the MicF–*ompF* duplex	107
4.10	Effect of StpA on the MicF–*ompF* duplex	108
5.1	Western immunoblot showing the specific reaction of the anti-StpA antibody	116
5.2	Growth-phase-dependent StpA levels in rich broth	117
5.3	Growth-phase-dependent StpA levels in minimal broth	118
5.4	Expression of StpA in rich and minimal media	118
5.5	H-NS mediates the growth-phase regulation of StpA in LB broth	119
5.6	Expression of H-NS in rich and minimal media	120
5.7	Expression of σ^s in rich and minimal media	120
5.8	StpA is required for full expression of σ^s	120
5.9	Under-expression of σ^s in the absence of StpA	121
5.10	Similar and disparate effects of StpA and H-NS on σ^s	122
5.11	Effect of a *stpA* mutation on *rpoS* mRNA levels	123
5.12	Effect of StpA and H-NS on *rpoS* mRNA levels	123
5.13	Effect of ethanol shock on the cellular content of StpA and σ^s	124
5.14	Effect of thermal shock on the cellular content of StpA	125
5.15	Effect of salt up-shock on the cellular content of StpA	126
5.16	Effect of salt down-shock on the cellular content of StpA	127
5.17	Induction of StpA and H-NS in macrophage-internalised *S. typhimurium*	128
5.18	Trans-acting factors and environmental conditions affecting expression of the *stpA* gene	135
6.1	Model summarising StpA-dependent regulation of *ompF* translation via MicF antisense RNA	142

(number shown is that of the page previous to the figure)

TABLES

1.1	Human pathogenic *E. coli* virulence factors	3
1.2	Properties of non-coding RNAs	14
1.3	Properties of major nucleoid proteins	19
1.4	Effectors of σ^s expression	33
2.1	*Escherichia coli* strains used in this study	40
2.2	Plasmids used in this study	41
2.3	Oligonucleotides used in this study	41
3.1	Effect of *stpA* and *hns* mutations on β-galactosidase expression from an *ompF–lacZ* gene fusion	80

(number shown is that of the page previous to the table)

Chapter 1

General Introduction

1.1 *Escherichia coli*

Escherichia coli is the most extensively studied microorganism. Over the years this facultatively anaerobic, Gram-negative rod, has been a model system for the study of bacterial molecular genetics, metabolism and cell division, cell wall biosynthesis, chemotaxis and genetic regulation (Neidhardt, 1996). The release of the entire genomic composition of *E. coli* (Blattner *et al.*, 1997) was a milestone in molecular biology. However, it served to remind us that we still have much to learn about this model microorganism. Indeed, the function of approximately 40% of the predicted genes has not been assigned (Blattner *et al.*, 1997), and many of these annotations are often based on reference models that are either spurious or irrelevant (Kyrpides and Ouzounis, 1999). Moreover, *E. coli* is continuously evolving. Approximately 2% of its DNA is composed of mobile genetic elements including bacteriophages, plasmids, transposons and pathogenicity islands, and horizontal transfer of these elements can lead to significant strain diversity and the spread of virulence determinants.

Although *E. coli* is predominately a non-pathogenic commensal microorganism of humans and animals, certain strains have acquired the ability to cause disease. In humans, pathogenic strains encoding virulence factors such as adhesins, invasins, toxins and capsules, can cause various diseases including several types of diarrhoea, urinary tract infections, sepsis and meningitis (Table 1.1; Kuhnert *et al.*, 2000; Puente and Finlay, 2001). Pathogenic *E. coli* have been classed into eight specific virotypes, based on possessing a particular set of virulence factors that determine the clinical manifestation of the disease. Enterotoxigenic *E. coli* (ETEC), enteroinvasive *E. coli* (EIEC), enterohaemorrhagic *E. coli* (EHEC), enteraggregative *E. coli* (EAEC), enteropathogenic *E. coli* (EPEC), and diffuse adhering *E. coli* (DAEC) infections result in diarrhoea of varying severity. *E. coli* strains that lead to urinary tract infections are known as uropathogenic *E. coli* (UPEC) while neonatal meningitis *E. coli* (NMEC) strains are responsible for meningitis or sepsis. The type of disease that ensues following infection by pathogenic *E. coli* (spread via the faecal-oral route primarily by ingestion of contaminated food or water), and the location of the disease within

the body is determined by the different virulence factors expressed by each virotype (summarised in Table 1.1).

Most of the pioneering research on *E. coli* has been carried out on *E. coli* K-12 or its near relatives. *E. coli* K-12 strains like MC4100, which was used in this study, were shown to be avirulent, and unable to colonise or survive in the environment (Blum *et al.*, 1996). MC4100 is a designated 'wild-type' laboratory strain (Table 2.1) and is often used in studies of gene regulation. It encodes a streptomycin resistance selectable marker, is *lac*$^-$ thereby facilitating studies with *lacZ* fusions, is easily transformed with plasmids, and is a suitable host for transduction.

1.2 Outer membrane

Unlike Gram-positive bacteria that are surrounded by a cytoplasmic (inner) membrane and a thick peptidoglycan-based cell wall, Gram-negative bacteria possess a cytoplasmic membrane, and are additionally covered by an extra membrane layer, which is located outside a thin peptidoglycan layer. This outer membrane simultaneously protects against a harsh environment while the embedded proteins carry out a number of tasks that are crucial to the bacterial cell. Although both the outer and inner lipid bilayer membranes contain proteins that assist in the passage of matter and information, they differ markedly in composition.

1.2.1 Outer membrane lipids

The lipid component of the cytoplasmic membrane is composed entirely of phospholipids such as phosphatidylethanolamine, phosphatidylglycerol and cardiolipin (Nikaido, 1996). In contrast, while the inner leaflet of the outer membrane is of similar composition, lipopolysaccharide (LPS) is exclusively located in the outer leaflet of the outer membrane (Nikaido, 1996). LPS is comprised of three parts. The lipid A region has six or seven fatty acid residues that extend inwards and these are essential for forming the hydrophobic outer leaflet of the outer membrane. The core oligosaccharide region connects the lipid A region to the protruding hydrophilic O-

Table 1.1. Human pathogenic **E. coli** *virulence factors*[a]

Type	Features	Main virulence factors
ETEC	Watery to cholera-like diarrhoea, common with infants and travellers	ETEC attachment to the intestinal mucosa of the small intestine is mediated by colonisation factors (CFs). 20 different, antigenically distinct CFs have been described; the main CFs in human ETEC are the CFA/I and CFA/II fimbrial structures. Once attached to the epithelial cells ETEC can produce heat-labile toxin (LT) and/or the heat-stable toxin (ST). LT is composed of one enzymic A subunit (cleaved into peptides A_1 and A_2) and five identical B subunits. Upon binding to its ganglioside GM_1 receptor on the epithelial cells LT is internalised by endocytosis. The A_1 peptide ADP-ribosylates the α-subunit of the GTP-binding protein, Gs, inhibiting its GTPase activity. Therefore, adenylate cyclase becomes constitutively active and intracellular cAMP levels rise. The leads to activation of the cAMP-dependent A kinase resulting in supranormal phosphorylation of chloride channel proteins such as CFTR. This leads to chloride ion efflux and a block in NaCl and fluid absorption into the cell resulting in watery diarrhoea. ST is a 19 amino acid enterotoxin that binds the guanylate cyclase C (GC-C) receptor located in the brush-boarder membrane of the epithelial cell. GC-C activation leads to a cascade of events including the accumulation of cGMP, which results in the activation of protein kinase A (PKA). PKA-dependent phosphorylation of chloride channel proteins such as CFTR results in net intestinal fluid secretion.
EIEC	Watery diarrhoea to dysentry	Virulence factors located on a 140-kb plasmid (pInv) allow EIEC invasion of colonic epithelial cells. Ipas (invasion plasmid antigens) A–D are secreted onto and into the host cell by a type III secretion system encoded by the products of more than 20 *mxi* and *spa* genes. Secreted Ipas trigger host cell membrane ruffling, actin rearrangements and macropinocytosis leading to bacterial engulfment. IpaB mediates lysis of the endocytic vacuole and bacteria multiply in host cell cytoplasm. The IcsA protein triggers actin nucleation at one pole of the bacterium. This action propels the bacteria through the endothelial cell and into adjacent cells. Apoptosis may be induced in macrophage.
EPEC	Watery diarrhoea, common with infants in developing world.	EPEC bound to epithelial cells of the small intestine result in attaching and effacing lesions (A/E). A/E lesions are marked by effacement of the brush-border microvilli at the sites of bacterial attachment leading to loss of absorptive surface. The initial non-intimate interaction of EPEC is mediated by bundle-forming pili (BFP), a type IV fimbrial adhesin. The products of 14 genes located on the 69-kb EAF plasmid direct the biosynthesis of BFP. After this initial interaction the LEE pathogenicity island encoded EspB, EspD and Tir protein are translocated onto and into the host cell by a LEE-encoded type III secretion apparatus. The EspA protein forms a large filamentous translocation organelle. During translocation Tir is phosphorylated and inserted into the host cell plasma membrane where it serves as a receptor for the bacterial outer membrane protein intimin. The intimin-Tir interaction triggers nucleation of the host cytoskeleton components resulting in the formation of actin rich pedestals below the adhering EPEC. Translocated Esps also trigger host cell signal transduction pathways: the enhancement of protein kinase C activity stimulates Cl^- secretion; phospholipase Cγ converts phosphaidyinositol–4,5–bisphosphate into inositol triphosphate and diacylglycerol, which stimulates the release intracellular Ca^{2+}; NF-κB and IL-8 stimulate the transmigration of polymorphonuclear cells.

EHEC	Diarrhoea, Haemorrhagic colitis, Haemolytic uremic syndrome.	EHEC possesses a LEE pathogenicity island that is functionally and structurally similar to EPEC LEE and thus EHEC infection also results in A/E lesions. EHEC secretes a Shiga-like toxin (Stx) that adopts an AB_5 conformation. The B subunits bind the toxin to the glycolipid receptor Gb_3. This allows the toxin to be internalised by receptor-mediated endocytosis. Toxin-receptor vesicles are transported to the golgi apparatus and then to the endoplasmic reticulum and finally translocated to the cytosol. The A subunit is cleaved into A_1 and A_2 domains. The catalytically active A_1 portion acts as a specific *N*-glycosidase that cleaves an adenine from the 28S ribosomal RNA that inhibits EF–1-dependent aminoacyl tRNA binding. This action blocks protein synthesis resulting in death of intoxicated cells. Translocation of toxins across gut barrier can lead to renal and neurological conditions. EHEC also possess a 60-Mda plasmid, p0157, which encodes several potential virulence factors including a haemolysin, a catalase-peroxidase, a serine protease and a type II secretion system.
EAEC	Watery to mucoid diarrhoea, mainly infection of infants	The plasmid encoded aggregative adherence fimbriae I and II (AAF/I and AAF/II) facilitate adherence of EAEC in aggregates to intestinal cells. This colonisation leads to increased mucus secretion where bacterial cells remain embedded. Secreted heat-stable enterotoxins promote intestinal secretions. The EAEC heat-stable toxin 1 (EAST1) is structurally and functionally similar to ETEC ST. Some EAEC also produce the Pet and Pic virulence factors. These belong to the autotransporter class of bacterial proteins
DAEC	Watery diarrhoea	Diffuse adherence pattern to tissue culture cells is associated with four different adhesins including F1854 fimbriae, an afimbrial adhesin called AIDA-I, and a mannose-resistant haemagglutinin. Some DAEC secrete Esp homologues that result in A/E lesions similar to EPEC and EHEC.
UPEC	Urinary tract infections such as dysuria, pyleonephritis	Most UPEC express P pili or type I fimbriae. P pili bind to the glycolipid Galα(1,4)Gal, and type I fimbriae bind to mannose-containing glycolipid receptors of uroepithelial cells. Afimbrial adhesins also aid the tight interaction of UPEC with uroepithelial cells. The coupling of P pili with its receptor signals the secretion of a bacterial iron-acquisition system and triggers the release of ceramides in the host cell, which trigger signal transduction events and subsequent cytokine production. Most UPEC produce a secreted haemolysin (HlyA) that when bound to calcium can insert into the host membrane to form a pore leading to lysis of the host cell. Cytotoxic necrotising factor 1 induces host cell cytoskeleton rearrangements that impairs migration and proliferation of bladder cells.
NMEC	Neonatal meningitis, sepsis	*E. coli* that cause septic deseases produce a capsule that blocks complement and antibody deposition on the surface. Adhesins such as type I fimbriae mediate attachment to the oropharynx of neonates while S-fimbrial adhesins mediate binding to cells of brain ventricles and to cellular fibronectin. The IbeA and IbeB proteins are important for invasion of the cenrtal nervous system.

[a]Information shown is summarised from the detailed reviews of Kuhnert *et al.* (2000) and Puente and Finlay (2001).

antigen polysaccharide. Gram-negative bacteria expressing the O-antigen are said to be 'smooth', whereas bacteria where this polysaccharide is not expressed are termed 'rough'. Curiously, laboratory strains of *E. coli* are rough, although the information for synthesising LPS is actually present in the *E. coli* K-12 genome (Blattner *et al.*, 1997). Other polysaccharides that are associated with the outer membrane include the enterobacterial common antigen (ECA) which is present in all members of the Enterobacteriaceae (Nikaido, 1996), and capsular polysaccharides, of which there are two types. The K-antigen is the major surface polysaccharide and has a varying structure specific to each serotype, whereas other capsular polysaccharides are similar to LPS but do not possess lipid A moiety (Whitfield and Roberts, 1999).

Outer membrane polysaccharides play a valuable protective role for the bacterial cell. The negatively charged carbohydrate chains serve to avoid surface phagocytosis, primarily by electrostatic repulsion. The high degree of structural diversity obtainable also helps avoiding attack by antibodies and digestive enzymes. LPS (also called endotoxin) is also a powerful immunostimulatory molecule which activates the innate host defense system and can lead to endotoxic (septic) shock (Darveau, 1998). Importantly, polysaccharides also provide a permeability barrier to hydrophobic compounds such as antibiotics, detergents, and bile salts (Vaara, 1993). This is primarily mediated by the tight interaction and reduced mobility of the saturated, fatty acid side chains of the membrane-embedded LPS molecules. While this reduced permeability protects the cell from noxious agents, it is still necessary for nutrients and waste products to traverse the membrane at a rapid rate. This is made possible by the presence of various transport proteins.

1.2.2 Outer membrane proteins

About 50% of the outer membrane mass is proteinaceous, either in the form of integral membrane proteins or as lipoproteins (Koebnik *et al.*, 2000). Murein lipoprotein is the prototypic example of a lipoprotein, and sequence analysis suggests there may be up to twelve other lipoproteins encoded in the *E. coli* genome

(Blattner *et al.*, 1997). The murein lipoprotein is connected to a diglyceride and a fatty acid residue at a modified cysteine. These three fatty acid chains are proposed to penetrate the inner leaflet of the outer membrane, with the rest of the hydrophilic protein is in the periplasm, perhaps covalently attached to peptidoglycan (Nikaido, 1996). In this way the murein lipoproteins (and other lipoproteins) play a structural role and anchor the outer membrane to the rest of the cell. The abundant OmpA porin also serves to stabilise the outer membrane (Nikaido, 1996).

Some integral membrane proteins allow the transmembrane diffusion of hydrophilic solutes through water-filled channels. These can be classed into three groups: non-specific or general porins (discussed in Section 1.3), substrate-specific porins, and TonB-dependent transport systems (Nikaido, 1992; Koebnik *et al.*, 2000). Due to the hydrophobic nature of the outer membrane all of the outer membrane integral proteins adopt a regular β-sheet secondary structure. In this way the formation of hydrogen bonds between adjacent β-strands stabilises the protein. The resulting structure is termed a β-barrel (Schulz, 2000). Interestingly, only bacterial outer membrane proteins adopt a β-barrel conformation, whereas the proteins of the cytoplasmic membrane exclusively adopt transmembrane α–helices. It is generally assumed that this differentiation originates from the biogenesis of outer membrane proteins whose polypeptide chains have to cross the inner membrane, where they would get stuck if they were too hydrophobic.

The substrate-specific porins are passive channels with specificity for certain molecules. The best-studied example is the LamB porin (maltoporin) that is specifically responsible for the facilitated passage of maltose and maltodextrins across the outer membrane, and *lamB* expression is induced as part of the maltose regulon (Nikaido, 1996). The LamB β-barrel has a row of non-polar amino acids lined up by polar residues, and this creates a 'greasy slide' allowing movement of the sugar through the channel (Schulz, 2000). To actively transport a solute against a concentration barrier, or for the transport of large ligands (vitamin B_{12} or an iron-

siderophore complex) requires an input of energy. This is provided by the proton-motive force of the inner membrane through the action of three proteins designated TonB, ExbB and ExbD (Braun *et al.*, 2001). For example, the monomeric FhuA porin transports iron into the cell through association with the energy-transducing TonB protein. The ligand (ferrichrome) binds to this porin. However, these porins are folded such that N-terminal part of the protein folds into the lumen of the barrel to plug the pore. Upon the action of the energised TonB protein conformational changes occur in the FhuA porin that releases the bound ligand and removes the plug, thus allowing for solute translocation (Braun *et al.*, 2001).

There are other proteins in the outer membrane whose synthesis is induced in response to various conditions. OmpX is synthesised in large amounts in stress situations and is thought to bind attacking proteins such as complement factors (Schulz, 2000). Protein components of several export systems and secretion pathways, or proteins involved in the biogenesis of flagella, fimbriae and pili are all induced when needed. Bacteria also carry enzymes within their outer membranes, such as phospholipase A and the OmpT protease (Nikaido, 1996). However, the functions of these are not clear. The TolC protein is involved in protein export and multidrug efflux of small molecules and large proteins from the cytoplasm, by interacting with an inner membrane substrate-specific translocase (Koronakis *et al.*, 2000). In this way export is achieved in a single step and the intervening periplasm is bypassed.

Outer membrane proteins are relatively hydrophilic, yet they must be transported across a hydrophobic barrier and through aqueous environments before their insertion into the outer membrane with the correct topology. There are several factors that facilitate this journey (reviewed in Bernstein, 2000). *E. coli* outer membrane proteins contain amino-terminal signal sequences that target them to the outer membrane. The cytoplasmic SecB molecular chaperone maintains the preprotein (during translation or post-translation) in a loosely folded conformation

and presents the signal sequence to the SecYEG complex (Collier *et al.*, 1988). The SecYEG complex is a dedicated protein-conducting channel (translocon) in the inner membrane. A ribosome-translocon complex can allow the translocation of proteins by continuing translation. This may be aided by the SecA protein which can drive translocation using the energy of ATP hydrolysis (Berstein, 2000). Three recently identified proteins located in the periplasm (Skp, PpiD, and SulA) may keep the outer membrane proteins in an unfolded conformation. In particular the Skp protein can specifically associate with unfolded, but not folded, outer membrane proteins, and hence could be an outer membrane protein-specific chaperone (Bernstein, 2000). Contact with the outer membrane LPS then stimulates the outer membrane proteins to adopt the β-barrel structure and to integrate into the membrane.

1.3 OmpF and OmpC

The OmpF, OmpC and PhoE porins are general porins that produce relatively non-specific channels allowing the passive diffusion of small hydrophilic molecules across the membrane. As with other outer membrane proteins, the crystal structures of OmpF and PhoE show that they adopt a β-barrel structure (Cowan *et al.*, 1992), which is depicted in Fig. 1.1A for the OmpF porin, and this structure is also predicted for the OmpC porin (Nikaido, 1996). OmpF and OmpC are homotrimers and each monomer forms a channel (Fig. 1.1B). The crystal structure of OmpF reveals a β-barrel composed of 16 anti-parallel β-strands. The β-strands are tilted at a 45° angle with respect to the membrane. The loops connecting the β-strands are short on the periplasmic side (1-4 amino acids), but they are often long and variable in sequence among porins from enteric bacteria on the external side. These loops serve as receptors for bacteriophage and colicins and thus each porin is a receptor for different bacteriophage (Nikaido, 1996). Additionally the loops form an extensive vestibule that increases the area of the solute collection domain.

The third loop (L3) of OmpF is not externally extended but instead folds back into the lumen of the pore. L3 contains several negatively charged residues that interact

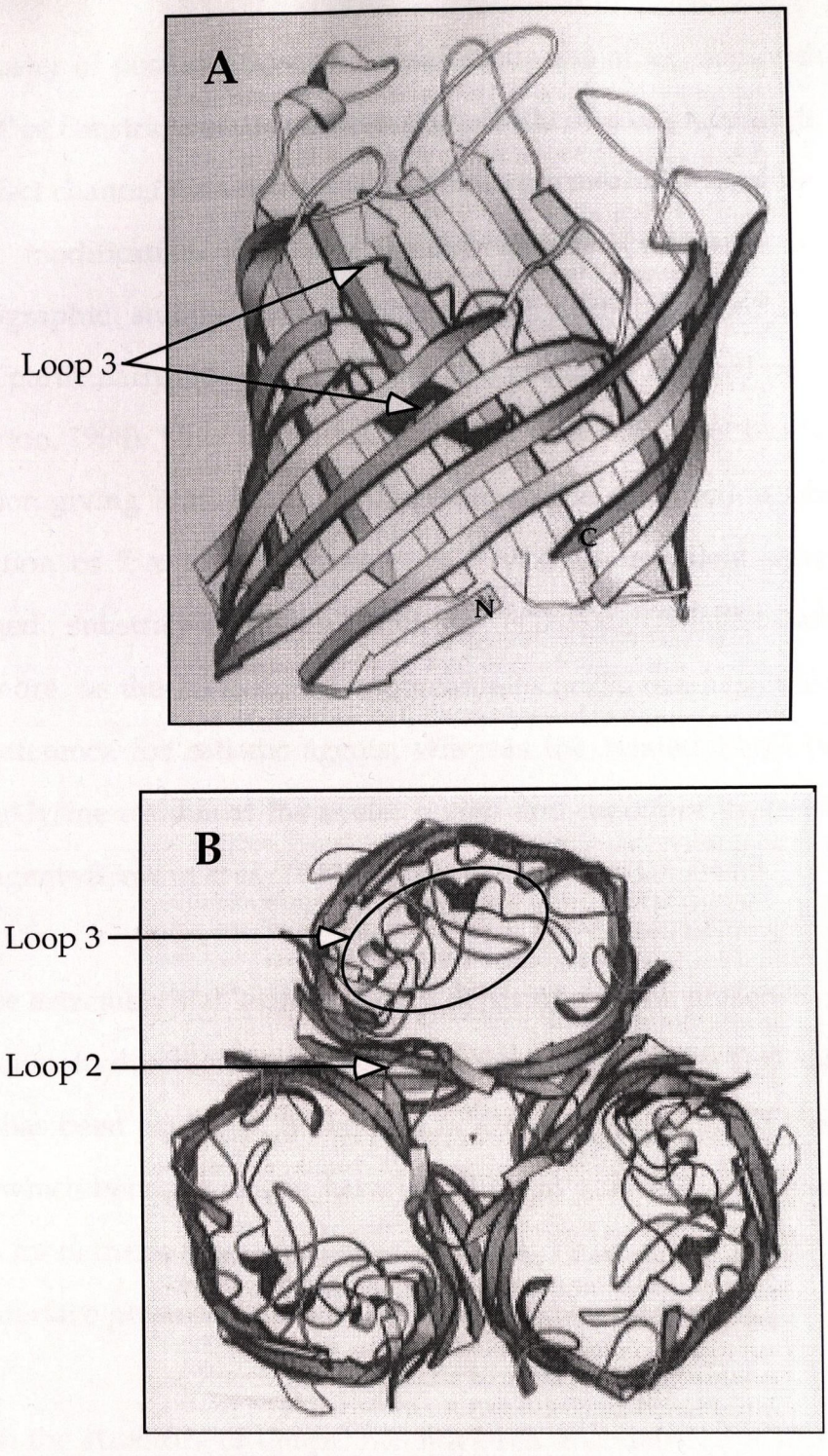

Fig. 1.1. Folding pattern of the OmpF porin

A. Ribbon plot of the monomeric β-barrel OmpF channel that is comprised of 16 anti-parallel β-strands. The centre of the channel is restricted by the infolding of loop 3.

B. Ribbon plot of the OmpF trimer as viewed looking down through the channels. The constriction of the channel by loop 3 is clearly visible and the 'latching' loop 2 that stabilises OmpF monomer interactions is indicated. Adapted from Nikaido (1996).

with a cluster of positively charged residues on the other side of the barrel creating an 'eyelet' or constriction site (Cowan *et al.*, 1992). The implication is that electrostatic forces affect channel dimension and therefore permeability, and this is supported by chemical modification and site-directed studies (Schirmer and Phale, 1999). Crystallographic studies also highlight that non-electrostatic properties of L3 residues, particularly side-chain size, are also crucial to channel permeability (Klebba and Newton, 1998). Thus, OmpF has a wide entrance and exit but has a short central constriction giving it an hourglass-like shape. The constriction site of OmpF has a cross-section of 7 x 11 Å (Cowan *et al.*, 1992), in excellent agreement with the determined substrate-exclusion limit of 600 Da (Nikaido and Saier, 1992). Furthermore, as the L3 loop of OmpF contains acidic residues, the OmpF porin has slight preference for cationic agents, whereas the related PhoE porin contains an additional lysine residue at the eyelet region and therefore preferentially transports anionic agents (Cowan *et al.*, 1992).

Porins are extremely stable and are only denatured in the presence of 2% SDS or 5 M guanidinium hydrochloride at temperatures above 70°C. This exceptionally high stability has been explained in the case of OmpF. It is primarily due to the latching loop L2 which bends over the barrel wall of an adjacent monomer and physically links the monomeric porins together (Fig. 1.1; Phale *et al.*, 1998). The hydrophobic trimer interface presumably also contributes to this stability.

Although the structure of OmpC has not been elucidated, it is likely to be similarly organised to OmpF and PhoE porins. However, a comparison of the penetration rates of solutes of various sizes by measuring the osmotic swelling rates of proteoliposomes showed that the OmpC pore diameter is smaller than that of OmpF (Nikaido, 1992). One major difference between OmpC and OmpF is the presence of an additional 15-residue stretch in loop L4. It is possible that this loop also folds into the lumen of the pore (as well as loop L3) further narrowing the pore size (Nikaido, 1996). So although the OmpC pore (~1.06 nm) is slightly narrower than the OmpF

pore (~1.1 nm), the permeation of fairly large (>300 Da), hydrophobic, or anionic compounds is greatly decreased in the OmpC channel.

1.4 Regulation of porin gene expression

The faster rate of substrate diffusion through the OmpF channel than through the smaller OmpC channel could have implications for bacterial survival, with particular diffusion rates favoured under certain growth conditions. Indeed, enteric bacteria in the human intestine, where toxin and nutrient concentrations are high, exclusively express the OmpC porin (Mederios *et al.*, 1987). In contrast, bacteria in nutrient-poor conditions such as fresh water preferentially express the OmpF porin (Nikaido, 1996; Pratt *et al.*, 1996). By preferentially expressing the smaller OmpC channel bacteria lose ~50% permeability to glucose and other small nutrients. However, larger, more hydrophobic or negatively charged compounds such as bile salts are efficiently excluded (Nikaido, 1996). Moreover, in nutrient-poor conditions the wider OmpF channel can allow the more efficient uptake of nutrients.

An *E. coli* cell harbours a constant total of ~10^5 OmpC and OmpF porin trimers in its outer membrane (Nikaido, 1996). However, the ratio of OmpF to OmpC varies depending on the environmental conditions. For example, the *ompF* gene is expressed when cells are grown in a low-osmolarity environment, whereas *ompC* is expressed when cells are grown under conditions of high osmolarity. This response to osmolarity is exerted at the level of *ompF* and *ompC* transcription via the well-characterised EnvZ-OmpR two-component signal transduction system (see below). In addition, *ompF* expression is controlled at a post-transcriptional level by the MicF antisense RNA, and *micF* expression is regulated in response to several *trans*-acting factors (Section 1.4.2). Thus, it is clearly important that the bacterial cell modulates the level of each porin expressed in the outer membrane, and interfering with the outer membrane porin composition can adversely affect bacterial physiology. Indeed, an *ompF ompC* double mutant of *Salmonella typhimurium* SL1344 was attenuated in a mouse model of infection (Chatfield *et al.*, 1991) and an *ompC* single

mutant of *Shigella flexneri* was also severely impaired for virulence in mice (Bernardini *et al.*, 1993).

1.4.1 EnvZ-OmpR

The essence of the EnvZ-OmpR two-component system, like other signal transduction systems, is the conversion of signal recognition, to gene activation or other cellular processes. The usual arrangement of a two-component system is a histidine protein kinase serving as a signal receptor, and its cognate response regulator modulating specific gene expression. EnvZ is a transmembrane histidine kinase that monitors osmotic pressure (Kim and Forst, 2001). The amino-terminal part of the protein located in the periplasm is the sensor kinase domain. Upon activation of this sensor kinase domain by a change in osmotic pressure, the carboxy-terminal catalytic domain of the protein located in the cytoplasm is phosphorylated at the highly conserved His-243 residue by an autokinase activity. This phosphate group is subsequently transferred to the conserved Asp-55 residue of OmpR. OmpR is a response regulator that is composed of a regulator domain and an output domain. This aspartyl-phosphate group on the OmpR (OmpR-P) regulator domain leads to structural changes in the OmpR-P output domain, which allows the response regulator to carry out its function. OmpR-P is an active transcription factor that binds the upstream promoter regions of the *ompF* and *ompC* genes, and other genes, and differentially modulates their expression. EnvZ also acts as a phosphatase dephosphorylating OmpR-P (Hoch, 2000).

The *ompF* gene and the *ompC* gene are efficiently expressed even although they possess poor –35 and –10 elements. Hence, other *cis*-acting sequences in the *ompF* and *ompC* promoter regions were shown to be necessary for maximal expression (Mizuno and Mizushima, 1990). These *cis*-acting sequences were necessary to mediate efficient interaction of OmpR-P with the *ompF* and *ompC* promoters as revealed by mutagenesis and footprinting studies (Pratt and Silhavy, 1995). The 20-bp OmpR-P-binding sites are designated F1, F2, and F3 in the case of the *ompF*

promoter, and C1, C2 and C3 in the case of the *ompC* promoter. When these sites are occupied by OmpR-P the *ompF* and *ompC* promoters are efficiently transcribed. Furthermore, there is an additional site (F4) within the *ompF* promoter region that when occupied by OmpR-P results in *ompF* transcriptional repression (Fig. 1.3; Pratt and Silhavy, 1995; Head *et al.*, 1998).

A model has been proposed by Bergström *et al.* (1998) to explain OmpR-mediated regulation of *ompF* and *ompC* expression. In medium of low osmolarity the cellular OmpR-P level is reduced as the ratio of EnvZ kinase to phosphatase activity decreases. This level of OmpR-P is sufficient to co-operatively interact with the F1 and F2 sites, and loosely with the F3 site of the *ompF* promoter (Fig. 1.2). This allows for OmpR-P to contact the C-terminal domain of the α-subunit of RNA polymerase and to activate *ompF* transcription. *ompC* expression is not induced under conditions of low osmolarity because OmpR-P can only interact with the C1 site. The DNA-bending protein, integration host factor (IHF), also serves to repress *ompC* expression (Huang *et al.*, 1990). On the other hand, in response to high osmolarity the kinase–phosphatase ratio of EnvZ increases and thus the cellular concentration of OmpR-P is greater. As a result of this increase OmpR-P can interact with the F4 site of the *ompF* promoter by co-operatively interacting with the OmpR-P molecules already bound at the F1-F2-F3 sites, and as a result the *ompF* promoter region is proposed to loop back to block *ompF* transcription (Fig. 1.2). The IHF protein stabilises this repressive nucleoprotein loop complex (Ramani *et al.*, 1992; Pratt and Silhavy, 1995). At the *ompC* promoter the C2 and C3 sites are now occupied and facilitate transcriptional activation of *ompC*. Notably, the unphosphorylated form of OmpR has only weak affinity for the promoters (Head *et al.*, 1998). Thus, *ompF* and *ompC* are reciprocally regulated by the cellular level of OmpR-P, which in turn is determined by the kinase and phosphatase activities of EnvZ. Recent *in vitro* data also suggests that the interaction of OmpR-P with its target DNA shifts the EnvZ-mediated equilibrium between OmpR and OmpR-P dramatically towards OmpR-P

Fig. 1.2. OmpR-mediated regulation of* ompF *and* ompC *porin gene expression
The OmpR response regulator modulates transcriptional regulation of the *ompF* and *ompC* genes in response to changes in osmotic pressure. The phosphorylated form of OmpR (OmpR-P, illustrated as ovoids) binds as a dimer to each of four binding sites (designated F1, F2, F3 and F4) upstream of the *ompF* transcription start site (illustrated as an arrow), and to three binding sites upstream of the *ompC* transcription start site (designated as C1, C2 and C3). At low osmolarity, the low level of OmpR-P in the cell binds the F1 and F2 sites, and loosely binds to the F3 site resulting in *ompF* expression. Only the C1 site in the *ompC* regulatory region is occupied at low osmolarity and hence *ompC* is poorly transcribed. At high osmolarity, as the OmpR-P concentration increases, OmpR-P also binds to the F4 site by interacting with the OmpR-P molecules bound to the F3 site. As a result the *ompF* regulatory region forms a repression loop which blocks transcription of *ompF*. At high osmolarity OmpR-P also co-operatively binds to the C2 and C3 sites allowing *ompC* transcription. Based on the data of Bergström *et al.* (1998).

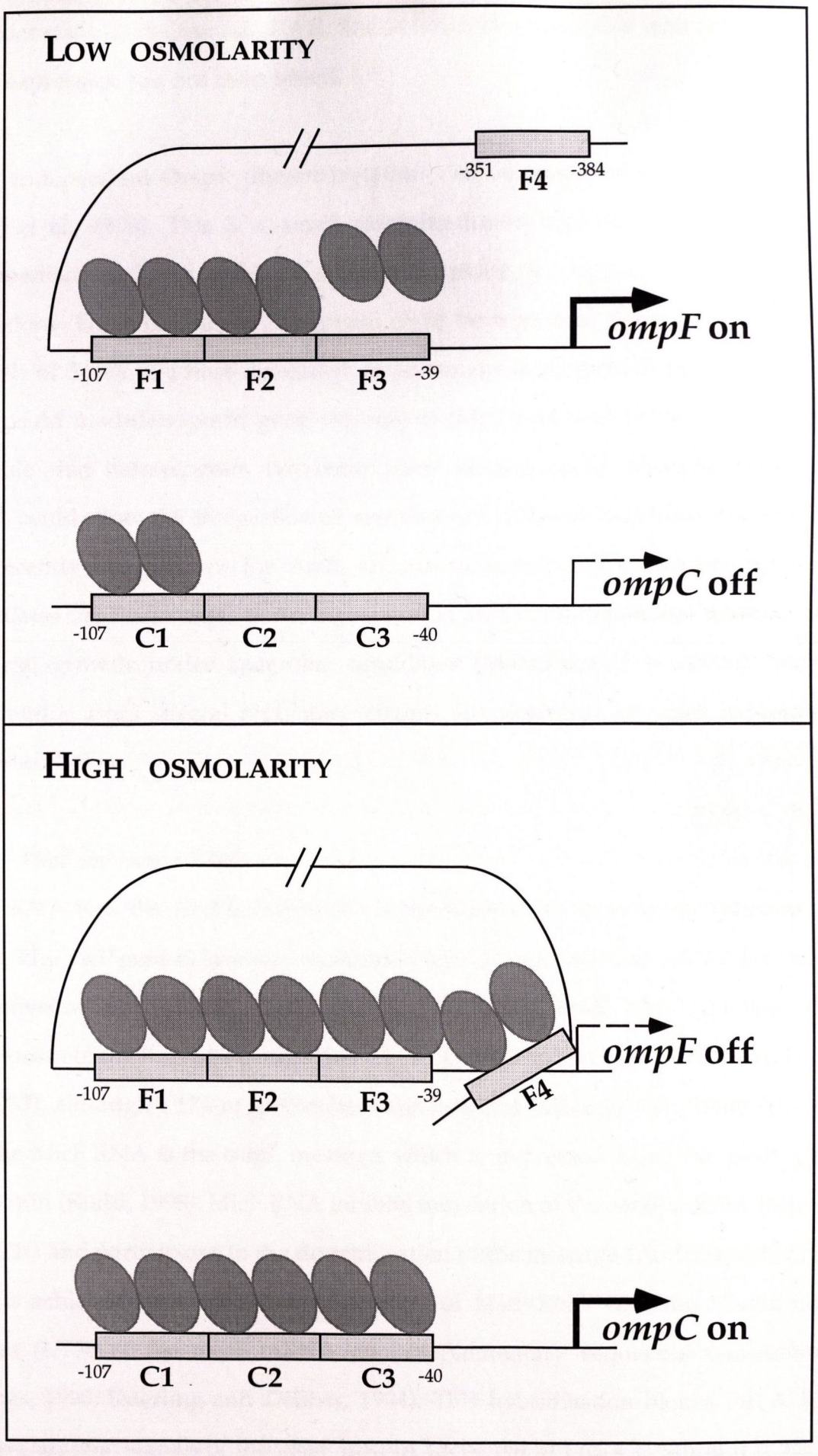
LOW OSMOLARITY
-351
F4
-384
-107
F1
F2
F3
-39
ompF on
-107
C1
C2
C3
-40
ompC off
HIGH OSMOLARITY
-107
F1
F2
F3
-39
F4
ompF off
-107
C1
C2
C3
-40
ompC on

(Buckler *et al.*, 2000; Qin *et al.*, 2001). The *in vivo* relevance of this with respect to porin gene expression has not been tested.

EnvZ-independent OmpR phosphorylation can be mediated by acetyl phosphate (Pratt *et al.*, 1996). This is a small phospho-donor molecule that is a metabolic intermediate and the level of acetyl phosphate is dependent on the growth conditions. Therefore, acetyl phosphate could be a general signal that differentiates growth of *E. coli* in a host-associated environment from growth in fresh-water and thus could modulate porin gene expression (McCleary and Stock, 1994). It is also possible that heterologous two-component kinases could phosphorylate OmpR which could allow the integration of signals from different regulatory systems. This has recently been shown for ArcB, an anaerobic-responsive histidine kinase that modulates *ompF* and *ompC* porin expression in an OmpR-dependent manner during bacterial growth under anaerobic conditions (Matsubara *et al.*, 2000). Morover, information from several regulatory circuits also converge on *micF* expression as discussed below.

1.4.2 MicF antisense RNA

MicF RNA was the first unlinked antisense RNA to be discovered (Mizuno *et al.*, 1984). The *micF* gene is located immediately upstream of *ompC* at 48.22 min on the *E. coli* physical map (Rudd, 1998) and is transcribed from the opposite strand. Expression of *micF* results predominantly in a 93-nt unprocessed RNA (Andersen *et al.*, 1987), although a 174-nt species has been detected (Mizuno *et al.*, 1984). The target for the MicF RNA is the *ompF* message which is expressed from the *ompF* gene at 21.23 min (Rudd, 1998). MicF RNA inhibits translation of the *ompF* mRNA (Mizuno *et al.*, 1984) and participates in the destabilisation of the message (Andersen *et al.*, 1989). This is achieved by a specific hybridisation of MicF RNA with the 5'–untranslated region (UTR) of the *ompF* mRNA via complementary sequences (Andersen and Delihas, 1990; Esterling and Delihas, 1994). This hybridisation blocks the AUG and Shine-Dalgarno signals of the *ompF* mRNA (depicted in Fig. 4.1; Schmidt *et al.*, 1995)

and in the presence of other factors the *ompF* message is destabilised (Andersen and Delihas, 1990). MicF could act be exposing or creating a RNase-sensitive site within *ompF* mRNA that enhances turnover, or be preventing ribosome loading which promotes turnover (Kushner, 1996).

Transcriptional modulation of *micF* occurs in response to a variety of *trans*-acting factors and environmental conditions (Fig. 1.3). The structurally related MarA, SoxS and Rob proteins (XylS-AraC family of transcriptional regulators) all activate *micF* expression in response to salicylate, antibiotics, oxidative stress, and cationic antimicrobials (Chou *et al.*, 1993; Cohen *et al.*, 1993; Ariza *et al.*, 1995; Jair *et al.*, 1995; 1996; Bennick *et al.*, 2000; Oh *et al.*, 2000). Collectively MarA, SoxS and Rob activate a common set of promoters termed the *mar* regulon, and hence *micF* is a member of the *mar* regulon. This activation is achieved by binding of the regulators to the 'marbox' located at –51 to –32 with respect to the *micF* transcription initiation site (Li and Demple, 1996; Martin *et al.*, 1999).

The nucleoid associated proteins H-NS (histone-like nucleoid structuring protein), Lrp (leucine-responsive regulatory protein) and HU (heat-unstable nucleoid protein) all modulate *micF* expression. Lrp and H-NS repress *micF*, and direct binding of these proteins to the *micF* promoter region has been demonstrated (respectively Ferrario *et al.*, 1995; Suzuki *et al.*, 1996). In contrast, the HU protein is necessary to stimulate *micF* expression (Painbeni *et al.*, 1997). It remains to be determined if these nucleoid proteins modulate *micF* expression in response to specific environmental parameters.

An unbalanced phospholipid composition in the outer membrane was shown to activate *micF* expression. However, how this is achieved is unclear (Inoue *et al.*, 1997). The cellular MicF RNA level also accumulates in response to different environmental stimuli including an upward shift in the temperature or osmolarity of the growth medium, or by the addition of ethanol to the medium (Andersen *et al.*, 1989). In most

Fig. 1.3. Effectors of **ompF** *porin gene expression*

Diagram summarising the environmental conditions and *trans*-acting factors that modulate *ompF* porin gene expression at the transcriptional and post-transcriptional levels. Closed arrows indicate *trans*-acting factors that negatively influence transcription of *ompF,* or transcription from the divergent *micF-ompC* promoters. Open arrows are effectors that positively influence transcription arising from the *ompF* promoter, and from the *micF-ompC* promoters. Green lines depict environmental conditions known to modulate *ompF* or *micF* expression, and the proteins that mediate the response to these different parameters, if known, are indicated. The resulting cellular content of the MicF antisense RNA can then influence *ompF* mRNA translation. If the sum total of the information converging on the *micF* protmoter leads to represssion of *micF* (e.g., growth in LB broth), the *ompF* mRNA is assessible to ribosomes and is freely translated. If the cell is stressed (e.g., thermal up-shock), *micF* expression is induced, and the accumulation of MicF RNA leads to formation of the MicF RNA/*ompF* mRNA duplex, where the *ompF* mRNA translation initiation signals are sequestered by MicF RNA binding. This inhibits ribosome loading, and therefore translation. The destabilised *ompF* message is then degraded by cellular RNases.

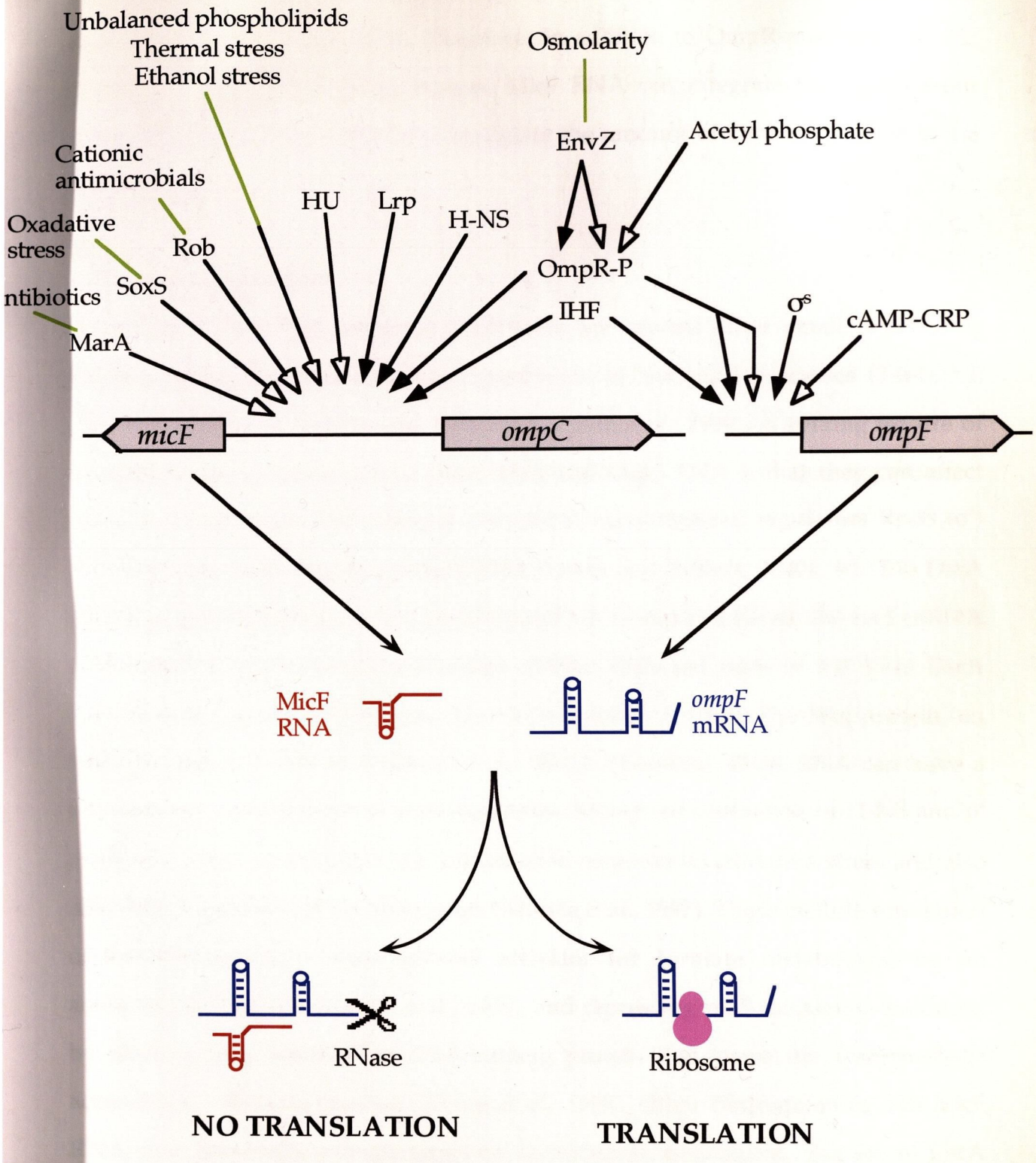
Unbalanced phospholipids
Thermal stress
Ethanol stress
Osmolarity
EnvZ
Acetyl phosphate
Cationic antimicrobials
HU
Lrp
H-NS
Oxadative stress
Rob
OmpR-P
SoxS
IHF
σs
cAMP-CRP
ntibiotics
MarA
micF
ompC
ompF
MicF RNA
ompF mRNA
RNase
Ribosome
NO TRANSLATION
TRANSLATION

cases described above when the cellular MicF level increases or decreases, there is a corresponding reciprocal effect on OmpF protein levels, consistent with the direct repressive effect of MicF RNA. Therefore, in addition to OmpR-mediated osmotic control of *ompC* and *ompF* expression, MicF RNA can integrate the signals from several other regulatory circuits to modulate the amount of OmpF expressed in the outer membrane.

1.5 Non-coding RNAs

In addition to the MicF antisense RNA there are several other small, non-coding RNAs (riboregulators) in *E. coli* that participate in biological processes (Table 1.2; reviewed in Wagner and Simons, 1994; Wassarman *et al.*, 1999). A striking feature of some *trans*-acting RNAs such as DsrA RNA and OxyS RNA is that they can affect more than one target. For example, the global transcriptional regulators RpoS (σ^s) and H-NS are both targets of DsrA RNA (Lease and Belfort, 2000a, b). The DsrA RNA–*hns* mRNA interaction enhances *hns* mRNA turnover whereas the *rpoS* mRNA is stabilised by DsrA (Lease and Belfort, 2000b). Different parts of the 85-nt DsrA RNA mediate these activities, and this riboregulation requires the Hfq protein, an RNA-chaperone co-factor (Sledjeski *et al.*, 2001). Therefore, DsrA RNA can have a far-reaching global impact on gene regulation through co-ordination of H-NS and σ^s expression. The 109-nt OxyS RNA is induced in response to oxidative stress and also affects the expression of multiple genes (Altuvia *et al.*, 1997). These include repression of *fhlA* translation (a transcriptional activator for formate metabolism) by an antisense mechanism (Altuvia *et al.*, 1998), and repressing *rpoS* translation indirectly by titrating Hfq, which is an RNA-binding protein that keeps the *rpoS* message accessible to ribosome loading (Zhang *et al.*, 1998). Other riboregulators, like MicF RNA, may affect only a single target by an antisense mechanism. The 360-nt CsrA RNA regulates carbohydrate metabolism by facilitating the decay of the *glgCAP* operonic mRNA by hybridisation with the translation initiation region of the mRNA. The CsrB protein may antagonise this interaction by sequestering the CsrA RNA (Franch and Gerdes, 2000). The DicF RNA has significant complementarity to the *ftsZ*

Table 1.2. Properties of non-coding RNAs[a]

RNA[b]	Gene	Length (nt)	RNA biogenesis	Main features	Selected reference
CsrB	*csrB*	369	Unknown	Associates with the RNA-binding protein CsrA and inhibits CsrA-mediated degradation of mRNA	Romeo (1998)
DicF	*dicF*	53	Processed from polycistronic transcript by RNase E (5′-end), RNase III (3′-end)	Represses translation of *ftsZ*, a protein involved in the cell division process	Wassarman *et al.* (1999)
DsrA	*dsrA*	87	Primary transcript	Stabilises *rpoS* mRNA and destabilises *hns* mRNA via interactions with the RNA-binding Hfq protein	Sledjeski *et al.* (2001)
GcvB	*gcvB*	130	Primary transcript	Represses expression of *oppA* and *dppA* mRNAs, the products of which are periplasmic-binding proteins of the major peptide transport system	Urbanowski *et al.* (2000)
MicF	*micF*	93	Primary transcript	Represses *ompF* mRNA translation; crosslinks to a 80-kDa protein	Andersen *et al.* (1989)
OxyS	*oxyS*	109	Primary transcript	Represses translation of *rpoS* via interaction with the Hfq protein. Also represses translation of *fhlA*, a transcriptional activator for formate metabolism	Zhang *et al.* (1998)
RNase P	*rnpB*	377	Processed from primary transcript by RNase E (3′-end)	Catalytic RNA which, as a ribonucleoprotein complex with the RNase P protein, is involved in RNA processing	Wassarman *et al.* (1999)
RprA	*rprA*	106	Primary transcript	Stimulates *rpoS* mRNA translation	Majdalani *et al.* (2001)
Spot 42	*spf*	109	Primary transcript	Associates with the nucleoid and ribosomes	Wassarman *et al.* (1999)

tmRNA	*ssrA*	363	Processed from primary transcript by RNase P (5′-end), RNase III (3′-end)	Marks proteins whose biosynthesis has stalled for degradation, by the co-translational addition of a tmRNA–encoded tag to the incomplete polypeptide	Karzai *et al.* (2000)
4.5S	*ffs*	114	Processed from primary transcript by RNase P (5′-end)	Component of the signal recognition particle which targets proteins containing a signal peptide to the secretory apparatus. Also involved in translation by enhancing the release of elongation factor G from the ribosome	Wassarman *et al.* (1999)
6S	*ssrS*	184	Processed from dicistronic transcript	Binds to the σ^{70}-holoenzyme form of RNA polymerase and acts to reduce its activity in stationary phase	Wassarman *et al.* (2000)

[a]This is an updated, modified table to that of Wassarman *et al.* (1999). [b]Only small RNAs that are expressed from the *E. coli* chromosome, and for which a physiological role has been elucidated, are included. Wassarman *et al.* (2001) and Argaman *et al.* (2001) list other identified small RNAs whose functions are currently unknown.

mRNA in the region surrounding the Shine-Dalgarno region. When DicF RNA is over-expressed, the resulting under-representation of the FtsZ protein prevents cell division (Wassarman *et al.*, 1999).

Natural occurring antisense RNAs are also often associated with control of accessory genetic elements such as plasmids, transposons, and bacteriophages (reviewed in Wagner and Simons, 1994). In several of these cases the antisense RNA has perfect complementarity with its target RNA due to divergent transcription of the target and antisense RNAs from overlapping DNA templates. The RNAI antisense RNA controls the cellular copy number of ColE1-based plasmids by interfering with the RNAII primer, which is necessary for the initiation of plasmid replication (Wagner and Brantl, 1998). The *hok–sok* system of plasmid R1 is a representative control mechanism of plasmid-borne killer systems, whereby R1 plasmid-less cells are killed thus ensuring stable maintenance of the plasmid. Translation of the *hok* mRNA, the product of which is a small protein that renders the cell membrane permeable, is negatively influenced by association with the Sok antisense RNA (Wagner and Simons, 1994). An antisense RNA also controls Tn*10* transposition. The IS*10* elements at the ends of the Tn*10* transposon encode the *tnp* mRNA (also called RNA-IN) coding for the transposase. The IS*10* antisense RNA, termed RNA-OUT, sequesters the RNA-IN ribosome-binding site and thereby prevents transposase expression (Wagner and Simons, 1994). A similar mechanism of antisense control involving double-stranded RNAs that destabilise a target RNA is conserved in plants and higher eukaryotes. This is termed post-transcriptional gene silencing. RNA silencing in these cases is deemed important for host–antiviral defense and transposon silencing (Cogoni and Macino, 2000).

Some non-coding RNAs expressed from the *E. coli* chromosome are not post-transcriptional regulators of gene expression (riboregulators) *per se*, but instead have intrinsic cellular activities. For example, the RNA signal recognition particle facilitates protein translocation across the inner membrane. The tmRNA targets aberrant

protein products of truncated mRNAs for rapid degradation. Finally, the catalytic RNase P RNA is a component of RNase P, a key enzyme in RNA processing (Table 1.2; Wassarman *et al.*, 1999).

It is clear that there are several small functional RNAs in *E. coli* and presumably there are numerous more examples to be uncovered. This raises the question: Why use small RNAs for regulation of biological processes? One hypothesis is that small RNAs are more economical by avoiding the energetic cost of synthesising a protein (Lease and Belfort, 2000b). This may be true for the stable DsrA and OxyS RNAs that can modulate several targets during times of stress. However, the plasmid-copy-number regulatory RNAs are inherently unstable. It is more likely that it is the versatility of RNA structure and stability, coupled with the energetic costs of producing small RNAs, which have led to their ubiquitous use in regulation of diverse biological processes.

1.6 The nucleoid

If stretched out in a linear form the ~4.6 million bp chromosome of *E. coli* would have a total length of ~1.5 mm. Within bacterial cells the chromosome(s) must be structured so as to function in multiple biological processes simultaneously including transcription, translation, replication, recombination, and physical movement. A typical *E. coli* cell is about 1 μm by 0.5 μm in size and microscopic visualisation of fluorescently labelled DNA shows that the chromosome must fit into half this space (Talukder *et al.*, 1999). This DNA-occupied space and its associated proteins is altogether called the bacterial nucleoid (reviewed in Pettijohn, 1996; Trun and Marko, 1998). Therefore, the chromosomal DNA must be compacted 1000-fold into a highly ordered structure that is permanently accessible to allow the above-mentioned biological processes to occur.

1.6.1 Structure of DNA in the nucleoid

Long DNA molecules in an aqueous environment are not linear or circular, but instead are in a 'random coil conformation', where fixed lengths of the molecule twist and turn randomly due to the effects of Brownian motion. This can reduce the effective length of the DNA molecule from 1.5 mm to 10 μm (Trun and Marko, 1998). However, such an entangled molecule is completely disorganised and would be insufficient to carry out the physical and biochemical properties associated with a bacterial chromosome. Instead, electron micrographs (Kellenberger, 1990) and moving pictures (Hinnebusch and Bendich, 1997; Bendich, 2001) of isolated chromsomes showed the DNA in a rosette form with loops (domains) emanating from a dense node, or as a network of looped strands lacking a node. The elements that form the anchor of the loops are not precisely known but may be caused by intra-molecular DNA-strand associations due to recombination junctions, tangles and knots (Bendich, 2001). It is also possible that the interactions of repetitive extragenic palindromic (REP) elements, which are periodically distributed throughout the chromosome, could create loops of DNA perhaps when complexed with IHF or other proteins (Bachellier *et al.*, 1999; Ussery *et al.*, 2001). In this rosette form the DNA is significantly more compacted and organised.

DNA supercoiling plays a role in chromosome condensation. Moreover, negatively supercoiled DNA has excess free energy and therefore has the potential to influence transactions that depend on local melting of the DNA helix as well as influencing DNA-protein interactions. Hence, supercoiling is an important aspect of the process of DNA transcription, replication and recombination (Cozzarelli, 1980; Dorman *et al.*, 1990; Drlica, 1990; Dorman, 1995). The *E. coli* chromosome is negatively supercoiled, and the degree of supercoiling of the different domains is independent, i.e., supercoils cannot move between different domains (Sinden and Pettijohn, 1981). The overall supercoiling properties of the different domains are determined primarily by the antagonistic effects of DNA gyrase, which introduces negative supercoils and removes positive supercoils, and DNA topoisomerase I, which relaxes supercoiled

DNA (Dorman, 1995). It was estimated that one single-stranded DNA break per 100-kbp introduced by gamma irradiation was required to relax the superhelical tension of a single DNA domain. In other words, each independent domain encompasses 100-kbp of DNA and therefore each *E. coli* genome would have approximately 45 DNA domains (Sinden and Pettijohn, 1981; Pettijohn, 1996). So supercoiling of the DNA imparts long-range order on the structure of the chromosome changing the global shape of a circular molecule from a 'random coil' to a 'rosette-like' conformation. This leads to a ~25-fold compaction of the chromosome (Pettijohn, 1996). Moreover, topological changes in one domain due to transcription, replication or DNA repair need not affect the overall conformation of the chromosome. Also as each domain has a different superhelical tension, different sets of supercoiling-responsive genes in different domains could be co-ordinately regulated. However, this has yet to be proved conclusively.

RNA represents about 30% of the total weight of isolated nucleoids. Indeed, the major protein associated with the DNA is RNA polymerase (Pettijohn, 1996). However, the role of RNA in nucleoid structure has not been established. Although treatment of isolated nucleoids with RNase causes them to unfold, the nucleoid of a bacterial cell growing in the presence of rifampicin (prevents RNA transcription) is more compact (Cunha *et al.*, 2001 and references therein). Further experimentation is required to precisely link a role for RNA in chromosome organisation.

The concentration of RNA and protein in the cytoplasm of an *E. coli* cell is ~340 mg ml^{-1} whereas the concentration of DNA is the nucleoid is much lower at ~75 mg ml^{-1} (Trun and Marko, 1998; Ellis, 2001). Hence, a significant portion of the cell (~20-30%) is physically occupied by molecules and, therefore, that space is physically unavailable to other macromolecules. This is termed macromolecular crowding or the excluded volume effect (reviewed in Ellis, 2001) and it has a significant influence on the nucleoid structure for two reasons. Firstly, DNA is condensed by the crowding effect where collisions between DNA and non-DNA-interacting

macromolecules of the cytoplasm will collapse the DNA into a compact structure (Pettijohn, 1996). Secondly, under these crowded conditions there is more chance of the DNA associating with one of the abundant nucleoid-associated proteins such as IHF, HU, H-NS (Section 1.7) and FIS (factor for inversion stimulation), which play an important role in maintaining the DNA in a compact functional state.

1.6.2 Nucleoid proteins

Compaction of the eukaryotic chromosomes is different to that of the prokaryotic chromosome (Bendich and Drlica, 2000), although in both cases proteins are involved. These are nucleoid proteins in prokaryotes, and their counterparts in eukaryotes, called histones. The best-characterised level of DNA condensation in eukaryotes involves the formation of nucleosome structures. Here, 146-bp of double stranded DNA wrap around the core of a histone octomer (Wu and Grunstein, 2000), while the tails of the histone proteins extend from this nucleosome core. Modification of the histone tails by (de)acetylation, methylation, phosphorylation, and ubiquitination enables regulation of diverse physiological functions such as transcription, DNA repair and replication (Wu and Grunstein, 2000). In contrast, bacterial nucleoid proteins form unstable complexes with DNA and consequently their role in affecting global structure of the chromosome is not well defined.

The nucleoid proteins of *E. coli* include IHF, H-NS, HU, FIS, Lrp, StpA (suppressor of td^- phenotype A), Dps (DNA-binding protein from starved cells), Hfq (host-factor for bacteriophage Q_β), CbpA (curved DNA-binding protein A), CbpB (curved DNA-binding protein B, also called Rob), DnaA (product of $dnaA^{ts}$ gene), and IciA (initiator of chromosome initiation A). The properties of some of these proteins are given in Table 1.3.

Although all of the nucleoid proteins can bind DNA non-specifically with physiological significant affinities, FIS, IHF, Lrp, Rob and DnaA show higher affinity for specific sequences (Talukder and Ishihama, 1999), and therefore a DNA-binding

Table 1.3. Properties of major nucleoid proteins[a]

Protein	Number of amino acids	Mass (kDa)	Structure[b]	DNA target[c]	Cellular localisation[d]	Exponential phase expression[e]	Stationary phase expression[e]	Cellular functions other than transcription	Selected reference
Dps	167	19.0	Dodecamer (X-ray)	Sequence non-specific	Uniformly within nucleoid	6000	118,000	DNA protection	Wolf *et al.* (1999)
FIS	98	11.2	Homodimer (X-ray)	GNtYAaWWWtTRaNC	6–10 specific foci	60,000	Very low	DNA recombination, replication	Finkel and Johnson (1993)
IHF	IHFα, 99 IHFβ, 94	11.2 10.7	Heterodimer (X-ray)	WATCAANNNNTTR	Uniformly within nucleoid	15,000	50,000	DNA recombination, replication	Goosen and van de Putte (1995)
HU	HU-1, 90 HU-1, 90	9.2 9.5	Heterodimer (X-ray, NMR)	Kinked, gapped, three or four way junctions	Uniformly within nucleoid	55,000	30,000	DNA recombination, replication	Dorman *et al.* (1999)
H-NS	137	15.4	Dimer-oligomer? (NMR-partial)	Sequence non-specific, preference for curved DNA	Uniformly within nucleoid	20,000	18,000	DNA recombination	Dorman *et al.* (1999) Williams and Rimsky (1996)
Lrp	167	19.0	Homodimer	YAGHAWATTWTDCTR	Not determined	3000	1000		Calvo and Matthews (1994)
StpA	133	15.3	Dimer-oligomer?	Sequence non-specific, preference for curved DNA	Uniformly within nucleoid	~200–500	Very low	RNA chaperone	Dorman *et al.* (1999) Williams and Rimsky (1996)

[a]This is an updated, modified table to that of McLeod and Johnson (2001). [b]Methods used to determine an atomic structure are parenthetically denoted, if available. [c]All nucleoid proteins can bind DNA non-specifically. However in some cases a preferred binding site or structure is given. Y = C or T, R = G or A, W = A or T, H = C, T or A, D = A, G or T, N = any base. [d]Data from Talukder *et al.* (2000). [e]Data expressed as molecules per cell from Talukder and Ishihima (1999), except data for StpA that are estimated based on this study.

site for each protein can be deduced. Using these protein-binding sequences it is possible to search the *E. coli* genome in an attempt to determine the distribution and location of other such DNA sequences. This has recently been done for the IHF and FIS protein-binding sites (Ussery *et al.*, 2001). They predicted between 600–1000 IHF binding-sites in the genome, many of which are clumped in large areas that appear to lie between regions of highly expressed genes. Furthermore, 130 IHF sites directly overlap the periodically distributed REP sites (Ussery *et al.*, 2001), which could have implications for the anchorage points of DNA domains as discussed in Section 1.6.1. Although the FIS protein binding sequence is somewhat degenerate (Table 1.3), Ussery *et al.* (2001) predict in the region of 6000 such sites in the *E. coli* genome, and that many of these sites are located directly on either side of the replication terminus. Consistent with this, indirect immuno-fluorescent microscopy revealed that the FIS protein accumulates at 6–10 distinct loci in the nucleoid (Talukder *et al.*, 2000). It should also be noted that a significant proportion of the IHF and FIS binding sites were located within 100-bp of predicted open-reading frames (Ussery *et al.*, 2001).

Although HU and H-NS are abundant, sequence non-specific, DNA-binding proteins, they may preferentially interact with certain DNA structures. HU specifically binds to DNA recombination and repair intermediates such as gapped or kinked DNA. Therefore HU may be considered to be a sensor of DNA damage, and is also important in maintaining the superhelical density of the DNA. Indeed, the HU protein was shown to be evenly distributed throughout the nucleoid by indirect immuno-fluorescent microscopy (Talukder *et al.*, 2000) and and by the fact that HU-GFP and DAPI co-localise on the nucleoid (Wery *et al.*, 2001). H-NS preferentially interacts with curved DNA (Talukder and Ishihama, 1999; Sonnenfield *et al.*, 2001) which could influence its role in chromosome organisation. Moreover, overproduction of H-NS leads to a highly condensed nucleoid (Spurio *et al.*, 1992). In an *hns* mutant there is an increased degree of supercoiling of the chromosomal DNA (Mojica and Higgins, 1997) and *in vitro* H-NS constrains DNA supercoils (Tupper *et al.*, 1994). A model for H-NS-mediated compaction of DNA was recently proposed

based on visualisation of H-NS-plasmid DNA complexes by atomic force microscopy (Dame *et al.*, 2000). When two H-NS-bound DNA strands are close together, the bound proteins can interact with an additional DNA strand, or another molecule bound to that strand to form an intramolecular bridge. Further oligomerisation of the H-NS molecules will lead to distinct foci of highly compacted DNA, and oligomerisation of H-NS molecules in the different foci of different strands will lead to high DNA condensation through network formation (Dame *et al.*, 2000). It is possible that H-NS bound to regions of DNA curvature *in vivo* (foci) could enhance DNA compaction in a similar manner.

It is difficult to determine directly the role of nucleoid proteins in the organisation of the chromosome *in vivo*, as generally single nucleoid protein mutations have little effect on the overall nucleoid structure (Trun and Marko, 1998). It is probably best to think of these proteins as a group that functions together for DNA condensation. Hence, under-representation of one or two of the nucleoid proteins can be compensated by the other members of the group. Consistent with this concept the abundance of twelve species of nucleoid proteins was shown to undergo inter-changeable expression during the different stages of growth (Table 1.3; Talukder *et al.*, 1999). The order of accumulation in exponential phase was FIS>Hfq>HU>StpA>H-NS>IHF>Rob>Dps>Lrp>DnaA>IciA>CbpA (see below for explanation of underlining). These results are in general agreement with previously reported values. However, a notable exception is the level of StpA. Several laboratories have reported that the expression of StpA is very low in wild-type bacteria, primarily due to promoter silencing mediated by the paralogous protein H-NS (Chapter 5; Sondén and Uhlin, 1996; Zhang *et al.*, 1996; Free and Dorman, 1997). Among these twelve proteins, the intracellular levels are maximal for the nine proteins during exponential phase. These nine proteins play regulatory roles in replication of the genome and transcription of growth-related genes. For example, FIS positively regulates expression of the stable RNAs (Finkel and Johnson, 1993). In stationary phase the order of abundance is Dps>IHF>HU>Hfq>H-

NS>StpA>Rob>DnaA>Lrp>IciA>CbpA>FIS (Talukder *et al.*, 1999). This change in nucleoid protein composition is accompanied by a compaction of the genomic DNA in stationary phase. This is primarily mediated by the dodecameric Dps protein which coats the DNA in a protective form and sequesters iron ions, thereby preventing oxidative damage (Wolf *et al.*, 1999). Additionally this serves to silence the genome. As stationary-phase bacteria experience nutrient limitation and other stresses, the only genes expressed are those for protection and adaptation to the stress (Ishihama, 1999).

Therefore, in combination with the physical properties that govern DNA discussed in Section 1.6.1, including random coiling, the built-in loop-domain substructure, and supercoiling, the nucleoid proteins and the crowded cellular environment all contribute to maintaining the 1.5 mm *E. coli* genome in a 1000-fold compacted functional structure.

1.7 H-NS

The H-NS protein was originally identified as a heat-stable transcription factor (Jacquet *et al.*, 1971), and was later shown to play an important role in the structure and functioning of the nucleoid (Varshavsky *et al.*, 1977). The H-NS protein (then called H1) was isolated by Busby *et al.* (1979), but soon after several laboratories isolated the gene as loss-of-function mutations when selecting for a variety of phenotypes. The mutations (*osmZ*, *drdX*, *bglY*, *pilG*, *virR*, reviewed in Ussery *et al.*, 1994) seemed unrelated but were mapped to the same locus at 27.8 min on the chromosome, the position of *hns*. Thereafter, the ability of H-NS to associate preferentially with curved DNA (Falconi *et al.*, 1988; Yamada *et al.*, 1991) and to condense DNA *in vivo* and *in vitro* was realised (Spassky *et al.*, 1984; Spurio *et al.*, 1992), highlighting its important role in nucleoid organisation. However, it was also realised that *hns* mutations had pleiotropic effects on many other cellular functions. These included stimulating the transposition of bacteriophage Mu and IS*1*, increasing the frequency of chromosomal deletions, and effects on gene expression from a

number of unlinked and unrelated genes and operons as discussed below (Atlung and Ingmer, 1997; Williams and Rimsky, 1997; Shiga *et al.*, 2001).

1.7.1 Control of gene expression by H-NS

The cellular content of at least 60 proteins was more than 4-fold altered in intensity in an *hns* mutant compared to a wild-type strain when analysed by two-dimensional gel electrophoresis (Hommais *et al.*, 2001). The majority of these proteins (49) were expressed at a higher level in the *hns* mutant, while 11 proteins were under-expressed in the *hns* mutant. The pleiotropic effect of H-NS was further highlighted by a comparative analysis of the messenger RNA expression profiles for otherwise isogenic *hns*$^+$ and *hns*$^-$ strains using DNA arrays (Hommais *et al.*, 2001). Approximately 5% of the annotated genes in *E. coli* (~250 genes) were expressed at significantly different levels in the *hns*$^-$ strain compared to the wild-type. Of the affected genes 80% were induced in the *hns* mutant. Of these H-NS–regulated genes 21% had well-known roles, or were predicted to be involved in information pathways such as transcription and translation, 35% were regulated in response to multiple environmental conditions and were cell wall components, 8% were involved in intermediate metabolism, 7% had other cellular functions and 34% of the genes differentially expressed in an *hns* mutant were of unknown function (Hommais *et al.*, 2001).

As noted above, H-NS, directly or indirectly, modulates gene expression primarily in a negative manner and H-NS-dependent repression of the *proU* (Jordi and Higgins, 2000), *rrnB* (Schröder and Wagner, 2000), and *bglGFB* (Schnetz and Wang, 1996) operons has been studied in detail. H-NS-repressed genes are often counter-regulated by environmental conditions or *trans*-acting factors that positively stimulate gene expression. For example, *proU* expression is induced at high osmolarity (Higgins *et al.*, 1988) and the FIS protein stimulates *rrnB* expression (Schröder and Wagner, 2000). Under such inducing conditions the H-NS-mediated repression is effectively removed, and therefore H-NS can play an important role in

the timing of gene expression. Indeed, inappropriate expression of the virulence traits of pathogenic *Shigella* (Dorman *et al.*, 2001), *Salmonella* (Harrison *et al.*, 1994) and EPEC (Bustamante *et al.*, 2001; Sánchez-SanMartín *et al.*, 2001) are controlled by the H-NS protein.

Several models, which could apply independently or in combination, have been proposed to explain the diverse regulatory properties of H-NS. H-NS can affect the expression of genes indirectly by altering the supercoiling state of the DNA (Higgins *et al.*, 1990; Hulton *et al.*, 1990). In this way, a change in the cellular H-NS content or activity can modulate DNA topology and therefore simultaneously affect many unlinked genes. However, it is likely that H-NS can only modulate transcription from supercoiling-sensitive promoters in this fashion. Another model of H-NS-mediated repression that is common to transcriptional repressor in general is occlusion of RNA polymerase-promoter contact (McLeod and Johnson, 2001). At the *E. coli proU* promoter some of the H-NS-binding sites overlap the promoter region, and transcription is prevented as RNA polymerase can not form productive complexes (Ueguchi and Mizuno, 1993). H-NS can also act as a transcriptional silencer (Göransson *et al.*, 1990) and bind directly to an appreciable region of DNA that, thereafter, is inaccessible to RNA polymerase and other *trans*-acting regulatory factors. The *bglGFB* operon is a classic example where transcription is severely restrained by H-NS in this manner (Higgins *et al.*, 1988; Schnetz and Wang, 1996; Yarmolinsky, 2000 for a review). H-NS can associate with extended regions of the *bgl* promoter region both up- and down-stream of the transcription initiation site. It is possible that H-NS initially contacts the A–T-rich silencer element in the *bgl* promoter region (nucleation site) and that this leads to polymerisation along the DNA (Schnetz and Wang, 1996). Indeed, H-NS has been shown to polymerise co-operatively along DNA (Spurio *et al.*, 1997). At the *rrnB P1* promoter, although the H-NS-binding sites overlap the –35 promoter recognition element, RNA polymerase can still form an open complex when H-NS is bound. However, the transcription complex is only capable of synthesising three-nucleotide-long abortive products, as RNA polymerase

is trapped by H-NS and incapable of proceeding into the elongation phase (Schröder and Wagner, 2000). H-NS can also act through other regulatory proteins by controlling their expression, aiding their DNA binding, or stabilising a nucleoprotein complex. Indeed, at the *E. coli nir* promoter a higher-order nucleoprotein complex composed of H-NS, IHF and FIS, forms an inhibitory promoter architecture that counteracts FNR-dependent activation (Browning *et al.*, 2000).

Whatever the exact mechanism of H-NS-dependent transcriptional repression, what is common is that the promoter regions of H-NS-target genes are often A–T-rich and curved (Atlung and Ingmer, 1997). Indeed, the average intrinsic curvature of a sample of 39 genes regulated by H-NS was 10% higher than the average upstream regions for all genes in *E. coli* (Ussery *et al.*, 2001). Furthermore, several reports show that H-NS has higher affinity for curved DNA than for linear DNA *in vitro* (Yamada *et al.*, 1991; Owen-Hughes *et al.*, 1992; Zuber *et al.*, 1994; Talukder and Ishihima, 1999; Sonnenfield *et al.*, 2001). The preferential interaction of H-NS with curved DNA may stem from the close proximity of the DNA strands (directly either side of the intrinsic bend) which may bring bound H-NS molecules in close proximity and thus enhance protein–DNA or protein–protein oligomerisation (Dame *et al.*, 2001). DNA curvature has been shown to play an important role in H-NS-dependent gene expression. For example, the *Shigella flexneri* VirF protein is the main regulator of virulence gene expression, and its expression is active at 37°C but not at low temperatures. H-NS represses *virF* expression by binding to two sites of the promoter region at temperatures below 32°C. In between the two H-NS-binding sites is a region of intrinsic curvature that undergoes a structural transition at temperatures above 32°C. This antagonises H-NS binding to both sites allowing *virF* expression (Falconi *et al.*, 1998; Dorman *et al.*, 2001).

In a number of cases H-NS is necessary for full expression of a target gene. For example, flagella biosynthesis requires the positive activation of the *flhDC* operon by H-NS, giving rise to the FlhD and FlhC master regulators that control transcription

of the flagellar regulon (Soutourina *et al.*, 1999; Bertin *et al.*, 2001). Additionally several components of the transcription and translation machinery were under-expressed in an *hns* mutant (Hommais *et al.*, 2001). H-NS has also been reported to modulate gene expression at a post-transcriptional level in both a positive and negative way. In the case of the maltose regulon H-NS is necessary to stimulate expression of MalT, the positive regulator of the operon (Johansson *et al.*, 1998). In contrast, H-NS down-regulates expression of RpoS (σ^s), the stress-induced sigma factor at the level of translation and protein stability (Barth *et al.*, 1995; Yamashino *et al.*, 1995). Hence, many *rpoS*-dependent genes are affected by the cellular H-NS content. However, in all of the above examples it is not clear if the effects are a direct or indirect consequence of H-NS.

1.7.2 Regulation of hns

Given that H-NS has both a positive and negative influence on gene expression at the transcriptional and post-transcriptional levels and is also crucial for nucleoid organisation, it is perhaps not surprising that *hns* expression is itself modulated by several *trans*-acting factors. Indeed, the *hns* gene is subject to autoregulation, as the expression of *hns* is increased by ~4-fold in a strain devoid of functional H-NS (Free and Dorman, 1995; Atlung and Ingmer, 1997). Other nucleoid proteins modulate *hns* expression. The H-NS homologue StpA represses transcription of *hns* (Zhang *et al.*, 1996), whereas the FIS protein enhances *hns* expression directly by interacting with the promoter region, and indirectly by competing with H-NS (Falconi *et al.*, 1996). The production of *hns* mRNA is mainly confined to exponential growth (Free and Dorman, 1995). It is likely that this is achieved through a relief of autoregulation, as H-NS molecules would be required to match the rapid rate of DNA synthesis for nucleoid condensation. In stationary phase, when DNA synthesis stops the *hns* mRNA level concomitantly declines (Free and Dorman, 1995).

In general, it appears that *hns* expression is not significantly altered by environmental conditions, whereas many H-NS-target genes are. Temperature

increases, osmotic shock, carbon starvation, and growth in minimal medium all fail to affect the cellular content of H-NS (Dorman *et al.*, 1999). However, *hns* mRNA and protein levels are induced by ~4-fold by lowering the incubation temperature from 37°C to 10°C. This cold-shock enhancement is due to the CspA protein (La Teana *et al.*, 1991; Giangrossi *et al.*, 2001). CspA is a single-stranded-DNA-binding protein that recognises CCAAT sequences, and its interaction with such a site at the 5′–end of the *hns* gene may enhance *hns* transcription (Giangrossi *et al.*, 2001). H-NS protein levels are also reported to increase ~3-fold upon phosphate deprivation (Van Bogelen *et al.*, 1996). *hns* expression is also repressed at the post-transcriptional level by the DsrA regulatory RNA as discussed in Section 1.5.

1.7.3 Structure of H-NS

Genetic and biochemical data showed that the 137-residue H-NS protein, and the 134-residue H-NS-homologue StpA are composed of two distinct functional domains separated by a flexible linker (Fig. 1.4; Cusick and Belfort, 1998; Dorman *et al.*, 1999). The N-terminal part of the proteins (residues 12–65) is the oligomerisation domain and the protease-sensitive linker region extends from residues 76–88. The DNA/RNA-binding domains of H-NS and StpA are localised to the C-terminal region of the protein between residues 90–120. Oligomerisation of H-NS is crucial to its diverse roles in DNA organisation and regulation of gene expression (Williams *et al.*, 1996; Ueguchi *et al.*, 1997). While it is clear that self-association of H-NS is mediated through the N-terminal 64 amino acids, the oligomeric state that H-NS adopts is the subject of considerable debate. Indeed, the oligomeric state of H-NS has variously been reported to predominately exist as dimers (Ueguchi *et al.*, 1997), trimers (Smyth *et al.*, 2000; Renzoni *et al.*, 2001) and tetramers (Spurio *et al.*, 1997; Ceschini *et al.*, 2000). The inconsistency of these reports is likely to be due to differing experimental conditions and methods of analysis. Indeed, Ceschini *et al.* (2000) have highlighted that H-NS oligomerisation *in vitro* is strictly dependent on the protein concentration, and strongly affected by temperature and buffering cations. Whatever the *in vivo* oligomeric state of H-NS, it is likely to self-associate through a

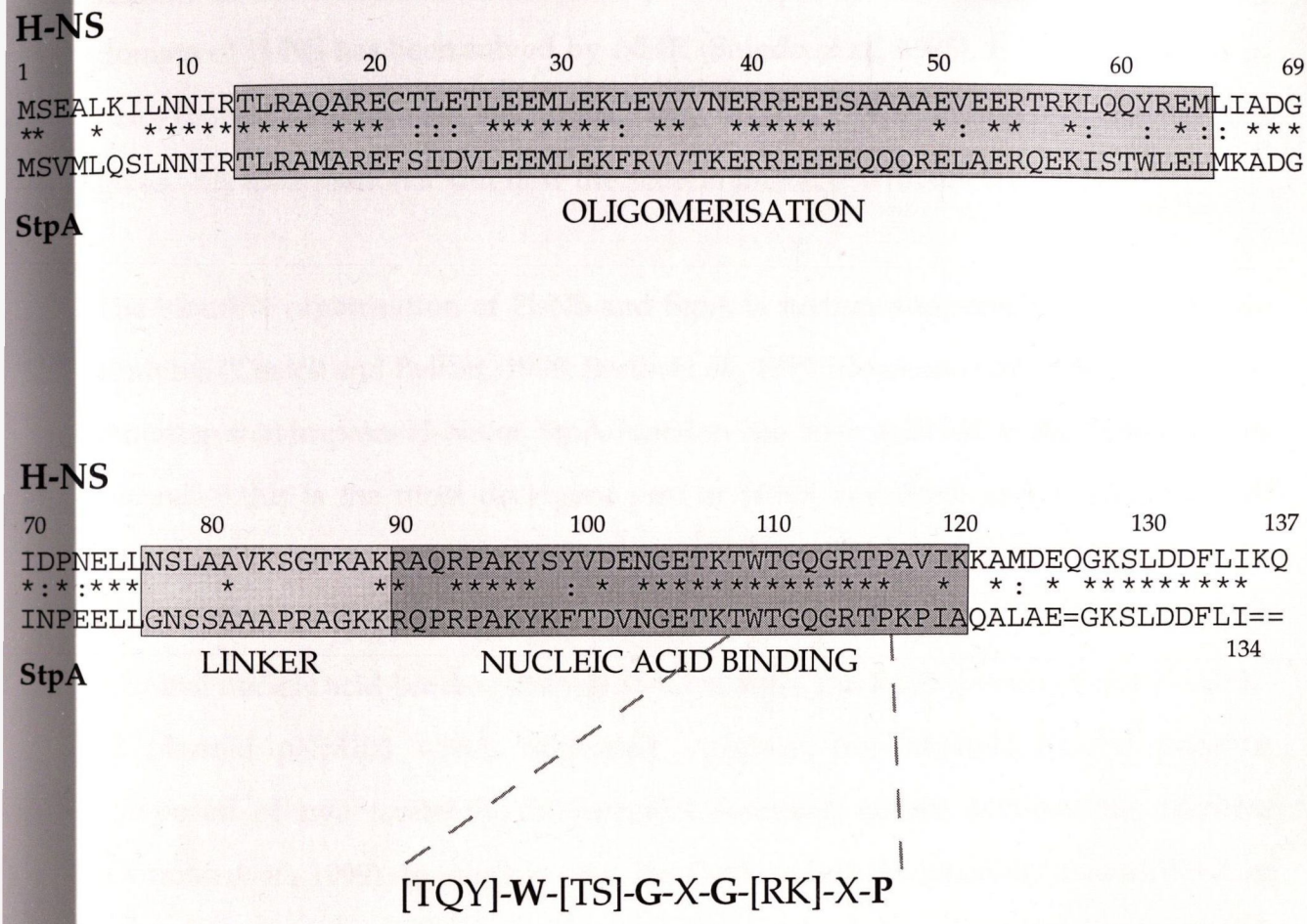

Fig. 1.4. Bipartite organisation of H-NS and StpA

Alignment of the H-NS and StpA protein sequences. An asterix symbol (*) between the sequences indicates residue identity; colons (:) indicate residue similarity. The two-domain organisation of StpA and H-NS is depicted with the oligomerisation domains and nucleic acid-binding domains separated by the linker region. The consensus sequence based on an alignment of 41 H-NS-like proteins (data not shown; protein names listed in Fig. 1.5) is indicated with conserved residues in boldface.

coiled-coil element (Renzoni *et al.*, 2001) which is an oligomerisation element in several transcription factors. A low resolution three-dimensional structure of a 47-residue N-terminal truncate of H-NS that incorporates the nucleic acid-interacting domain of H-NS has been solved by NMR (Shindo *et al.*, 1995). It adopts a mixed α-helix–β-sheet structure but has no similarity to other DNA-binding proteins and thus gives little information about how the protein interacts with nucleic acids.

The bipartite organisation of H-NS and StpA is further supported by phylogenetic analyses (Cusick and Belfort, 1998; Bertin *et al.*, 1999; Dorman *et al.*, 1999). Firstly, no mutation that impairs H-NS or StpA function has been selected in the linker region. Secondly, this is the most divergent part of H-NS and StpA and is composed of amino acids that commonly occur in other linkers (Dorman *et al.*, 1999). Thirdly, several plasmid- and pathogenicity island-encoded H-NS homologues possess the C-terminal nucleic acid-binding domain. For example, the KorB protein of the *E. coli* K-12 plasmid pKM101 which negatively regulates the conjugal mating pore, is composed of two tandemly duplicated, C-terminal, nucleic acid-binding domains (Dorman *et al.*, 1999). In another case, the Orf4 protein encoded on plasmid R446 of *E. coli* K-12, which modulates conjugation pilus expression, and an identical protein from plasmid pACM1 of *Klebsiella oxytoca* consist of a C-terminal nucleic acid-binding domain fused to an unrelated N-terminal domain. Similarly, the Ler protein encoded on the locus of enterocyte effacement (LEE) pathogenicity island of EPEC, which activates LEE transcription (Bustamante *et al.*, 2001; Sánchez-SanMartín *et al.*, 2001), and the Ler protein of EHEC contain the H-NS nucleic-acid-binding domain. These examples highlight that the C-terminal nucleic acid-binding domain of H-NS (and StpA) function independently, and suggest that domain switches and duplications have occurred in evolution.

1.8 H-NS-like proteins

Given this intriguing two-domain structure for the 137-residues and 134-residue H-NS and StpA proteins, respectively, and the functional diversity that H-NS-related

proteins possess, it was of interest to search for other homologues in the finished and unfinished genome sequencing databases found at the following websites:

http://www.ncbi.nlm.nih.gov/microb_blast/unfinishedgenome.html

http://www.genome.wisc.edu

Forty-one H-NS- and StpA-related proteins (Fig. 1.5) were identified using the BLASTP and TBLASTN programs (Altschul *et al.*, 1990). These proteins showed ~16% amino acid sequence identity with the entire H-NS or StpA protein sequences. However, this sequence identity is significantly greater over the C-termini of the proteins. Additionally, the theoretical analyses of these proteins using the 'Coils' software (http://www.isrec.isbsib.ch/software/COILS_form.html) suggest that their N-terminal domains are mainly α-helical and are predicted to adopt a coiled-coil structure. This configuration has been shown to mediate oligomerisation of H-NS (Smyth *et al.*, 2000, Renzoni *et al.*, 2001). Hence, the N-termini of the proteins are conserved at the level of function rather than sequence.

Curiously some bacteria encode three H-NS related proteins. For example, *Shigella flexneri* possesses H-NS and StpA proteins with 100% sequence identity at the amino acid level to *E. coli* H-NS and StpA proteins, and additionally has a third protein with 62% amino acid sequence identity with StpA, and 59% amino acid sequence identity with H-NS. This StpA-like protein is closely related (98.5% amino acid sequence identity) to a protein encoded on the *Salmonella typhi* plasmid pHCM1 (Fig. 1.5). Furthermore, UPEC strain CFT073 has three H-NS homologues. Again the H-NS and StpA protein are highly conserved (100% and 99.3% amino acid sequence identity respectively) with respect to those in *E. coli*. The third protein has 63% amino acid sequence identity with H-NS, and 52% amino acid sequence identity with StpA. However, no functional role has been assigned to these extra H-NS-related proteins.

It is interesting to note that when the relationship of the 41 H-NS- and StpA-like proteins is viewed as a phylogenetic tree (data not shown) or as a cladogram (Fig. 1.5), two sub-groups within the H-NS-family of proteins are discernable. One sub-

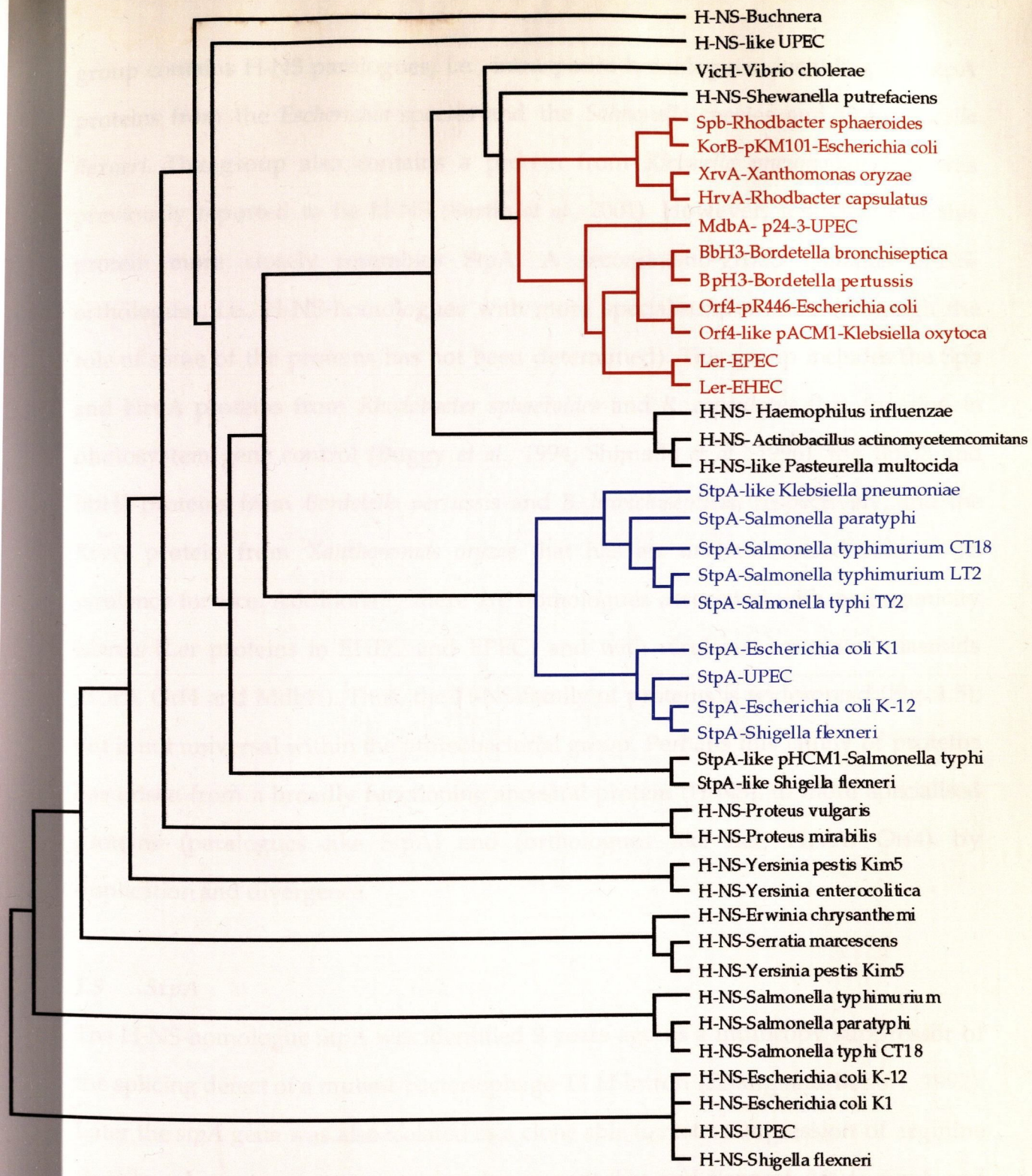

Fig. 1.5. Cladogram of H-NS- and StpA-like proteins

A cladogram showing the relationship among 41 identified H-NS- and StpA-like proteins obtained from finished and unfinished genome sequencing projects. The tree was created using the CLUSTALW program, then viewed and manually refined with the TREEVIEW software. Two sub-groups consisting of StpA proteins (intraspecies paralogues of H-NS; blue), and known or proposed H-NS-orthologues (red) are highlighted.

group contains H-NS paralogues, i.e., intraspecies homologues, including the StpA proteins from the *Escherichia* species and the *Salmonella* species and from *Shigella flexneri*. This group also contains a protein from *Klebsiella pneumoniae* that was previously reported to be H-NS (Bertin *et al.*, 2001). However, it is clear that this protein more closely resembles StpA. A second sub-group contains H-NS-orthologues, i.e., H-NS-homologues with more specialised functions (although the role of some of the proteins has not been determined). This group includes the Spb and HrvA proteins from *Rhodobacter sphaeroides* and *R. capsulatus* that function in photosystem gene control (Buggy *et al.*, 1994; Shimada *et al.*, 1996), the BpH3 and BbH3 proteins from *Bordetella pertussis* and *B. bronchisepticia*, respectively, and the XrvA protein from *Xanthomonas oryzae* that has an uncharacterised role in its virulence for rice. Additionally there are homologues associated with pathogenicity islands (Ler proteins in EHEC and EPEC) and with virulence associated-plasmids (KorB, Orf4 and MdbA). Thus, the H-NS-family of proteins is widespread (Fig. 1.5), but is not universal within the proteobacterial group. Perhaps this family of proteins has arisen from a broadly functioning ancestral protein (H-NS), to more specialised proteins (paralogues like StpA) and (orthologues like Ler, HrvA, Orf4) by duplication and divergence.

1.9 StpA

The H-NS-homologue StpA was identified 9 years ago as a multicopy suppressor of the splicing defect of a mutant bacteriophage T4 *td* intron (Zhang and Belfort, 1992). Later the *stpA* gene was also isolated as a clone able to restore repression of arginine decarboxylase gene expression in an *hns* mutant (Shi and Bennett, 1994). StpA and H-NS are 58% identical at the amino acid level and have a similar bipartite organisation (discussed in section 1.7.3; Fig. 1.4). Given this similarity it is no surprise that the paralogues have many overlapping biochemical activities. For example, both proteins preferentially interact with curved DNA in a sequence-independent manner (Zhang *et al.*, 1996; Sonnenfield *et al.*, 2001), restrain DNA supercoils, and inhibit transcription from a model promoter (Zhang *et al.*, 1996). Additionally StpA

and H-NS negatively cross-regulate the expression of each other's gene, and autoregulate their own expression (Sondén and Uhlin, 1996; Zhang *et al.*, 1996). The dominant effect is repression of *stpA* by H-NS, and thus the cellular content of H-NS is orders of magnitude greater than that of StpA (Free and Dorman, 1997; Johansson and Uhlin, 1999). This difference in expression is reflective in the growth rate and proteomic profile of *stpA*$^-$, *hns*$^-$ and *stpA*$^-$ *hns*$^-$ strains. A *stpA* mutant grows at a similar rate as a wild-type strain and there is little detectable effect in the proteome, whereas a *hns* mutant strain is slow growing and the expression of 60 proteins is affected (Zhang *et al.*, 1996; Hommais *et al.*, 2001). However, a *stpA hns* double mutant is more severely affected in growth rate and in its proteomic profile when compared to an *hns* mutant (Zhang *et al.*, 1996). These data suggest that StpA can substitute for some, but not all, of the phenotypes of *hns* mutants. Additionally, StpA and H-NS have functional differences, at least *in vitro*. The StpA protein is 10-times more efficient in RNA-related activities such as stimulating strand annealing of complementary RNA oligonucleotides, and in *trans*-splicing assays of the bacteriophage T4 *td* intron (Zhang *et al.*, 1995, 1996; Cusick and Belfort, 1998). StpA was also shown to be an RNA chaperone *in vivo* and able to resolve an exonic trap in the T4 bacteriophage *td* gene (Clodi *et al.*, 1999).

Therefore, it is possible that the physiological role of StpA could involve RNA transactions, perhaps under H-NS-derepressing or *stpA*-inducing conditions. As a first step to identifying a more independent role for StpA, Free and Dorman (1997) analysed the level of the *stpA* message under different environmental conditions. They showed that the *stpA* gene was only transiently expressed during exponential growth in LB broth, but was expressed at a more sustained level throughout exponential phase in minimal media in a Lrp-dependent manner. Furthermore, *stpA* expression was induced by raising the incubation temperature from 30°C to 37°C, and by osmotic stress, and was repressed by carbon starvation and DNA relaxation (Free and Dorman, 1997, Dorman *et al.*, 1999).

StpA could also affect cellular processes by forming heteromeric complexes with H-NS. Data from two-dimensional gel analysis indicate that certain genes require both StpA and H-NS for normal regulation (Zhang *et al.*, 1996). Although StpA and H-NS may act independently, the results would also be consistent with a StpA-H-NS heteromeric complex. Indeed, chemical cross-linking studies have shown that StpA and H-NS can heterodimerise both *in vitro* (Williams *et al.*, 1996) and *in vivo* (Johansson *et al.*, 2001), and that this interaction is necessary to protect the StpA protein from degradation by the Lon protease (Johansson and Uhlin, 1999; Johansson *et al.*, 2001). Moreover, an *in vivo* regulatory effect of such a StpA-H-NS heteromeric complex has recently been determined. The *bgl* operon, derepressed in an *hns* mutant, can be repressed by the amino-terminal domain of H-NS targeted to the promoter by the DNA-binding domain of StpA (Free *et al.*, 1998; Johansson *et al.*, 2001). This repression of *bgl* by truncated H-NS is dependent on a high-specificity interaction with StpA when there are low levels of the truncate. However, repression can be achieved in a StpA-independent manner when H-NS truncate levels are abundant (A. Free, M. E. Porter, P. Deighan, C. J. Dorman, In Press). Therefore, with differential expression and turnover of the H-NS and StpA proteins (Johansson and Uhlin, 1999), the levels of homomultimers and heteromultimers can be regulated, which can differentially affect cellular processes.

It is also possible that StpA and H-NS can interact with other proteins that share a similar N-terminal coil-coiled domain. This is particularly intriguing in light of the finding that *Shigella flexneri* and UPEC contain an extra H-NS-related gene (Fig. 1.5). Moreover, an unrelated protein shown to interact with H-NS is the Hha protein. An H-NS-Hha association has been shown *in vitro*, and significantly, the two proteins co-operate in regulation of the haemolysin operon in the recombinant haemolytic plasmid pANN2.2-312 *in vivo* (Nieto *et al.*, 2000). This is achieved via the formation of a novel nucleoid protein complex in the regulatory region.

Currently there are no examples of genes significantly (>1.7-fold) regulated by StpA alone. However, this is likely due to the low level of *stpA* expression in a wild-type stain grown under standard laboratory conditions. However, some genes are differentially regulated in an *hns*$^-$ strain (where *stpA* expression is induced) compared to a *stpA*$^-$ *hns*$^-$ strain. For example, both StpA and H-NS are necessary to stimulate expression of the stringently regulated genes such as *crp*, *fis* and the stable RNAs (Johansson *et al.*, 2000). This positive expression is mediated through an unusual DNA topology, where H-NS and StpA are proposed to maintain the stringently regulated promoters in a highly supercoiled conformation that is more efficiently transcribed. In another case, the translation of MalT, a positive regulator of the maltose regulon, is decreased in a *stpA hns* double mutant. However the exact mechanism of translation stimulation has not been determined (Johansson *et al.*, 1998).

1.10 The stress sigma factor

The product of the *rpoS* gene, RpoS or σ^s, is a σ-subunit of RNA polymerase and is the master regulator of the 'general stress response' in *E. coli* and other Gram-negative bacteria (reviewed in Hengge-Aronis, 1996, 2000; Loewen *et al.*, 1998). As σ^s functions predominately in response to certain stress conditions, its activity and cellular content has accordingly to be tightly controlled. Indeed, σ^s expression is regulated at the level of transcription, translation and protein stability (Lange and Hengge-Aronis, 1994; reviewed in Nogueira and Springer, 2000; Hengge-Aronis, 2000). This control over σ^s expression is exerted by *cis*–acting elements and more than 20 different *trans*-acting factors, including three small untranslated RNAs (Table 1.4).

σ^s acts to regulate the general stress response of *E. coli* by directing RNA polymerase towards a different set of genes. The RNA polymerase holoenzyme (E) containing σ^s (E σ^s) preferentially recognises an extended –10 promoter element with a cytosine nucleotide and a thymidine nucleotide at the –13 and –14 positions (Becker and

Table 1.4. Effectors of σ^s expression

Effector [a]	Selected reference
***rpoS* transcription**	
[b]Promoters *nlpD*P1, *nlpD*P2 and *rpoS*P	Lange *et al.* (1995)
BarA (+)	Mukhopadhyay *et al.* (2000)
Crr (-)	Ueguchi *et al.* (2001)
CRP-cAMP (-)	Lange and Hengge-Aronis (1994)
ppGpp (+)	Lange *et al.* (1995)
Homosrine lactone (+)	Huisman and Kolter (1994)
Inorganic polyphosphate (+)	Shiba *et al.* (1997)
***rpoS* mRNA structure/translation**	
[b]TIR –translation initiation region	Cunning *et al.* (1998)
Hfq (+)	Muffler *et al.* (1996)
H-NS (-)	Yamashino *et al.* (1995)
LeuO (-)	Klauck *et al.* (1997)
DnaK (+)	Muffler *et al.* (1997)
DsrA RNA (+)	Lease and Belfort (2000)
OxyS RNA (-)	Zhang *et al.* (1998)
HU (+)	Balandina *et al.* (2001)
RprA RNA (+)	Majdalani *et al.* (2001)
Crr (-)	Ueguchi *et al.* (2001)
CspC/CspE (+)	Phadtare and Inouye (2001)
UDP-glucose (-)	Böhringer *et al.* (1995)
σ^s proteolysis	
[b]Turnover element	Becker *et al.* (1999)
ClpXP (+)	Schweder *et al.* (1996)
RssB (+)	Zhou *et al.* (2001)

Table 1.4 continued

Effector [a]	Selected reference
σ^s proteolysis	
RssA (-)	Muffler *et al.* (1996)
H-NS (+)	Yamashino *et al.* (1995)
DnaK (-)	Muffler *et al.* (1997)
Acetyl phosphate (+)	Zhou *et al.* (2001)
LrhA (+)	Gibson and Silhavy (1999)

[a](+) and (-) indicate a positive or negative influence of the effector on *rpoS* transcription, *rpoS* mRNA stability/translation or σ^s turnover

[b]*cis*-acting elements

Hengge-Aronis, 2001). These nucleotides act as a discriminator region and contact specific amino acid residues in region 2.5 of σ^s that are not present in the corresponding region 2.5 in σ^{70}, the general sigma factor of *E. coli* (Becker and Hengge-Aronis, 2001). This allows E σ^s to redirect transcription towards signature promoters whose products confer stress-protective and adaptive functions. Nucleoid proteins such as H-NS, Lrp and IHF also confer sigma factor selectivity (Hengge-Aronis, 2000), perhaps via direct contact with σ^s or by modulating the architecture of the E σ^s-dependent promoter.

Examples of E σ^s-dependent proteins include (i) Dps, which protects DNA from oxidative damage, (ii) exonuclease III, a component involved in DNA repair, and (iii) UspB, a protein induced in response to many stresses and mediates σ^s-dependent resistance to ethanol (reviewed in Hengge-Aronis, 2000).

1.11 *Overview*

A crucial aspect of bacterial survival is the ability to adapt rapidly to fluctuations in the environment. To accomplish this bacteria must be able to sense these changes and react appropriately to alter the expression of the desired genes. Modulating the amount of the OmpF porin present in the outer membrane of *E. coli* is likely to be an integral component of bacterial adaptation to changing environments. Expression of the wide OmpF porin may be advantageous during times of starvation and facilitate bacteria to scavenge and import scarce nutrients. However, in an environment rich in toxic agents such as bile salts, OmpF porin expression is down-regulated, thereby slowing down the penetration of the harmful agents.

OmpF expression is reciprocally regulated with the OmpC porin by the EnvZ-OmpR two-component system at the transcriptional level. Additionally, the MicF antisense RNA modulates translation of the *ompF* message in response to information relayed from several regulatory circuits. The abundant nucleoid protein H-NS is one such protein that controls OmpF expression indirectly, by affecting the level of *micF* transcription. By two-dimensional gel analysis it was revealed that the H-NS-homologue StpA was also involved in modulating OmpF porin expression.

The aim of the work described here was to define the role for StpA in OmpF porin expression, and thereby to elucidate if the paralogous proteins StpA and H-NS affect *ompF* gene expression by similar or distinct mechanisms. This was achieved by a series of genetic and biochemical studies carried out *in vivo* (Chapter 3) and *in vitro* (Chapter 4). The expression of StpA was monitored in response to different environmental parameters, and the alternative sigma factor (σ^s), which is itself induced by stress conditions, was shown to require StpA for full expression (Chapter 5). In combination this work shows that StpA and H-NS are differentially expressed, and, importantly, that both paralogues modulate *ompF* porin gene expression by distinct mechanisms, the primary mechanism for StpA-dependent control involving RNA transactions.

Chapter 2

Materials and Methods

2.1 *Chemicals and growth media*

2.1.1 *Chemicals, reagents and radionucleotides*

All chemicals and reagents used in this study were purchased from BDH Chemicals Ltd, Bio-Rad, Clontech, Edge Biosystems, Fisons, Gelman Sciences, Gibco-BRL, Novagen, Pall, Pharmacia, Pierce, Promega, Qiagen, Roche Molecular Biochemicals, Sigma Chemical Company, New England BioLabs or Stratagene. DNA restriction and modifying enzymes were obtained from New England Biolabs or Roche Molecular Biochemicals. Radionucleotides were supplied by NEN Life Sciences. Custom automated sequencing was performed by MWG Biotech. In addition, several molecular biology 'kits' were used during this study. The basic principle of each kit is briefly described in the appropriate sections below, without giving an exhaustive protocol.

2.1.2 *Growth media*

Escherichia coli can grow rapidly in minimal media such as M9-broth which contains a carbon source (generally glucose which also acts as an energy source) and salts which supply nitrogen, phosphorus and other trace metals. From these starting materials the bacteria can make all the amino acids, nucleotide precursors, vitamins and other metabolites required for growth. In contrast, all of these are supplied in a rich broth such as Luria-Bertani (LB) broth.

Ingredients for preparing minimal or rich growth medium were obtained from Difco or Oxoid. All media were sterilised by autoclaving at 120°C for 20 min prior to use, or storage at room temperature. Additional solutions not suitable for autoclaving, e.g., amino acid or antibiotic solutions, were sterilised by filtration through 0.2 µm Acrodisc Filters (PALL). All quantities listed below are for the preparation of 1 litre of medium in distilled, deionised water (ddH_2O).

LB broth and LB agar plates

LB agar plates were used throughout this study for reviving bacterial strains from frozen stocks, general culturing of strains, and selection of transformants and transductants. Bacterial strains were routinely grown in Luria-Bertani (LB) broth unless otherwise stated.

LB broth: 10 g Oxoid tryptone, 5 g Yeast extract, 5 g NaCl

LB agar: 10 g Oxoid tryptone, 5 g Yeast extract, 5 g NaCl, 15 g agar

MacConkey Lactose agar plates

MacConkey Lactose agar plates were used to indicate the levels of β-galactosidase activity of bacterial colonies. A constituent of MacConkey base is phenol red, a pH indicator which turns red under acidic conditions. β-galactosidase-expressing colonies are a red colour due to the production of acidic metabolic products during the fermentation of lactose. In contrast colonies not expressing, or expressing very low levels of β-galactosidase are white or a pale pink colour.

MacConkey lactose agar: 40 g Difco MacConkey agar base, 10 g lactose, 15 g agar

LB-salicin agar plates

LB-salicin agar plates were used as an aid to confirm the *hns* status of bacteria by monitoring phospho-β-glucosidase activity. *hns*$^-$ strains allow derepression of the *bgl* operon and consequent production of phospho-β-glucosidase, an enzyme which catabolises aromatic β-glucosides such as salicin. Thus, colonies grown on salicin-containing plates in the presence of the pH indicator bromothymol blue are a yellow colour. Colonies where the *bgl* operon is silenced (*hns*$^+$) are blue. LB-salicin plates were prepared by adding to molten LB agar: 0.5% filter-sterilised salicin and 10 ml sterilised bromothymol blue stock solution {2% (v/v) bromothymol blue, 50% (v/v) ethanol and 0.2-N NaOH}.

M9 minimal medium

M9 minimal medium was prepared from a sterilised 10 x concentrate of M9 salts {60 g $Na_2HPO_4.7H_2O$, 15 g KH_2PO_4, 2.5 g NaCl and 5 g NH_4Cl L^{-1} ddH_2O (pH 7.4)}. One litre of medium: 100 ml of M9 concentrate, 2 ml 1-M $MgSO_4$, 100 µl 1-M $CaCl_2$, and 10 ml of 40% glucose.

Antibiotics, X-Gal and IPTG

All stock antibiotic solutions were stored in aliquots at –20°C and those prepared in water were sterilised by filtration through 0.2 µm Acrodisc Filters (PALL). Carbenicillin was prepared as a 100 mg ml^{-1} stock solution in ddH_2O and used in media at a concentration of 100 µg ml^{-1}. Kanamycin, spectinomycin and streptomycin were prepared as 50 mg ml^{-1} stock solutions in ddH_2O and used at a final concentration of 50 µg ml^{-1}. Tetracycline was prepared as a 10 mg ml^{-1} stock solution in 100% ethanol and used at a final concentration of 10 µg ml^{-1}. Chloramphenicol was prepared as a 20 mg ml^{-1} stock solution in 100% ethanol, and used at a final concentration of 20 µg ml^{-1}. Rifampicin was prepared fresh on day of use as a 250 mg ml^{-1} stock solution in 100% methanol and used at a final concentration of 250 µg ml^{-1}.

X-Gal (5-bromo-4-chloro-3-indoyl-β-D-galactoside), a chromogenic substrate for β-galactosidase was prepared as a 20 mg ml^{-1} stock solution in *N,N*-dimethyl formamide and stored in the dark at –20°C. X-Gal was used in agar plates at a final concentration of 20 µg ml^{-1}.

IPTG (isopropyl-β-D-thiogalactopyranoside), a gratuitous inducer of the *lac* promoter through inactivation of the LacI repressor, was prepared as a 100-mM stock solution in ddH_2O, filter sterilised, and stored at –20°C. IPTG was used at a final concentration of 0.5-mM in broth cultures to induce expression of *stpA*.

2.2 *Bacterial strains and culture conditions*

2.2.1 *Bacterial strains*

All bacterial strains used in this study were derivatives of *Escherichia coli* K-12 and are listed in Table 2.1. Bacterial strains were maintained as permanent stocks in 7.7% DMSO (dimethyl sulphoxide) in LB broth and stored at –70°C.

2.2.2 *Bacterial culture conditions*

While studying StpA-dependent OmpF expression (Chapter 3), bacterial cultures were grown overnight in 3 ml LB medium at 37°C with antibiotic selection, diluted to an optical density at 600 nm (OD_{600}) of 0.005 in 25 ml fresh LB broth in a 250 ml flask, and grown until an OD_{600} of ≈0.6 before harvesting.

To investigate the effect of environmental stimuli on the cellular content of StpA, H-NS or σ^s (Chapter 5), wild-type *E. coli* MC4100 was grown overnight in 3 ml LB medium at 37°C in a test tube with antibiotic selection. Following dilution to an OD_{600} of 0.005 in 200 ml fresh LB medium in a 2-L flask, growth was continued to an OD_{600} of ~0.3. The culture was then split into 25 ml aliquots in 250 ml flasks, which were treated directly with the desired environmental stress. These include a stress induced by an upward or downward shift in the temperature of the growth medium, hereafter referred to as thermal up-shock and down-shock, respectively, and stress induced by the addition of NaCl or ethanol to the growth medium, hereafter referred to as osmotic up-shock and ethanol shock, respectively. A stress was also induced by decreasing the osmolarity of the growth medium (hereafter referred as salt down-shock). To achieved this the 25 ml aliquots of culture were pelleted at 37°C, washed and resuspended in 25 ml of pre-warmed broth containing the required concentration of NaCl. When studying growth-phase regulation of StpA, H-NS or σ^s, strain MC4100 was grown overnight in either LB or M9 broth at 37°C in a test tube with antibiotic selection. Following dilution to an OD_{600} of 0.005 in 200 ml fresh LB or M9 broth in 2-L flasks, the cultures were incubated for up to 24 h

Table 2.1. **Escherichia coli** ***strains used in this study***

Strain	Relevant characteristics[a]	Reference / source
BGL1	CSH26 Δ(*pro-lac*) *ara thi* (λ*bgl-lacZ*)	Ohta *et al.* (1999)
BL21(DE3)	F⁻ *dcm ompT hsdS gal*	Studier and Moffatt (1986)
CJD1125	GM37 *hns2* Δ*stpA*::Tc^R	Free *et al.* (1998)
CJD1600	MC4100 Δ*stpA*::Tc^R	This work
CJD1601	MC4100 Δ*stpA*::Tc^R *hns-206*::Ap^R	This work
CJD1602	MH225 Δ*stpA*::Tc^R	This work
CJD1603	MH225 *hns-206*::Ap^R	This work
CJD1604	MH225 Δ*stpA*::Tc^R *hns-206*::Ap^R	This work
CJD1605	MH513 Δ*stpA*::Tc^R	This work
CJD1606	MH513 *hns-206*::Ap^R	This work
CJD1607	MH513 Δ*stpA*::Tc^R *hns-206*::Ap^R	This work
CJD1608	SM3001 Δ*stpA*::Tc^R	This work
CJD1609	SM3001 *hns-206*::Ap^R	This work
CJD1610	SM3001 Δ*stpA*::Tc^R *hns-206*::Ap^R	This work
CJD1612	MC4100 / pMicF	This work
CJD1613	CJD1600 / pMicF	This work
CJD1614	PD32 / pMicF	This work
CJD1615	CJD1601 / pMicF	This work
CJD1616	CJD1601 / pACYC184	This work
CJD1617	CJD1601 / pYCStpA	This work
CJD1618	CJD1601 / pAF201	This work
CJD1620	CJD1610 / pACYC184	This work
CJD1621	CJD1610 / pYCStpA	This work
CJD1622	CJD1601 / pAF201	This work
GM37	MC4100 φ (*proU-lacZ*⁺)	Higgins *et al.* (1988)
MC4100	F⁻ λ⁻ *araD139* Δ(*argF-lac*)*U169 rpsL150 relA1 flbB5301 deoC ptsF25 rbsR*	Casadaban (1976)

Table 2.1 continued

Strain	Relevant characteristics[a]	Reference / source
MH225	MC4100 *malQ7* ϕ(*ompC-lacZ*$^+$) 10-25	Hall and Silhavy (1979)
MH513	MC4100 *araD*$^+$ ϕ(*ompF-lacZ*$^+$) 16-23	Hall and Silhavy (1981)
PD32	MC4100 *hns-206*::Ap^R	Dersch *et al.* (1993)
SM3001	MC4100 Δ*micF1* Km^R	Matsuyama and Mizushima (1985)
TO26	BGL1 *hns*::Km^R *stpA*::Sp^R	Otha *et al.* (1999)
XL-1 Blue	*recA1 endA1 gyrA96thi-1 hsdR17 supE44 relA1 lac* [F′*proAB lacI*^{q}ZΔM15Tn*10*(Tc^R)]	Stratagene

[a]Antibiotic resistance markers are abbreviated as follows: Tc^R, resistance to tetracycline; Ap^R, resistance to ampicillin; Km^R, resistance to kanamycin; Sp^R, resistance to spectinomycin.

Table 2.1. **Escherichia coli *strains used in this study***

Strain	Relevant characteristics[a]	Reference / source
BGL1	CSH26 Δ(*pro-lac*) *ara thi* (λ*bgl-lacZ*)	Ohta *et al.* (1999)
BL21(DE3)	F⁻ *dcm ompT hsdS gal*	Studier and Moffatt (1986)
CJD1125	GM37 *hns2* Δ*stpA*::Tc^R	Free *et al.* (1998)
CJD1600	MC4100 Δ*stpA*::Tc^R	This work
CJD1601	MC4100 Δ*stpA*::Tc^R *hns-206*::Ap^R	This work
CJD1602	MH225 Δ*stpA*::Tc^R	This work
CJD1603	MH225 *hns-206*::Ap^R	This work
CJD1604	MH225 Δ*stpA*::Tc^R *hns-206*::Ap^R	This work
CJD1605	MH513 Δ*stpA*::Tc^R	This work
CJD1606	MH513 *hns-206*::Ap^R	This work
CJD1607	MH513 Δ*stpA*::Tc^R *hns-206*::Ap^R	This work
CJD1608	SM3001 Δ*stpA*::Tc^R	This work
CJD1609	SM3001 *hns-206*::Ap^R	This work
CJD1610	SM3001 Δ*stpA*::Tc^R *hns-206*::Ap^R	This work
CJD1612	MC4100 / pMicF	This work
CJD1613	CJD1600 / pMicF	This work
CJD1614	PD32 / pMicF	This work
CJD1615	CJD1601 / pMicF	This work
CJD1616	CJD1601 / pACYC184	This work
CJD1617	CJD1601 / pYCStpA	This work
CJD1618	CJD1601 / pAF201	This work
CJD1620	CJD1610 / pACYC184	This work
CJD1621	CJD1610 / pYCStpA	This work
CJD1622	CJD1601 / pAF201	This work
GM37	MC4100 ϕ (*proU-lacZ*$^+$)	Higgins *et al.* (1988)
MC4100	F⁻ λ⁻ *araD139* Δ(*argF-lac*)*U169 rpsL150* *relA1 flbB5301 deoC ptsF25 rbsR*	Casadaban (1976)

Table 2.1 continued

Strain	Relevant characteristics[a]	Reference / source
MH225	MC4100 *malQ7* ϕ(*ompC-lacZ*$^+$) 10-25	Hall and Silhavy (1979)
MH513	MC4100 *araD*$^+$ ϕ(*ompF-lacZ*$^+$) 16-23	Hall and Silhavy (1981)
PD32	MC4100 *hns-206*::Ap^R	Dersch *et al.* (1993)
SM3001	MC4100 Δ*micF1* Km^R	Matsuyama and Mizushima (1985)
TO26	BGL1 *hns*::Km^R *stpA*::Sp^R	Otha *et al.* (1999)
XL-1 Blue	*recA1 endA1 gyrA96thi-1 hsdR17 supE44 relA1 lac* [F′*proAB lacI*^{q}ZΔM15Tn*10*(Tc^R)]	Stratagene

[a]Antibiotic resistance markers are abbreviated as follows: Tc^R, resistance to tetracycline; Ap^R, resistance to ampicillin; Km^R, resistance to kanamycin; Sp^R, resistance to spectinomycin.

with samples harvested periodically. Every effort was made to ensure that growth and harvesting of bacteria for comparative experiments were done in an identical manner.

It is important to note that strains PD32 (MC4100 *hns*) and CJD1601 (MC4100 *stpA hns*) are prone to acquire secondary mutations to alleviate their slower growth defects. To help minimise this, all agar plates were kept at 4°C for no longer than 5 days and *hns* and *stpA hns* mutants were grown only in rich medium. Additionally, colony morphology, growth rates, and *bgl* phenotypes were strictly monitored.

2.3 *Plasmids and oligonucleotides*

2.3.1 *Plasmids*

Plasmids used in this study are listed in Table 2.2 together with relevant details and source. Any necessary details of plasmid construction will be described in the appropriate result chapters.

2.3.2 *Oligonucleotides*

The sequences, nomenclature and purpose of all oligonucleotides used in this study are listed in Table 2.3. Oligonucleotides were purchased from MWG-Biotech.

2.4 *Transduction with bacteriophage P1*

Throughout this study the temperate bacteriophage P1 *cml cI.100* (Sternberg and Maurer, 1991) was used to transduce bacterial DNA from a donor to a recipient *E. coli* strain. P1 *cml* encodes the temperature-sensitive Clr repressor, which is stable at 30°C and prevents lytic growth, but is unstable at 42°C. Hence, the transition from lysogeny to lytic growth can be induced by a temperature up-shock. The lytic cycle involves production of a bacteriophage-encoded nuclease that fragments the bacterial chromosome. Degradation of these fragments is slow and so they remain fairly large during the P1 lytic cycle. Occasionally, one of these large bacterial DNA

Table 2.2. Plasmids used in this study

Plasmid	Relevant characteristics[a]	Reference / source
pACYC184	P15A replicon, Cm^R Tc^R	New England Biolabs
pAF201	H-NS in pACYC184	A. Free
pAF311	*stpA*+ 6 histidine tag cloned downstream of IPTG-inducible T7 promoter in pBluescript. Ap^R	A. Free
pBADStpA	arabinose-inducible *stpA*	This work
pBADStpAH6	arabinose-inducible *stpA-His6*	This work
pBAD33	arabinose-inducible promoter	Guzman *et al.* (1995)
pBluescript II KS	routine cloning vector. Ap^R	Stratagene
pBR322	routine cloning vector. Ap^R	New England Biolabs
pDIA17	*lacI* repressor	P. Bertin
pHP45	Source of Ω Sm^R/Sp^R cassette	Prentki and Krisch (1984)
pMEP540	*hupA* riboprobe	M. Porter
pMicF	*micF* promoter cloned upstream of lacZ in pQFΩSm. Sm^R/Sp^R	This work
pM/C	*micF-ompC* promoter region in pBluescript KS. Ap^R	This work
pQF50	*lacZ* promoterless trap vector. Ap^R	Farinha and Kropinski (1990)
pQFΩSm	Ω Sm^R/Sp^R cassette interrupting β-lactamase gene in pQF50. Ap^S, Sm^R/Sp^R	This work
pSPT18	SP6/T7 *in vitro* transcription vector. Ap^R	Roche Molecular Biochemicals
pYCStpA	StpA in pACYC184	Williams *et al.* (1996)
p18ompF	*ompF* riboprobe	This work
p18ompC	*ompC* riboprobe	This work

Table 2.2 continued

Plasmid	Relevant characteristics[a]	Reference / source
p18micF	*micF* riboprobe	This work
p18rpoS	*rpoS* riboprobe	This work

[a]Antibiotic resistance markers are abbreviated as follows: Cm^R, resistance to chloramphenicol; Ap^R, resistance to ampicillin; Sp^R, resistance to spectinomycin; Sm^R, resistance to streptomycin.

Table 2.3. Oligonucleotides used in this study

Name	[a]Sequence 5′ – 3′	Purpose
blaH	GATGATAAGCTGTCAAACATG	*bla* promoter probe for EMSA
blaS	GGTTATTGTCTGATGAGCGG	*bla* promoter probe for EMSA
micF3	GGTGAATTCGCTATCATCATTAACTTTA	cloning *micF* riboprobe (*Eco*RI)
micF4	GACAAGCTTAAAAAAAACCGAATGCGAGG	cloning *micF* riboprobe (*Hin*dIII)
micF5	GTTATTAACCCTCTGTTATAT	*micF-ompC* promoter probe for EMSA and curved DNA analysis
micF6	CATGCCATGGTAGGGGTAAACAGACATTCA	cloning *micF-lacZ* fusion (*Nco*I)
		micF-ompC promoter probe for EMSA and curved DNA analysis
micF7	GGAAGATCTGTTATTAACCCTCTGTTATAT	cloning *micF-lacZ* fusion (*Bgl*II)
micF-T7-F	AAATTAATACGACTCACTATAGGCTATCATCATTAACTTTATTTT	*micF in vitro* transcription (T7 promoter)
micF-T7-R	AAAAAAAACCGAATGCGAGGCATCCGG	*micF in vitro* transcription
micFPE	TAGGGGTAAACAGACATTCAG	*micF* promoter mapping
ompC-T7-F	AAATTAATACGACTCACTATAGTTGCCGACTGATTAATGAGGG	*ompC in vitro* transcription (T7 promoter)
ompC-T7-R	CTTTGAAGCCAAGACGCATGTAGG	*ompC in vitro* transcription
ompF1	GTGATCGTCCCTGCTCTGTT	cloning *ompF* riboprobe

ompF2	CCAGTAGCCCACTGTTCAGC	cloning *ompF* riboprobe
ompF-T7-F	AAATTAATACGACTCACTATAGAGACACATAAAGACA CCAAACTCTC	*ompF in vitro* transcription (T7 promoter)
ompF-T7-R	GATCTACTTTGTTGCCATCTTTGT	*ompF in vitro* transcription
hnsN	ATGAGCGAAGCACTTAAAATT	*hns* DNA probe
hnsC	TTATTGCTTGATCAGGAAATC	*hns* DNA probe
rpoS2	CAGGAATTCCTGGACTTATCGAAGAGGG	cloning *rpoS* riboprobe (*Eco*RI)
rpoS3	CAGAAGCTTCTTCATATCGTCATCTTGCGTG	cloning *rpoS* riboprobe (*Hin*dIII)
stpANheI-F	CCTAGCTAGCTTTTTTTGTTTTGGCGTTAAAAGGT	cloning *stpA and stpA H6* under control of inducible promoter in pBAD33 (*Nhe*I)
stpASalI-R	ACGCGTCGACTTAGATCAGGAAATCGTCGAG	cloning *stpA* under control of inducible promoter in pBAD33 (*Sal*I)
stpAH6SalI-R	ACGCGTCGACCTAGTGATGATGATGATGATGGATCAG	cloning *stpAH6* under control of inducible promoter in pBAD33 (*Sal*I)
stpAN	ATCCGTAATGTTACAAAGTTTA	*stpA* DNA probe
stpAC	GATCAGGAAATCGTCCAGAGA	*stpA* DNA probe

[a]Underlined sequence represents restriction endonuclease cleavage site or T7 promoter sequence, as indicated in parenthesis in the Purpose column.

fragments (~100-kbp) can be packaged into the bacteriophage particle, instead of bacteriophage DNA. These transducing particles can represent between 0.3% and 6% of total bacteriophage particles in any P1 lysate. When a transducing particle attaches to a recipient bacterium, the DNA within the bacteriophage head is injected into the cell and is available for crossing over to the chromosome by homologous recombination.

2.4.1 *Preparation of a high titre P1* **cml** *lysate*

To prepare a P1 *cml* lysate the bacteriophage was firstly used to infect the donor strain (Cm^S), where injected P1 DNA circularises and remains as a free supercoiled DNA molecule. This host strain is now a lysogen. The P1 DNA is replicated in tandem with chromosomal replication and each daughter cell receives a P1 circle (prophage). A lysogen was made by incubating 100 µl of an overnight LB culture of the appropriate donor strain with 100 µl of the P1 *cml* lysate stock (grown on wild-type *E. coli* MC4100). To aid bacteriophage adsorption to bacterial cells 5-mM $CaCl_2$ was added and the mixture was incubated for 30 min at 30°C with aeration. This was then plated onto LB agar plates supplemented with chloramphenicol and incubated overnight at 30°C. Bacteriophage P1 is engineered so as to encompass a Tn*9* transposon encoding chloramphenicol resistance, thus allowing the identification of lysogens as chloramphenicol-resistant colonies.

A high titre lysate was prepared from the desired lysogen by a procedure detailed in Silhavy *et al.* (1984). Of an overnight culture of the lysogen (grown at 30°C with selection) 50 µl of was used to inoculate 10 ml of LB broth. The culture was grown for 90 min at 30°C with aeration (OD_{600} of ~0.1), and induction of the P1 lysogen achieved by incubation in a 42°C waterbath for 20 min. The culture was further incubated at 37°C for 90 min to allow completion of the lytic cycle, resulting in bacterial lysis and release of bacteriophage. To this 100 µl chloroform was then added and cellular debris pelleted by centrifugation at 5,000 r.p.m for 10 min at 4°C.

The supernatant containing the high titre lysate was transferred to a 13 ml Sarstedt tube and the lysate maintained sterile by the addition of 100 µl chloroform.

2.4.2 *Transduction with P1* cml

Genetic markers were moved to recipient *E. coli* strains using the bacteriophage P1 *cml* lysates (approximately 10^9-10^{10} bacteriophage ml^{-1}) according to Silhavy *et al.* (1984). The recipient strain was grown overnight in 5 ml of LB broth at 37°C. Cells were pelleted by centrifugation at 5,000 r.p.m for 5 min, and resuspended in 2.5 ml of sterile MC solution (10-mM $MgSO_4$, 5-mM $CaCl_2$). Recipient cells and bacteriophage were added to 5 tubes in the following ratios:

Tube no.	Volume recipient cells	Volume P1 *cml* lysate
1	100 µl	-
2	100 µl	10 µl
3	100 µl	50 µl
4	100 µl	100 µl
5	-	100 µl

The tubes were incubated in a 37°C waterbath for 30 min to permit bacteriophage adsorption to cells. To this 100 µl 1-M sodium citrate was then added followed by 1 ml of pre-warmed (37°C) LB broth. Sodium citrate is added to chelate the Ca^{2+} and Mg^{2+} ions, thus preventing loss of transductants by further reinfection of cells by virulent bacteriophage. Tubes were incubated for 60 min at 37°C to allow phenotypic expression of the transduced marker. Bacteria were then pelleted by centrifugation, resuspended in 100 µl of LB broth and spread onto appropriate selection plates for overnight incubation at 37°C. Plates corresponding to tubes 1 and 5 control for reversion, and bacterial contamination of the P1 *cml* lysate, respectively. Transductants from plates corresponding to tubes 2, 3 and 4 were single colony purified twice consecutively at 37°C, then tested for the presence of a stable lysogen by streaking onto LB agar plates with chloramphenicol and incubating at 30°C.

2.5 *Transformation of* E. coli *with plasmid DNA*

Plasmid DNA was transformed into *E. coli* by two different methods as described in Ausubel *et al.* (1990). Either *E. coli* cells were made competent by treatment with calcium chloride coupled with a heat-shock uptake of plasmid DNA, or transformation by electroporation, a high-voltage electroshock treatment. Greater transformation efficiencies can be achieved with electroporation (up to 10^{10} transformants μg^{-1} DNA; Ausubel *et al.*, 1990) than can be achieved with the $CaCl_2$ method (typically 5×10^6 transformants μg^{-1} DNA; Sambrook *et al.*, 1989). The $CaCl_2$ method is more cost effective and was routinely used for the transformation of plasmid DNA or ligation mixes. Electroporation was only sometimes used for transformation of precipitated ligation mixes where greater efficiency was required.

2.5.1 *Preparation of calcium chloride-competent cells*

An overnight culture of the strain to be made competent for transformation was used to inoculate 100 ml of LB broth and grown to an OD_{600} ≈0.2–0.4. The cells were pelleted by centrifugation at 3,500 r.p.m for 5 min, and the bacterial pellet resuspended in 100 ml of ice-cold 0.1 M $CaCl_2$. After incubation on ice for 30 min cells were again harvested as described above, and resuspended in 50 ml ice-cold 0.1-M $CaCl_2$. Following a 30-min incubation on ice, cells were again collected and resuspended in 2 ml of cold $CaCl_2$ solution (60-mM $CaCl_2$, 15% glycerol, 10-mM PIPES, pH 7). At this stage cells were distributed into 200 µl aliquots and used directly or snap-frozen on dry ice and stored at –70°C.

2.5.2 *Transformation of calcium chloride-competent cells*

DNA (0.1–1 µg) to be transformed, in a volume not exceeding 10 µl, was added to the 200 µl aliquot of competent cells and left on ice for 30 min, thus allowing the DNA to contact the bacterial surface. The tubes were then placed in a 42°C water bath for 2 min before returning to ice for 2 min. This heat-shock treatment allows uptake of the plasmid DNA through the $CaCl_2$-induced competent bacterial membrane by an unknown mechanism, and appears to temporarily inactivate

intracellular nucleases. Of LB broth 1 ml was added the culture, which was then incubated at 37°C for 1 h to allow phenotypic expression of the plasmid-borne antibiotic resistant marker. Subsequently, 10 µl and 100 µl samples of the transformation mix were plated onto appropriate selection plates. Cells to which no DNA had been added were treated in the same way and thus served as a control for contamination. Following overnight incubation at 37°C single colony transformants were purified on fresh selective agar plates.

2.5.3 *Preparation of electrocompetent cells*

Typically 100 µl of an overnight culture of the strain to be made electrocompetent for transformation was used to inoculate 100 ml of LB broth and grown to an OD_{600} ≈0.3-0.5. The cells were pelleted by centrifugation at 3,500 r.p.m for 5 min and the bacterial pellet resuspended in 100 ml of sterile, ice-cold ddH_2O. After 30 min incubation on ice, cells were again pelleted and resuspended in 100 ml cold ddH_2O and further incubated on ice for 30 min. Following another centrifugation step cells were resuspended in 10 ml of ice-cold 10% (v/v) glycerol, incubated on ice for 10 min, pelleted, and finally resuspended in 2 ml of cold 10% (v/v) glycerol. Aliquots (40 µl) were used directly or snap frozen on dry ice and stored at –70°C.

2.5.4 *Transformation of electrocompetent cells*

The DNA to be electroporated (50–200 ng in 2 µl sterile water) was added to the 40 µl aliquot of electrocompetent cells and incubated on ice for 2 min. The mixture was then transferred to a pre-chilled electroporation cuvette (EquiBio, 0.2 cm gap width). The cuvette was placed in the Gene Pulser chamber (Bio-Rad) and an electroshock delivered. To the cuvette 1 ml of pre-warmed LB broth was added and the contents transferred to a sterile tube and incubated at 37°C with aeration for 1 h. This incubation allows phenotypic expression of the antibiotic resistance marker. Subsequently, 10 µl and 100 µl of the transformation mix was plated onto appropriate selection plates. Cells to which no DNA had been added were treated in

the same way and thus served as a control for contamination. Following overnight incubation at 37°C transformants were single colony purified.

2.6 *Assays based on spectrophotometry*

2.6.1 *Monitoring bacterial growth*

The growth of bacterial cultures was monitored by measuring the optical density of the culture at a wavelength of 600nm (OD_{600}). For routine measurement of OD_{600}, including estimation of cell quantity for β-galactosidase assays (Section 2.5.4), 0.1–1.0 ml of the culture was transferred into a plastic disposable cuvette (Greiner) and brought to a final volume of 1 ml with LB broth or M9 broth as necessary. The OD_{600} value was measured in a spectrophotometer against a cuvette containing only LB broth or M9 broth. This value was linear in the range 0.1–0.6 and was multiplied by the dilution factor if necessary.

2.6.2 *Assessing quantity and purity of RNA*

For quantitative Northern blotting the concentration of RNA was determined by measuring the absorbance at 260 nm (A_{260}). RNA samples were diluted 1:333 in 1 ml diethylpyrocarbonate (DEPC) treated-ddH_2O (DEPC-treated ddH_2O). Samples were placed into a quartz cuvette and the A_{260} measured. The quartz cuvette was washed twice with DEPC-treated ddH_2O between samples, and each sample was measured in duplicate. The concentration of RNA was determined based on an A_{260} value of 1 = 40 μg ml^{-1} RNA, and calculated using the formula given below (Sambrook *et al.*, 1989). The purity of the RNA samples was assessed by measuring the A_{280}. For pure RNA uncontaminated by proteins or residual phenol, the ratio of A_{260} to $A_{280} \approx 2$.

$$\frac{40 \times A_{260}}{3} = \text{RNA Concentration } (\mu g\ \mu l^{-1})$$

2.6.3 *Determination of protein concentration by the Bradford assay*

Protein concentration was determined using a Bio-Rad Protein Assay which is based on the method of Bradford (1976), and measures the differential colour change (shift in absorbance from 465 to 595 nm) of Coomassie Brilliant Blue G-250 when protein binding occurs. The concentrations of His-tagged purified StpA and H-NS were calculated by measuring several serial dilutions of either protein. The resulting OD_{595} measurements were compared to a standard curve determined by measuring several known concentrations of lysozyme (similar MW to StpA and H-NS).

2.6.4 *Assay of β-galactosidase activity*

Transcriptional levels are routinely quantified by the β-galactosidase assay in which the *lac* genes are placed under the regulatory control of the promoter of a target gene. The transcription-regulating properties of the promoter are reflected in levels of the stable β-galactosidase enzyme, the product of the *lacZ* gene (Miller, 1992). In bacterial cells β-galactosidase cleaves the β-galactoside linkage of lactose, resulting in the formation of galactose and glucose. The resulting products, glucose and galactose then enter the glycolytic pathway. Several synthetic substrates such as ONPG (*o*-nitrophenyl-β-D-galactopyranoside) and X-Gal contain the β-galactoside linkage and thus can be hydrolysed by β-galactosidase. In the case of ONPG, which is colourless, cleavage results in the production of galactose, and *o*-nitrophenol, which is intensely yellow. Therefore, assaying the concentration of *o*-nitrophenol reports on the cellular level of β-galactosidase, which is determined by the activity of the target promoter.

The β-galactosidase assay used in this study was a modified, scaled-down version of that of Miller (1992). Bacterial culture (100 µl) to be assayed was transferred in duplicate into tubes containing 675 µl of Z-buffer, 50 µl of $CHCl_3$ and 25 µl of 0.1% SDS. Tubes were vortexed briefly to enhance permeabilisation and then incubated for 5 min at 28°C before addition of 150 µl of ONPG (4 mg ml^{-1} in ddH_2O). Incubation was continued until a straw yellow colour was obtained (typically corresponding to

an OD_{420} reading ≈ 0.1–0.6). The reaction was stopped with the addition of 375 µl 1-M Na_2CO_3, and the tubes were centrifuged at 14,000 r.p.m for 5 min to pellet cellular debris. Of the supernatant 1 ml was transferred into a plastic cuvette and the OD_{420} determined. The amount of β-galactosidase activity was expressed in arbitrary Miller units and calculated as follows:

$$\text{Miller units} = \frac{1000 \times OD_{420}}{t \times V \times OD_{600}}$$

t = Reaction time in min (from addition of ONPG to addition of Na_2CO_3)

V = Volume of cells added in ml.

Each assay was performed in duplicate, and the mean values were determined from at least 3 independent experiments. Unless otherwise indicated standard deviations were less than 10%.

Z buffer: {60-mM $Na_2HPO_4.2H_2O$, 40-mM $NaH_2PO_4.2H_2O$, 50-mM β-mercaptoethanol, 10-mM KCl, 1-mM $MgSO_4.7H_2O$ L^{-1} ddH_2O (pH 7)}

2.7 *Preparation of plasmid and chromosomal DNA*

2.7.1 *Small-scale isolation of plasmid DNA*

When analysing the outcome of putative cloning reactions plasmid DNA was routinely purified from *E. coli* strains using a variation of the alkali-lysis method described by Ausubel *et al.* (1990). A pellet from a 1.5 ml sample of an overnight culture was resuspended in 100 µl of solution I. Of freshly made solution II 200 µl was added and the contents mixed by inversion and incubated for 5 min on ice. Of solution III 150 µl was then added, the contents mixed, and the tube left on ice for 5 min. Debris was pelleted by centrifugation at 14,000 r.p.m for 5 min and the supernatant transferred to a tube containing 400 µl of 1:1 phenol:chloroform. Following vortexing the tube was centrifuged at 14,000 r.p.m for 2 min. The aqueous phase was transferred to a tube containing 20 µl 0.5% polyacrylamide and 1 ml of

cold ethanol. Plasmid DNA was precipitated, the pellet washed in 70% ethanol, dried and resuspended in 30 µl of ddH_2O containing 1 µl RNase–DNase free (Roche Molecular Biochemicals).

Solution I: {50-mM glucose, 25-mM Tris-HCl (pH 8.0), 10-mM EDTA}, resuspension buffer, EDTA will sequester divalent cations necessary for DNase activity.

Solution II: {0.2-N NaOH, 1% (w/v) SDS}, lysis buffer, denatures proteins and DNA.

Solution III: {60 ml 5-M potassium acetate, 11.5 ml glacial acetic acid, 28.5 ml ddH_2O}, neutralising buffer, proteins and chromosomal DNA precipitate, plasmid DNA re-anneals and remains in the supernatant.

2.7.2 *Small-scale isolation of high purity plasmid DNA*

The Wizard Plus *SV* Miniprep Kit (Promega) was routinely used to extract plasmid DNA from 3 ml of cultures according to the guidelines provided. The procedure is based on a modified alkaline-lysis method where bacteria are lysed and proteins denatured (SDS) in the presence of protease inhibitors. RNA is then degraded (RNase), and chromosomal and plasmid DNA denatured (NaOH). The lysis mixture is then neutralised with salts causing protein and chromosomal DNA precipitation. Plasmid DNA rapidly re-anneals and debris is pelleted by centrifugation. The supernatant containing plasmid DNA is washed and desalted through a mini-column and eluted in 100 µl ddH_2O.

When comparing pMicF plasmid copy number in wild-type, *stpA*, *hns* and *stpA hns* mutant backgrounds (Chapter 3), 7 ml samples of cultures were harvested at an OD_{600} of 0.6. The lysis step was carried out for an extra 5 min (10 min in total) to minimise potential interference of the different mutant strains lysing to differing degrees.

2.7.3 *Large-scale preparation of high purity plasmid DNA*

The Qiagen midi-plasmid purification kit was used to extract plasmid DNA from 100 ml overnight cultures of *E. coli* according to the guidelines provided. Purification is based on a modified alkaline-lysis procedure similar to that described in section 2.7.1, followed by binding of plasmid DNA to a column-based anion-exchange resin under low salt and pH conditions. A medium salt wash removes RNA, proteins, and other impurities, and the plasmid DNA is eluted with a high-salt buffer. The DNA is then precipitated with isopropanol, desalted, and resuspended in 100 µl ddH_2O.

2.7.4 *Purification of chromosomal DNA*

Purification of chromosomal DNA for Southern blot analysis was performed using the AGTC Bacterial Genomic DNA Purification Kit (Edge Biosystems). A 3-ml sample of an overnight culture was used for DNA extraction according to the guidelines provided. Briefly the procedure involves conversion of bacteria to sphaeroplasts (spherical cells from which most of the cell wall is removed) by incubation in a Tris-buffered solution containing lysozyme (cleaves peptidoglycan), sucrose (osmotic stress), and EDTA (chelates divalent metal ions that are necessary cofactors for protease and DNase activity). Efficient lysis is then achieved by heating to 65°C in the presence of SDS (protein denaturant), NaCl (osmotic shock) supplemented with RNase. Latex beads are added that bind and clump denatured proteins and cellular debris. The mixture is centrifuged (debris pellets) and chromosomal DNA is extracted from the supernatant by precipitation with isopropanol. Chromosomal DNA is desalted, dried and uniformly resuspended in a final volume of 100 µl ddH_2O.

2.8 *Manipulation of DNA in vitro*

2.8.1 *Restriction endonuclease cleavage of DNA*

Typically 0.5–2.0 µg of plasmid DNA or purified PCR product was cut with 10 U of restriction enzyme in a 30 µl volume containing the reaction buffer supplied with the

enzyme. For double digests involving simultaneous cleavage of DNA by two endonucleases, a suitable buffer was chosen in which both enzymes had >75% activity. Alternatively, double digests were performed sequentially in suitable buffers with ethanol precipitation of the DNA between digestions. Reactions were incubated at 37°C for 1–2 h unless otherwise recommended. Chromosomal DNA was digested overnight with 30 U of restriction enzyme in a 40 µl volume at 37°C.

2.8.2 *Phosphatase treatment of restriction endonuclease-cleaved DNA*

Cleavage of DNA by restriction enzymes leaves a 5′-protruding and 3′-recessive or 5′-blunt end phosphoryl groups on the DNA. These phosphoryl termini are required for formation of phosphodiester bonds between adjacent ends of DNA (inter- or intra-molecular). Consequently, removal of the 5′-phosphoryl group of vector DNA molecules prior to use in cloning reactions prevents self-ligation and decreases the vector background in cloning strategies. Alkaline phosphatase was used to dephosphorylate 5′-phosphoryl groups when a blunt-ended cloning was performed, or if cloning into a single restriction site. Vector DNA was digested with restriction endonucleases for 1–2 h and then 1 U of calf intestinal alkaline phosphatase (New England BioLabs) and 1 x dephosphorylation buffer (supplied with the enzyme) were added, and incubation at 37°C continued for an additional 60 min.

2.8.3 *Purification of linear DNA*

Linear DNA fragments (PCR products or cleaved DNA) were purified for cloning, or for the preparation of (labelled) probes, using the Wizard PCR Prep DNA purification system (Promega). The linear DNA fragments were purified directly, or from an agarose gel slice. For this, the DNA was electrophoresed through a 1 x TAE agarose gel containing 1 µg ml^{-1} of ethidium bromide. The desired DNA fragment was cut out using a surgical blade and purified following the guidelines supplied. Briefly, the procedure entails mixing DNA (from PCR reactions or a gel slice) in a buffer that provides the ions and environment where DNA is selectively bound with high affinity to a silica-based resin. The resin is then trapped in a mini-column and

macromolecules, primers, salts and other impurities removed by passing 80% isopropanol through the mini-column using a syringe. The resin is dried and DNA is eluted in ddH_2O.

2.8.4 *Ligation of DNA molecules*

T4 DNA ligase catalyses the ATP-dependent formation of phosphodiester bonds between adjacent 5′-phosphoryl and 3′-hydroxyl ends in double-stranded DNA. Bacteriophage T4 DNA ligase supplied with the Rapid DNA ligation Kit (Roche Molecular Biochemicals) was routinely used to clone digested insert DNA into appropriately digested vectors according to the manufacturer's directions. Reactions were performed by incubating an estimated molar ratio of purified vector:insert DNA (1:3 for sticky ends, 1:5 for blunt ends) in a 20 µl volume with 1 µl of T4 DNA ligase. DNA quantity was estimated by electrophoresing through a 1% TAE agarose gel and comparing band intensity to known standards. The mixture was incubated at room temperature for 30 min and typically a 10 µl sample was directly transformed into appropriate calcium-chloride-competent cells.

2.8.5 *Phenol extraction and ethanol precipitation of DNA or RNA*

Contaminating proteinaceous debris was removed from DNA and RNA solutions by phenol–chloroform extractions, and then concentrated by ethanol precipitation as detailed in Ausubel *et al.* (1990). For nucleic acid extractions an equal volume phenol–chloroform {1:1 v/v sodium acetate buffered phenol (pH 5.2)–chloroform} was mixed with the DNA or RNA sample (adjusted to a minimum volume of 400 µl if necessary), vortexed, and centrifuged for 30 sec at 14,000 r.p.m. The aqueous (top) layer was carefully removed and an equal volume of chloroform was added to remove traces of phenol. The contents were mixed and then separated by centrifuging at 14,000 r.p.m for 2 min. The DNA or RNA was concentrated by ethanol precipitation with linear polyacrylamide as carrier (Gaillard and Strauss, 1990). To the nucleic acid suspension 0.1 volumes of 3-M sodium acetate (pH 5.2), 5 µl of 0.05% polyacrylamide, and 2 volumes of 100% cold ethanol were added. The

contents were mixed and incubated on dry ice for 15 min before centrifugation at 14,000 r.p.m for 10 min. The pellet was washed in 200 µl of 70% ethanol, air-dried and resuspended in a suitable volume of ddH_2O.

2.9 *Polymerase Chain Reaction*

The polymerase chain reaction (PCR) was used for the amplification of DNA for preparation or confirmation of fragments during cloning strategies, and for generating probes for electrophoretic mobility-shift assays or southern blot analyses. The PCR method is based on the ability of a thermostable DNA polymerase to amplify DNA primed from oligonucleotides annealed to denatured single-stranded templates (Saiki *et al.*, 1988). The procedure involves thermal denaturation of the DNA template, thus allowing two specific oligonucleotides to hybridise to complementary sequences on opposite strands of the DNA flanking the sequence to be amplified. The annealed primers are orientated with their 3′-ends facing each other such that DNA polymerase in the presence of dNTPs and Mg^{2+} will extend across the region of the original DNA template between the primers. Each synthesised strand is complementary to one of the primers and can serve as template in further cycles of annealing and extension. The denaturation, annealing and extension steps are repeated for 25–35 cycles resulting in exponential amplification of the DNA region of interest.

2.9.1 *Amplification of DNA*

Two different thermostable polymerases were used in this study. *Taq* DNA polymerase (New England BioLabs) is a highly processive 5′–3′-DNA polymerase purified in recombinant form free of endo- or exo-nucleases. *Taq* polymerase lacks a 5′–3′ exonuclease activity (proof-reading) and was routinely used for PCR when it was unimportant if the product contained mutations, for example when checking plasmids for cloned inserts. *Pfx* polymerase (Gibco BRL) is also a highly processive 5′–3′-DNA polymerase free of endo- or exo-nucleases. *Pfx* harbours a 3′–5′ proof-reading exonuclease activity resulting in a reduced error rate of nucleotide

misincorporation. *Pfx* polymerase was used for the amplification of probes for electrophoretic mobility-shift assays, and for the amplification of DNA fragments for cloning purposes.

PCR reactions were carried out by mixing 5 µl 10 x *Pfx* buffer, 0.2-mM of each dNTPs, 100 pmol of each oligonucleotide, 1 U of *Pfx* polymerase, 1–3-mM $MgSO_4$, 10–100 ng template DNA and ddH_2O to a final volume of 50 µl in a 500 µl thin-walled PCR tube (Stratagene). PCR reactions using *Taq* DNA polymerase were performed as above, with the exception that 5 µl of 10 x *Taq* buffer (includes 1.5-mM $MgCl_2$) and 1 U of *Taq* polymerase were used. Reactions were set-up on ice and immediately placed into the Peltier Thermal Cycler. One tube contained no template DNA and served as a negative control. Routinely the reaction cycles were as follows:

1. 94°C, 2 min [denaturation]
2. oligo annealing temperature[a], 30 sec
3. 72°C, 1 min [extension[b]]
4. 94°C, 1 min [denaturation]
5. steps 2–4 above repeated, 30 cycles
6. 72°C, 10 min [final extension and renaturation]

[a]The annealing temperature was typically set at 5°C below the theoretical melting temperature (Tm) of the oligonucleotides being used. The Tm was calculated using the formula Tm = 2 x (A+T) + 4 x (G+C), where A, T, G and C refer to the base composition of the oligonucleotide.

[b]Extension time depended on expected length of PCR product (~1 min per kilobase).

DNA sequences were amplified from purified chromosomal or plasmid DNA. PCR amplification was also carried out using template DNA from a cell lysate. Here, a single colony was scrapped from the agar plate with a plastic tip and resuspended in 100 µl of ddH_2O, boiled for 5 min and 5 µl used for each PCR reaction.

2.10 *Southern blotting*

The basic principle of Southern blotting (Southern, 1975) involves digestion and separation of DNA by agarose gel electrophoresis. The DNA is then denatured *in situ* and transferred to nylon membrane. Immobilised DNA is hybridised with a Digoxigenin-(DIG) labelled probe that can be detected by a chemiluminescent immunoassay and revealed by autoradiography. This sensitive technique was used to confirm the genetic structure of *stpA* and *hns* insertional mutants of *E. coli* following P1 *cml*-mediated transduction.

Chromosomal DNA (1–2 µg) was cut overnight with an excess of appropriate restriction endonuclease(s) to ensure complete digestion and subsequently separated by electrophoresis through a 1% agarose gel for 4 h. The resolved DNA was then *in situ* depurinated, denatured, and neutralised, prior to overnight capillary transfer to Biodyne B nylon membrane (PALL) according to the method outlined in Sambrook *et al.* (1989). The *in situ* treatment of the DNA allows transfer to proceed more efficiently by cleaving larger fragments, and makes detection more sensitive by denaturing double-stranded DNA. DNA was immobilised on the membrane by UV-crosslinking.

A DIG-labelled probe was synthesised by polymerase chain reaction (Section 2.9) using the PCR DIG Labelling Mix (Roche Molecular Biochemicals). The mix contains 2-mM dATP, 2-mM dCTP, 2-mM dGTP, 1.9-mM dTTP and 0.1-mM DIG-11-dUTP. Of this 5 µl was added to a 50 µl volume PCR reaction instead of standard dNTP mix. The PCR products synthesised using primer pairs stpAN / stpAC, and hnsN / hnsC (Table 2.3) incorporate the DIG-labelled nucleotides. The labelled probes were purified as described in Section 2.8.3, and eluted in a 50 µl volume. Typically 10 µl was used per 10 ml hybridisation solution. Hybridisation and detection of probe bound to immobilised targets was carried out as outlined in Section 2.14.4 with the exception that probe was denatured by heating to 95°C for 10 min then incubated on ice for 10 min prior to use.

2.11 *DNA sequencing*

The nucleotide sequences of DNA fragments of interest were determined using the dideoxy chain termination method described by Sanger *et al.* (1977). The chain termination method utilises DNA polymerase to synthesise a complementary copy of a single-stranded DNA template primed from a specific annealed oligonucleotide. When the polymerase selects a deoxynucleotide analogue, dideoxynucleotide (ddNTP), for incorporation by base-pair matching to the template DNA, chain elongation is terminated. Chain growth depends on the formation of a phosphodiester bond between the 3′-OH group at the end of the growing primer and the 5′-phosphate group of the incoming deoxynucleotide (dNTP). ddNTPs are efficiently recognised by DNA polymerase but lack a 3′-OH, and consequently this prevents further chain elongation. This method of sequencing is designed such that in doing four separate reactions, a ddNTP (G, A, C or T) is introduced at every position of the complementary DNA corresponding to the template. Incorporation of [^{35}S]dATP in the reaction mixtures allows newly synthesised DNA to be labelled. Reactions are then electrophoresed side-by-side on a high-resolution denaturing polyacrylamide gel allowing the sequence to be read following autoradiography.

Plasmid denaturation, primer annealing, labelling and terminations reactions were carried out using the T7 Sequencing Kit (Pharmacia Biotech) according to the guidelines supplied. Qiagen-purified plasmid DNA pM/C (2 µg) (Table 2.2) and 20 pmol of oligonucleotide micFPE (Table 2.3) were used.

2.11.1 *Denaturing polyacrylamide gel electrophoresis*

The products from sequencing and primer extension reactions were separated by electrophoresis on 7.5-M Urea, 6% polyacrylamide gels in 1 x TBE buffer. The gels were prepared by mixing together 24 ml of SequaGel concentrate, 10 ml of SequaGel Buffer and 66 ml of SequaGel Diluent (National Diagnostic). To this 300 µl of 10% (w/v) ammonium persulphate and 50 µl of *N,N,N′,N′*-tetramethylethylene diamine (TEMED) were also added. TEMED serves to enhance the formation of free radicals

from ammonium persulphate. These free radicals in turn catalyse the polymerisation of acrylamide and the formation of bisacrylamide crossbridges between polyacrylamide chains. The polymerised gel was pre-run in 1 x TBE (prepared with DEPC-treated ddH_2O) at 70 W until the temperature of the gel had reached at least 50°C. Heating to this temperature and the presence of urea in the gel help maintain the sequencing reactions and primer extension products in a denatured state. Prior to loading, the 5-µl samples were heated at 90°C for 5 min. The gel was the run at 70 W for 90–120 min, dried under vacuum and exposed to X-ray film.

2.12 *Autoradiography*

In this study autoradiography was used to visualise and quantitate on X-ray film; (i) radio-emissions from molecules that incorporated [α-^{35}S]dATP, [γ-^{32}P]ATP, [α-^{32}P]dUTP (sequencing reactions, primer extension products and RNA gel shift assays); (ii) non-radioactive chemiluminescent emissions derived from alkaline phosphatase or horseradish peroxidase cleavage of chromogenic reagents (Northern, Southern and Western blots). In each case Hyperfilm-MP (Amersham) was used. When photon emissions (chemiluminescent or radiation) strike a silver halide crystal (X-Ray film is coated with silver halides suspended in gelatin), the crystal adsorbs energy and releases an electron. This electron is attracted to a positively charged silver ion forming an atom of metallic silver. After an appropriate time the film was placed into a tray containing diluted Kodak LX-24 X-Ray developer for 3 min, a chemical solution which amplifies the signal by reducing exposed silver halide crystals to metallic silver. The film was washed briefly in water and then fixed in Kodak Industrex liquid fixer for a further 3 min. The fixer serves to convert any silver halide that was not reduced into soluble silver thiosulphate. Developed films were rinsed in a large volume of water overnight. For quantitative analysis of signal intensity (Northern and Western blotting) several exposures of varying times were taken.

2.13 *Isolation of RNA*

RNA is a chemically unstable molecule and prone to digestion by ubiquitous RNases that require no cofactors to function and can maintain activity even after autoclaving or boiling. For these reasons certain precautions were used when isolating or handling RNA. These included wearing gloves, and using separate designated tips, tubes and electrophoresis tanks. All solutions were prepared with DEPC-treated ddH_2O (1 ml DEPC L^{-1} ddH_2O), mixed overnight then autoclaved. DEPC inactivates any RNases in the ddH_2O by covalent modification. In addition, where possible, all steps in the isolation of bacterial RNA or *in vitro* transcription reactions were performed quickly and on ice.

Total RNA was extracted from 7-ml samples of mid-exponential phase cultures (OD_{600} of 0.6) by the hot-phenol method similar to that described previously (Krieg, 1996). Cells were harvested by centrifugation and resuspended in 0.5 ml of boiling lysis buffer {2% SDS, 10-mM EDTA, 50-mM sodium acetate (pH 5.3)}. Hot phenol (0.5 ml, pH 5.3) was added, and the samples vortexed vigorously before incubation at *c.* 90°C for 5 min. After a 10 min incubation on ice the aqueous layer was extracted twice with 1:1 phenol:chloroform and once with chloroform and the RNA precipitated with ethanol at –70°C. Following resuspension RNA concentration and purity was assessed by A_{260} and A_{280} measurements as described in Section 2.5.2.

2.14 *Northern blotting*

The principle of Northern blotting is that a transcript within immobilised RNA can be quantified after hybridisation with a specific probe. This sensitive technique was used to investigate the relative level of abundance and stability of the *ompF*, *ompC*, *rpoS*, *hupA* and MicF RNA transcripts as a function of the presence or absence of StpA and H-NS. The procedure involves (i) resolution of the RNA sample by denaturing gel electrophoresis (Section 2.14.1), (ii) transfer of resolved RNA to nylon membrane (Section 2.14.2) and (iii) hybridisation and detection of the RNA with

labelled probes (probe synthesis described in Section 2.14.3, hybridisation and detection procedures described in Section 2.14.4).

2.14.1 Denaturing electrophoresis of RNA

RNA molecules can contain a high degree of secondary structure and are consequently electrophoresed under denaturing conditions. In this study the denaturant used was formaldehyde for agarose gel electrophoresis and urea for polyacrylamide gel electrophoresis. Long formaldehyde-containing agarose gels were used initially when analysing the specificity of a newly prepared riboprobe (RNA probe antisense to the transcript of interest prepared by *in vitro* transcription) in Northern analysis. If probe specificity was confirmed (i.e., no signal was visualised from a strain mutated for the gene of interest) and the transcript was of the expected size, then further agarose electrophoresis was done using pre-cast denaturing 1.25% Reliant agarose gels (FMC).

Agarose gels (1%) containing formaldehyde were cast by mixing 1 g agarose, 10 ml of 10 x MOPS, 73 ml of DEPC-treated ddH_2O in a clean conical flask. The agarose was dissolved and allowed to cool to 60°C and then 17 ml of 37% formaldehyde was added (gel concentration of formaldehyde is 6.3%). Samples of total RNA (5 µg) were denatured prior to loading in 3 volumes of denaturing solution (50% formamide, 1 x MOPS) at 70°C for 5 min, transferred to ice for 5 min, then loaded with 0.1 volumes of loading buffer. Gels were run in 1 x MOPS buffer at 100 V for 1–3 h. RNA samples for electrophoresing through Reliant agarose gels was prepared in an identical manner.

Separation and detection of the MicF RNA was best-achieved using 8% polyacrylamide gels containing 7.5-M urea. The gels were prepared by mixing together 3.2 ml of SequaGel concentrate, 1 ml of SequaGel Buffer and 5.8 ml of SequaGel Diluent (National Diagnostic). To this 100 µl of 10% (w/v) ammonium persulphate and 10 µl of TEMED were added to enhance acrylamide polymerisation.

Samples of total RNA (50 µg) were denatured in 3 volumes of denaturing solution {50% formamide, 1 x TBE} at 70°C for 5 min, transferred to ice for 5 min, then loaded with 3 µl loading buffer. Electrophoresis was carried out in a vertical gel tank (Bio-Rad) in 1 X TBE buffer at 100 V.

10 x MOPS: {41.85 g 4-morpholinepropanesulphonic acid (MOPS), 6.8 g Sodium acetate.3 H_2O, 20 ml 0.5-M Na_2EDTA, made to 1 L with DEPC-treated ddH_2O, pH 7.0}

10 x TBE: {108 g Tris, 55 g Boric acid, 40 ml 0.5-M Na_2EDTA (pH 8.0) made to 1 L with DEPC-treated ddH_2O}

Load buffer: {50% (v/v) glycerol, 1-mM EDTA (pH 8.0), 0.25% bromophenol blue}

2.14.2 *Transfer of RNA or DNA to nylon membrane*

For Northern blot analysis of RNA and in Southern blot analysis of DNA, samples, which had been resolved by agarose gel electrophoresis were transferred to nylon membrane by capillary transfer, while electroblotting was used to transfer RNA from polyacrylamide gels. Capillary transfer was performed according to the method outlined in Sambrook *et al.* (1989) and transfer was to Biodyne B Nylon membrane 0.45 µm (PALL). RNA electrophoresed through polyacrylamide gels was transferred to Biodyne B Nylon membrane using a Mini Trans-blot electrophoretic transfer Cell (Bio-Rad) at 100 V for 60 min in 1 x TBE. RNA was then fixed to the membranes by UV-crosslinking.

2.14.3 In vitro *transcription of riboprobes*

RNA probes (riboprobes) for use in Northern blot analysis were synthesised from plasmids p18ompC, p18ompF, p18micF and p18rpoS (Table 2.2) by *in vitro* transcription using the DIG RNA Labelling Kit (Roche Molecular Biochemicals) following the guidelines supplied. The fragment of DNA corresponding to the probe of interest was cloned into vector pSPT18. This plasmid has T7 and SP6 bacteriophage promoters either side of the multiple cloning site. The plasmid was

then linearised appropriately (defines length of probe) such that, following T7-based transcription, an antisense probe to the RNA transcript of interest is synthesised. The reaction is carried out in the presence of DIG-dUTP as a component of the dNTP mix and thus DIG-dUTP gets incorporated into the transcribed riboprobe.

2.14.4 *Hybridisation and detection of probe bound to immobilised targets*

Hybridisation and detection of DIG-labelled RNA or DNA probes (used for Southern blotting) were carried out following the detailed instructions in the DIG System User's Guide for Filter Hybridisation (1995). Briefly, the procedure involves overnight incubation of the probe with the nylon membrane at 68°C. Non-specific hybridised probe is removed by a series of stringency washes (decreasing salt concentration, increasing temperature). The membrane is then incubated with an Anti-DIG-alkaline phosphatase-antibody conjugate (Anti-DIG-AP-conjugate, Roche Molecular Biochemicals) that recognises the immobilised DIG moiety that was incorporated into the probe. In the presence of a suitable chemiluminescent substrate (CDP-Star, Roche Molecular Biochemicals), the alkaline-phosphatase-mediated enzymic dephosphorylation reaction results in a luminescent signal that visualises hybridised molecules by autoradiography (Section 2.10).

2.15 *Primer Extension*

MicF RNA can be transcribed from two promoters, resulting in an abundant 93-nt species and a less prominent 174-nt species in wild-type *E. coli* (Mizuno *et al.*, 1984; Andersen *et al.*, 1987). Primer extension analysis was used to investigate if there was StpA- or H-NS-dependent promoter preference for *micF* transcription initiation. The principle of primer extension is that a ^{32}P-labelled primer hybridises with its complementary RNA transcript. The addition of reverse transcriptase and dNTPs directs the synthesis of a DNA strand that is complementary to the RNA template. Extension stops when the 5'-end of the mRNA template is encountered resulting in a single-stranded DNA molecule of defined origin whose length is determined by the transcription start site of the RNA molecule. The start site is then identified by

electrophoresis of the synthesised cDNA alongside a DNA sequencing reaction that was generated using the same primer.

2.15.1 5′-end labelling of DNA using [γ^{32}P]ATP

Primer micFPE (Table 2.3) is complementary to a portion of MicF RNA 40-bp from the transcription start site of the 93-nt species and 121-bp from the start site of the proposed 174-nt species. The primer was labelled with [γ-^{32}P]ATP using bacteriophage T4 polynucleotide kinase (T4 PNK; New England BioLabs), which catalyses the transfer and exchange of a phosphate group from the γ-position of ATP to the 5′-hydroxyl terminus of the primer. To this 20 pmoles of micFPE (1 pmol μl^{-1}) was mixed with 50 μCi of [γ^{32}P]ATP (10 mCi ml^{-1}, 5,000 Ci mmol^{-1}), 3 μl of 10 x kinase buffer (supplied with enzyme) and 15 U of T4 PNK in a 1.5-ml screw-cap Eppendorf tube. The reaction was incubated for 30 min at 37°C. The labelled oligonucleotide was then precipitated with 3 μl 3-M sodium acetate (pH 5.2), 2 μl of 0.05% polyacrylamide and 90 μl of 100% ethanol on dry ice for 10 min. Following centrifugation, the pellet was washed with 70% ethanol, dried, and resuspended in 20-μl DEPC-treated ddH_2O (≈1 pmol μl^{-1}).

2.15.2 Primer-RNA annealing and cDNA synthesis

Total cellular RNA was isolated from mid-exponential phase cultures of wild-type strain MC4100, CJD1600 (MC4100 *stpA*), PD32 (MC4100 *hns*), CJD1601 (MC4100 *stpA hns*) and SM3001 (MC4100 *micF*) as described in Section 2.11.1. Approximately 30–50 μg of each RNA sample was mixed with 2 pmol of ^{32}P-labelled oligonucleotide micFPE (Table 2.3) and 40 U of RNase inhibitor (Gibco-BRL) in a final volume of 50 μl. RNA was denatured by incubating at 90°C for 5 min. The template and primer were annealed by cooling on ice for 15 min. Synthesis of cDNA was performed with the addition of the following to the template-primer reactions; {14 μl of ddH_2O, 1-mM each dNTP, 10-mM dithiothreitol, 20 μl of First Strand Buffer, 200 U of Superscript II RT reverse transcriptase (Gibco BRL)}. Reactions were incubated at 42°C for 90 min. RNA was then degraded by the addition of 50 U of RNase–DNase

free (Roche Molecular Biochemicals) for 30 min. The cDNA extension products were purified by phenol–chloroform and chloroform extractions and concentrated by ethanol precipitation (Section 2.8.5). The DNA pellets were resuspended in 6 µl of ddH_2O and 4 µl of PE loading dye. Extension products were analysed by denaturing PAGE (Section 2.11.1) alongside the DNA sequencing reactions.

5 x First Strand Buffer: {250-mM Tris-HCl (pH 6.8), 375-mM KCl, 15-mM $MgCl_2$}

PE loading dye: {95% (v/v) formamide, 20-mM EDTA, 0.05% (w/v) bromophenol blue, 0.05% (w/v) xylene cyanol FF}

2.16 *Gel mobility-shift analysis of RNA–protein interactions*

The association of purified StpA or H-NS, with *ompF*, *ompC* and MicF RNAs were analysed by gel mobility-shift assay. This procedure takes advantage of the decrease in electrophoretic mobility of an RNA when complexed with a protein, thus allowing bound and unbound RNA populations to be discriminated by non-denaturing polyacrylamide gel electrophoresis. Gel shift analyses were carried out by (i) preparation of RNA probes described in Section 2.16.1, and (ii) formation and separation of StpA:RNA and H-NS:RNA complexes described in Section 2.16.2.

2.16.1 **In vitro** *synthesis of labelled RNA*

Specific RNA targets were synthesised by *in vitro* transcription reactions with T7 RNA polymerase using PCR products as templates. The T7 promoter sequence (5′-TAATACGACTCACTATAG-3′) was designed to be the 5′-end of primers micFT7-F, ompFT7-F, ompCT7-F (Table 2.3). With appropriate 3′-end primers (Table 2.3), a 93-nt *micF*, 213-nt *ompF* and 268-nt *ompC* (starting from respective major +1 transcription initiation sites) templates were amplified by PCR and thus flanked by the T7 promoter sequence. PCR products were purified as described in Section 2.8.3.

Approximately 200 ng of *micF*, *ompF* and *ompC* templates were used for *in vitro* transcription reactions with T7 RNA polymerase. The 30-µl reaction mixture

contained 3 µl of 10 x transcription buffer, 1 µl of RNase inhibitor (Gibco-BRL), 13 µl of DEPC-treated ddH_2O, 2 µl of rUTP (0.65-mM final concentration), 1 µl of [α-^{32}P]dUTP (NEN), 3 µl of rGTP-rATP-rCTP mix (each 1-mM final concentration) and 2 µl of T7 RNA polymerase (New England BioLabs). The reaction was incubated for 2 h at 37°C. Template DNA was degraded by addition of 1 µl (40 U) DNaseI–RNase free (New England BioLabs) for 30 min. Synthesised RNA was purified by phenol–chloroform and chloroform extractions followed by ethanol precipitation (Section 2.7.5). Cold RNA was synthesised in a similar manner with the exception that rUTP was used at a final concentration of 1-mM and [α-^{32}P]dUTP was omitted.

2.16.2 Formation and separation of RNA–protein complexes

Labelled *ompF-213*, *ompF-268* and MicF RNAs (3 ng) were used for each 15-µl reaction in 1 x BS buffer {40-mM HEPES (pH 8.0), 100-mM potassium glutamate, 10-mM magnesium aspartate, 0.022% NP40, 0.1 mg ml^{-1} BSA}. tRNA (300 ng, 100-fold excess) was included as non-specific competitor. This buffer was chosen as both StpA and H-NS are proficient for nucleic acid binding and oligomerisation under these conditions (Bertin *et al.*, 1999). Two other buffers were tested. However, the StpA-RNA and H-NS-RNA interactions were slightly more efficient in this buffer (data not shown). RNA probes were firstly denatured by heating to 65°C for 5 min and then cooled to 37°C. His-tagged purified StpA (1 µl, purification described in Section 2.20) or H-NS (a generous gift from S. Rimsky) was added to the reactions in a series of 2-fold dilutions {200 ng (0.82 µM), 100 ng (0.41 µM) or 50 ng (0.20 µM)}. One tube contained no protein but instead 1 µl of storage buffer was added (the same buffer used for protein dilutions). Tubes were incubated at 37°C for 10 min. Prior to electrophoresis 4 µl 50% glycerol was added to each tube.

Native polyacrylamide gels (10%) were used to resolve RNA and RNA:protein complexes. They were prepared by mixing together 2.5 ml of 10 x TBE, 16.6 ml of Protogel (National Diagnostic), 2.5 ml of 50% glycerol and 26.9 ml of DEPC-treated ddH_2O. To this 500 µl of 10% (w/v) ammonium persulphate and 50 µl of TEMED

were added to enhance acrylamide polymerisation. The contents of the gel-shift reactions were loaded and electrophoresed for 6 h at 100 V in 0.5 x TBE. Protein:RNA complexes were found to be stable whether the gels were migrated at 4°C or at room temperature; electrophoresis was routinely performed at room temperature.

StpA storage buffer: {350-mM NaCl, 50-mM Tris-HCl (pH7.9), 1-mM EDTA, 0.5-mM DTT, 0.1-mM PMSF, 30% glycerol}

2.17 *Formation of the* MicF–ompF *duplex*

The 93-nt MicF antisense RNA is proposed to form an RNA–RNA duplex with *ompF* mRNA via a 25-bp complementary region (Fig. 4.1). The MicF RNA–*ompF* mRNA duplex was formed *in vitro*. The 93-nt MicF RNA and the 213-nt 5′-end of the *ompF* mRNA were synthesised and labelled by *in vitro* transcription as described in Section 2.16.1. The RNAs were annealed by incubation in a buffer containing 50-mM Tris-HCL (pH 7.5), 5-mM $MgCl_2$, and 25-mM KCl (TMK, a physiological buffer used in the isolation of ribosomes). Initially duplex formation was performed by adding an increasing amount of the *ompF* transcript with a fixed amount of MicF RNA (6 ng). RNAs were denatured by heating to 65°C followed by cooling to 37°C. The RNAs were maintained for 60 min at 37°C for renaturation and duplex formation. Two tubes contained only MicF RNA or *ompF-213* mRNA in TMK buffer and served as markers for RNA migration. Under these conditions duplex formation was best achieved when there was an excess of *ompF-213* mRNA. Subsequently, further experiments were carried out with a 3-fold excess of labelled *ompF-213* mRNA. Annealed (slower-moving) complexes were separated from non-duplexed RNA by migration through 5% native polyacrylamide gels (prepared as in Section 2.16.2 with 8.33 ml of Protogel and 36.2 ml of ddH_2O) for 15 h at 4°C in 0.5 x TBE. The MicF–*ompF-213* RNA duplex was stabilised by migration at 4°C.

2.18 *Effect of StpA on MicF–ompF-213 RNA duplex formation*

StpA is an RNA chaperone and has a role in OmpF porin expression involving MicF RNA. Therefore, the influence of StpA on MicF–*ompF-213* RNA duplex formation was analysed *in vitro*. The 93-nt MicF RNA (~6 ng) and the 213-nt *ompF* RNAs (~3-fold molar excess) were incubated in a 15 µl volume in TMK buffer, heated to 65°C, then slowly cooled to 37°C. To the tubes 1 µl of His-tagged purified StpA was added in a series of 2-fold dilutions {100 ng (0.40 µM), 50 ng (0.20 µM), 25 ng (0.10 µM)}. One tube contained no protein but instead 1 µl of StpA storage buffer (Section 2.14.2) was added, the same buffer used for protein dilutions. Two tubes contained only MicF RNA or *ompF-213* mRNA in TMK buffer and served as markers for RNA migration. Tubes were incubated for 1 h at 37°C and resolved by electrophoresis through 5% native polyacrylamide gels as described in Section 2.16.

In this assay a low concentration of StpA and a high concentration of RNA transcripts were used. This was to prevent all of the RNAs being sequestered in protein:RNA complexes leaving none available for duplex formation. Even at the highest concentration used (0.40 µM), there was no detectable up-shift of either *ompF-213* or MicF RNAs. It should be noted that TMK buffer was as suitable for StpA:RNA interactions as BS buffer (data not shown).

2.19 *Gel mobility-shift analysis of DNA–protein interactions*

The association of purified StpA with the *micF–ompC* promoter region was analysed by gel mobility-shift assay. A 448-bp *micF–ompC* probe was amplified by PCR with *Pfx* polymerase (Gibco-BRL) using oligos micF4 / micF5 (Table 2.3), and *E. coli* MC4100 chromosomal DNA as template. A 200-bp curved *bla* promoter region (a positive control for StpA binding, Bertin *et al.*, 1999) was similarly amplified using the primer pair blaH / blaS and plasmid pBR322 as template. Amplified probes were purified as detailed in Section 2.8.3, and labelled as described above in Section 2.15.1. Approximately 5 ng of probe was incubated with increasing concentrations of His-tag purified StpA (Section 2.20) from 0–100 ng (0–0.62 µM) for 15 min at room

temperature in 10-µl reaction cocktail containing 40-mM HEPES (pH 8), 100-mM potassium glutamate, 10-mM magnesium aspartate, 0.022% NP40, 0.1 µg ml^{-1} BSA, and 10% glycerol. Protein-DNA complexes were resolved by electrophoresis through an 8% polyacrylamide gel for 6 h at 4°C. The gel was dried and examined by autoradiography.

A second procedure was used which included an excess of competitor DNA (Bertin *et al.*, 1999). Plasmid pRR322 was digested into 8 fragments with *Taq*I and *Ssp*I restriction enzymes. One restricted fragment is 217-bp and contains the sequence of the curved *bla* promoter. The *micF–ompC* promoter region was amplified and purified as a 404-bp PCR product using primer pair micF5 / micF6 (Table 2.3). This probe and digested pBR322 were incubated with 0–200 ng (0–1.24 µM) StpA in the reaction buffer described above. The products were electrophoresed through 3% molecular screening agarose (Roche Molecular Biochemicals) for 5 h at 100 V. The gel was stained with 1 µg ml^{-1} ethidium bromide and viewed under UV illumination.

2.20 *Purification of StpA*

Plasmid pAF311 (Table 2.2) is a pBluescript-based plasmid which harbours a C-terminal six histidine fusion to the *stpA* gene cloned downstream of the T7 polymerase promoter. Induction of *stpA* expression was done in strain BL21(DE3)/pDIA17. *E. coli* strain BL21(DE3) (Table 2.1) contains phage T7 gene *1* (gene coding for T7 RNA polymerase) under the control of the *lacUV5*-inducible promoter. This construct was integrated at the λ*att* site using the lambda cloning vector DE3 (Studier and Moffatt, 1986). In addition, strain BL21(DE3) is deficient in the OmpT and Lon proteases. Plasmid pDIA17 (Table 2.2) encodes the LacI repressor that completely silences the *lacUV5* giving tight control over *stpA* induction. Upon addition of the gratuitous inducer IPTG, the LacI-mediated repression of the *lacUV5* promoter is effectively removed and T7 RNA polymerase is produced. T7 RNA polymerase then initiates selective transcription from the plasmid-borne T7 promoter sequence upstream of the *stpA* gene.

One litre of culture was grown at 30°C to mid-exponential phase in LB broth and *stpA* expression induced by addition of 0.5-mM IPTG for 2 h. Cells were pelleted by centrifugation and resuspended in binding buffer {60-mM imidazole, 500-mM NaCl, 20-mM Tris-HCl (pH 7.9), 1-mM PMSF} supplemented with 200 μg ml^{-1} lysozyme. The mixture was frozen on dry ice and left at –20°C overnight. After thawing complete lysis was achieved by sonication. Cell debris was pelleted by centrifugation for 10 min at 14,000 r.p.m and the soluble extract (15 ml) retained.

StpA purification from the crude extract was performed by metal affinity chromatography using the His-Bind Kit (Novagen). The His-Bind resin within the column contains immobilised Ni^{2+} ions that can retain the His-tag sequence by electrostatic interaction. Imidazole serves as a competitor with histidine (His-tag) for the Ni^{2+} ions and therefore an increasing concentration of imidazole will elute the target protein from the column.

The soluble extract was passed over a pre-equilibrated His-Bind 900 column (Novagen). The column was washed with binding buffer and then with wash buffer {100-mM imidazole, 0.5-M NaCl, 20-mM Tris-HCl (pH 7.9), 1-mM PMSF} to remove proteins weakly associated with the resin. StpA-H6 was recovered by elution with 500-mM imidazole and was estimated to be 70% pure by SDS-PAGE (see below) followed by Coomassie staining (Section 2.21.1). Impurities were further removed by re-passing the fractions containing StpA-H6 over another His-bind 900 column. After washing StpA-H6 was again eluted with 500-mM imidazole and judged to be ~98% pure by SDS-PAGE followed by Coomassie staining. Purified StpA was dialysed into storage buffer {350-mM NaCl, 50-mM Tris-HCl (pH 7.9), 1-mM EDTA, and 0.5-mM DTT, 0.1-mM PMSF, 30% glycerol} and stored in aliquots at –20°C.

2.21 *SDS-PAGE*

Proteins were separated by discontinuous 12% polyacrylamide gel electrophoresis as described in Sambrook *et al.* (1989). The discontinuous buffer system uses buffers of

different pH and composition in the stacking and separating gels. Consequently protein migration through the large pores in the stacking gel (5% acrylamide) is fast and the proteins become concentrated into a narrow band. However, migration through the narrow pores of separating gel (12% acrylamide) is according to size. Both gels were prepared with 0.1% SDS. Since most proteins bind SDS in a constant weight ratio, this leads to identical charge densities for denatured proteins. Hence proteins migrate according to size not charge.

A 12% separating gel was prepared by mixing 2 ml of Protogel (National Diagnostics) 1.25 ml 1.5-M Tris-HCl (pH 8.8), 50 µl of 10% SDS, and 1.7 ml of ddH_2O. Immediately prior to pouring, 50 µl of 10% (w/v) ammonium persulphate and 5 µl TEMED were added to the gel mix to promote polymerisation. The separating gel was then overlaid with 200 µl propan-2-ol (excludes oxygen) and allowed to polymerise for 30 min. The stacking gel was made by the mixing of 0.833 ml of Protogel (National Diagnostics), 1.25 ml 0.5 M Tris-HCl (pH 6.8), 50 µl of 10% SDS and 2.87 ml of ddH_2O. The gel was electrophoresed in 1 x Tris-glycine running buffer {25-mM Tris-HCl, 250-mM glycine (pH 8.3), 0.1% (w/v) SDS}. Prior to loading 10 µl total cell protein extracts (Section 2.24.1) were denatured at 90°C for 10 min. Electrophoresis was performed at 150 V for 60–90 min.

2.21.1 *Staining of proteins*

Gels were washed in ddH_2O prior to staining with GelCode Blue Stain Reagent (Pierce) for 1 h according to the guidelines supplied. Gels were then destained in ddH_2O. This stain uses the colloidal properties of Coomassie G-250 for protein binding and staining but has no affinity for the polymerised gel.

2.22 *Preparation and analysis of outer membrane fractions*

The outer membranes of *E. coli* were prepared by differential extraction with *N*-laurylsarcosine (Sarkosyl) using a modified procedure to those described by Nikaido (1994). The principle is based on the ability of this detergent to disaggregate and

solubilise proteins and other components of the cytoplasmic membrane in a bacterial lysate. In contrast, as Sarkosyl has a similar charge density per surface area as lipopolysaccharide (LPS), i.e., mimics LPS, it does not disaggregate the LPS-based outer membrane.

A Sarkosyl-insoluble fraction containing the outer membranes was prepared from mid-exponential phase cultures (OD_{600} = 0.6) as follows: 20-ml samples of culture were harvested, washed and resuspended in 0.6 ml of ice-cold sonication buffer {10% sucrose, 50-mM Tris-HCl (pH 7.5), 100-mM NaCl, 1-mM EDTA, 5-mM dithiothreitol} and incubated with 200 μg ml^{-1} lysozyme on ice for 20 min. Complete lysis was achieved by sonication and cellular debris cleared by centrifugation at 10,000 r.p.m for 5 min. The supernatant was then incubated with 0.5% Sarkosyl for 30 min at room temperature. The insoluble outer membrane fraction was harvested by centrifugation at 18,000 r.p.m for 30 min and resuspended in 100 μl of 1 x final sample buffer. Samples (15 μl) were boiled and then separated by 8-M urea–12% SDS-PAGE (Section 2.21) for 95 min at 150 V (the presence of urea in the gel aids in the disaggregation and subsequent separation of the hydrophobic trimeric porins). Gels were stained with GelCode Blue Stain Reagent (Pierce).

2.23 *StpA antiserum*

Immunising a New Zealand White rabbit with His-tagged purified StpA generated antibodies specifically reactive against StpA. The initial injection was with 300 μg of StpA solubilised in Freund's complete adjuvant. Two further boosts were administered at two weekly intervals each with 300 μg of protein in Freund's incomplete adjuvant. The generation of anti-StpA antibodies was monitored by Western immunoblotting, and after a primary test bleed when the titre was revealed to exceed 1:5000 the rabbit was exsanguinated. The resulting serum was absorbed against the *E. coli* strain CJD1600 (MC4100 Δ*stpA*) lysate. The lysate was prepared by harvesting 100 ml of culture at OD_{600} = 1. This pellet was resuspended in 1 ml of sonication buffer and lysis achieved by 3 cycles of freeze-thaw, sonication, and finally

boiling for 10 min. Of this serum 500 µl was absorbed overnight at 4°C against an equal volume of the lysate. Insoluble material was removed by centrifugation at 14,000 r.p.m for 30 min. The supernatant was retained and stored in aliquots at –20°C and used at a 1:1000 dilution in Western immunoblot analysis.

2.24 *Western immunoblot analysis*

Western immunoblottng is a sensitive technique whereby proteins (antigens) are (i) solubilised with SDS and β-mercaptoethanol (Section 2.24.1) and separated by SDS-PAGE (Section 2.21), (ii) irreversibly transferred to nitrocellulose membrane (Section 2.24.2), (iii) the membrane is incubated with primary antibody, and the antigen–antibody complexes detected with a secondary antibody and revealed by a chemiluminescent assay (Section 2.24.3).

2.24.1 *Preparation of total cellular extracts*

Crude protein extracts for Western immunoblot analysis were prepared as described below. Overnight cultures were harvested directly, or diluted to an optical density at 600 nm of 0.005. Bacteria were further grown under various environmental conditions until required for harvesting. At this stage the OD_{600} was measured and an appropriate volume of cells removed. This volume corresponded to 2 ml of culture per 1 OD_{600} unit. Bacteria were pelleted, washed in PBS and snap-frozen on dry ice. The pellets were then resuspended in 100 µl of 2 x final sample buffer (FSB) diluted in sonication buffer, and boiled for 10 min. Typically 10 µl of this crude extract was used for immuno-detection of StpA, H-NS or σ^s in Western immunoblot analyses.

2 x FSB: {150-mM Tris-HCl (pH 6.8), 1.2% SDS, 30% glycerol, 15 ml of β-mercaptoethanol} made to 100 ml with ddH_2O.

Sonication buffer: {10% sucrose, 50-mM Tris-HCl (pH 7.5), 100-mM NaCl, 1-mM EDTA, 5-mM dithiothreitol}.

2.24.2 *Transfer of proteins to nitrocellulose membrane*

Following SDS-PAGE (Section 2.23), gels were electroblotted to 0.2 µm PROTAN nitrocellulose membrane (Schleicher and Schuell) using a Mini Trans-blot electrophoretic transfer cell (Bio-Rad) filled with transfer buffer (25-mM Tris, 192-mM glycine, 20% methanol), at 20 V for 14 h at 4°C. Equal protein loading and consistent transfer to the nitrocellulose membrane were confirmed by staining the membrane with Ponceau S solution {0.2% Ponceau S (Sigma), 3 % trichloroacetic acid} for 5 min followed by extensive washing with ddH_2O.

2.24.3 *Detection of bound antigens*

Nitrocellulose membranes were blocked for 1 h in blocking buffer {5% w/v nonfat dry milk, in phosphate-buffered saline (PBS)}. Anti-StpA (1:1000), anti-H-NS (1:1000, a generous gift from E. Bremer) and anti-RpoS (1:3000, a generous gift from R. Hengge-Aronis) antisera were diluted appropriately in blocking buffer and incubated with the membrane for 1 h at room temperature. The membrane was washed 3 x 5 min with PBS and then incubated in blocking buffer containing HRP-linked anti-rabbit IgG for 1 h. The membrane was again washed 3 x 5 min with PBS. In the presence of a suitable chemiluminescent substrate the horseradish-peroxidase-mediated enzymic reaction results in a luminescent signal that visualises the antigen–antibody complex which can by detected by autoradiography (Section 2.12). Typical exposures were from 45 sec to 10 min.

2.25 *Protein-protein crosslinking*

Analysis of purified StpA oligomerisation was performed by *in vitro* cross-linking. StpA concentration was adjusted to be 1.2 µM in 8 µl BS buffer (Section 2.16.2). After a 10 min incubation at room temperature 2 µl of a solution containing a mixture of zero-length chemical cross-linker 1-ethyl-3-(3'-dimathylaminopropyl) carbodimide (EDC), and the catalyst *N*-hydroxy-succinimide (NHS) was added to the protein {final concentration of 50-mM EDC and 200-mM NHS (Grabarek and Gergely, 1990; Williams *et al.*, 1996)}. In the presence of these reagents some of the carboxyl groups

of StpA will be converted to succinimidyl esters. Crosslinking then arises from substitution of the ε-amino group of a lysine residue from one StpA protein by the succinimidyl ester of another. The cross-linking reaction was incubated at room temperature for 60 min and the reaction was stopped by the addition of 10 µl of 2 x FSB (Section 2.20). The products of cross-linking reactions and of control reactions carried out in an identical manner but in the absence of the cross-linking reagents were separated by SDS-PAGE (Section 2.23), and StpA-StpA complexes were detected by Western immunoblotting (Section 2.24).

2.26 *Analysis of DNA curvature*

The H-NS and StpA proteins have been reported to show specificity for interacting with curved DNA (Talukder and Ishihima, 1999 and references therein; Sonnenfield *et al.*, 2001). As a preferential interaction of H-NS with the *micF–ompC* promoter region was previously reported (Suzuki *et al.*, 1996) and this was also verified for the StpA protein in this study (Fig. 3.12), it was of interest to determine if the *micF–ompC* promoter region showed features of curved DNA. *In silico* analysis of promoter curvature was calculated with the Bend.it server (http://www2.icgeb.trieste.it/), using the DNase I-based bendibility parameters of Brukner *et al.* (1995). The results of this analysis suggested that regions of the *micF-ompF* divergent promoters were sharply curved. This was confirmed experimentally. A 448-bp fragment of the *micF–ompC* region was amplified using *Pfx* polymerase and the primer pair micF4 / micF5. The purified fragment was subject to 8% native polyacrylamide gel electrophoresis at 4°C. Under these conditions curved DNA shows anomalously slow electrophoretic mobility.

Chapter 3

Defining the role of StpA in OmpF porin expression

3.1 *Introduction*

The discovery nine years ago that the intensively studied DNA-binding protein H-NS in *Escherichia coli* has an intracellular homologue, StpA, that is 58% identical at the level of amino acid sequence, raised questions about the roles of these proteins when acting individually and in combination. Initially it was perceived that StpA was a 'molecular back-up' for H-NS (Sondén and Uhlin, 1996; Zhang *et al.*, 1996). This was because of its low level of expression under standard laboratory conditions, and the lack of any detectable phenotype associated with a *stpA* mutation. Now it is accepted that, although both proteins may work in concert for many roles and even heteroligomerise, StpA is functionally distinct from H-NS. Most notably StpA is more proficient in RNA-related activities (Zhang *et al.*, 1996; Cusick and Belfort, 1998; Deighan *et al.*, 2000).

3.1.1 *Proteomic profile for* **stpA** *and* **hns** *mutants*

Given the interrelatedness of the StpA and H-NS proteins, it was of interest to examine the global regulatory effects of *stpA* and *hns* mutations. This was carried out by two-dimensional gel electrophoresis of total cellular extracts prepared from cells grown to mid-exponential phase in minimal medium (Free and Dorman, 1997a). As shown previously, a number of protein spots were altered in intensity in an *hns* mutant when compared to the wild-type strain (Zhang *et al.*, 1996; Laurent-Winter *et al*, 1997; Hommais *et al.*, 2001). There were very few differences in protein profiles of a *stpA* mutant compared to wild-type, suggesting that in the presence of H-NS, the StpA protein does not make a significant contribution to global gene regulation (Zhang *et al.*, 1996; Sondén and Uhlin, 1996). However, when a double *stpA hns* mutant was made, the expression pattern of many proteins was affected, more so than in the *hns* single-mutant background. Some of these proteins that are synthesised at a reduced level in the *stpA hns* double-mutant background compared to the wild-type strain are indicated in Fig. 3.1A (upper panal). Thirty proteins produced at an elevated level in a *stpA hns* mutant background are also highlighted

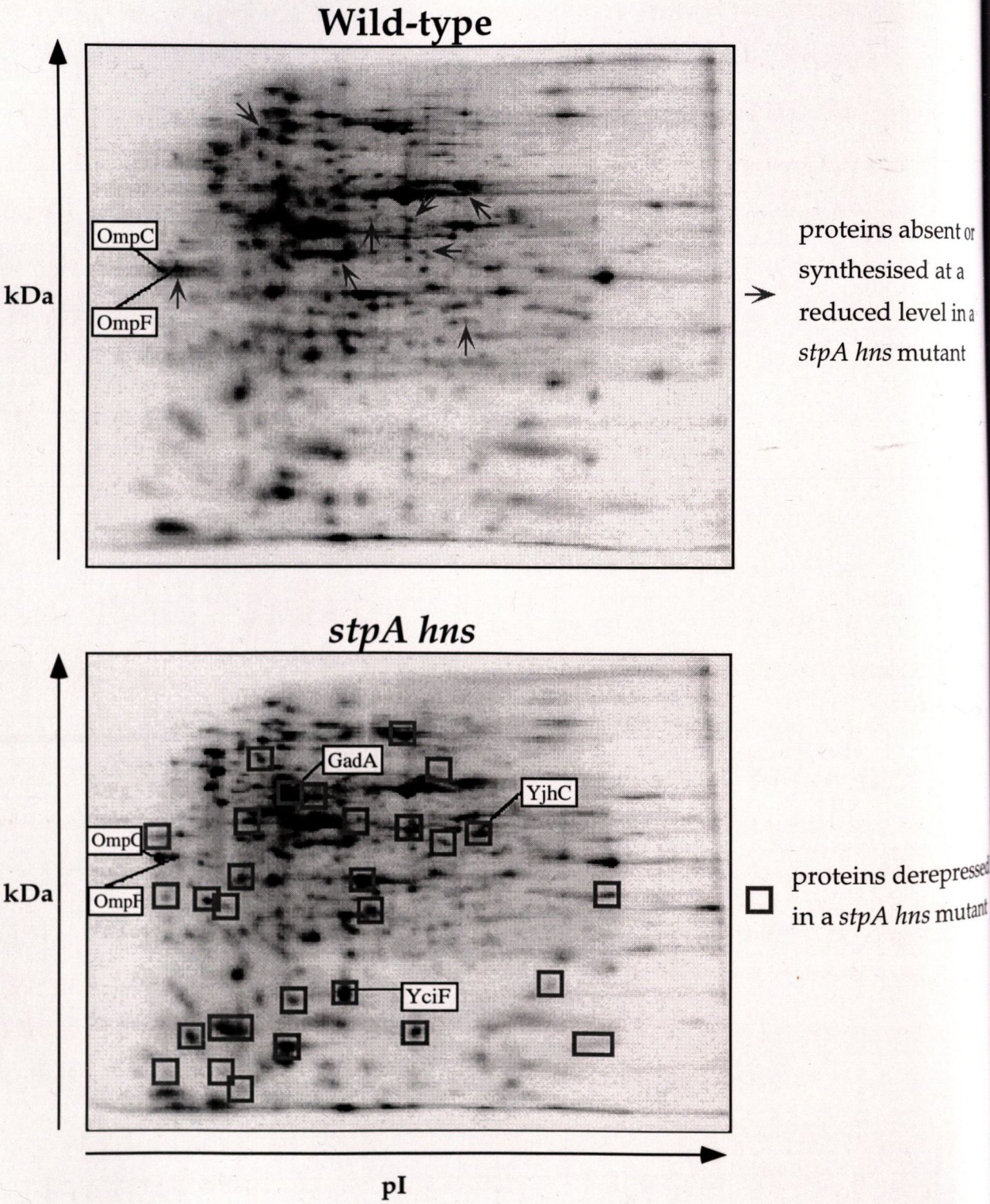
A
Wild-type
kDa
OmpC
OmpF
proteins absent or synthesised at a reduced level in a *stpA hns* mutant
stpA hns
kDa
GadA
YjhC
OmpC
OmpF
YciF
proteins derepressed in a *stpA hns* mutant
pI

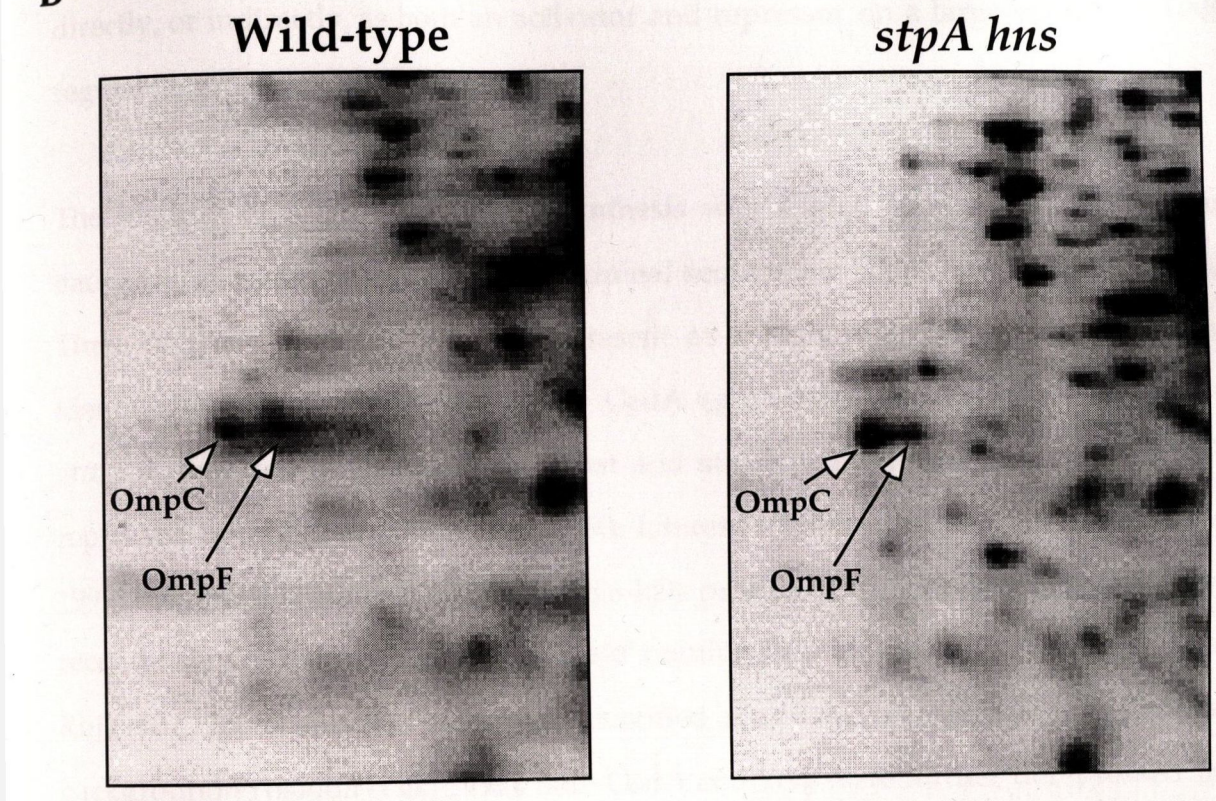

Fig. 3.1. Proteomic profiles for wild-type **E. coli** *GM37 and its* **stpA hns** *double mutant derivative*

A. Two-dimensional gel electrophoresis of total protein extracts from wild-type *E. coli* GM37 and its *hns2* Δ*stpA*::Tc^R derivative strain CJD1125. Bacteria were grown to mid-exponential phase in M9 minimal medium and newly synthesised proteins pulse-labeled with ^{35}S-methionine. Proteins with pI values in the range 3.0–10.0 and molecular mass in the range 10–100 kDa are resolved. Proteins absent or synthesised at reduced levels in strain CJD1125 are indicated in the upper panal by arrowheads. Proteins whose synthesis is induced in strain CJD1125 are indicated in the lower panel by boxes. The positions of the OmpF, GadA, YciF and YjhC proteins as identified by N-terminal sequencing, together with that of the OmpC protein as identified by comparison with the Swiss-2DPAGE database, are indicated.

B. The regions of the two-dimensional gels from (**A**) containing the OmpF and OmpC proteins are enlarged to show the clear downregulation of synthesis of the OmpF porin in the *hns2* Δ*stpA*::Tc^R strain CJD1125 compared with the wild-type parent strain GM37.

in Fig 3.1A (lower panal). Taken together, these data suggest that StpA can act directly, or indirectly, as both an activator and repressor on a large subset of H-NS-regulated genes.

The identity of 4 proteins whose synthesis was altered in the *stpA hns* mutant background was determined by N-terminal sequencing (Free and Dorman, 1997a). Three of these proteins that were present at a higher level in the mutant were identified as GadA, YciF and YjhC. GadA (glutamate decarboxylase alpha), an enzyme required for protection against acid stress, was previously reported to be repressed by H-NS (Yoshida *et al.*, 1993; Laurent-Winter *et al.*, 1997; de Biase *et al.*, 1999; Hommais *et al.*, 2001). YciF is a 18.6-kDa protein of unknown function that was recently shown to be a member of the σ^s regulon in *Salmonella typhimurium* (Ibanez-Ruiz *et al.*, 2000), and was previously identified as a protein elevated in an *hns* mutant background (Yoshida *et al.*, 1993). Both GadA and YciF were further derepressed in a *stpA hns* background compared to in the *hns* single-mutant background (Free and Dorman, 1997a). YjhC is a putative dehydrogenase in the *leuXA-fecE* intergenic region. No data on the regulation or function of YjhC has been published previously.

The fourth protein was synthesised at a reduced level in the *stpA hns* mutant background compared to the wild-type strain (Fig. 3.1B), and had the N-terminal sequence AEIYNKDGNK. This sequence matches exactly to amino acid residues 23–32 of OmpF and residues 22–31 of PhoE, corresponding to the mature form of these outer membrane porins following cleavage of the N-terminal signal sequences. With the help of the Swiss-2DPAGE expression maps [http://www.expasy.ch] a comparison of the identified positions of PhoE and OmpF suggested it was more likely that the protein spot observed was OmpF. Moreover, the PhoE porin, which is derepressed by phosphate starvation, would not be significantly expressed under the experimental conditions used in this analysis (Neidhardt, 1996).

3.1.2 *H-NS regulates OmpF porin expression*

Previous work had indicated that H-NS is required for full expression of the OmpF porin (Graeme-Cook *et al.*, 1989; Laurent-Winter *et al.*, 1997), and that this involved a role for H-NS in repressing *micF* transcription (Suzuki *et al.*, 1996). The product of the *micF* gene, MicF RNA, is a post-transcriptional repressor of OmpF expression. MicF RNA can hybridise with the 5'-end of the *ompF* mRNA via complementary sequences, sequestering the *ompF* mRNA translation start signals which results in inactivation and destabilisation of the *ompF* message (Mizuno *et al.*, 1984; Andersen *et al.*, 1989; Andersen and Delihas, 1990; Schmidt *et al.*, 1995). Thus, in an *hns* mutant *micF* transcription was elevated and consequently OmpF porin levels were reduced.

Two-dimensional gel electrophoresis revealed a very strong negative effect of the *stpA* mutation on OmpF synthesis on top of any effect caused by mutating *hns* (Free and Dorman, 1997a). Since there are many regulatory facets to OmpF expression including post-transcriptional repression by an antisense RNA, it was of interest to determine if StpA and H-NS exerted their effect on OmpF porin expression in a similar or distinct manner. Thus, the aim of the work described in this chapter was to define the role of StpA in OmpF porin expression.

3.2 *Results*

3.2.1 *Construction and characterisation of strains*

To elucidate the role for StpA in OmpF expression a series of strains were firstly constructed and characterised. The Δ*stpA*::Tc^R allele (Zhang *et al.*, 1996) has an internal deletion of the *stpA* gene replaced by the *tetAR* genes, which confer a decreased permeability and subsequent resistance to tetracycline. The *hns-206*::Ap^R allele (Dersch *et al.*, 1993) contains a 2.7-kb Ω-Ap^R cassette inserted into the unique *Hpa*I site within the *hns* gene. This cassette encodes β-lactamase, an enzyme that inactivates carbenicillin. P1 *cml*-mediated transduction was used to mobilise these alleles for strain construction (Table 2.1). Southern blotting with a *stpA*-specific probe (Fig. 3.2) and a *hns*-specific probe (Fig. 3.3) confirmed the correct integration of the alleles. In addition, the Δ*stpA*::Tc^R and *hns-206*::Ap^R lesions were confirmed to be complete null mutations for *stpA* and *hns* by Western immunoblot analysis (Fig. 5.1 and data not shown, respectively).

The double-mutant strain CJD1601 showed a clear reduction in growth rate compared to the wild-type strain, as monitored by measuring the optical density of the culture at 600 nm throughout the growth phase (Fig. 3.4). The generation time of strain CJD1601 during the exponential phase of growth was 53 min compared to 39 min for the single *hns* mutant (PD32). Both the *stpA* single mutant (CJD1600) and the wild-type strain MC4100 grew with a doubling time of 29 min. In addition, the *stpA hns* double-mutant strain stopped growing at a lower optical density than the other strains (Fig. 3.4). These growth properties are in agreement with global regulatory features of StpA and H-NS described in Section 3.1.1.

3.2.2 *Effect of* StpA *and* H-NS *on OmpF porin expression*

The results from the two-dimensional electrophoresis indicated that OmpF porin level was more strongly down-regulated in the *stpA hns* double mutant than in the *hns* single-mutant background (Free and Dorman, 1997a). This was confirmed by

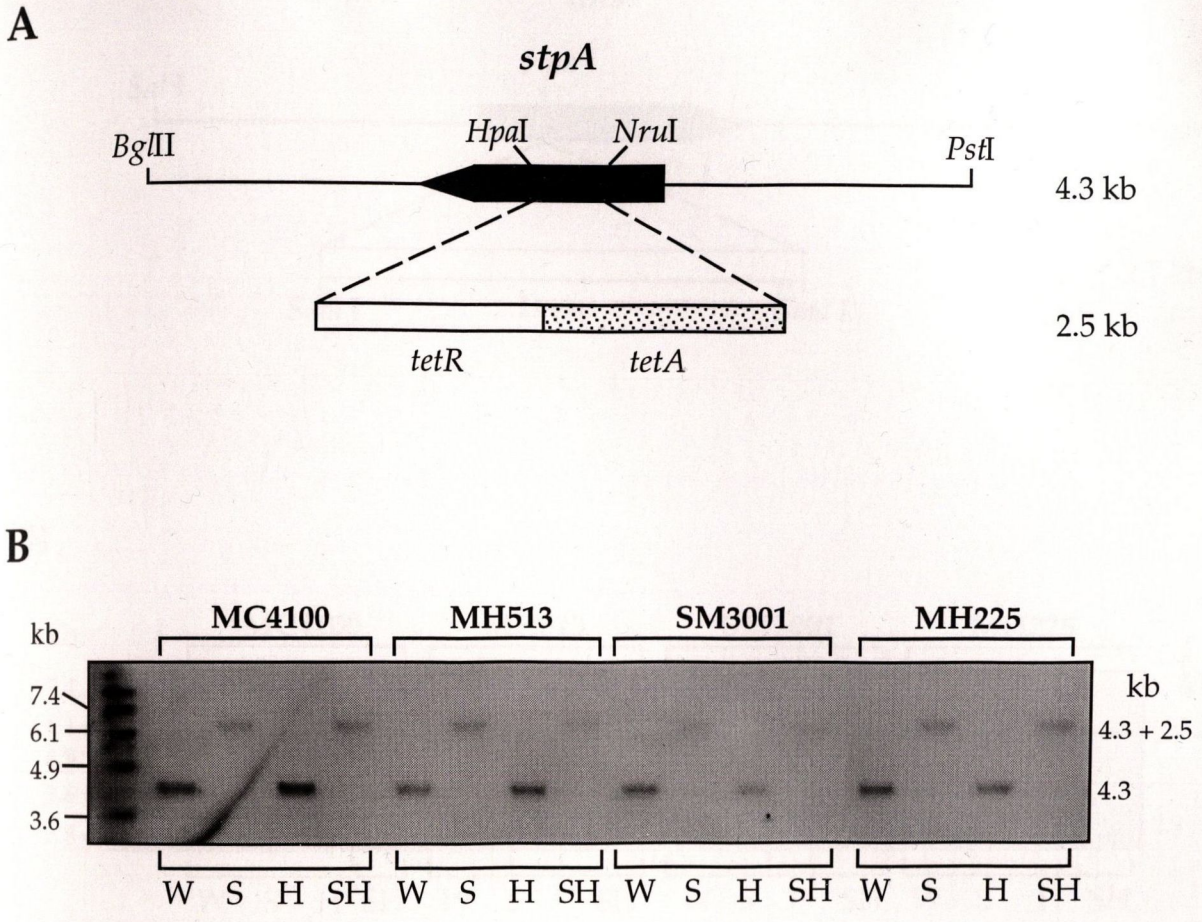

Fig. 3.2. Genetic confirmation of **stpA** *mutants*

A. Schematic representation of the *E. coli stpA* gene. The *stpA* gene, shown as an arrow, was replaced with a 2.5 kb fragment encoding the *tetR-tetA* genes (Δ*stpA*::Tc^R mutant strain a gift from M. Belfort).

B. Southern blot confirming disruption of *stpA*-coding sequences. The Δ*stpA*::Tc^R allele was moved by P1 transduction into MC4100, MH513, SM3001 and MH225 backgrounds as indicated. Following chromosomal digestion with restriction endonucleases *Bgl*II and *Pst*I, the wild-type *stpA* gene migrates on a 4.3-kb fragment, and the interrupted *stpA* gene migrates on a 6.8-kb fragment. Strain genotypes (W, wild-type; S, Δ*stpA*::Tc^R; H, *hns-206*::Ap^R; SH, Δ*stpA*::Tc^R *hns-206*::Ap^R) are indicated below each lane.

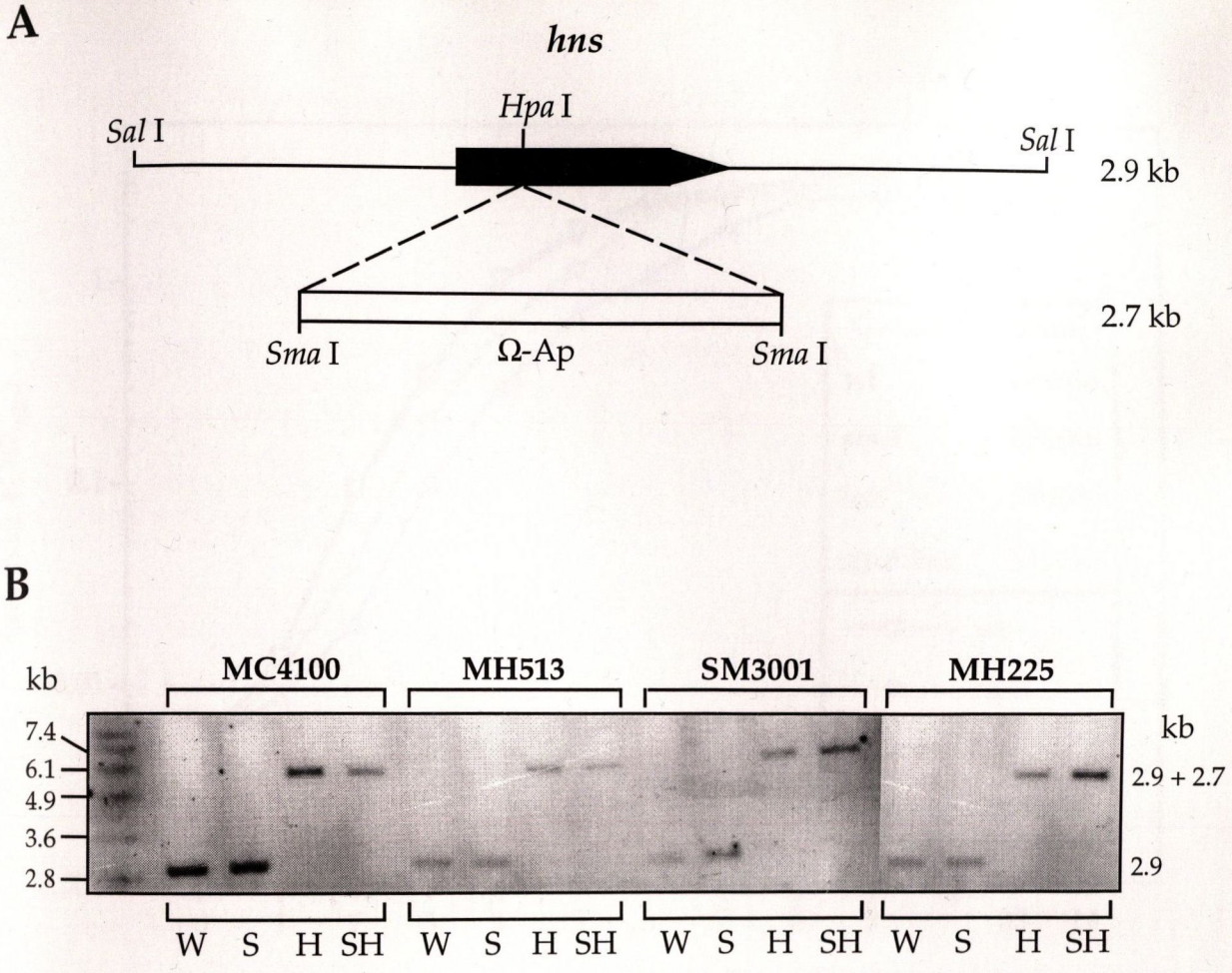

Fig. 3.3. Genetic confirmation of **hns** *mutants*

A. Schematic representation of the *E. coli hns* gene. In the *hns* mutant, coding sequence shown as an arrow, was interrupted by a 2.7-kb Ω-ApR cassette (*hns-206*::Ap^R mutant strain PD32, a gift from E. Bremer).

B. Southern blot confirming disruption of *hns*-coding sequences. The *hns-206*::Ap^R allele was moved by P1 transduction into MC4100, MH513, SM3001 and MH225 backgrounds as indicated. Following chromosomal digestion with *Sal*I restriction endonuclease, the wild-type *hns* gene migrates on a 2.9-kb fragment and the interrupted *hns* gene migrates on a 5.6-kb fragment. Strain genotypes (W, wild-type; S, Δ*stpA*::Tc^R; H, *hns-206*::Ap^R; SH, Δ*stpA*::Tc^R *hns-206*::Ap^R) are indicated below each lane.

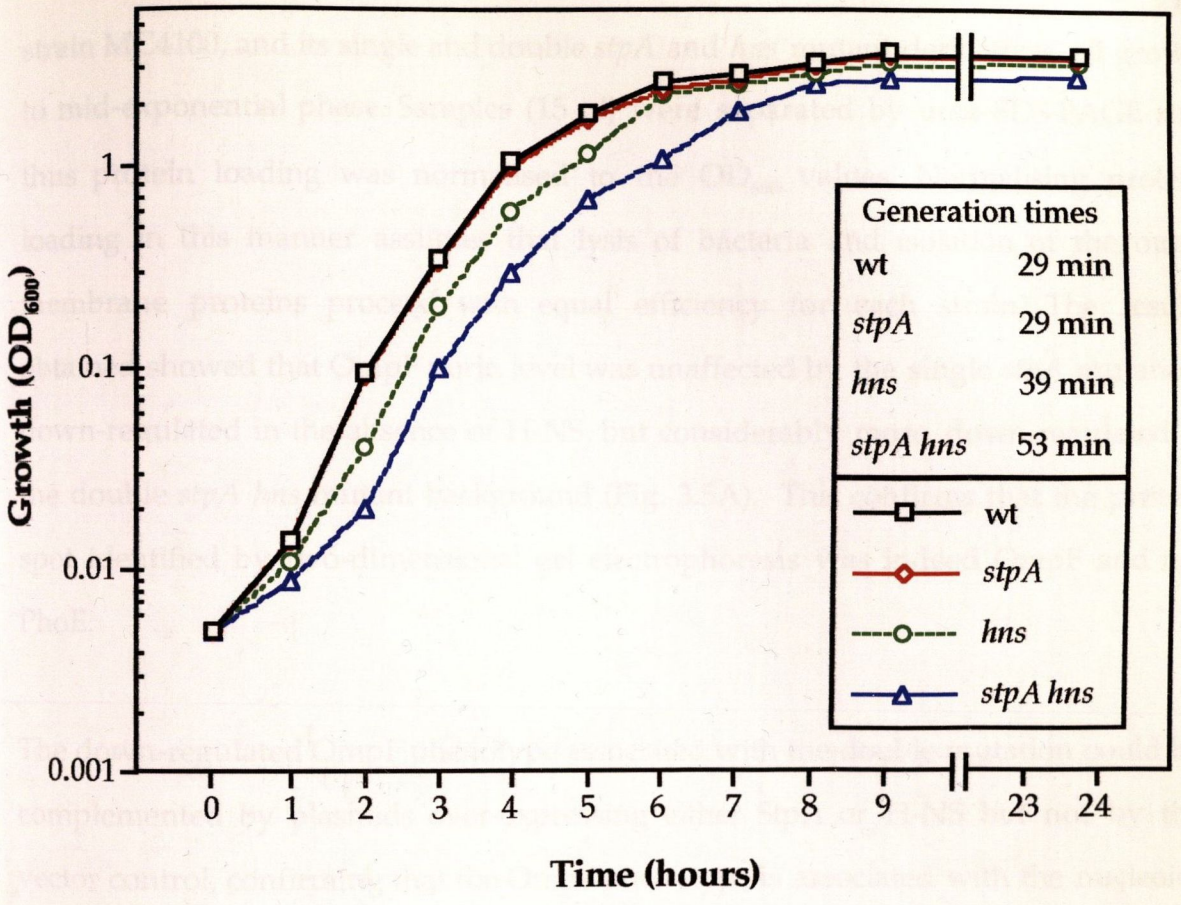

Fig. 3.4. Growth curves of wild-type and mutant strains in LB broth

Growth curves of wild-type MC4100, CJD1600 (*stpA*), PD32 (*hns*) and CJD1601 (*stpA hns*) strains in LB broth at 37°C. Overnight cultures were diluted to an OD_{600} of 0.005, and bacterial growth monitored by measuring OD_{600} at the indicated times. The generation time for each strain during the exponential phase of growth is indicated.

one-dimensional gel electrophoresis of outer membrane proteins. The outer membrane proteins were extracted as a Sarkosyl-insoluble fraction from wild-type strain MC4100, and its single and double *stpA* and *hns* mutant derivatives, all grown to mid-exponential phase. Samples (15 µl) were separated by urea–SDS-PAGE and thus protein loading was normalised to the OD_{600} values. Normalising protein loading in this manner assumes that lysis of bacteria and isolation of the outer membrane proteins proceed with equal efficiency for each strain. The results obtained showed that OmpF porin level was unaffected by the single *stpA* mutation, down-regulated in the absence of H-NS, but considerably more down-regulated in the double *stpA hns* mutant background (Fig. 3.5A). This confirms that the protein spot identified by two-dimensional gel electrophoresis was indeed OmpF and not PhoE.

The down-regulated OmpF phenotype associated with the double mutation could be complemented by plasmids over-expressing either StpA or H-NS but not by the vector control, confirming that the OmpF phenotype is associated with the nucleoid-associated proteins (Fig. 3.5B). This complementation additionally restores growth of the double-mutant strain to a wild-type rate, although Western immunoblot analysis shows that expression of both StpA and H-NS from the pACYC184-based plasmids is several times more than the wild-type level (data not shown and Fig. 5.1). This confirms that the under-expression of OmpF in the *stpA hns* strain is due to a direct effect of the nucleoid proteins and not associated with growth rate.

Previously it was shown that OmpC porin expression was elevated in the absence of H-NS (Graeme-Cook *et al.*, 1989; May *et al.*, 1990; Suzuki *et al.*, 1996; Laurent-Winter *et al.*, 1997). Curiously, increased OmpC protein level was not observed with the *hns-206* mutation (Fig. 3.5A), although *ompC* mRNA was slightly elevated (Fig. 3.6B). However, when the outer membrane proteins were isolated from another double *stpA hns* mutant strain, TO26 (*stpA*::Sp^R *hns*::Km^R), and compared to its wild-type parent BGL1 (Table 2.1), the OmpC porin level was found to be elevated and the

Fig. 3.5. Urea–SDS-PAGE of outer membrane porins

A. The expression patterns of outer membrane porins OmpC, OmpF, and OmpA, are shown for strains MH225 (*ompC*), MH513 (*ompF*), MC4100 (wild-type), CJD1600 (Δ*stpA*::Tc^R), PD32 (*hns-206*::Ap^R) and CJD1601 (Δ*stpA*::Tc^R *hns-206*::Ap^R). The porin profiles of strains BGL1 (wild-type) and TO26 (*stpA*::Sp^R *hns*::Km^R) are also shown.

B. Complementation of the downregulated OmpF level in a *stpA hns* mutant by a plasmid encoding functional StpA or H-NS. Plasmid pACYC184 is a cloning vector control; pYCStpA is derived from pACYC184 and encodes wild-type StpA; pAF201 is also derived from pACYC184 and encodes wild-type H-NS. Outer membrane extracts were prepared from bacteria grown to mid-exponential phase in LB medium and analysed by 8-M urea–12% SDS-PAGE. The positions of OmpC, OmpF, and OmpA are shown as verified by comparison with strains MH225 and MH513. The relevant strain genotypes are indicated below each lane. The experiments were performed twice and representative gels are shown.

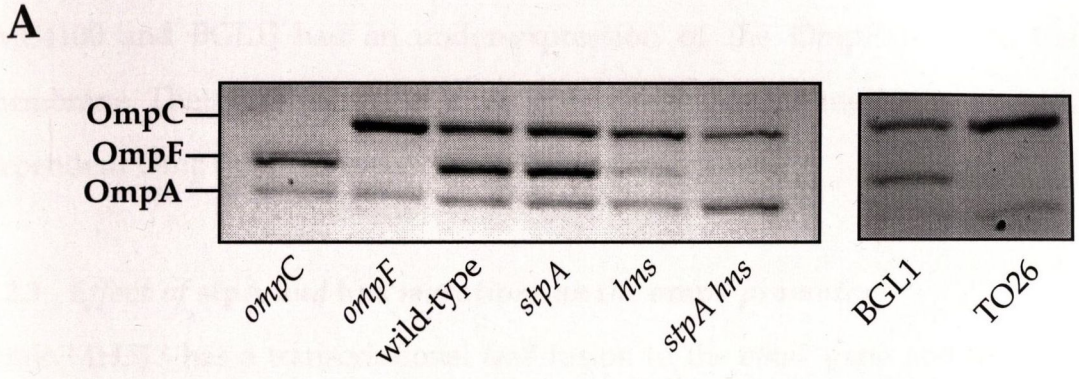
A
OmpC
OmpF
OmpA
ompC
ompF
wild-type
stpA
hns
stpA hns
BGL1
TO26

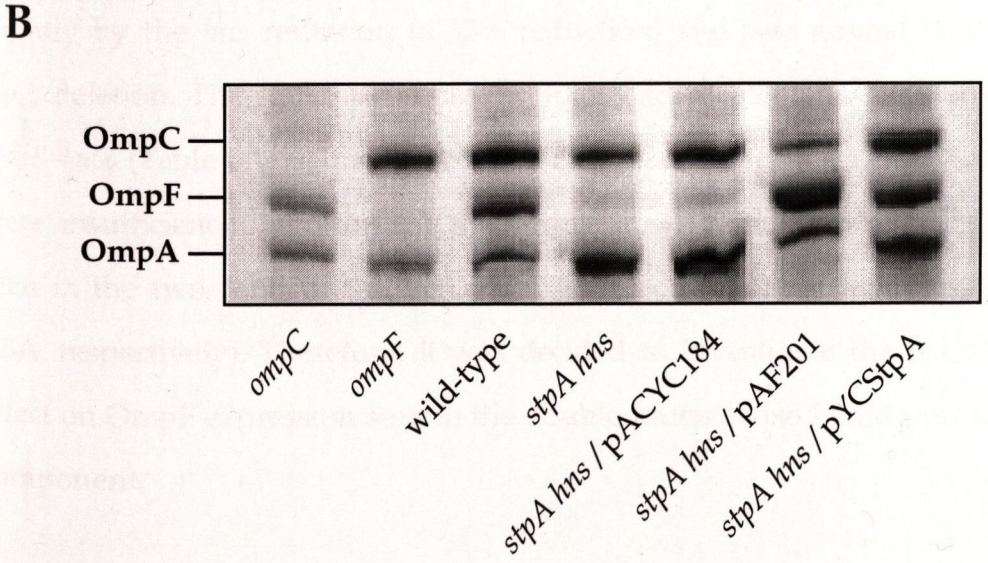
B
OmpC
OmpF
OmpA
ompC
ompF
wild-type
stpA hns
stpA hns / pACYC184
stpA hns / pAF201
stpA hns / pYCStpA

OmpF porin level severely reduced. It is possible that the mucoid nature associated the *hns-206* allele in the MC4100 background could interfere with efficient lysis and subsequent detergent-based extraction of the outer membrane, compared to the less mucoid strain TO26 (data not shown). In any case, both of the allele pairs [Δ*stpA*::Tc^R *hns-206*::Ap^R] and [*stpA*::Sp^R *hns*::Km^R] in different *E. coli* genetic backgrounds [MC4100 and BGL1] had an under-expression of the OmpF porin in the outer membrane. Therefore, it was of interest to investigate the mechanism behind StpA-dependent OmpF expression.

3.2.3 *Effect of* stpA *and* hns *mutations on the* ompF *promoter*

Strain MH513 has a transcriptional *lacZ* fusion to the *ompF* gene and this reports on changes in the activity of the *ompF* promoter. Derivatives of strain MH513 were constructed that harboured a deletion of the *stpA* gene (Δ*stpA*::Tc^R), or the insertionally inactivated *hns* allele *hns-206*::Ap^R, or both lesions. Beta-galactosidase activity measurements showed that the level of *ompF–lacZ* expression was affected slightly by the *hns* mutation (a 32% reduction) and was almost unaffected by the *stpA* deletion. The *stpA hns* double mutant had a 64% reduction in expression of *ompF–lacZ* (Table 3.1). Although contributing, these effects on *ompF–lacZ* expression were insufficient to account for the strong down-regulation of the OmpF protein seen in the two- and one-dimensional gel electrophoretic analyses (Figs. 3.1 and 3.5A, respectively). Therefore, it was decided to investigate the possibility that the effect on OmpF expression seen in the double mutant also had a post-transcriptional component.

3.2.4 *StpA and H-NS regulate* ompF *post-transcriptionally*

The effects of the *stpA* and *hns* mutations on the steady state level of the *ompF* message were measured by Northern analysis. Total RNA was extracted from strain MC4100 and its *stpA* and *hns* mutant derivatives grown to mid-exponential phase, and *ompF* mRNA detected with a specific riboprobe (Fig. 3.6, lanes 1–4). The results showed that the level of *ompF* mRNA was unaffected by the *stpA* lesion, whereas a

Table 3.1. Effect of **stpA** *and* **hns** *mutations on β-galactosidase expression from an* **ompF–lacZ** *gene fusion*

Strain	Relevant details	β-Galactosidase acivity[a]	*P*[b]
MH513	*ompF–lacZ*	502 (27)	
CJD1605	*ompF–lacZ ΔstpA*::Tc^R	494 (25)	NS
CJD1606	*ompF–lacZ hns-206*::Ap^R	342 (38)	<0.005
CJD1607	*ompF–lacZ ΔstpA*::Tc^R *hns-206*::Ap^R	182 (4)	<0.0001

[a]Mean β-galactosidase activities from four independent experiments are expressed in Miller units with standard deviations in brackets.

[b]Student's *t*-test versus control strain MH513. NS implies not statistically significant

Fig. 3.6. Effects of **stpA, hns** *and* **micF** *mutations on* **ompF** *mRNA level*

A. Northern blot of total RNA extracted form cells grown to mid-exponential phase in LB medium hybridized with an *ompF*-specific riboprobe.

B. Northern blot of total RNA extracted form cells grown to mid-exponential phase in LB medium hybridized with an *ompC*-specific riboprobe. In (**A**) and (**B**) the relevant strain genotypes are indicated below each lane.

C. Table showing densitometric analyses of the data in (**A**). The data are expressed relative to wild-type for *stpA*, *hns*, and *stpA hns* strains, and relative to *micF* for *micF stpA*, *micF hns*, and *micF stpA hns* strains. The experiment was performed three times and representative gels and typical data are shown.

A

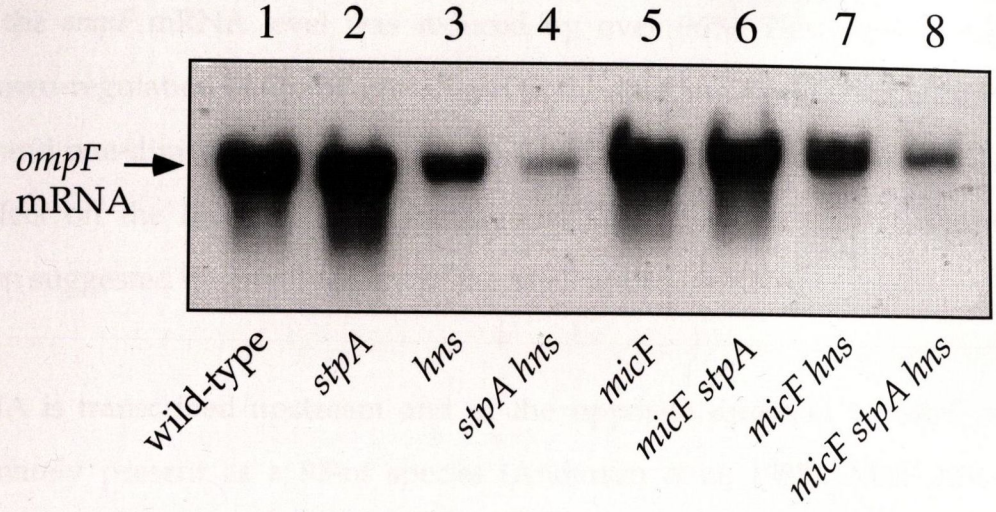

B

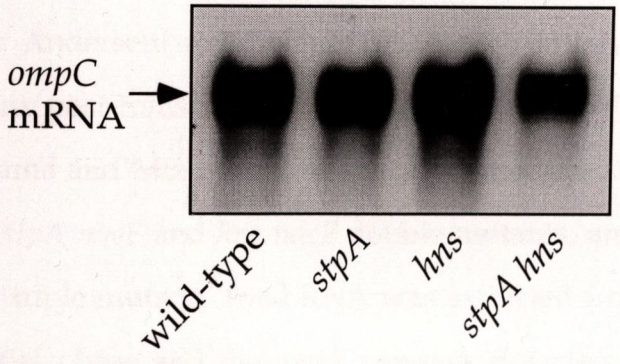

C

stpA and *hns* alleles	Strain	
	Wild-type[a]	*micF*[b]
wild-type	1	1
stpA	1	1
hns	0.3	0.5
stpA hns	0.04	0.1

[a]level of *ompF* mRNA relative to wild-type
[b]level of *ompF* mRNA relative to *micF* mutant

70% decrease was detected in the absence of H-NS. However, in the *stpA hns* double mutant, the *ompF* mRNA level was reduced by over 96%. This showed that the strong down-regulation of OmpF porin level in the *stpA hns* double mutant detected by two- and one-dimensional electrophoresis (Fig. 3.1 and 3.5A) was primarily due to an effect on the level of *ompF* message in the cell. This post-transcriptional regulation suggested the involvement of the MicF antisense RNA.

MicF RNA is transcribed upstream and in the opposite direction to *ompC* and is predominately present as a 93-nt species (Andersen *et al*; 1987). MicF RNA has significant sequence homology to the 5'-end of the *ompF* message and hybridisation of the RNAs results in a poorly translated complex (Mizuno *et al.*; 1984; Andersen *et al.*, 1989; Andersen and Delihas, 1990). The involvement of MicF RNA in StpA-dependent post-transcriptional expression of *ompF* was tested. The Δ*micF1* allele (Matsuyama and Mizushima, 1985) was introduced into strains CJD1600 and PD32 creating *stpA micF* and *hns micF* double mutants, and into CJD1601 creating a *micF stpA hns* triple mutant. Total RNA was extracted from these strains grown to mid-exponential phase and the *ompF* message detected by Northern analysis (Fig. 3.6, lanes 5–8). The results showed that, in the absence of *micF*, the *stpA* single mutation again had little effect on the *ompF* mRNA level, whereas a 50% decrease was detected in the *hns* background. Moreover, the *ompF* mRNA level was reduced by 10-fold in the *micF stpA hns* triple mutant, in contrast to the 25-fold reduction in a *micF*$^+$ background (Fig. 3.6C). This suggested that the effect on *ompF* mRNA observed in the *stpA hns* double mutant was primarily mediated through the MicF antisense RNA.

Overall the *ompF* and *ompC* genes are 44% identical at the nucleotide level. However, over 90-bp stretches of the genes this sequence homology can be as high as 95%. As a control for riboprobe specificity, the effect of the *stpA*, *hns* and *stpA hns* mutations on *ompC* mRNA level was measured by Northern analysis (Fig. 3.6B). The *stpA* null mutation had little effect on the *ompC* mRNA level, but there was a detectable

increase in the *hns* mutant strain, consistent with H-NS having a role as a transcriptional repressor at this promoter (Graeme-Cook *et al.*, 1989; Suzuki *et al.*, 1996). The level of *ompC* mRNA was slightly decreased when the *stpA* allele was introduced into the *hns* background. These results are in contrast to the level of *ompF* mRNA detected with the same RNA samples confirming riboprobe specificity.

It should be noted that complete restoration of *ompF* mRNA levels to a wild-type level was not seen in either *hns* or *stpA hns* backgrounds by deleting the *micF* locus. This suggests that not all control of OmpF by H-NS or StpA is entirely *micF*-dependent. There are other examples where down-regulated OmpF production via *micF* activation is only partially reversed by deletion of the *micF* gene (Misera and Reeves, 1987; Andersen *et al.*, 1989; Rosner *et al.*, 1991). In addition the Δ*micF1* mutation used in this and other studies itself has effects, as it increases OmpC production as a result of extension of the deletion into the *ompC* regulatory region, and OmpF production is slightly decreased (Matsuyama and Mizushima, 1985).

However, it was observed that the low level of OmpF expressed in the outer membrane in a *stpA hns* mutant could be restored to wild-type levels by a plasmid over-expressing the StpA protein (Fig. 3.7). This complementation could not be achieved in a *micF stpA hns* triple mutant suggesting that complementation of OmpF by StpA is an effect that alone works via the MicF RNA. These data confirmed that StpA-dependent regulation of *ompF* expression involved MicF RNA, which could be mediated via destabilisation of the *ompF* message.

3.2.5 *Effect of* **stpA** *and* **hns** *mutations on stability of the* **ompF** *message*

The antibiotic rifampicin binds the β-subunit of RNA polymerase inhibiting RNA synthesis. Bacteria in cultures sensitive to treatment with rifampicin will produce no additional RNA thus allowing the determination of the half-life for a particular message that is present in the cell. Strain MC4100 and its *stpA* and *hns* single- and double-mutant derivatives were grown to mid-exponential phase and *de novo*

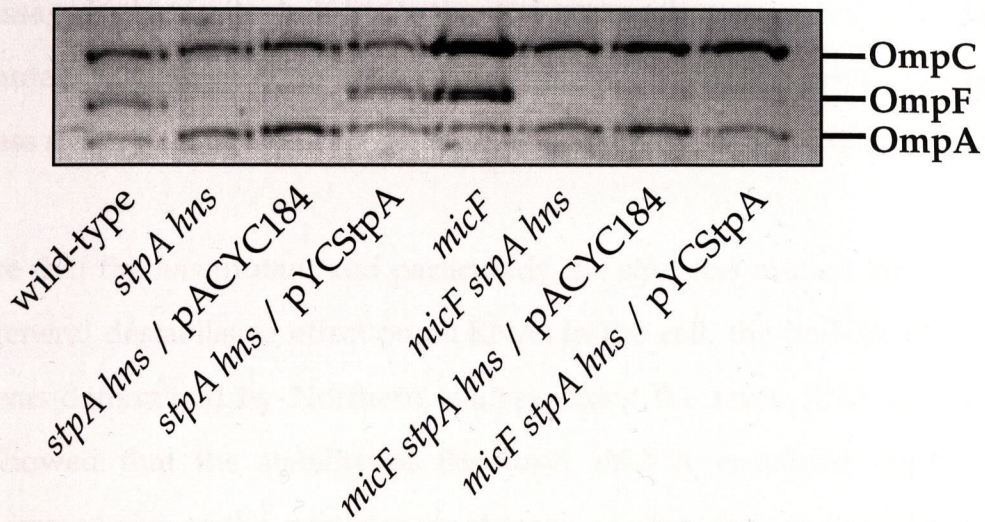

Fig. 3.7. Complementation of down-regulated OmpF porin levels

Urea–SDS-PAGE of outer membrane porins showing complementation of the down-regulated OmpF level in a *stpA hns* mutant by a plasmid encoding functional StpA in the presence and absence of *micF*. Plasmid pACYC184 is the cloning vector control and pYCStpA is derived from pACYC184 and encodes wild-type StpA. Outer membrane proteins were extracted from bacteria cultured to mid-exponential phase in LB medium. The positions of OmpC, OmpF, and OmpA are shown and relevant strain genotypes are indicated below each lane. The experiment was repeated twice and a representative gel is shown.

transcription stopped by the addition of rifampicin. Samples of culture for RNA extraction were harvested before and after rifampicin addition in a time-course experiment, and the *ompF* message detected by Northern analysis (Fig. 3.8). The results showed that the *ompF* mRNA had a half-life of 8 min in wild-type *E. coli*. The *ompF* message had a similar half-life in the *stpA* mutant, but was reduced by 2-fold in an *hns* mutant. Significantly, in the *stpA hns* double mutant the *ompF* message was ≈5-fold less stable than in wild-type with a calculated half-life of 1.6 min.

To ensure that the *hns* mutant and particularly the *stpA hns* mutant strains did not exert a general destabilising effect on all RNAs in the cell, the half-life of the *hupA* mRNA was determined by Northern analysis using the same RNA samples. The results showed that the stability of the *hupA* mRNA remained approximately constant irrespective of the presence or absence of *stpA* and/or *hns* (Fig. 3.8B), in contrast to the stability of the *ompF* mRNA. This was consistent with the idea that StpA and H-NS were acting specifically through MicF RNA, which then brought about the destabilisation of the *ompF* message.

3.2.6 *The promoter choice for* micF *transcription initiation is independent of StpA and H-NS*

MicF RNA was initially identified as a 174-nt (6S) RNA in *E. coli* by S1 nuclease mapping (Mizuno *et al.*, 1984). Andersen *et al.* (1987) further characterised MicF RNA and discovered a more abundant 93-nt RNA (4.5S), which corresponds to nucleotides G82 → U174 of the 174-nt species. Both RNAs are transcribed from independent promoters and both contain the region of sequence complementarity to the 5'-end of the *ompF* mRNA. However, *lacZ*-fusion experiments showed that the 6S promoter was at least 30-fold weaker that the 4.5S promoter in a wild-type strain (Andersen *et al.*, 1987). The *micF* transcription start site was mapped by primer extension to determine if there was StpA- or H-NS-dependent promoter bias for transcription initiation. Total RNA was extracted from the wild-type strain MC4100 and its *stpA* and *hns* mutant derivatives. RNA was also extracted from a *micF* mutant to serve as

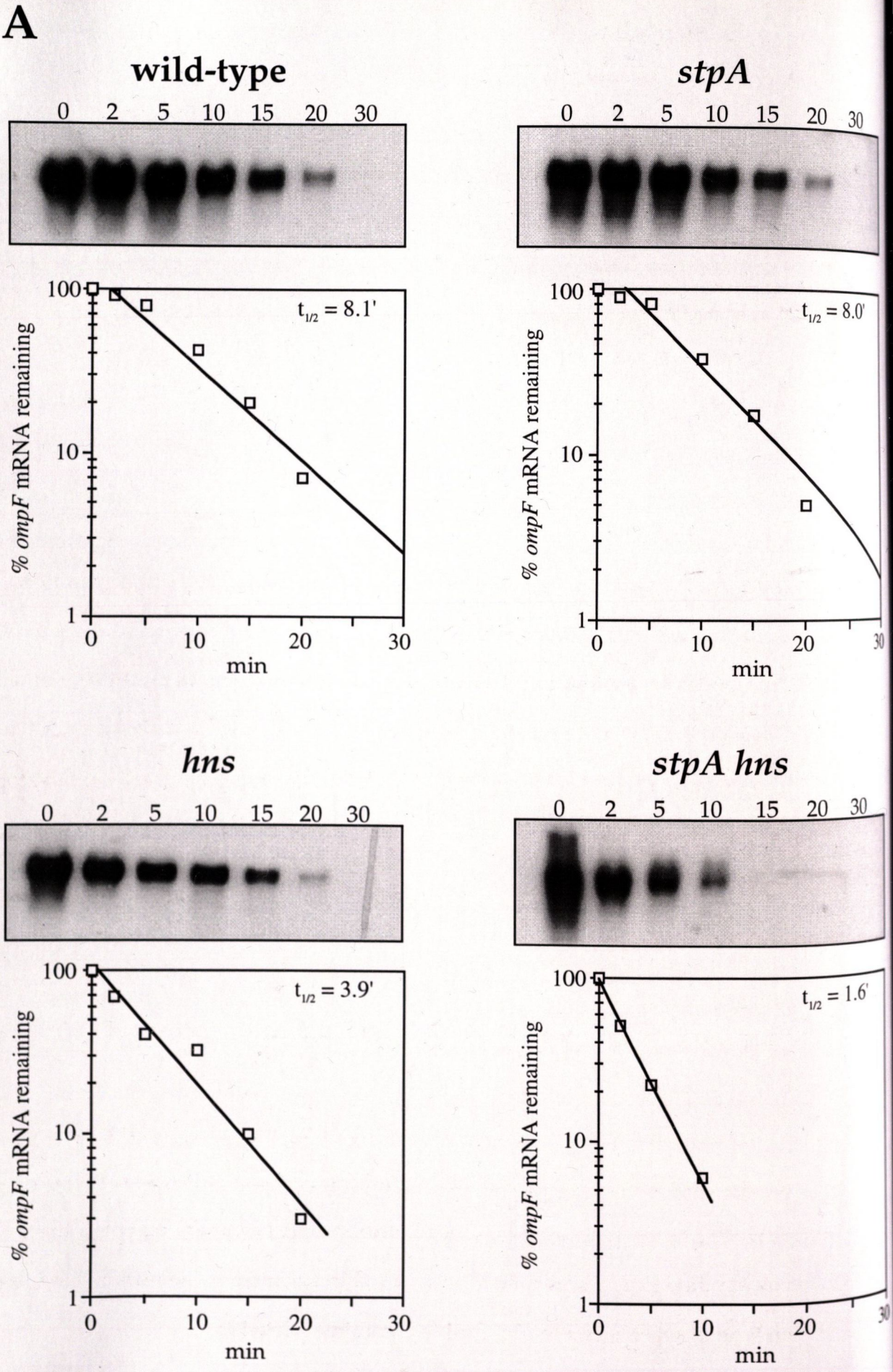
A
wild-type
0 2 5 10 15 20 30
100
10
1
% ompF mRNA remaining
t1/2 = 8.1'
0 10 20 30
min
stpA
0 2 5 10 15 20 30
100
10
1
% ompF mRNA remaining
t1/2 = 8.0'
0 10 20 30
min
hns
0 2 5 10 15 20 30
100
10
1
% ompF mRNA remaining
t1/2 = 3.9'
0 10 20 30
min
stpA hns
0 2 5 10 15 20 30
100
10
1
% ompF mRNA remaining
t1/2 = 1.6'
0 10 20 30
min

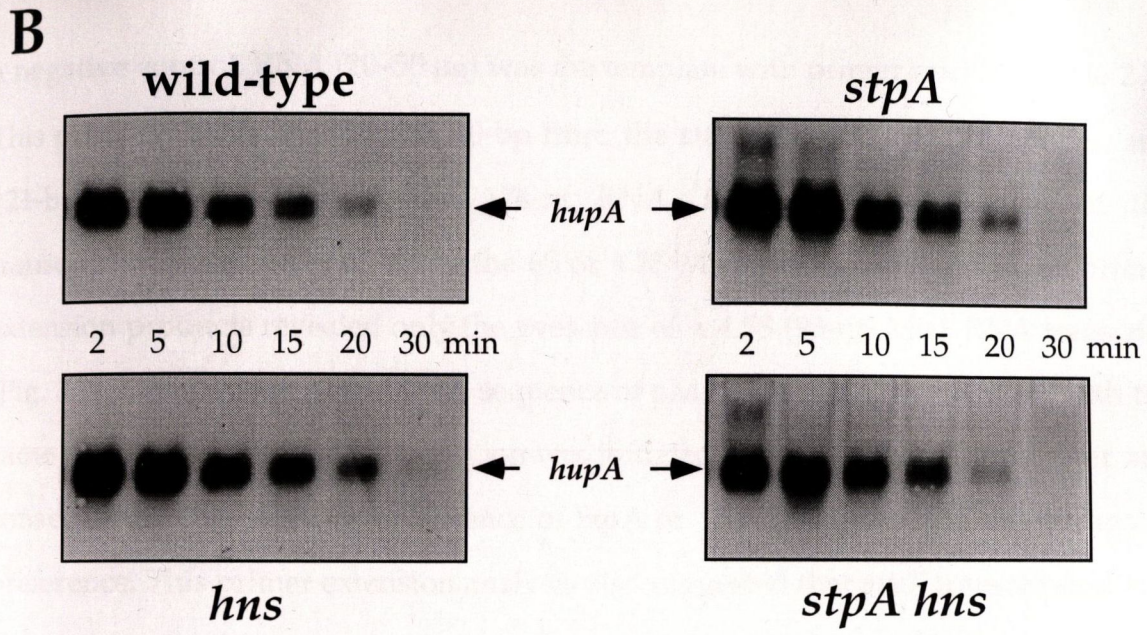

Fig. 3.8. ompF mRNA stability

A. Northern blot analysis showing the effects of *stpA* and *hns* mutations on *ompF* mRNA stability. Total RNA was isolated form wild-type strain MC4100, and its *stpA, hns,* and *stpA hns* mutant derivatives grown to mid-exponential phase in LB medium, and probed with an *ompF*-specific riboprobe. Numbers above each lane refer to the time in minutes after (0, 2, 5, 10, 15, 20, 30) rifampicin treatment to stop *de novo* transcription. Each blot has been exposed to film for different time periods and consequently comparisons between blots are not meaningful. Shown below the respective blot for each strain is a semilogarithmic plot of *ompF* mRNA decay based on densitometric analyses of several different exposures. The half-life ($t_{1/2}$) calculated from each plot is indicated. The experiment was repeated twice and typical data and representative gels are shown.

B. Northern blot analysis showing *hupA* mRNA decay in wild-type strain MC4100, and its *stpA, hns,* and *stpA hns* mutant derivatives. The same RNA samples as used in (**A**) were probed with an *hupA*-specific riboprobe. Numbers between the gels refer to the time in minutes following rifampicin treatment. The autoradiographs shown have been exposed to film for identical time periods.

a negative control. RNA (20–50 μg) was the template with primer micFPE (Table 2.3). This primer was designed to be 40-bp from the start of the 93-nt RNA species, and 121-bp from the start of the 174-nt RNA, facilitating identification of the transcriptional start sites of either the 6S or 4.5S MicF RNAs. Analysis of the primer extension products revealed only the presence of a 4.5S (93-nt) MicF RNA transcript (Fig. 3.9). Comparison of the DNA sequence of pM/C (Table 2.2) generated with the same primer implied that transcription was initiated from the *micF* P2 promoter and consequently the presence or absence of StpA or H-NS did not bias this promoter preference. This primer extension analysis also suggested that *micF* transcription was elevated in a *stpA hns* mutant.

3.2.7 *Interaction of StpA with the curved* micF–ompC *promoter region*

H-NS was shown previously to bind a fragment of DNA encompassing the *micF–ompC* divergent promoters (Suzuki *et al.*, 1996). It was of interest to determine if purified StpA could also interact with this promoter region. Prior to this *micF–ompC* promoter curvature was assessed. Curved DNA sequences are common in bacterial gene promoters (Van Wye *et al.*, 1991), and the relationship between intrinsic curvature and DNA-binding by H-NS has been suggested in a number of cases (Yamada *et al.*, 1991; Atlung and Ingmer, 1997; Jordi *et al.*, 1997; Dorman *et al.*, 1999; Talukder and Ishishama, 1999).

The curvature propensity plot for the 448-bp sequence of the *micF–ompC* promoters was calculated with the Bend.it server (http://www2.icgeb.trieste.it/), using the DNase I-based bendibility parameters of Brukner *et al.* (1995). Analysis revealed the presence of several smaller peaks and one conspicuous peak of sharply increased curvature, which corresponds to the region of DNA encompassing the start of the OmpC open-reading frame (Fig. 3.10A). The presence of curvature in this region was verified experimentally by analysing the 448-bp PCR-amplified *micF–ompC* promoter region by polyacrylamide gel electrophoresis at 4°C (Fig. 3.10B). The DNA fragment migrated at a slower rate than the marker DNA, as expected for curved DNA. When

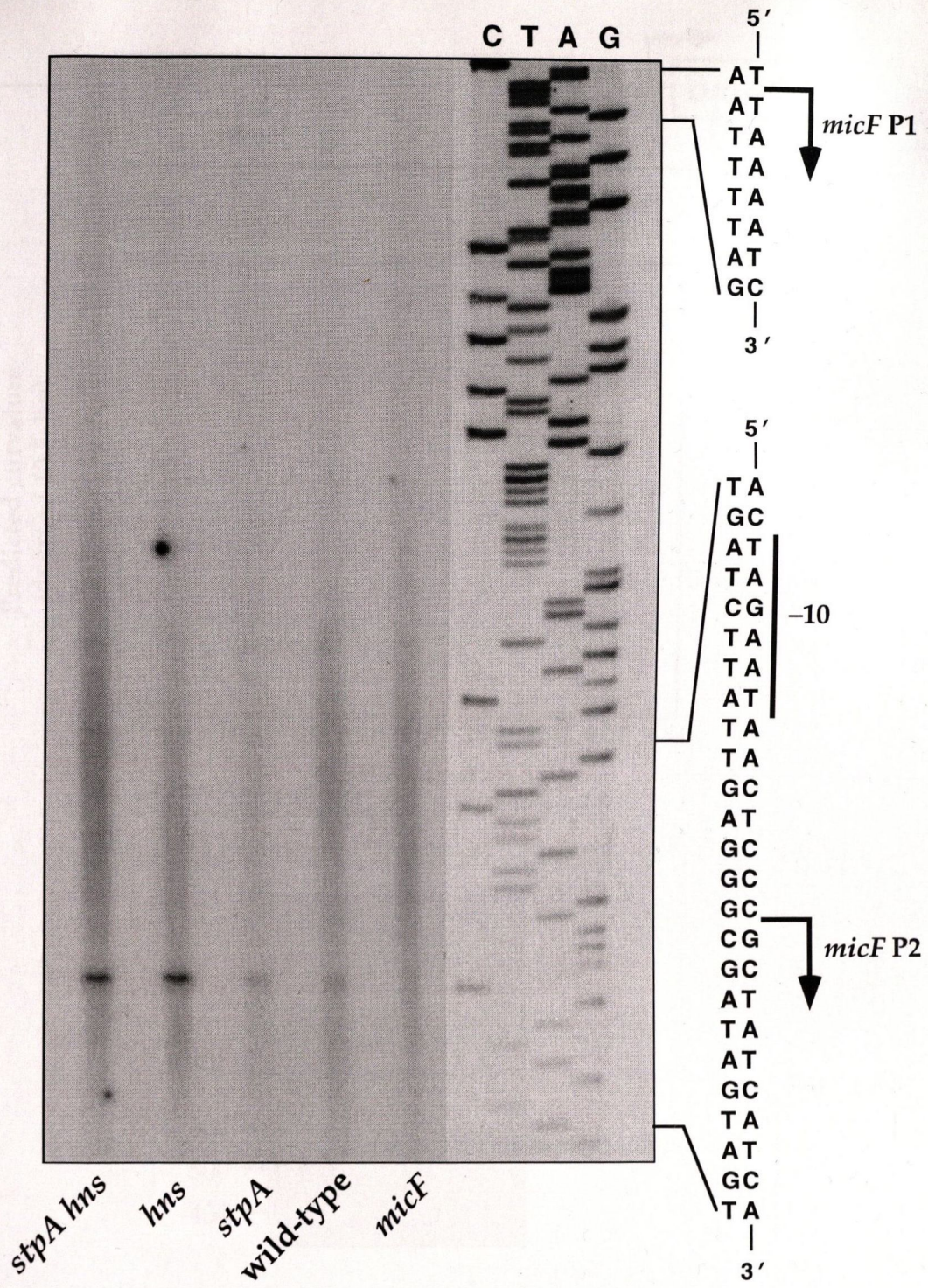

Fig. 3.9. Effects of StpA and H-NS on micF promoters

Primer extension of *in vivo*-produced MicF RNA. Total RNAs (20–50 μg) prepared from mid-exponential phase cultures of MC4100 (wild-type), CJD1600 (*stpA*), PD32 (*hns*), CJD1601 (*stpA hns*) and SM3001 (*micF*) were used as templates for primer extension analysis with ^{32}P–end-labeled primer micFPE. Sequencing lanes with the same primer and plasmid pM/C as a template are shown alongside. The sequence read and that of the complementary strand are presented. The +1 of *micF* P1, and the +1 and –10 sequences of *micF* P2 are indicated. The primer extension reactions and the sequencing lanes have been exposed to film for different time periods.

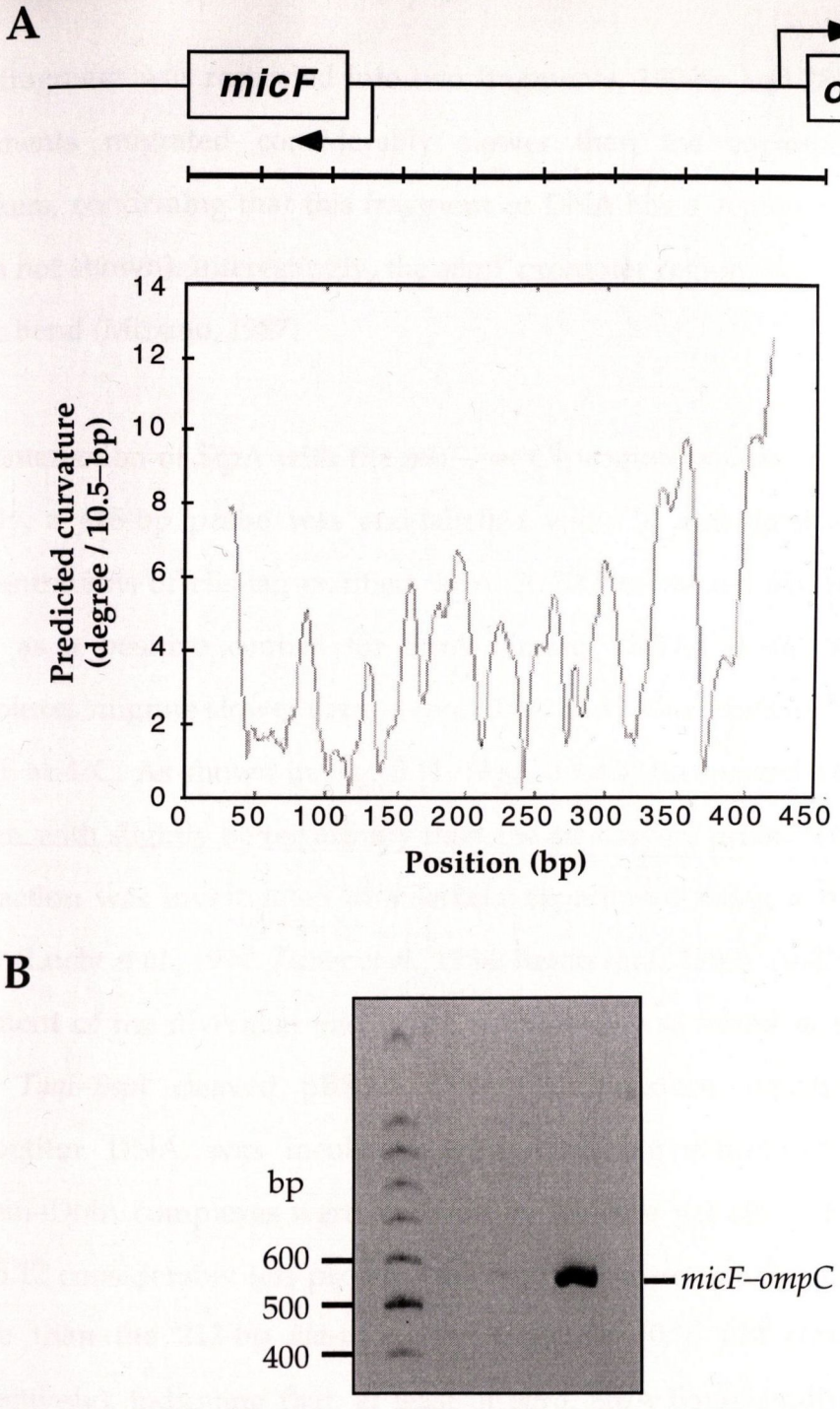

Fig. 3.10. The **micF–ompC** *promoter region is curved*

A. The curvature of a 448-bp region encompassing the *micF–ompC* promoters was predicted using the Bend.it server (http://www2.icgeb.trieste.it/). A schematic representation of this region and the propensity plot indicating curvature {degrees per 10.5 bp (one helical turn)} plotted against the position in the sequence is shown.

B. Native 8% polyacrylamide gel electrophoresis of the 448-bp *micF–ompC* promoter region at 4°C. The gel was visualised by staining with ethidium bromide and DNA size standards are indicated, as is the position of migration of the 448-bp promoter fragment.

this fragment was restricted into two fragments, 160-bp and 288-bp in length, both fragments migrated considerably slower than the corresponding non-curved markers, confirming that this fragment of DNA has a region of intrinsic curvature (data not shown). Interestingly, the *ompF* promoter region was also shown to have a static bend (Mizuno, 1987).

The interaction of StpA with the *micF–ompC* promoters was analysed in two ways. Firstly, a 448-bp probe was end-labelled with ^{32}P and incubated with increasing concentrations of His-tag purified StpA. A 200-bp curved *bla* promoter probe was used as a positive control for StpA binding (Bertin *et al.*, 1999). Protein–DNA complexes migrate slower than native DNA and were separated by non-denaturing PAGE at 4°C. As shown in Fig. 3.11, StpA bound the curved *micF–ompC* promoter region with slightly better affinity than the *bla* control probe. The specificity of the interaction was investigated in a second experiment using a competitive gel-shift assay (Lucht *et al.*, 1994; Zuber *et al.*, 1994; Bertin *et al.*, 1999). A 404-bp PCR-amplified fragment of the divergent *micF–ompC* promoters was mixed in equimolar amounts with *Taq*I–*Ssp*I cleaved pBR322 DNA. The mixture, containing an excess of competitor DNA, was incubated with increasing concentrations of StpA, and protein–DNA complexes were analysed by agarose gel electrophoresis. As seen in Fig. 3.12 considerably less protein was required to retard the *micF–ompC* promoter probe than the 217-bp *bla*-promoter fragment (0.15 μM compared to 1.2 μM, respectively), indicating that, at least *in vitro*, StpA binds avidly to the *micF–ompC* divergent promoter region.

3.2.8 *Control of micF transcription*

It was likely that in the double mutant CJD1601 the inhibitory effect of StpA and H-NS on *micF* expression was removed, and the resulting increased MicF RNA level could enhance the inactivation and degradation of the *ompF* message. To elucidate whether StpA and H-NS affected *micF* expression at a transcriptional or at a post-

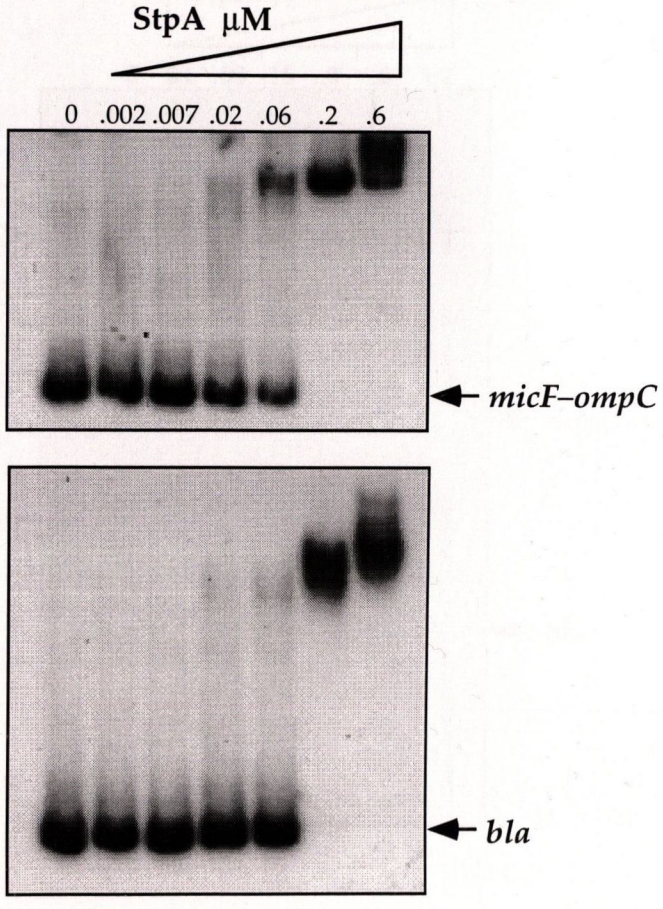

Fig. 3.11. StpA interacts with the **micF–ompC** *promoter region*

Gel mobility shift assay showing the interaction of StpA with the curved *micF–ompC* and β-lactamase (*bla)* promoter regions. Both probes were end-labelled with ^{32}P and incubated with the indicated concentrations of purified StpA at room temperature. Protein–DNA complexes were separated by 5% native polyacrylamide gel electrophoresis at 4°C. The migration of free *micF–ompC*- and *bla*-promoter probes are indicated.

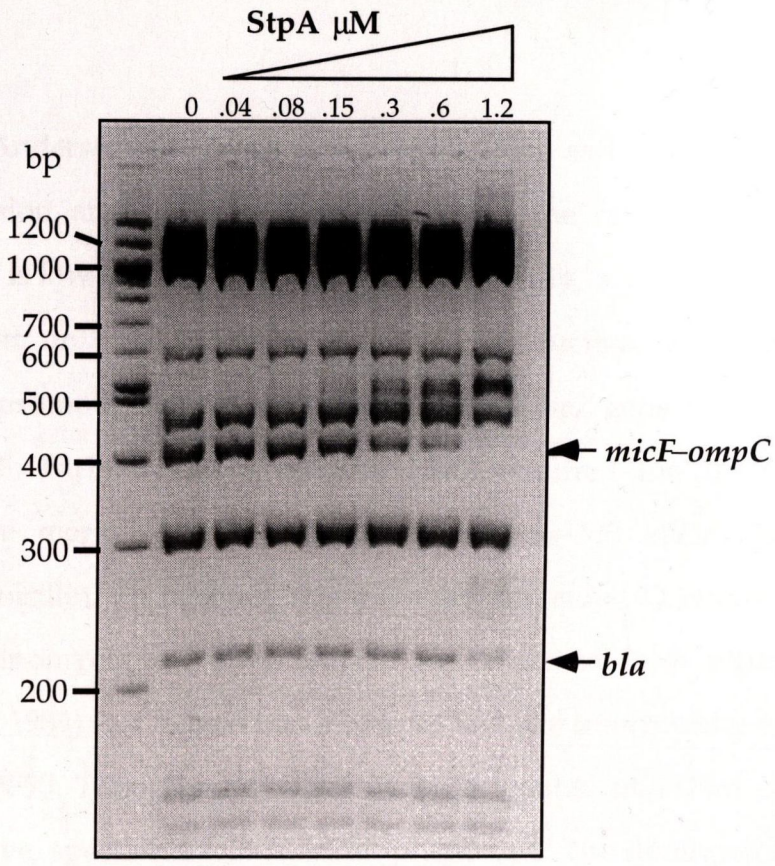

Fig. 3.12. StpA specifically interacts with the **micF–ompC** *promoter region*

Competitive gel mobility shift assay showing the specific binding of StpA with the *micF–ompC* promoter region. The DNA fragments from *Taq*I – *Ssp*I digested pBR322 were mixed with a 404-bp PCR amplimer of the *micF–ompC* promoter region and separated by migration through 3% molecular screening agarose. The mixtures were pre-incubated with purified StpA at the indicated concentrations. The migration of the free *micF–ompC* and β-lactamase (*bla*) promoter-containing fragments are indicated. The positions of molecular size markers are indicated in bp.

transcriptional level, a β-galactosidase assay was used to monitor changes in *micF* promoter activity.

Previous studies (Andersen *et al.*, 1989; Suzuki *et al.*, 1996) and results obtained from the primer extension analysis (Fig. 3.9) highlighted the fact that expression of chromosomal *micF* is low in wild-type *E. coli*. Consequently, a plasmid-based system was used to report on *micF* promoter activity. Construction of a transcriptional fusion of the *micF* promoter region to the promoterless *lacZ* gene in plasmid pQF50 (30 copies per cell; Farinha and Kropinski, 1990) required the insertion of an additional selective marker within pQF50, as the *hns-206* allele also encodes resistance to carbenicillin. To facilitate this a *Sma*I-blunt-ended Ω cassette encoding resistance to spectinomycin and streptomycin was digested from plasmid pHP45 (Pentki and Krisch, 1984) and ligated into a unique *Sca*I site interrupting the *bla* gene within plasmid pQF50. This plasmid which was designated pQFΩSm conferred a carbenicillin-sensitive, spectinomycin-resistant phenotype. The divergent *micF–ompC* promoter region (–335 to +58 with respect to the transcriptional start site for the 93-nt MicF RNA) was then amplified by PCR using the oligonucleotide pair micF6 / micF7 (Table 2.3). The oligonucleotides incorporated restriction enzyme recognition sites for *Nco*I and *Bgl*II respectively. Plasmid pQFΩSm and the 393-bp amplimer were digested with restriction enzymes *Nco*I and *Bgl*II to allow ligation, with the *micF* promoter reading into the *lacZ* gene. The sequence of the entire promoter containing fragment was verified, and resultant plasmid designated pMicF (Fig. 3.13).

Plasmid pMicF was transformed into wild-type MC4100, CJD1600 (*stpA*), PD32 (*hns*) and CJD1601 (*stpA hns*) backgrounds. All strains were grown to mid-exponential phase and β-galactosidase activity measured. To control for any effect of the *stpA* and *hns* alleles on pMicF copy number, 7-ml samples of culture were harvested and saved for plasmid DNA isolation, concomitantly with harvesting samples for the β-galactosidase assay. Plasmid DNA was extracted, linearised with *Afl*II, and analysed

by agarose gel electrophoresis. The results presented in Fig. 3.14A, revealed that the level of *micF–lacZ* expression in the wild-type and *stpA* mutant strains was approximately equal, as was pMicF copy number (Fig. 3.14A inset). This indicates that StpA does not regulate the activity of the *micF* promoter in the presence of H-NS. In the *hns* mutant, *micF–lacZ* expression was elevated by about 50% compared with wild-type. However, analysis of pMicF copy number showed that it had declined by about 3-fold in this background. Hence, the level of β-galactosidase was an underestimate; the adjusted value indicated a 4.5-fold activation of *micF* by the *hns* mutation (Fig. 3.14A, dark shading). In the *stpA hns* background *micF–lacZ* expression was elevated by 2.5-fold. However, pMicF copy number was also higher; the adjusted value indicated only a slight increase (1.7-fold) in *micF* promoter activity, much lower than that seen in the *hns* background. Thus, the strong reduction in *ompF* mRNA stability measured in the *stpA hns* strain was not due to an effect of StpA, either alone or in combination with H-NS, on *micF* transcription.

An effect of the *stpA* and *hns* alleles on plasmid copy number was intriguing. The reduction in pMicF copy number in the *hns* mutant may have been due to increased *stpA* expression, as the levels returned to slightly above wild-type in the *stpA hns* double mutant. To confirm that the effect of the alleles was specific to plasmid DNA, strain MC4100 and its *stpA* and *hns* mutant derivatives were grown to mid-exponential phase, and samples harvested for extraction of plasmid and chromosomal DNA. In addition, when the cultures reached OD_{600} 0.6, the number of viable colonies was confirmed to be approximately equal by plating out a sample of the culture onto LB-agar supplemented with spectinomycin. This was to ensure that the OD_{600} values were accurate (not influenced by the mucoid nature of *hns* mutant), and that there was not a large amount of anucleate cells in the culture. This is a phenotype that has been associated with *hns* mutants, albeit it at low frequency in rich broth (Kaidow *et al.*, 1995). Analysis of the chromosomal and plasmid DNAs revealed that the effect of *stpA* and *hns* was indeed specific to plasmid DNA, as there was no difference in chromosomal DNA levels (Fig. 3.14B).

Fig. 3.14. Effect of* stpA *and* hns *mutations on expression of a* micF–lacZ *transcriptional fusion

A. Histogram shows β-galactosidase activity in the wild-type strain MC4100 and *stpA*, *hns*, and *stpA hns* mutants carrying plasmid pMicF (*micF–lacZ* fusion). Strains were grown to mid-exponential phase in LB medium. Stippled shading shows data before normalisation for plasmid copy number; dark shading shows normalised data. Inset shows an agarose gel representing levels of linearised pMicF plasmid DNA extracted from each strain concomitantly with samples for the β-galactosidase assay (loaded in the same order as the histogram labelling). The data expressed in Miller units represent the average of four independent experiments and standard deviations were less than 12%.

B. Agarose gel showing the effect of *stpA* and *hns* mutations on plasmid DNA. Wild-type strain MC4100 and its *stpA*, *hns*, and *stpA hns* mutant derivatives were grown to mid-exponential phase in LB medium. Samples of culture were extracted for the isolation of plasmid and chromosomal DNAs. Samples (10 μl) of plasmid DNA (linearised) and 2 μl samples of chromosomal DNA from each background as indicated, were electrophoresed through a 0.8% agarose gel alongside molecular size markers (M). The position of the 10-kb DNA marker is indicated.

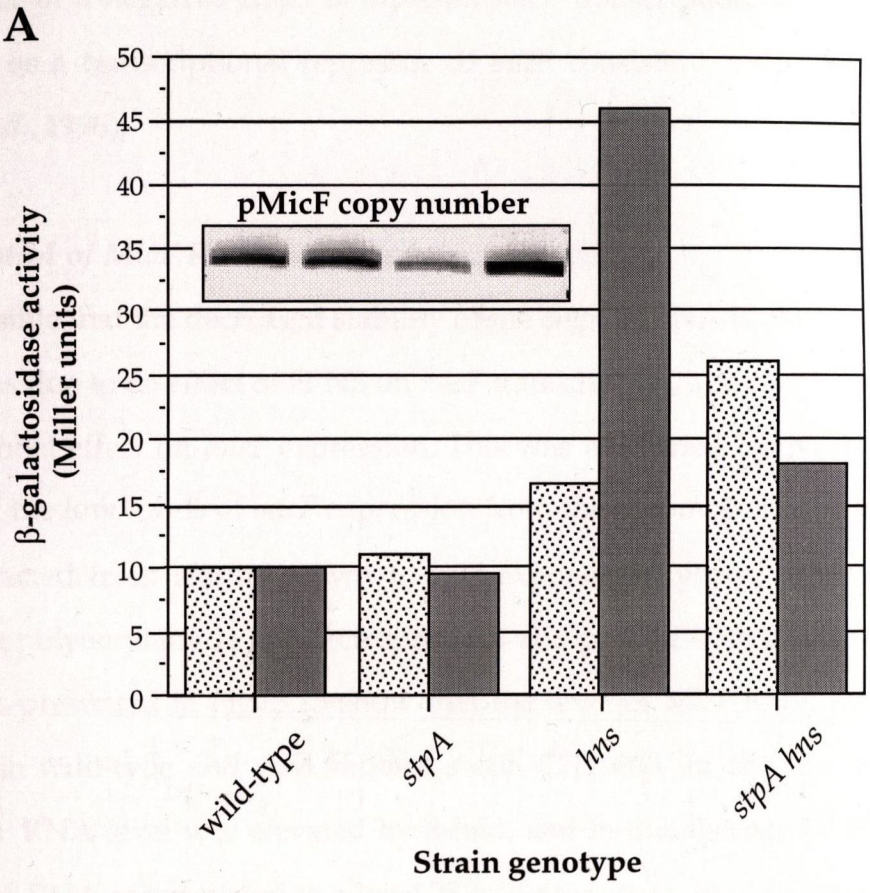
A
β-galactosidase activity (Miller units)
50
45
40
35
30
25
20
15
10
5
0
pMicF copy number
wild-type
stpA
hns
stpA hns
Strain genotype

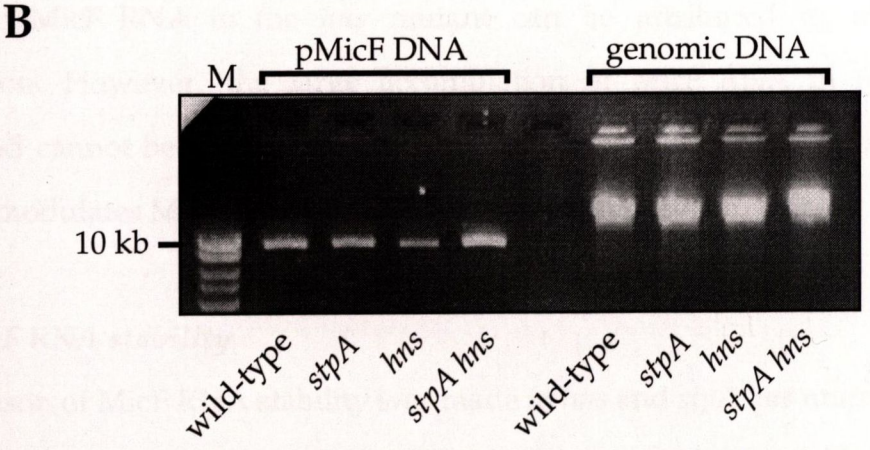
B
M
pMicF DNA
genomic DNA
10 kb
wild-type
stpA
hns
stpA hns
wild-type
stpA
hns
stpA hns

Although the changes in plasmid copy number complicated this analysis, there was no evidence of a negative effect of StpA on *micF* transcription, whereas H-NS was proven to be a transcriptional repressor of *micF* consistent with a previous report (Suzuki *et al.*, 1996).

3.2.9 *Control of MicF RNA*

It was possible that the decreased stability of the *ompF* mRNA in the *stpA hns* double mutant was due to an effect of H-NS on *micF* transcription, and that StpA had a post-transcriptional effect on *micF* expression. This was examined by Northern blotting. Because of the low levels of *micF* expression from the chromosome, 50 µg samples of RNA (extracted from strains grown to mid-exponential phase) were separated by denaturing polyacrylamide gel electrophoresis and probed with a specific riboprobe. The results presented in Fig. 3.15 show that the level of MicF RNA was similar and very low in wild-type and *stpA* mutant strain CJD1600. In the *hns* mutant strain PD32, MicF RNA level was elevated by 8-fold, and in the absence of both StpA and H-NS, MicF RNA accumulated to a level 25-fold more than that detected in the wild-type. This increase could be restored to near wild-type level with a plasmid encoding functional StpA. Taken together with the results from the *micF–lacZ* fusion, the increase in MicF RNA in the *hns* mutant can be attributed to transcriptional derepression. However, the large accumulation of MicF RNA in the *stpA hns* background cannot be accounted for by transcriptional derepression and indicates that StpA modulates MicF RNA at a post-transcriptional level.

3.2.10 *MicF RNA stability*

A comparison of MicF RNA stability was made in *hns* and *stpA hns* mutant strains by growing the strains to mid-exponential phase, prior to treatment with rifampicin to stop *de novo* transcription. Samples of culture for RNA extraction were harvested before and after rifampicin addition in a time-course experiment, and the MicF RNA transcript detected by Northern analysis (Fig. 3.16). The half-life of MicF RNA was measured to be 2.3 min in the *hns* mutant, whereas the antisense message was ≈ 5-

Fig. 3.15. Effect of StpA and H-NS on MicF RNA level

A. Northern blot showing MicF RNA levels from *E. coli* strains grown to mid-exponential phase in LB medium. Total RNA was isolated and electrophoresed through 8% polyacrylamide gel, electro-blotted to nylon membrane, and probed with a MicF-specific riboprobe. The relevant strain genotypes are indicated below each lane. pACYC184 is vector control and pYCStpA is derived from pACYC184 and encodes wild-type StpA.

B. Histogram showing densitometric analyses of the data in (**A**), expressed as a percentage of the most intense band shown. The experiment was performed three times and a representative gel and typical data are shown.

C. As a loading control the same RNA samples as used in (**A**) were probe with a *hupA*-specific riboprobe.

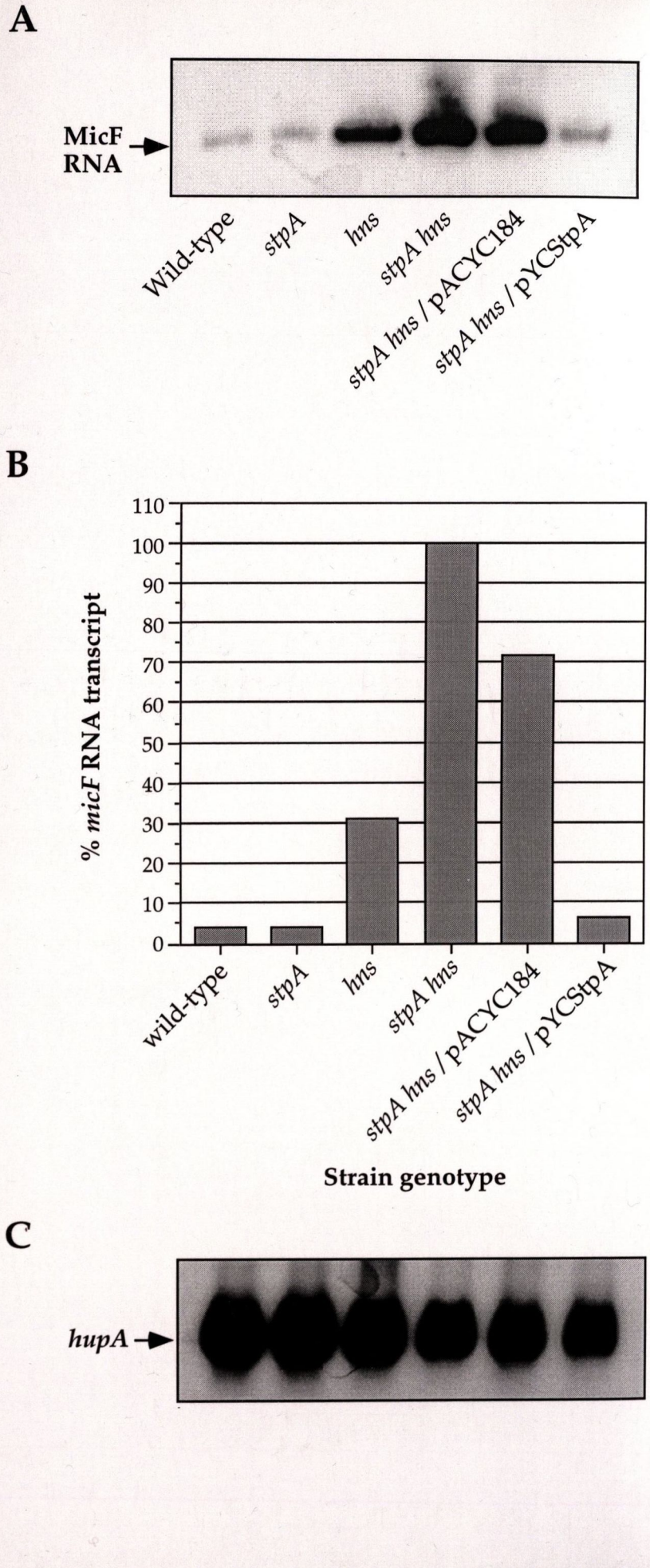
A
MicF RNA
Wild-type
stpA
hns
stpA hns
stpA hns / pACYC184
stpA hns / pYCStpA
B
% micF RNA transcript
110
100
90
80
70
60
50
40
30
20
10
0
wild-type
stpA
hns
stpA hns
stpA hns / pACYC184
stpA hns / pYCStpA
Strain genotype
C
hupA

Fig. 3.16. MicF RNA stability

A. Northern blot indicating the decay of MicF RNA in *hns* and *stpA hns* mutant strains. Strains PD32 (*hns*) and CJD1601 (*stpA hns*) were grown to mid-exponential phase and RNA isolated at fixed time points after rifampicin treatment to stop *de novo* transcription. Numbers above each lane refer to the time in minutes after (0, 2, 5, 10, 15, 20, 30) rifampicin treatment. Each blot has been exposed to film for different time periods and, consequently, comparisons between blots are not meaningful.

B. Semilogarithmic plot of MicF RNA decay based on densitometric analyses of the blots in (**A**); PD32 (open symbols), and CJD1601 (closed symbols). The half-life ($t_{1/2}$) calculated for MicF RNA in each strain background is indicated. The experiment was repeated three times and typical data and representative gels are shown.

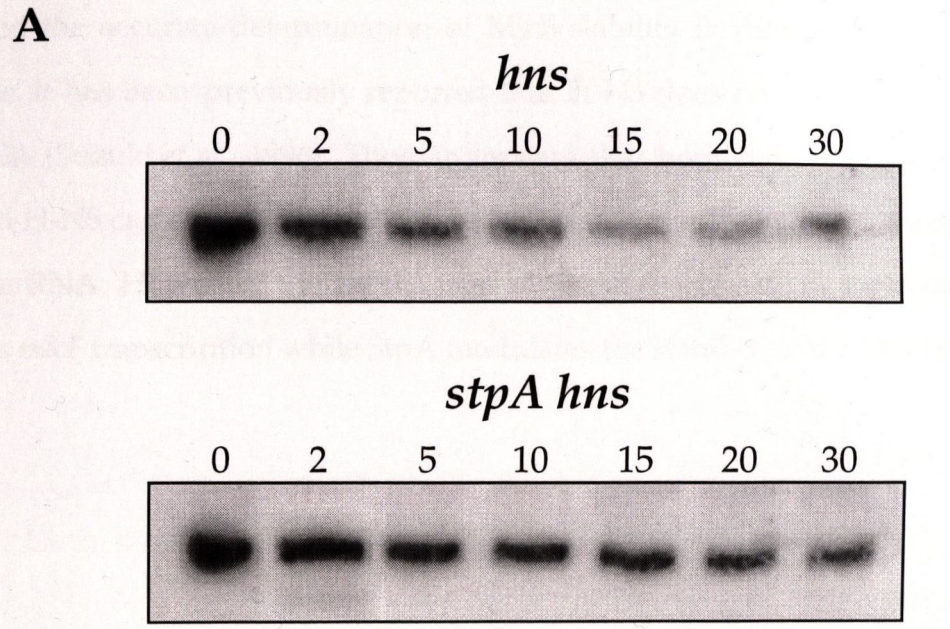
A
hns
0 2 5 10 15 20 30
stpA hns
0 2 5 10 15 20 30
B
100
10
1
% MicF RNA remaining
0 4 8 12 16 20 24 28 32
min
stpA hns
t1/2 = 12.6'
hns
t1/2 = 2.3'

fold more stable in the *stpA hns* background with a calculated half-life of 12.6 min. The low level of *micF* expression in the wild-type strain and in a *stpA* mutant strain prevented the accurate determination of MicF stability in these *hns*$^+$ backgrounds. However, it has been previously reported that H-NS does not affect the stability of MicF RNA (Suzuki *et al.*, 1996). Thus, it appears that both the paralogous proteins StpA and H-NS can effect OmpF porin expression primarily mediated through MicF antisense RNA. However, the mechanism at work is distinct in each case; H-NS regulates *micF* transcription while StpA modulates the stability of the MicF RNA.

3.3 *Discussion*

Following the identification of StpA as an intracellular analogue to H-NS (Zhang and Belfort, 1992), much work has been carried out to elucidate its cellular role. The results described in this chapter define a specific role for StpA in the expression of the outer membrane porin protein OmpF in *Escherichia coli*. This study was initiated following an analysis of the proteomic profiles for wild-type, *stpA*, *hns*, and *stpA hns* strains by two-dimensional gel electrophoresis (Free and Dorman, 1997a). Several spots were identified as being either up- or down-regulated in a *stpA hns* double-mutant strain when compared to a wild-type strain (Fig. 3.1). One of these spots, identified by N-terminal sequencing to be OmpF, was strongly down-regulated in the *stpA hns* background. In previous work, this porin was shown to be reduced in expression in the absence of H-NS (Graeme-Cook *et al.*, 1989; Suzuki *et al.*, 1996; Laurent-Winter *et al.*, 1997). The results of the proteomic study and of the one-dimensional analysis of the outer membrane proteins (Figs. 3.1 and 3.5A) indicated a very strong negative effect of the *stpA* mutation on top of any effect caused by mutating *hns*. This suggested that in addition to H-NS, StpA could influence OmpF expression.

StpA-dependent control of OmpF expression was primarily mediated via a novel regulatory mechanism involving destabilisation of the MicF antisense RNA. Post-transcriptional regulation of *ompF* via the *micF* locus has been well studied. Over-expression of MicF RNA inhibits translation of the *ompF* message and decreases the level of the *ompF* mRNA (Mizuno *et al.*, 1984; Andersen *et al.*, 1989). A specific hybridization between MicF RNA and the 5'-end of *ompF* mRNA (Schmidt *et al.*, 1995) and interaction with an 80-kDa MicF RNA-binding protein aids in this destabilisation (Andersen and Delihas, 1990). Previously, MicF RNA had been shown to accumulate in an *hns* mutant. This was attributed entirely to transcriptional derepression of *micF* in the absence of H-NS, as no effect on the stability of MicF RNA was observed (Suzuki *et al.*, 1996). The results of transcriptional data from a

plasmid-borne *micF–lacZ* fusion (Fig. 3.14), and Northern analysis of MicF RNA level (Fig. 3.15) in the *hns-206* background confirmed this view. In contrast, the 25-fold accumulation of MicF RNA in the *stpA hns* double mutant compared to the 8-fold increase in the *hns* background is not a consequence of further derepression of *micF* transcription (Figs. 3.14; 3.15). If anything, StpA is required for efficient transcription from this promoter, as β-galactosidase activity is actually lower in the *stpA hns* background than in the *hns* mutant. Instead, measurements of the stability of MicF RNA showed a clear 5-fold increase in the half-life of this message in the *stpA hns* double mutant compared to the *hns* single mutant (Fig. 3.16). It should be noted that mutations in *stpA* or *hns* did not have a general stabilising effect on all RNAs in the cell. Indeed, the *ompF* transcript was significantly more destabilised in the *stpA hns* background than in the *hns* single mutant (Fig. 3.8). This is presumably brought about by the difference in steady state MicF RNA levels in these backgrounds (Fig. 3.15). In addition the half-life of the *hupA* message was constant irrespective of the *stpA* or *hns* phenotype of the cell (Fig. 3.8B). Therefore, although StpA and H-NS both affect the accumulation of MicF RNA in the cell, H-NS regulates transcription of the *micF*, whereas StpA modulates the stability of the antisense RNA.

It is perhaps not surprising that StpA has an influence on the expression of OmpF at the level of RNA interactions. Although StpA and H-NS share 58% sequence identity at the protein level, StpA is a superior RNA chaperone than H-NS. RNA chaperones are defined as proteins that act within the cell to promote correct RNA folding by preventing misfolding and resolving misfolded forms (Herschlag, 1995). Indeed, StpA was initially identified on the basis of its ability to resolve misfolding and thereby to promote formation of the catalytically active structure of the self-splicing *td* intron of bacteriophage T4 (Zhang and Belfort 1992; Zhang *et al.*, 1995). Furthermore, StpA was shown to be 10-fold more efficient than H-NS at accelerating strand annealing of complementary RNA oligonucleotides and in stimulating a *trans*-splicing reaction of a group-I *td* intron *in vitro* (Zhang *et al.*, 1996; Cusick and Belfort, 1998; Clodi *et al.*, 1999). It is possible that in wild-type cells StpA can bind the MicF

RNA, maintaining or folding the RNA in a structure that impedes its interaction with the *ompF* mRNA. Alternatively, StpA may bind the *ompF* message and thereby prevent the interaction with MicF RNA. MicF RNA may then be a degraded by RNase E, previously shown to degrade MicF RNA *in vitro* (Schmidt and Delihas, 1995). The molecular mechanism of StpA-dependent control of OmpF expression via MicF RNA will be addressed in more detail in Chapter 4.

The effect of StpA on *micF* expression was only observed in an *hns*$^-$ background. There are two possible reasons for this. Firstly, expression of *micF* is low when cells are grown to mid-exponential phase in LB-broth (Figs. 3.13; 3.14; Suzuki *et al.*, 1996). Hence the substrate for StpA action is not abundant. Secondly, *stpA* expression is itself low in rich media when H-NS is present (Zhang *et al.*, 1996; Free and Dorman, 1997), so the StpA protein is not present at high levels. Perhaps StpA plays a role in modulating the expression of OmpF under different environmental conditions where H-NS repression of *stpA* and *micF* has been removed, or *stpA* and *micF* expression are otherwise induced. Indeed, *micF* expression can be induced by many environmental conditions including elevated growth temperature or changes in osmolarity (Andersen *et al.*, 1989), and unlike the *hns* gene, *stpA* expression also responds to these stimuli (Sondén and Uhlin, 1996; Free and Dorman, 1997). Exposure to ethanol (Andersen *et al.*, 1989), the superoxide-generating agent paraquat (Chou *et al.*, 1993; Pomposiello and Demple, 2000), ubiquitous cationic antimicrobial peptides (Oh *et al.*, 2000), or salicylate (Rosner *et al.*, 1991; Cohen *et al.*, 1988, 1993) also induce *micF* expression. Furthermore, StpA protein levels are induced by a variety of environmental conditions even in the presence of H-NS (environmental regulation of StpA expression is discussed in Chapter 5).

OmpC porin expression was previously shown to be derepressed in the absence of H-NS (Graeme-Cook *et al.*, 1989; Suzuki *et al.*, 1996; Laurent-Winter *et al.*, 1997). In this study, using the *hns-206* allele, an increase in *ompC* promoter activity (data not shown), and *ompC* mRNA was also detected (Fig. 3.6). The *micF* promoter which is

transcribed upstream from, and in the opposite direction to *ompC*, responded in a similar manner. Hence, *micF–lacZ* and MicF RNA levels were elevated in the *hns* mutant strain (Figs. 3.14; 3.15). Increased MicF RNA levels were transcribed from the *micF* P2 promoter, producing the 93-nt MicF RNA species, and there was no promoter bias for *micF* transcription initiation irrespective of the StpA or H-NS phenotype of the cell (Fig. 3.9). When the *stpA* and *hns* mutations were combined, both *ompC* mRNA and *micF–lacZ* levels were actually lower than in the *hns* single mutant (MicF RNA was higher; however, this is due to its increased stability). This suggests that StpA is required for efficient performance of the divergent *micF–ompC* promoters. Consistent with this, purified StpA bound with better affinity to a probe encompassing the *micF–ompC* promoters than to the control *bla* probe in two distinct gel mobility-shift assays (Figs. 3.11; 3.12). *In silico* analysis suggested that the *micF–ompC* divergent promoter region was curved and this was confirmed experimentally (Fig. 3.10). H-NS-like proteins show preferential binding to curved DNA regions (Bertin *et al.*, 1999; Sonnenfield *et al.*, 2001). It is conceivable that StpA, in addition to controlling OmpF expression, may modulate OmpC expression when its more dominant homologue is absent. StpA binding to the *micF–ompC* promoter region may be required for stimulating transcription. Alternatively this binding may occlude the interaction of other regulatory proteins.

Although the results from this study indicated that StpA-dependent *ompF* expression is primarily mediated via modulation of MicF RNA stability, it is likely that StpA makes other contributions to OmpF expression, particularly in the absence of H-NS. Data using the *ompF–lacZ* transcriptional fusion showed that the *stpA hns* double mutation caused a 64% reduction in β-galactosidase activity compared to the wild-type strain, whereas the *hns* mutation alone caused a 30% reduction (Table 3.1). The precise location of this *lacZ* fusion to the *ompF* gene is not well defined and hence it may not be a pure transcriptional fusion. However, others have observed a similar effect of *hns* mutations on *ompF–lacZ* activity using the same fusion (Graeme-Cook *et al.*, 1989) or a defined transcriptional fusion (Suzuki *et al.*, 1996). Therefore, it seems

that H-NS can subtly affect *ompF* promoter activity under standard growth conditions, to which StpA may also be able to contribute, perhaps under conditions when *stpA* expression is induced.

Additionally there was significant down-regulation of the *ompF* transcript and protein in *hns* and *stpA hns* backgrounds also deleted for *micF* (Figs. 3.6; 3.7). Down-regulated OmpF production via *micF* activation also occurs when bacteria are exposed to ethanol (Andersen *et al.*, 1989), salicylate (Rosner *et al.*, 1991) or mutated at the *tolC* locus (Misera and Reeves, 1987), and these effects are also only partly reversed in a *micF* mutant. Thus, in addition to *micF*, a second anti-*ompF* translational activity is implicated in the effects of StpA and H-NS (ethanol, salicylate and *tolC*) on OmpF production. This could be mediated through the 80-kDa MicF RNA-binding protein, which can also bind *ompF* mRNA *in vitro* and is necessary for *ompF* turnover (Andersen and Delihas, 1990). Alternatively the RNA-binding protein StpA could contribute to *ompF* mRNA stability directly, maintaining the transcript in a stable conformation and protecting it from the degradation machinery. It should also be remembered that the *micF* lesion itself significantly increases OmpC and slightly reduces OmpF porin levels (Matsuyama and Mizushima, 1985), which may obscure the *hns* and *stpA hns* effects on OmpF.

Nevertheless, it is likely that in wild-type *E. coli* the majority of H-NS- and StpA-dependent OmpF expression occurs through modulation of MicF RNA stability. The reciprocal expression profiles for the *ompF* and MicF RNAs observed in the *hns* and *stpA hns* mutant background are consistent with this (Figs. 3.6; 3.15). Additionally, both the accumulation of MicF RNA and the subsequent under-expressed level of OmpF in the outer membrane in the double mutant can be complemented by a plasmid encoding StpA (Figs. 3.15; 3.7). Complementation of the reduced OmpF level did not occur in a *micF* mutant.

Several DNA-binding proteins including H-NS (Suzuki *et al.*, 1996), HU (Painbeni *et al.*, 1997), Lrp (Ferrario *et al.*, 1995), Rob (Ariza *et al.*, 1995), SoxS (Chou *et al.*, 1993) and MarA (Cohen *et al.*, 1988; Jair *et al.*, 1995) are known to regulate *micF* promoter activity and consequently modulate *ompF* mRNA translation. The findings presented in this chapter also implicate a role for StpA in OmpF porin expression, and identify an important novel facet of this regulatory apparatus, namely, destabilisation of MicF antisense RNA by StpA.

A model summarising this work is presented in Fig. 3.17. In wild-type cells *micF* expression is low due to transcriptional repression mediated by H-NS (represented by squares), and any MicF RNA molecules that do appear are destabilised by StpA (represented by circles), either directly, or indirectly through another factor (X). In this way the *ompF* mRNA is unaffected by the antisense RNA and is efficiently translated, thus protected from degradation. When H-NS is removed from the cell (or *micF* expression is induced) the level of MicF antisense RNA increases. In the absence of StpA, MicF RNA is stable and remains available for base pairing with complementary sequences at the 5′-end of the *ompF* message. This RNA–RNA interaction renders the *ompF* message non-proficient for translation, and as a result it is more susceptible to endonucleolytic cleavage by cellular RNase (represented by scissors).

Fig. 3.17. Model summarising StpA and H-NS-dependent post-transcriptional regulation of OmpF expression

In wild-type cells, H-NS (illustrated by squares) represses transcription of the *micF* gene, leading to low levels of the MicF antisense RNA in the cell. It is proposed that StpA (illustrated by circles) destabilises the MicF RNA by direct interaction, or indirectly through another factor (X). This antagonises the interaction between MicF RNA and *ompF* mRNA allowing ribosome loading and efficient *ompF* mRNA translation. In the *stpA hns* double mutant, transcription of *micF* is enhanced due to the absence of H-NS, and the MicF RNA is more stable in the absence of StpA. Consequently the RNA–RNA interaction between MicF and *ompF* proceeds efficiently. In this way, the *ompF* message is rendered non-proficient for translation and is more susceptible to nucleolytic cleavage by cellular RNases (illustrated by scissors).

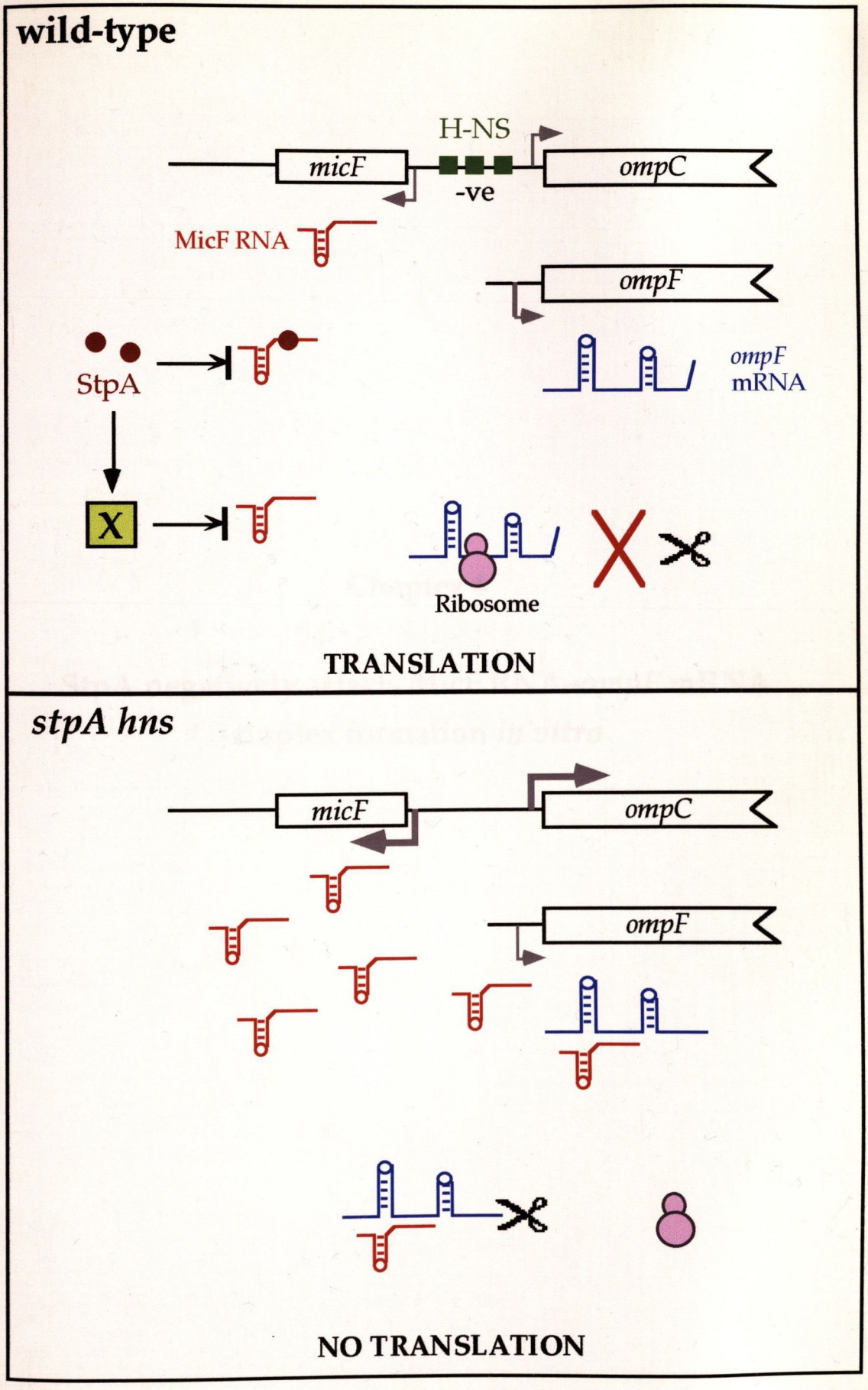
wild-type
H-NS
micF
ompC
-ve
MicF RNA
ompF
StpA
ompF
mRNA
X
Ribosome
TRANSLATION
stpA hns
micF
ompC
ompF
NO TRANSLATION

Chapter 4

StpA negatively affects MicF RNA–*ompF* mRNA duplex formation *in vitro*

4.1 *Introduction*

The 93-nt MicF RNA was the first antisense RNA to be discovered that is unlinked to its target gene (Mizuno *et al.*, 1984). MicF RNA post-transcriptionally regulates the expression of *ompF* in *Escherichia coli* in response to a variety of stresses (reviewed in Pratt *et al.*, 1996) by hybridising with the 5′-untranslated region (UTR) of the *ompF* mRNA via complementary sequences (Mizuno *et al.*, 1984; Andersen and Delihas, 1990). This results in an RNA–RNA complex where the Shine-Dalgarno and translation initiation start codon of the *ompF* mRNA are sequestered, thereby inhibiting translation (Schmidt *et al.*, 1995; Delihas *et al.*, 1997; Fig. 4.1C). In the presence of other factor(s) the *ompF* message is specifically destabilised and degraded (Andersen and Delihas, 1990).

4.1.1 *RNA structure*

All RNA molecules adopt elaborate secondary and tertiary structures that are intimately linked with their functions *in vivo*. These secondary structures include short *A*-form helical regions resulting from Watson–Crick pairing of complementary stretches interspersed with hairpins, mismatches, internal loops, bulges and pseudoknots. This framework of secondary structure is connected by tertiary associations including non-canonical (non-Watson–Crick) pairings, base triplets, and electrostatic, hydrophobic and hydrogen bonding interactions of complementary surfaces (Draper, 1996; Conn and Draper, 1998). Furthermore the compact three-dimensional conformation of RNA may be stabilised by, or depend upon, association with monovalent or divalent cations and water mediated interactions (Shiman and Draper, 2000).

4.1.2 *MicF RNA and* ompF-213 *mRNA structures*

Secondary structural models of the MicF RNA, the *ompF-213* mRNA (a 213-nt region of the 5′-end of the *ompF* mRNA) and the MicF RNA–*ompF-213* mRNA duplex have

been determined by enzymic and chemical probes of conformation and phylogenetic comparisons (Schmidt *et al.*, 1995; Delihas *et al.*, 1997). The deduced structures of MicF RNA and *ompF-213* mRNA are depicted in Fig. 4.1A and B. The model for *ompF-213* mRNA shows two major stem-loops and one minor stem-loop structures (Fig. 4.1A). Stem-loop I contains two non-canonical pairs (U24:G68 and C37:A54) while stem-loop II contains a U136:G174 non-canonical pair. Such mismatched bases create large localised changes in the *A*-form helical twist of the RNA molecule that can provide opportunities for tertiary folding and specific recognition by protein side chains (Conn and Draper, 1998; Cusack, 1999). The Shine-Dalgarno ribosome-binding site is part of stem-loop IA while the AUG translation initiation codon is in a single-stranded region. The structural model for the MicF RNA predicts two stem-loops with a long 27-nt single-stranded region at the 5′-end of the RNA (Fig. 4.1B). Two G:U non-canonical pairs are present, viz., G29:U50 in stem-loop I and G70:U82 in stem-loop II. The six unpaired uridine residues at the end of stem II form a typical Rho-independent transcriptional termination element.

4.1.3 *MicF RNA*–ompF *mRNA interaction*

The MicF antisense RNA was proposed to hybridise with the 5′-UTR of the *ompF* message via complementary sequences (Mizuno *et al.*, 1984; Andersen *et al.*, 1987). This was verified experimentally when a MicF RNA–*ompF-213* mRNA duplex was annealed *in vitro* (Andersen and Delihas, 1990). A line diagram depicting the RNA–RNA duplex determined from enzymic and chemical probing studies (Schmidt *et al.*, 1995) and revised by Delihas *et al.* (1997) to include phylogenetic comparisons, is shown in Fig. 4.1C. The RNA–RNA duplex is an imperfect 25-nt duplex which forms over nucleotides 1–33 of MicF RNA and nucleotides 95–120 of the *ompF* mRNA. Probing studies show that stem-loop I of MicF RNA, and the minor stem-loop IA of *ompF* mRNA, must unfold to allow formation of the duplex. When complexed with MicF RNA, the *ompF* message is inefficiently translated as the ribosome-binding site and AUG translation initiation codon (which must be free to

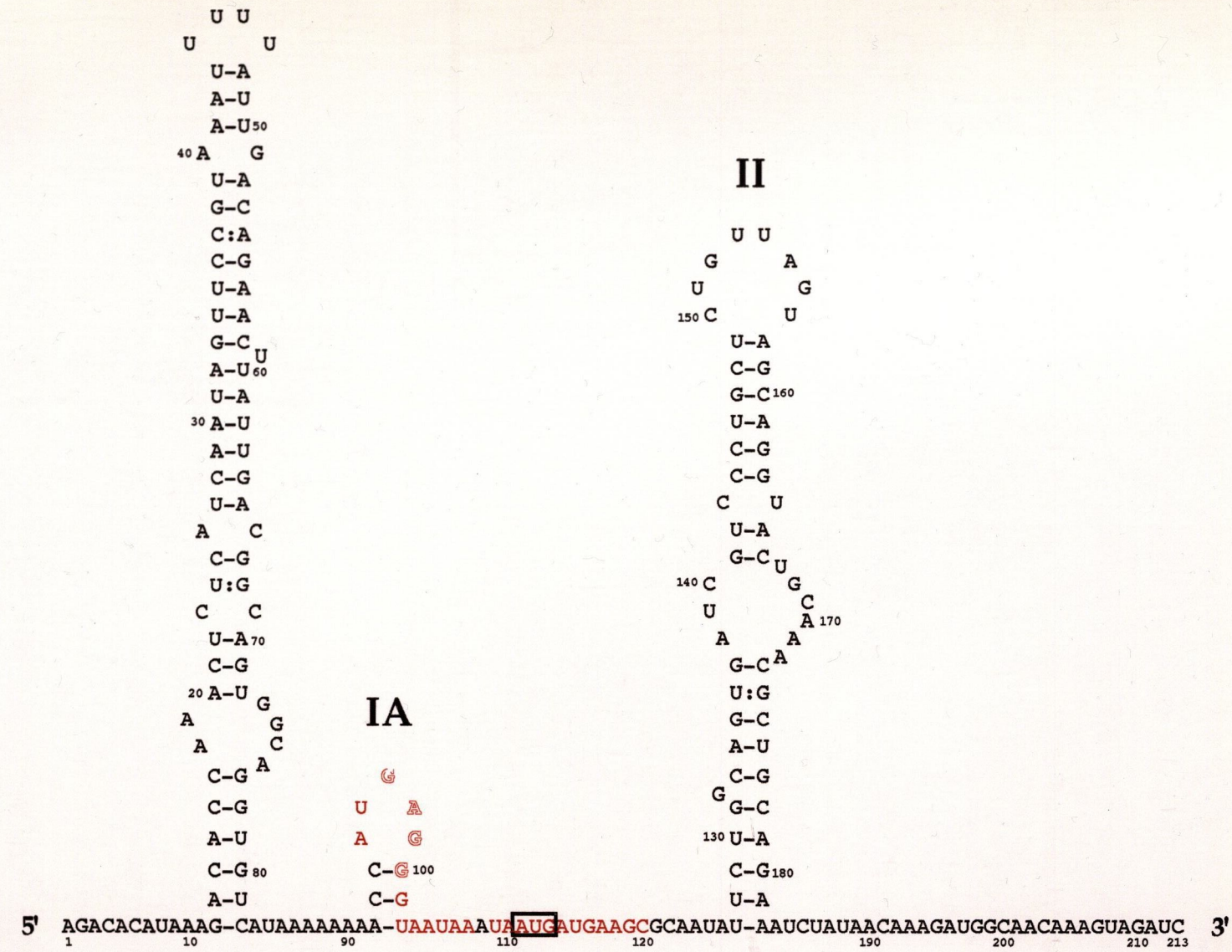
A
I
II
IA
5' AGACACAUAAAG-CAUAAAAAAAA-UAAUAAAUAAUGAUGAAGCGCAAUAU-AAUCUAUAACAAAGAUGGCAACAAAGUAGAUC 3'
1
10
90
110
120
190
200
210
213

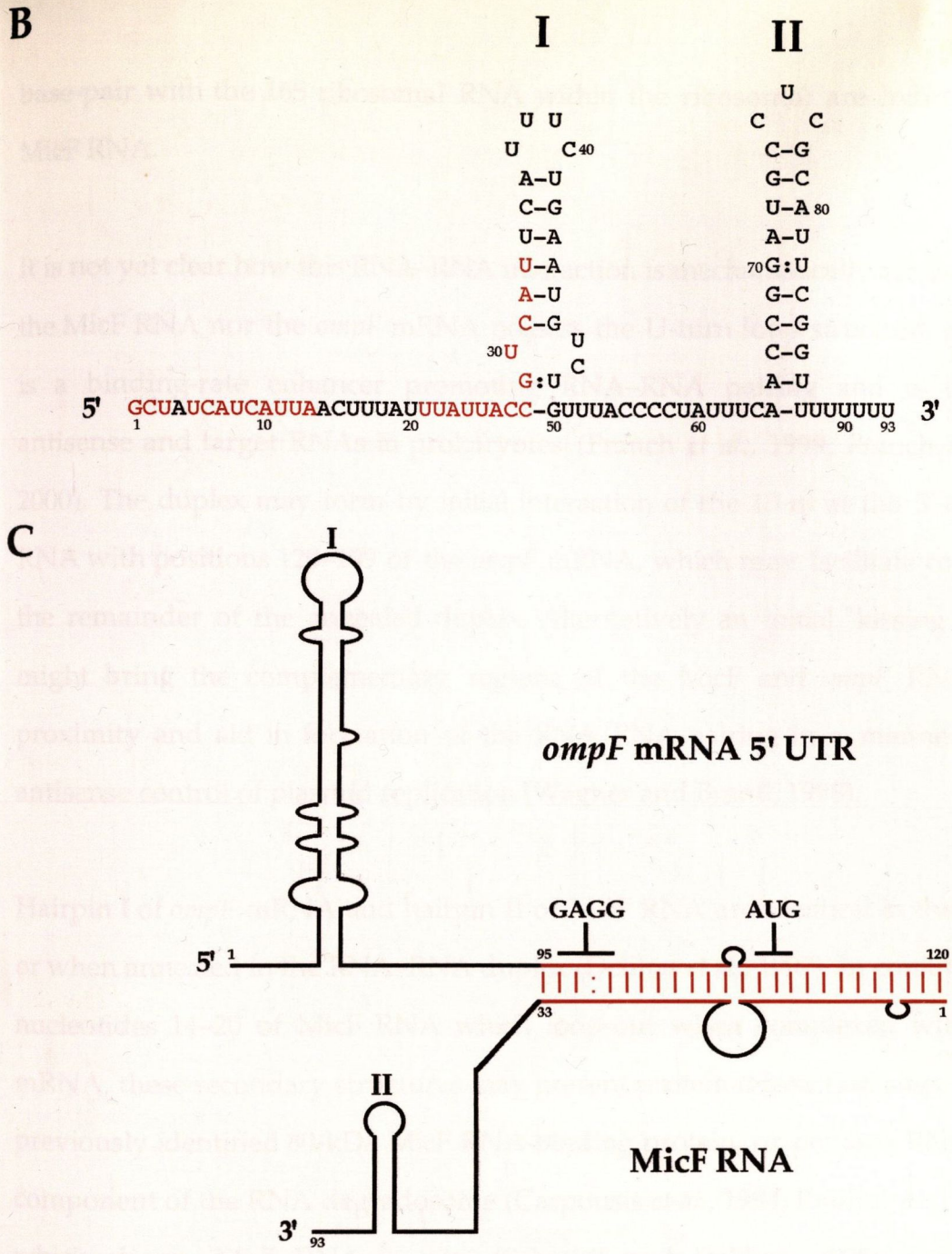

Fig. 4.1. RNA secondary structures

The proposed secondary structural models of the *ompF-213* mRNA and the 93 nt MicF RNA are shown in (**A**) and (**B**), respectively. Regions of MicF RNA and *ompF-213* mRNA indicated in red anneal to form the MicF RNA–*ompF-213* mRNA duplex as depicted by the line diagram in (**C**). The *ompF-213* mRNA model shows the Shine-Dalgarno sequence GAGG indicated by outline lettering and the translation initiation codon AUG is boxed. Stem-loops are labelled above the appropriate structure, as is the position of every tenth nucleotide. Watson–Crick pairings are shown by the minus sign (-), whereas non-canonical pairings are indicated by a colon (:). The models shown were deduced by chemical and enzymic probes of conformation (Schmidt *et al.*, 1990) and modified by Delihas *et al.* (1997) to include phylogenetic comparisons.

base-pair with the 16S ribosomal RNA within the ribosome) are hybridised to the MicF RNA.

It is not yet clear how this RNA–RNA interaction is mechanistically achieved. Neither the MicF RNA nor the *ompF* mRNA possess the U-turn loop structural element that is a binding-rate enhancer promoting RNA–RNA pairing and is common in antisense and target RNAs in prokaryotes (Franch *et al.*, 1999; Franch and Gerdes, 2000). The duplex may form by initial interaction of the 13-nt at the 5'-end of MicF RNA with positions 120–109 of the *ompF* mRNA, which may facilitate completion of the remainder of the annealed duplex. Alternatively an initial 'kissing interaction' might bring the complementary regions of the MicF and *ompF* RNAs in close proximity and aid in formation of the RNA–RNA pairing in a manner similar to antisense control of plasmid replication (Wagner and Brantl, 1998).

Hairpin I of *ompF* mRNA and hairpin II of MicF RNA are identical in the free RNAs or when annealed in the RNA–RNA duplex (Delihas *et al.*, 1997). In combination with nucleotides 14–20 of MicF RNA which loop-out when complexed with the *ompF* mRNA, these secondary structures may present protein interaction sites. Indeed, the previously identified 80-kDa MicF RNA-binding protein, or perhaps RNase E, a key component of the RNA degradosome (Carpousis *et al.*, 1994; Rauhut and Klug, 1999) which cleaves MicF RNA *in vitro* (Schmidt and Delihas, 1995), may use such structures as docking sites.

The H-NS-like StpA protein was initially identified as an RNA chaperone able to resolve misfolding and thereby to promote formation of the catalytically active structure of the self-splicing group-I *td* intron (Zhang *et al.*, 1995). Importantly StpA can also function as a true RNA chaperone *in vivo* (Clodi *et al.*, 1999) and is superior to H-NS in RNA-related activities (Zhang *et al.*, 1996; Cusick and Belfort, 1998).

A series of *in vivo* experiments identified a role for StpA in modulating MicF RNA stability, which in turn controls *ompF* mRNA translation and stability (Chapter 3). Given that StpA is an RNA-binding protein with chaperone activity, it was therefore of interest to investigate if purified StpA protein could directly interact with the MicF or *ompF* transcripts, and consequently influence formation of the MicF RNA–*ompF* mRNA duplex *in vitro*.

4.2 *Results*

4.2.1 *Purification of StpA*

As a prelude to monitoring StpA–RNA interactions the StpA protein was firstly overexpressed using the T7 RNA polymerase expression system (Studier and Moffatt, 1986) and purified by affinity chromatography. Plasmid pAF311 (Table 2.2) was used and harbours the *stpA* gene with six C-terminal histidines cloned downstream of a T7-inducible promoter. As monitored by SDS-PAGE, recombinant StpA-H6 was overexpressed to a high level and approximately 80% of induced StpA remained in the soluble supernatant fraction (Fig. 4.2A and data not shown). StpA was purified from this fraction by nickel affinity chromatography, and was retained in the column, as little StpA was evident in the flow-through fraction (Fig. 4.2A). Bound StpA was eluted with 500-mM imidazole, which out-competes the C-terminal histidines for the Ni^{2+}. In this way only full-length StpA protein was purified and was judged to be greater than 98% pure by Coomassie staining (Fig. 4.2A). The StpA protein was dialysed into a suitable storage buffer and its integrity, purity and concentration confirmed by SDS-PAGE (Fig. 4.2B).

Prior to use in RNA gel-shift assays a series of tests was performed to ensure that purified StpA had functional properties *in vitro*, similar to those associated with the protein *in vivo*. Thus, the ability of StpA to oligomerise (Williams *et al.*, 1996; Bertin *et al.*, 1999) and its proficiency for nucleic acid interactions (Cusick and Belfort, 1998; Bertin *et al.*, 1999) were tested (see below). In addition the *in vivo* function of recombinant StpA was analysed to ensure that the six C-terminal histidines did not perturb the tertiary structure and hence functioning of the protein.

4.2.2 *Oligomerisation of StpA*

In vitro oligomerisation of StpA-H6 was carried in a cross-linking experiment using a mixture of the zero-length chemical cross-linker 1-ethyl-3-(3′-dimethylaminopropyl) carbodiimide (EDC), and the catalyst *N*-hydroxy-succinimide (NHS) (Grabarek and

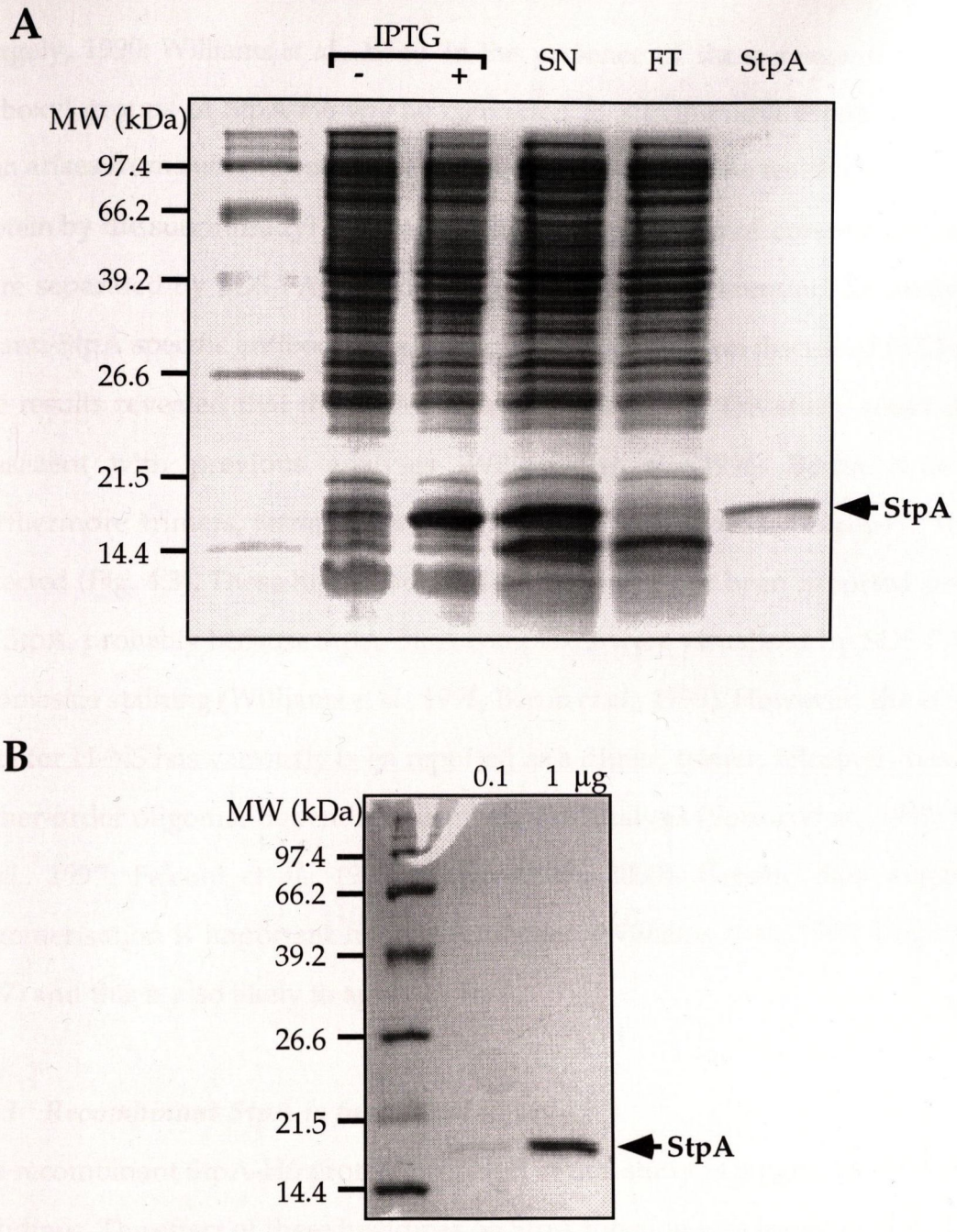

*Fig. 4.2. **Purification of StpA***

A. SDS-PAGE analysis of overexpression and purification of StpA. Strain BL21(DE3)/pDIA17 harbouring the StpA-overexpressing plasmid pAF311 was grown to mid-exponential phase and *stpA* expression induced with the addition of 0.5-mM IPTG. Protein samples of induced (+) and uninduced (-) culture, the soluble supernatent fraction (SN) prior to passage over a Ni^{2+}-charged column, and the flow-through fraction (FT) are all indicated above the gel. Purified StpA is also shown.

B. SDS-PAGE analysis of 0.1 and 1 µg samples of purified StpA to confirm protein concentration, purity and integrity.

Gergely, 1990; Williams *et al.*, 1996). In the presence of these reagents some of the carboxyl groups of StpA-H6 will be converted to succinimidyl esters. Cross-linking then arises from substitution of the ε-amino group of a lysine residue from one StpA protein by the succinimidyl ester of another. The products of cross-linking reactions were separated by SDS-PAGE and detected by Western immunoblot analysis with an anti-StpA specific antibody (Fig. 4.3; antibody preparation discussed in Chapter 5). The results revealed that the StpA-H6 protein purified in this study could dimerise, consistent with previous analyses (Williams *et al.*, 1996; Bertin *et al.*, 1999). Furthermore trimers, tetramers and higher-order oligomers of StpA-H6 were also detected (Fig. 4.3). These higher-order oligomers have not been reported previously for StpA, probably because StpA–StpA complexes were visualised by SDS-PAGE and Coomassie staining (Williams *et al.*, 1996; Bertin *et al.*, 1999). However, the oligomeric state for H-NS has variously been reported as a dimer, trimer, tetramer, hexamer or higher-order oligomer depending on method of analysis (Spurio *et al.*, 1997; Ueguchi *et al.*, 1997; Falconi *et al.*, 1998; Smyth *et al.*, 2000). Genetic data suggest that oligomerisation is important for H-NS function (Williams *et al.*, 1996; Ueguchi *et al.*, 1997) and this is also likely to apply to StpA.

4.2.3 *Recombinant StpA is functional* in vivo

The recombinant StpA-H6 protein prepared in this study is tagged by six C-terminal histidines. The effect of these histidines on StpA function was tested *in vivo*. The wild-type *stpA* gene and the *stpA* gene with the 3'-flanking histidine sequence were amplified by PCR and sub-cloned down-stream of the arabinose-inducible promoter in plasmid pBAD33 (Guzman *et al.*, 1995). The resulting plasmids, pBADStpA and pBADStpAH6, were transformed into the *stpA hns* double mutant strain CJD1125. This strain harbours a chromosomal *proU–lacZ* fusion that allows changes in transcription arising from the *proU* promoter to be monitored. The absence of StpA and H-NS result in derepressed *proU* expression. However, *proU* transcription can be partially repressed by a plasmid encoding functional StpA (Free *et al.*, 1998). Strain CJD1125 harbouring pBAD33 (control), pBADStpA, and pBADStpAH6 were grown

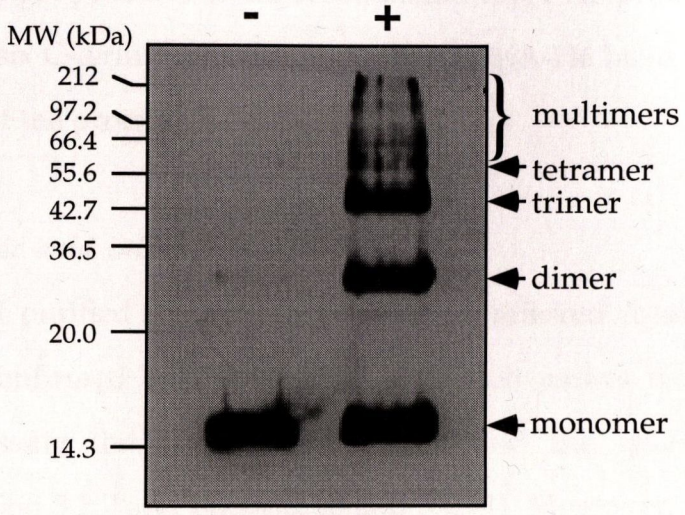

Fig. 4.3. Oligomerisation of StpA

Analysis of the *in vitro* protein–protein interactions of purified StpA by chemical cross-linking. StpA (100 ng) was incubated with (+) or without (-) EDC–NHS cross-linking reagents for 1 h at room temperature. Samples were separated by SDS-PAGE, transferred to nitrocellulose membrane and detected by Western immunoblotting with an anti-StpA-specific antibody. StpA monomers, dimers, trimers and tetramers and higher–order multimers are indicated.

in the absence and presence of arabinose (0.13-mM and 1.3-mM) and the induction of StpA and StpA-H6 monitored by Western immunoblot analysis (Fig. 4.4A). Both StpA and StpAH6 were expressed to a similar level. Analysis of LacZ expression from these strains showed that the *proU* promoter was repressed to a similar level by the wild-type StpA protein and the recombinant StpA-H6 protein (Fig. 4.4B). This confirms that the six C-terminal histidines flanking StpA-H6 have no effect on the *in vivo* functioning of the protein.

4.2.4 *StpA-nucleic acid interactions* in vitro

The proficiency of purified StpA-H6 (from here on referred to as StpA) to interact with DNA was confirmed by DNA gel mobility-shift assays using PCR-amplified probes encompassing the *bla*-promoter region and the *micF–ompC* promoters (described in Section 3.2.7 and Figs. 3.2.10 and 3.2.11). Moreover, purified StpA was also proficient for RNA associations as analysed by the RNA gel mobility-shift assay. RNA probes corresponding to the 93-nt MicF RNA, *ompF*-213 mRNA (213-nt 5′-end region of the *ompF* mRNA) and *ompC-268* mRNA (268-nt 5′-end region of the *ompC* mRNA), were synthesised by *in vitro* transcription using the corresponding PCR-amplified DNA regions as templates. Each template encompassed the T7 promoter recognition sequence {5′-TAATACGACTCACTATAG-3′}, allowing for efficient *in vitro* transcription with T7 RNA polymerase in the presence of [α-^{32}P]dUTP. RNA probes were incubated with increasing concentrations of StpA and protein–RNA complexes separated by native polyacrylamide gel electrophoresis and visualised by autoradiography (Fig. 4.5A). The results revealed that the purified StpA protein associated with RNA consistent with previous analyses (Zhang *et al.*, 1996; Cusick and Belfort, 1998). Additionally, no nuclease contamination was evident. This criterion was of particular importance when studying protein–RNA interactions.

Recombinant H-NS-H6 (a gift from S. Rimsky; Fig. 4.5B) was purified in a similar manner to that described in Section 4.2.1, and was also free for contaminating nucleases (data not shown). It was proficient for DNA binding (Bertin *et al.*, 1999) and

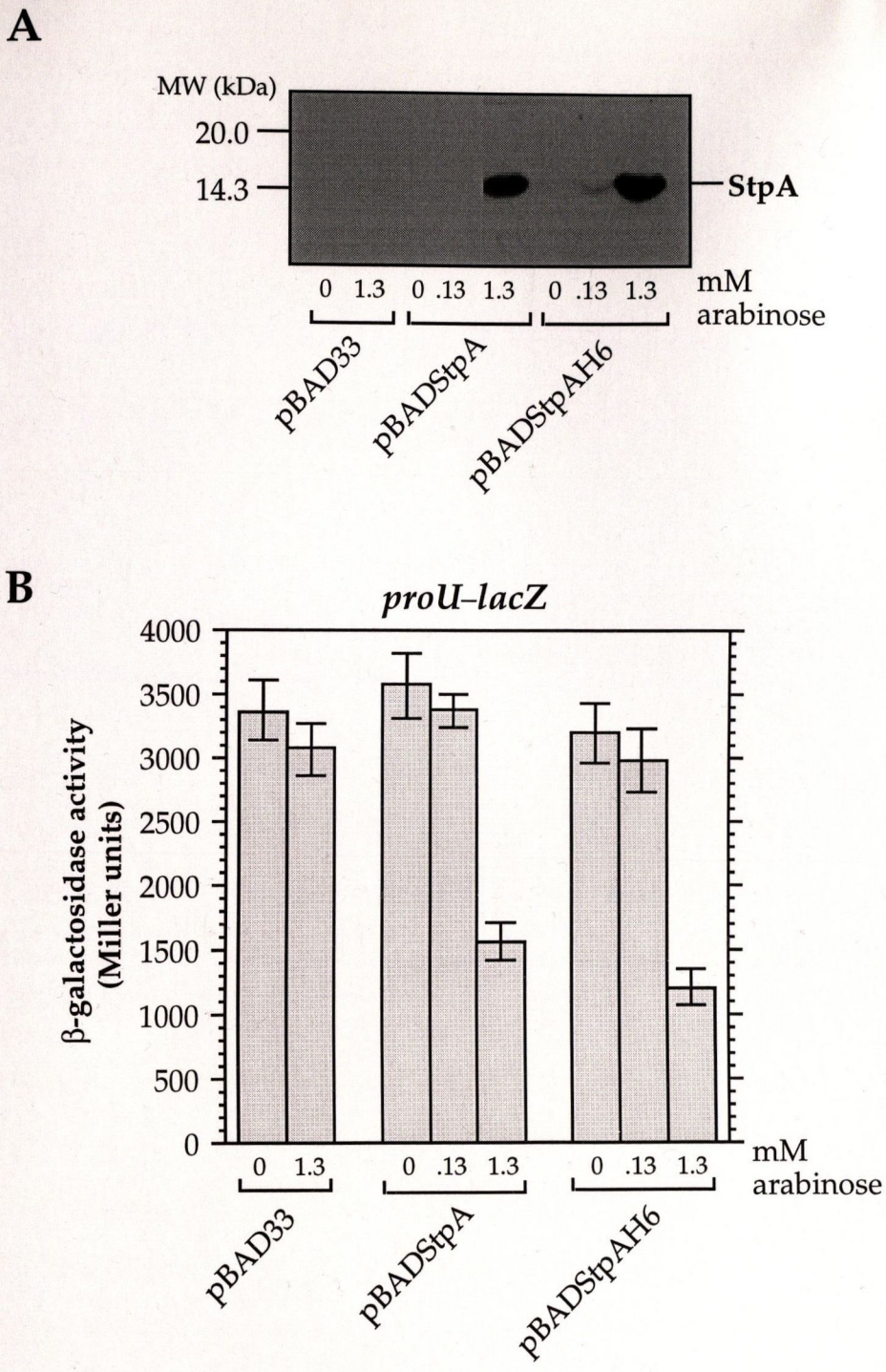

Fig. 4.4. ***Recombinant StpAH6 is functional*** **in vivo**

A. Over-expression of StpA and StpAH6 *in vivo.* Plasmids pBAD33 (control) pBADStpA and pBADStpAH6 were transformed into the *stpA hns* double mutant strain CJD1125 and grown overnight in LB broth in the absence (lane = 0) and presence (lanes = 0.13 and 1.3) of arabinose (0.13-mM and 1.3-mM) as indicated. Total protein cell extracts (normalised to the OD_{600} values) were separated by SDS-PAGE and probed with StpA-specific antiserum in Western immunobloting. The StpA antibody is described in Chapter 5.

B. Histogram shows β-galactosidase activity arising from a chromosomal *proU–lacZ* fusion, from samples of the same cultures as used in (**A**). The data expressed in Miller units represent the average of three independent experiments.

***Fig. 4.5. StpA–RNA interactions* in vitro**

A. RNA gel-shift assay. The 93-nt MicF RNA, and the *ompF-213* and *ompC-268* RNA probes were synthesised and labelled with ^{32}P by *in vitro* transcription and purified by phenol–chloroform extractions. Approximately 3 ng of each probe was incubated with increasing concentrations of purified StpA (0.1–0.8 μM) for 15 min at 37°C. Protein–RNA complexes were separated by migration through a 10% polyacrylamide gel and visualised by autoradiography.

B. Determination of StpA and H-NS protein concentrations. His-tag-purified H-NS (gift from S. Rimsky) and StpA (~0.25 and 0.5 μg) were separated by SDS-PAGE alongside a standard amount (0.25 and 0.5 μg) of lysozyme and BSA. Densitometric analyses of the protein bands was one method used for the determination of StpA and H-NS protein concentrations, which was required for comparative RNA gel-shift assays.

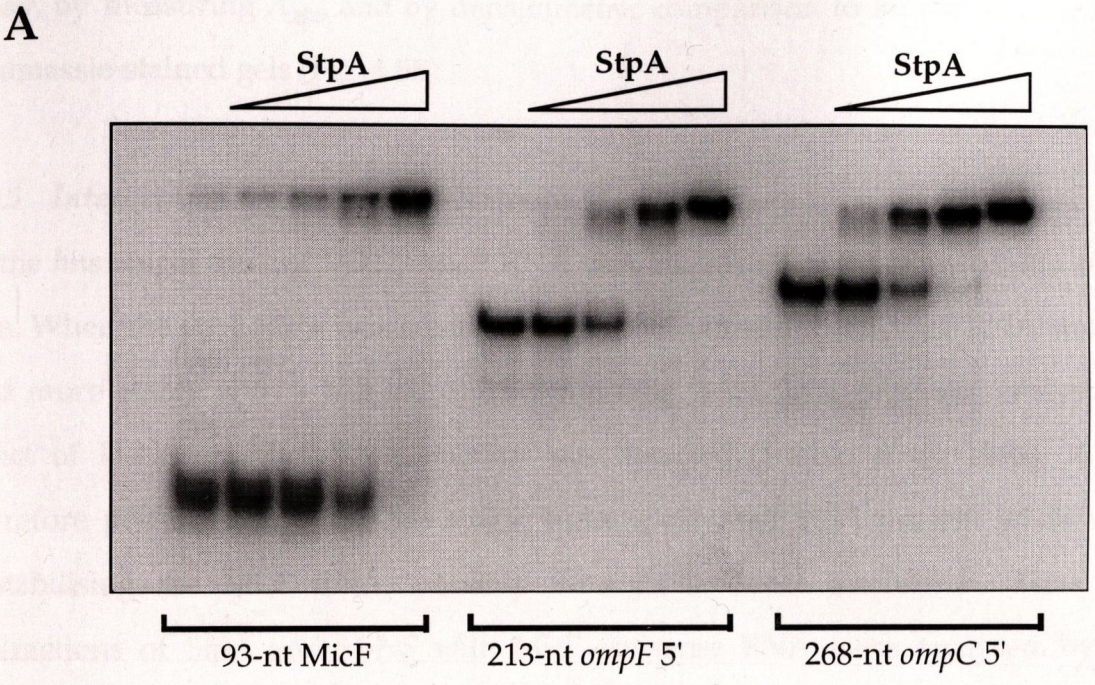
A
StpA
StpA
StpA
93-nt MicF
213-nt ompF 5'
268-nt ompC 5'

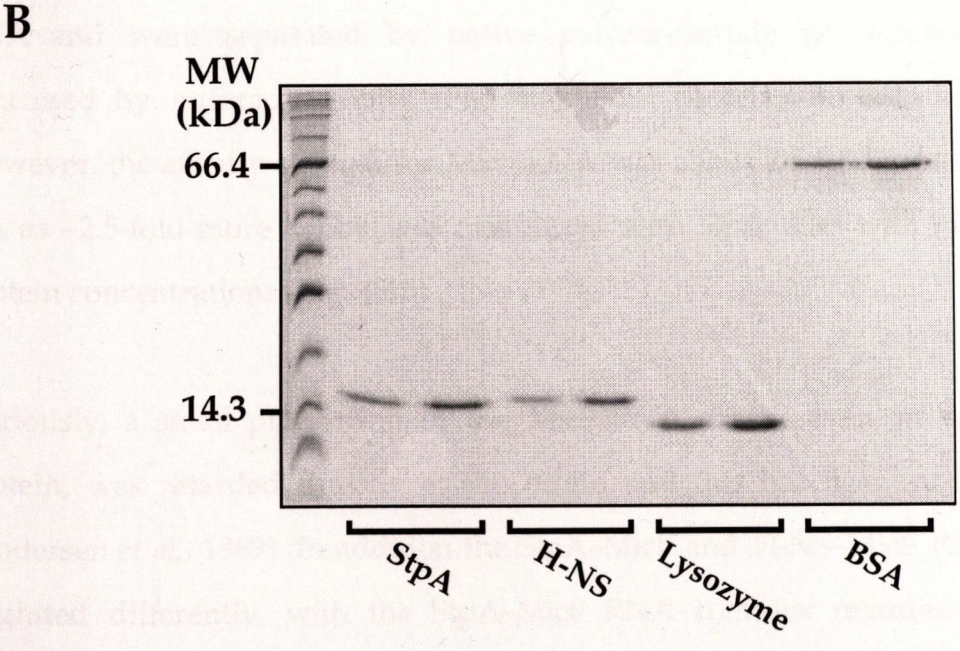
B
MW
(kDa)
66.4
14.3
StpA
H-NS
Lysozyme
BSA

could oligomerise *in vitro* (Williams *et al.*, 1996). For comparative use in RNA gel-shift assays StpA and H-NS concentrations were quantified using the Bio-Rad protein assay, by measuring A_{280}, and by densitometric comparison to known standards in Coomassie-stained gels (Fig. 4.5B).

4.2.5 *Interactions of StpA and H-NS with* MicF *RNA*

In the *hns* single mutant PD32, MicF RNA was calculated to have a half-life of 2.3 min. When the *stpA* allele was combined with the *hns* mutation, MicF RNA was ~5-fold more stable with a half-life of 12.6 min (Fig. 3.16). In a previous analysis no effect of H-NS on MicF RNA stability was detected (Suzuki *et al.*, 1996). It was therefore possible that in the *hns* single mutant, elevated StpA protein levels were destabilising the MicF RNA, possibly through a direct interaction. Thus, the interactions of StpA and H-NS with MicF antisense RNA were analysed by gel mobility-shift assay. The 93-nt MicF RNA (Fig. 4.1B) was synthesised and labelled with ^{32}P by *in vitro* transcription and incubated with identical, increasing concentrations of StpA or H-NS. Protein–RNA complexes migrate slower than free RNA and were separated by native polyacrylamide gel electrophoresis and visualised by autoradiography (Fig. 4.6). Both proteins bound the MicF RNA. However, the affinity of StpA for MicF RNA was about 2.5-fold greater than for H-NS, as ~2.5-fold more probe was complexed with StpA than with H-NS at similar protein concentrations (Fig. 4.6B).

Curiously, a small proportion of the MicF RNA probe, even in the absence of protein, was retarded directly at the origin and this has been noted previously (Andersen *et al.*, 1989). In addition the StpA–MicF and H-NS–MicF RNA complexes migrated differently, with the StpA–MicF RNA complex retarded in the wells, whereas the H-NS–MicF RNA complex migrated out of the wells. This was apparent even if the gels were electrophoresed for longer and may reflect higher-order conformations present in the 93-nt MicF RNAs. It is possible that StpA can chaperone

Fig. 4.6. Interactions of StpA and H-NS with **MicF** *RNA*

A. Gel mobility-shift analysis of StpA and H-NS interactions with the 93-nt MicF RNA. Purified StpA and H-NS at the indicated concentrations were incubated with ^{32}P-labelled MicF RNA for 15 min at room temperature in a buffer containing a 100-fold excess of competitor tRNA. Bound and free RNAs were separated by polyacrylamide gel electrophoresis and visualised by autoradiography. The position of migration of free MicF RNA is shown, and the top of the gel is indicated by the star symbol (*).

B. Graph showing densitometric analyses tracing the formation of the StpA–MicF RNA (broken line) and H-NS–MicF RNA (full line) complexes in (**A**), expressed as a percentage of the most intense protein–RNA complex shown.

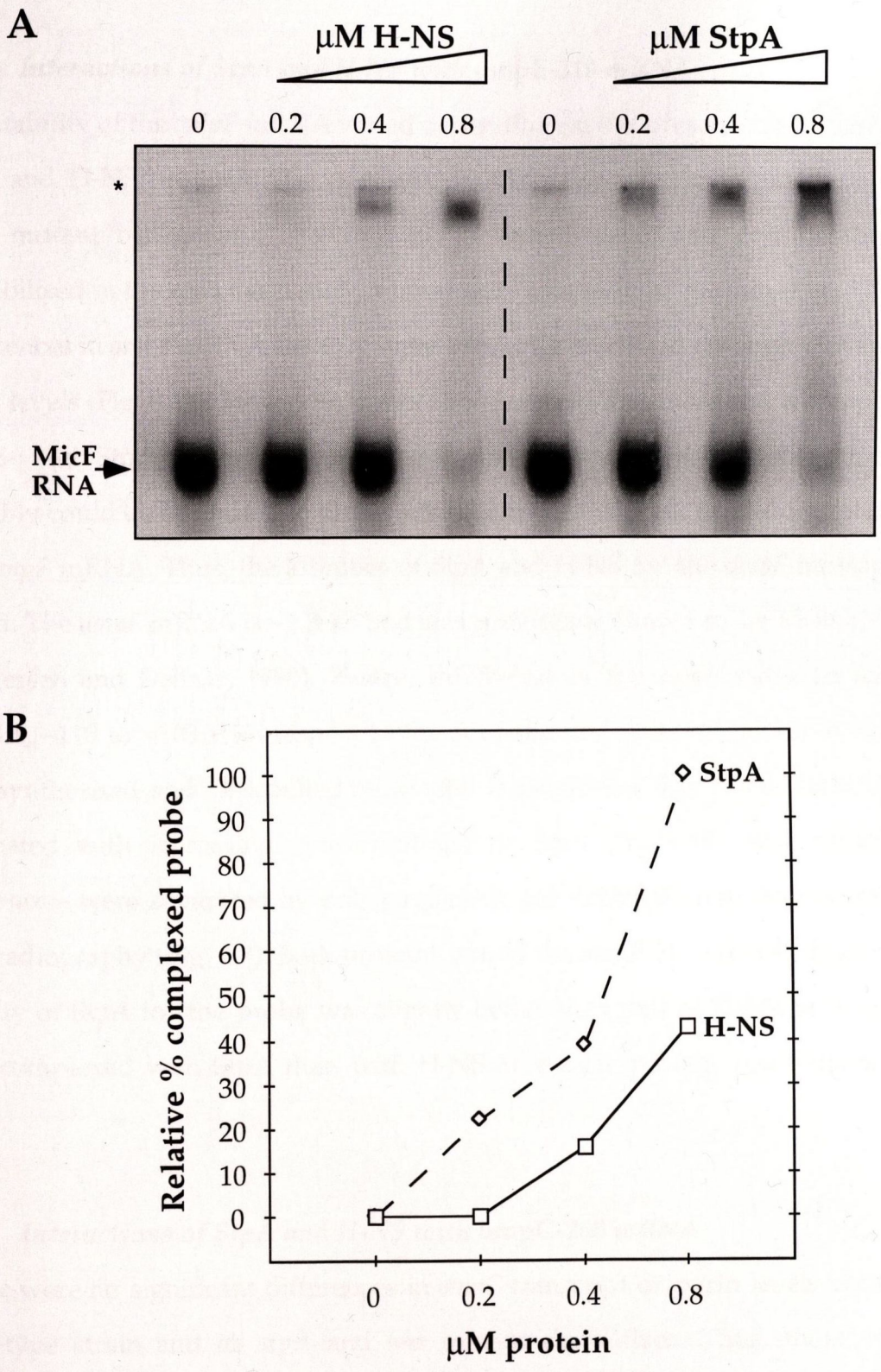
A
μM H-NS
μM StpA
0
0.2
0.4
0.8
0
0.2
0.4
0.8
*
MicF
RNA
B
Relative % complexed probe
100
90
80
70
60
50
40
30
20
10
0
StpA
H-NS
0
0.2
0.4
0.8
μM protein

the MicF RNA into a secondary structure with exposed nucleotide faces that allow the formation of these higher-order MicF–MicF RNA structures.

4.2.6 *Interactions of StpA and H-NS with* ompF-213 *mRNA*

The stability of the *ompF* mRNA varied depending on the presence or absence of the StpA and H-NS proteins. The calculated half-life was ~8 min in wild-type and the *stpA* mutant background, 3.9 min in an *hns* mutant, and considerably more destabilised in the *stpA hns* double mutant with a half life of 1.6 min (Fig. 3.8). These differences in *ompF* mRNA stability were primarily mediated through elevated MicF RNA levels (Fig. 3.15). However, it was also observed that there was a component of H-NS- and StpA-dependent *ompF* expression that was *micF*-independent, which possibly could be attributed to direct interactions of the StpA or H-NS proteins with the *ompF* mRNA. Thus, the affinities of StpA and H-NS for the *ompF* message were tested. The *ompF* mRNA is ~1.3-kb and was previously shown to be unstable *in vitro* (Andersen and Delihas, 1990). Hence, the 5'-end of the *ompF* message (*ompF-213* mRNA, –110 to +103 with respect to the A of the first AUG) (depicted in Fig. 4.1A) was synthesised and ^{32}P-labelled by *in vitro* transcription. The *ompF-213* mRNA was incubated with increasing concentrations of StpA or H-NS, and protein–RNA complexes were separated by polyacrylamide gel electrophoresis and visualised by autoradiography (Fig. 4.7). Both proteins bound the *ompF-213* mRNA. However, the affinity of StpA for the probe was slightly better than that of H-NS, as more probe was complexed with StpA than with H-NS at similar protein concentrations (Fig. 4.7B).

4.2.7 *Interactions of StpA and H-NS with* ompC-268 *mRNA*

There were no significant differences in *ompC* transcript or porin levels between the wild-type strain and its *stpA* and *hns* mutant derivatives. Thus, there was little evidence to suggest that either StpA or H-NS regulated *ompC* expression at a post-transcriptional level. Therefore, as a control the interaction of StpA and H-NS with a 268-nt probe encompassing the 5'-end of the *ompC* mRNA (–81 to +187 relative to

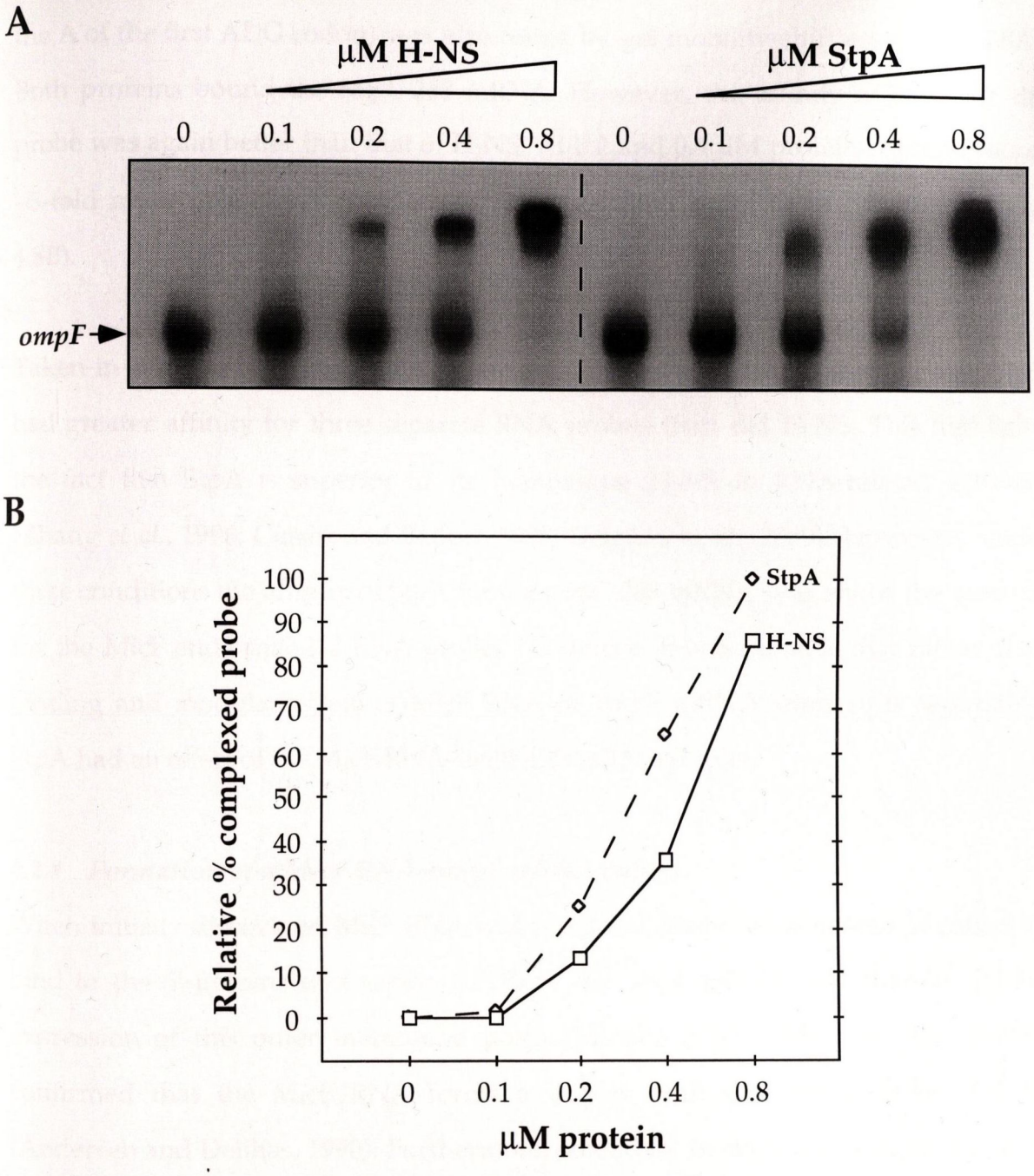

Fig. 4.7. Interactions of StpA and H-NS with **ompF-213 m*RNA***

A. Gel mobility shift-analysis of StpA and H-NS interactions with the *ompF-213* mRNA. Purified StpA and H-NS at the indicated concentrations were incubated with ^{32}P-labelled *ompF-213* mRNA for 15 min at room temperature in a buffer containing a 100-fold excess of competitor tRNA. Bound and free RNAs were separated by polyacrylamide gel electrophoresis and visualised by autoradiography. The position of migration of free *ompF-213* mRNA is indicated.

B. Graph showing densitometric analyses tracing the formation of the StpA–*ompF-213* (broken line) and H-NS–*ompF-213* mRNA (full line) complexes in (**A**), expressed as a percentage of the most intense protein–RNA complex shown.

the A of the first AUG codon) was also tested by gel mobility-shift assay (Fig. 4.8A). Both proteins bound the *ompC-268* mRNA. However, the affinity of StpA for the probe was again better than that of H-NS. At 0.2 and 0.4 μM protein concentrations, ~3-fold more probe was complexed with StpA than with the H-NS protein (Fig. 4.8B).

Taken in combination, the results of the gel mobility-shift assays showed that StpA had greater affinity for three separate RNA probes than did H-NS. This highlights the fact that StpA is superior to its homologue H-NS in RNA-related activities (Zhang *et al.*, 1996; Cusick and Belfort, 1998; Deighan *et al.*, 2000). However, under these conditions the affinity of StpA for the *ompC-268* mRNA was about the same as for the MicF and *ompF-213* RNA probes. Therefore, it was possible that rather than binding and modulating either MicF RNA or *ompF* mRNA transcripts separately, StpA had an effect of the MicF RNA–*ompF-213* mRNA duplex.

4.2.8 *Formation of a MicF RNA–*ompF *mRNA duplex*

When initially discovered MicF RNA was predicted (based on sequence identity) to bind to the 5′-untranslated region (UTR) of the *ompF* mRNA and thereby inhibit expression of this outer membrane porin (Mizuno *et al.*, 1984). *In vitro* studies confirmed that the MicF RNA forms a duplex with the *ompF* mRNA 5′-UTR (Andersen and Delihas, 1990). Furthermore, secondary structural models of the MicF RNA–*ompF* mRNA duplex have been developed from enzymic and chemical probing studies and *in silico* phylogenetic comparisons (Schmidt *et al.*, 1995; Delihas *et al.*, 1997; Fig. 4.1C). *In vivo*, StpA modulates the stability of MicF RNA, which in turn controls *ompF* mRNA stability via duplex formation. It was, therefore, of interest to anneal the MicF RNA–*ompF* mRNA duplex *in vitro*, and to investigate if purified StpA could influence the formation of this RNA–RNA hybrid.

Both the 93-nt MicF RNA and the *ompF-213* mRNA were synthesised and labelled by *in vitro* transcription. A standard amount of MicF RNA was incubated with

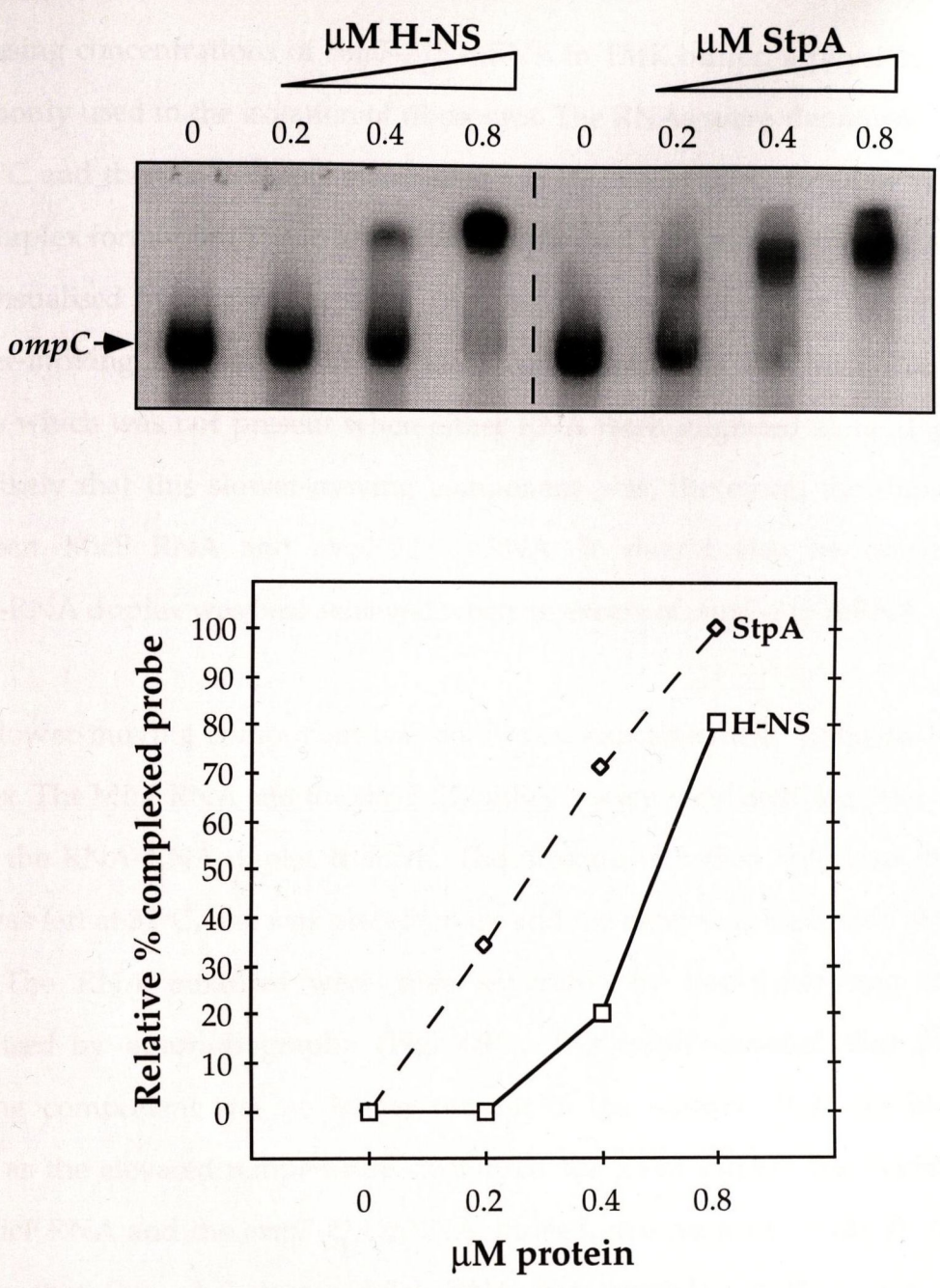

Fig. 4.8. Interactions of StpA and H-NS with **ompC-268** *mRNA*

A. Gel mobility shift analysis of StpA and H-NS interactions with the *ompC-268* mRNA. Purified StpA and H-NS at the indicated concentrations were incubated with ^{32}P-labelled *ompC-268* mRNA for 15 min at room temperature in a buffer containing a 100-fold excess of competitor tRNA. Bound and free RNAs were separated by polyacrylamide gel electrophoresis and visualised by autoradiography. The migration of free *ompC-268* mRNA is indicated.

B. Graph showing densitometric analyses tracing the formation of the StpA–*ompC-268* (broken line) and H-NS–*ompC-268* mRNA (full line) complexes in (**A**), expressed as a percentage of the most intense protein–RNA complex shown.

increasing concentrations of *ompF-213* mRNA in TMK buffer, a physiological buffer commonly used in the isolation of ribosomes. The RNAs were denatured by heating to 60°C and then cooled and maintained for 60 min at 37°C to allow renaturation and duplex formation. The mixtures were separated by non-denaturing PAGE at 4°C and visualised by autoradiography (Fig. 4.9A). It was apparent that there was a slower-moving component in the lanes containing both the MicF and *ompF-213* RNAs which was not present when either RNA were migrated alone (Fig. 4.9A). It was likely that this slower-moving component was, therefore, the duplex formed between MicF RNA and *ompF-213* mRNA. It should also be noted that the RNA–RNA duplex was best achieved when an excess of *ompF-213* mRNA was used.

The slower-moving component was confirmed experimentally to be an RNA–RNA duplex. The MicF RNA and the *ompF-213* mRNA were incubated together at 37°C to allow the RNA–RNA duplex to form. The mixture was then split into three tubes; one was left at 37°C, one was placed on ice and the other was incubated at 70°C for 3 min. The RNA mixtures were then separated by non-denaturing PAGE and visualised by autoradiography (Fig. 4.9B). The result revealed that the slower-moving component was no longer present in the mixture that was incubated at 70°C, as the elevated temperature denatured the 25-nt duplex that forms between the MicF RNA and the *ompF-213* mRNA. Indeed, in a previous study an RNA–RNA duplex that formed between MicF RNA and *ompF-150* mRNA was shown to denature at temperatures above 56°C (Andersen and Delihas, 1990).

4.2.9 *Effect of StpA on the MicF RNA–*ompF *mRNA duplex*

The model for StpA- and H-NS-dependent regulation of OmpF porin expression deduced from *in vivo* experiments showed that in wild-type *E. coli* H-NS repressed transcription of *micF*, while StpA impeded (directly or indirectly) the interaction of any MicF RNA molecules with the *ompF* mRNA, and subsequently the MicF RNA was destabilised (Fig. 3.17; Deighan *et al.*, 2000). The direct effect of StpA on formation of the RNA–RNA duplex was tested *in vitro*. The MicF RNA and *ompF-213*

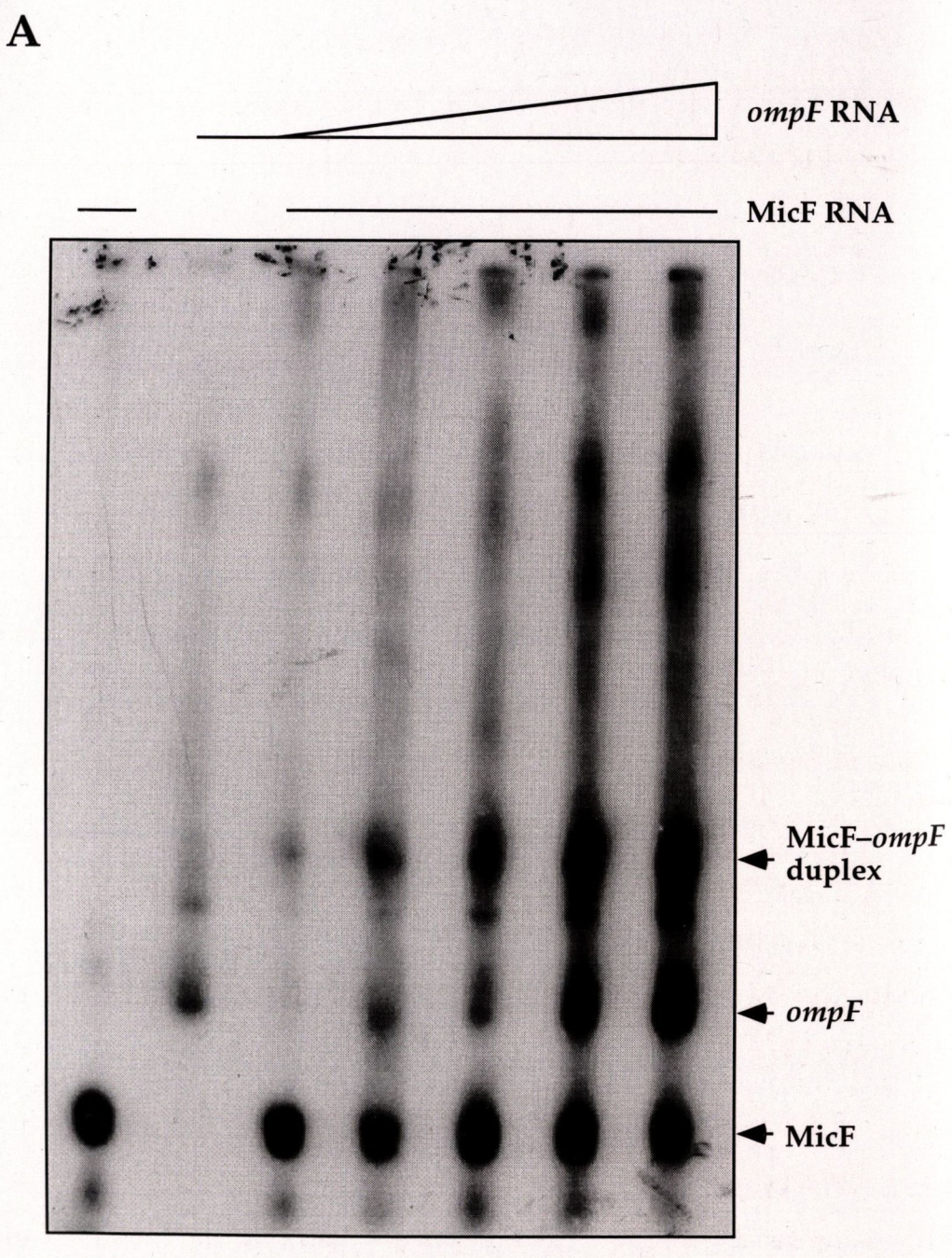
A
ompF RNA
MicF RNA
MicF–ompF duplex
ompF
MicF

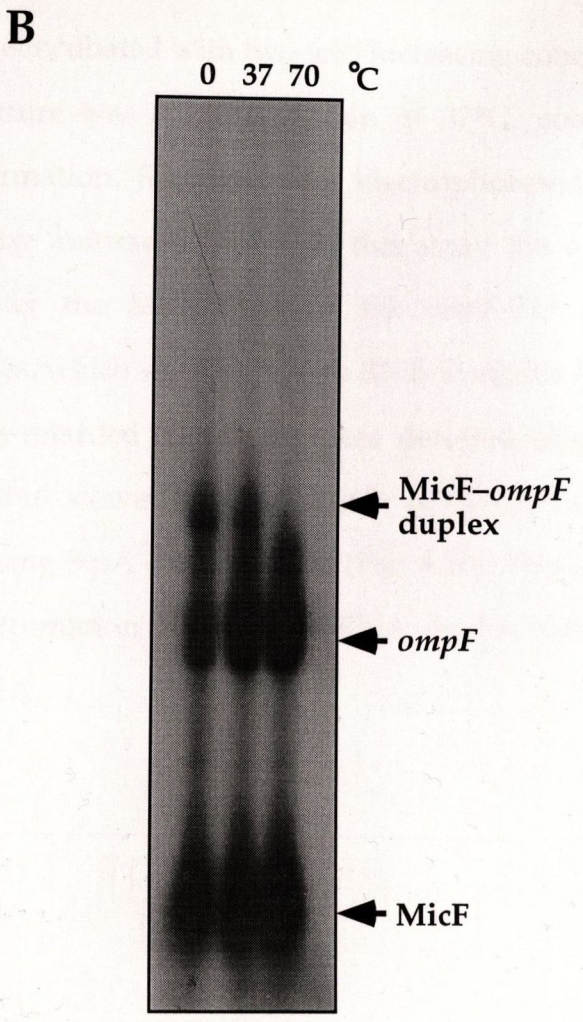

*Fig. 4.9. Formation of the MicF–***ompF** *duplex*

A. Non-denaturing 5% polyacrylamide gel showing the RNA–RNA duplex formed between MicF RNA and *ompF-213* mRNA. Both RNAs were synthesised and labelled with ^{32}P by *in vitro* transcription and purified by extraction with phenol–chloroform. A standard amount of MicF RNA was mixed with increasing amounts of *ompF-213* mRNA. Two tubes contained only MicF RNA or *ompF-213* mRNA and served as markers for migration. The RNAs were denatured at 60°C then incubated at 37°C to allow renaturation and duplex formation for 1 h prior to electrophoresis at 4°C. The slower-moving RNA–RNA duplex is indicated as are the free MicF and *ompF-213* RNAs.

B. Effect of temperature on the MicF–*ompF* duplex. MicF RNA and *ompF-213* mRNA were incubated together for 1 h at 37°C. The mixture was then split into three tubes which were placed at the indicated temperatures for 3 min. The RNAs were then separated by 5% non-denaturing PAGE. The slower-moving RNA–RNA duplex and the free MicF and *ompF-213* RNAs are labelled.

mRNA (in excess) were incubated with two-fold increasing concentrations of StpA in TMK buffer. The mixture was left for 60 min at 37°C, conditions which allow RNA–RNA duplex formation. Samples were electrophoresed by non-denaturing PAGE and visualised by autoradiography. In this assay the concentration of StpA used did not sequester the MicF RNA or the *ompF-213* mRNA probes into protein–RNA complexes, which would leave no RNA available for duplex formation. Indeed, no StpA–RNA-retarded complexes were detected (Fig. 4.10). However, it was revealed that the slower-moving MicF RNA–*ompF-213* mRNA duplex disappears with increasing StpA concentration (Fig. 4.10). This shows that at least *in vitro*, StpA can inhibit formation of the RNA–RNA duplex between the MicF RNA and the *ompF-213* mRNA.

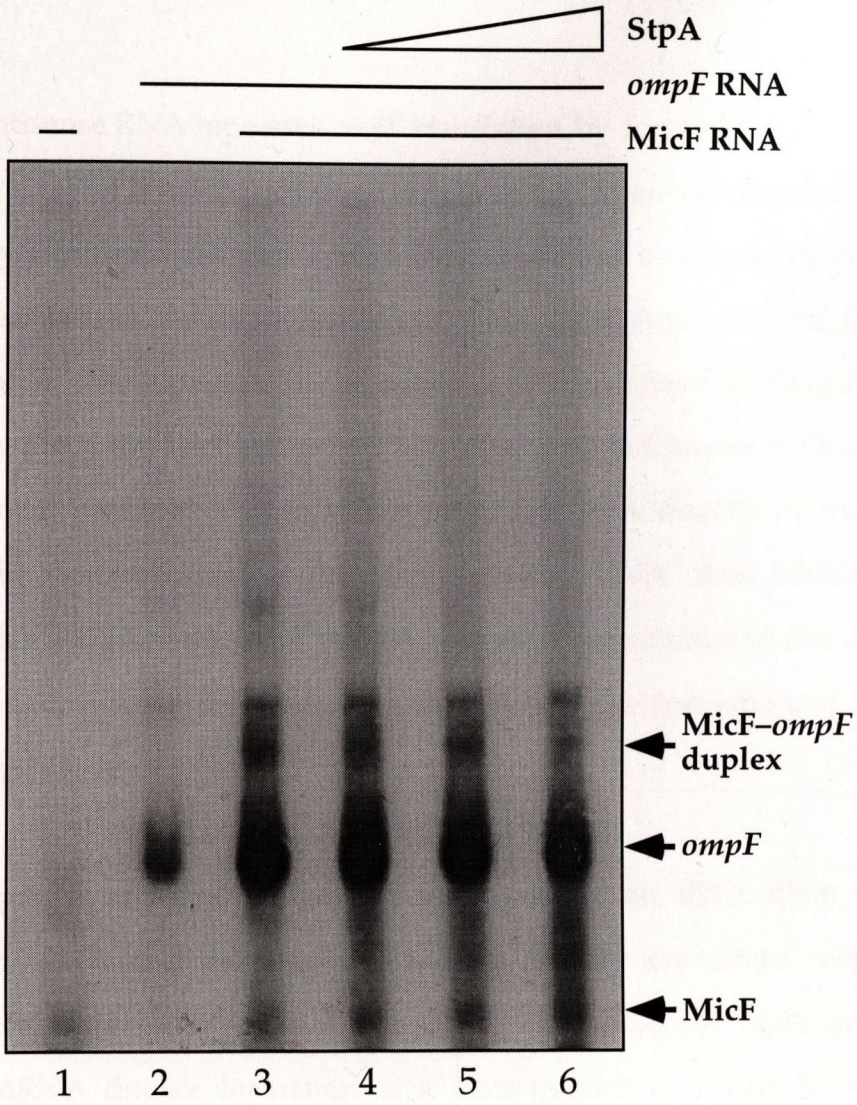

*Fig. 4.10. Effect of StpA on the MicF–*ompF *duplex*

5% native polyacrylamide gel showing the influence of StpA on MicF RNA–*ompF-213* mRNA duplex formation. A standard quantity of MicF RNA was mixed with an excess of *ompF-213* mRNA. The RNAs were denatured at 60°C and then incubated at 37°C for 1 h in the absence (lane 3) or presence of StpA (lane 4, 0.1 μM; lane 5, 0.2 μM; lane 6, 0.4 μM). Two tubes contained only MicF RNA or *ompF-213* mRNA (lanes 1 and 2 respectively) and served as markers for RNA migration. The slower–moving RNA–RNA duplex is indicated as are the free MicF and *ompF-213* RNAs.

4.3 *Discussion*

The 93-nt MicF antisense RNA represses *ompF* translation by forming an RNA–RNA duplex with the 5′-UTR of the *ompF* message due to complementary sequences. This results in a poorly translated complex and in the presence of a cognate protein the *ompF* mRNA is destabilised and degraded (Mizuno *et al.*, 1984; Andersen and Delihas, 1990). A series of *in vivo* experiments identified a role for StpA in OmpF porin expression that involved the MicF antisense RNA (discussed in Chapter 3; Deighan *et al.*, 2000). The model predicted that in wild-type *E. coli*, StpA directly or indirectly brought about the destabilisation of the MicF antisense RNA, thus inhibiting its interaction with the 5′-UTR of the *ompF* mRNA. The results described in this chapter show that purified StpA has a direct negative influence on the formation of a MicF RNA–*ompF-213* mRNA duplex *in vitro*.

The ability of StpA to negatively affect the formation of an RNA–RNA duplex between the MicF RNA and the *ompF-213* mRNA is fully consistent with data obtained *in vivo* (Chapter 3; Deighan *et al.*, 2000). This effect of StpA on MicF RNA–*ompF-213* mRNA duplex formation is a consequence of direct StpA–RNA interactions. When the MicF and *ompF-213* mRNAs were synthesised and ^{32}P-labelled by *in vitro* transcription and incubated together in a physiological buffer, a slower-moving component was visible that was not present when either RNA transcript was electrophoresed alone (Fig. 4.9A). Additionally this component was not present if the samples were heated to 70°C prior to native polyacrylamide gel electrophoresis (Fig. 4.9B). This confirms that the slower-moving component represents the annealed 25-nt RNA–RNA duplex between MicF RNA and *ompF-213* mRNA. Indeed, a similarly annealed MicF RNA–*ompF-150* mRNA duplex was experimentally calculated to denature at temperatures above 56°C (Andersen and Delihas, 1990). Intriguingly, if MicF RNA and *ompF-213* mRNA were annealed in the presence of StpA, there was a clear ~5-fold reduction in level of the RNA–RNA duplex (Fig. 4.10). Moreover, in this assay the StpA concentration used did not

sequester the transcripts into discrete StpA–MicF or StpA–*ompF-213* complexes; thus the RNAs were available for duplex formation.

There are several possible mechanisms as to how StpA could negatively affect duplex formation. StpA could impede the formation of the MicF RNA–*ompF-213* mRNA duplex by directly interacting with either the MicF or *ompF-213* RNAs. The resulting StpA–RNA association could be a steric barrier to further RNA–RNA interactions. Under the experimental conditions used in this study, which included a 100-fold excess of competitor tRNA, the StpA protein bound the MicF RNA and *ompF-213* mRNA probes with better affinity than did the H-NS protein (Figs. 4.6 and 4.7). This is consistent with other analyses (Zhang *et al.*, 1996; Cusick and Belfort, 1998). Moreover, reactions performed with a 500-fold excess of tRNA gave similar results and protein–RNA complexes could be out-competed with an increasing concentration of cold probe, validating the experiments (data not shown). However, a similar trend of StpA and H-NS binding was also observed using the *ompC-268* mRNA probe (Fig. 4.8). There is no *in vivo* evidence to suggest that StpA or H-NS control *ompC* expression post-transcriptionally, and consequently no reason to suspect that either protein should specifically interact with this RNA. Since the binding of StpA to all three probes was similar, it is likely that the observed negative influence of StpA on the MicF RNA–*ompF-213* mRNA annealed duplex is not mediated by prolonged stable association of StpA with either the MicF RNA or the *ompF-213* mRNA. Consistent with this, the affinity of StpA for the RNA probes was considerably weaker than for DNA probes under similar binding conditions (~0.2 μM compared to <0.1 μM to complex similar quantities of RNA and DNA probes, respectively; Figs. 3.11 and 4.5A). The recombinant StpA protein purified in this study (Fig. 4.2) was proficient for oligomerisation (Fig. 4.3) and this property is important for nucleic acid binding by H-NS-like proteins (Bertin *et al.*, 1999). In addition the six C-terminal histidines did not perturb the functioning of the protein *in vivo* (Fig. 4.4), and so are not likely to have an effect *in vitro*. However, it is possible that *in vivo*, or under different experimental conditions, that the StpA–RNA

associations proceeds more efficiently. Indeed, the strength of protein–RNA interactions is determined by positioning of chemical groups at the interface that allow for hydrophobic, ionic, hydrogen-bonding and shape complementarity interactions (reviewed in Cusack, 1999; Draper, 1999; Frankel, 2000). This interface is influenced by several variable experimental parameters including monovalent and divalent cation type and concentration, and water-mediated associations (Cusack, 1999; Draper, 1999).

For the MicF RNA–*ompF* mRNA duplex to anneal it is necessary that regions of secondary structure (and presumable tertiary structure) within the MicF RNA and the *ompF* message are unfolded. The 25-nt complementary region between the RNAs partially overlaps stem-loop IA of the *ompF* mRNA and the base of stem-loop I in the MicF RNA (depicted in red in Fig. 4.1). These regions must be single-stranded for duplex formation (Schmidt *et al.*, 1995; Delihas *et al.*, 1997; Fig. 4.1C). It is likely that in a population of MicF and *ompF-213* RNAs, a proportion of the molecules will be kinetically trapped in stable alternative conformations. This is a problem common to all RNA molecules purified under denaturing conditions and renatured *in vitro*, which also perhaps exists *in vivo* and is referred to as the 'RNA-folding problem' (Herschlag, 1995). In the case of the MicF and *ompF-213* RNAs some of these stable alternative secondary structures may have the 25-nt region of complementarity between the MicF and *ompF-213* RNAs exposed in a single-stranded domain, which would facilitate annealing of the RNA–RNA duplex. It is possible that StpA, an RNA-chaperone *in vitro* (Zhang *et al.*, 1995) and *in vivo* (Clodi *et al.*, 1999), can deter or resolve such alterations in structure (which may be considered as misfolded RNAs), fully consistent with the function of RNA chaperones (Herschlag, 1995). In this way StpA could have a negative influence on annealing of the MicF RNA–*ompF-213* mRNA duplex. The fact that no specific StpA–RNA complexes are formed but a concomitant ~5-fold decrease in the MicF RNA–*ompF-213* mRNA duplex is detected (Fig. 4.9), would support the idea that the effect of StpA may be operating through only a proportion of the RNA population. Furthermore, the different complexes

formed between StpA and H-NS with the MicF RNA suggests that in some way StpA can alter the MicF RNA secondary structure that allows the formation of higher-order conformations that are retarded directly in the wells (Fig. 4.6).

It is also possible that the negative effect of purified StpA on the RNA–RNA duplex between MicF RNA and the *ompF-213* mRNA arises from a direct interaction of StpA with the RNA–RNA duplex. The altered secondary structure of both the MicF and *ompF* RNAs upon interaction may create a binding site for the StpA protein, which could then destabilise the duplex structure. An interesting experiment to investigate this would be to firstly anneal the duplex *in vitro,* and then to add purified StpA for a period of time before analysing levels of the RNA–RNA association. This is distinct from the assay performed in this study that had all components incubated together at the start of the reaction.

Previously an 80-kDa protein partially purified from an *E. coli* extract was shown to bind the MicF RNA and to have weak affinity for the 5′-UTR of the *ompF* message (Andersen and Delihas, 1990). Together with MicF RNA binding to the *ompF* mRNA, this cognate protein may participate in destabilisation and degradation of the *ompF* message during thermal regulation of *ompF* expression (Andersen and Delihas, 1990). The findings presented in this study also implicate a direct role for the RNA chaperone StpA in negatively influencing the MicF RNA–*ompF* mRNA duplex. Taken in combination with the results discussed in Chapter 3, these data highlight that the StpA protein directly influences OmpF porin expression through the MicF antisense RNA.

Chapter 5

StpA expression and regulation of σ^s

5.1 *Introduction*

Expression of the *Escherichia coli stpA* and *hns* genes is subject to negative cross-autoregulation; i.e., each gene product can inhibit both its own gene promoter and that of the other (Sondén and Uhlin, 1996; Zhang *et al.*, 1996). The dominant effect is the repression of *stpA* by H-NS, which causes *stpA* expression to be low in wild-type bacteria (Sondén and Uhlin, 1996; Zhang *et al.*, 1996; Free and Dorman, 1997). Presumably due to this low expression of StpA in a *hns*$^+$ strain, there was no evidence of an associated phenotype with a *stpA* single mutation as monitored by two-dimensional gel electrophoresis (Sondén and Uhlin, 1996). Furthermore, the StpA and H-NS proteins were shown to be structurally and functionally similar (Bertin *et al.*, 1999). Therefore, it was envisaged that StpA might be a 'molecular back-up' for H-NS. However, recently it is becoming clear that the expression of *stpA* and *hns* differ considerably (Dorman *et al.*, 1999), and that the StpA protein is functionally different to H-NS, especially with respect to RNA-related activities (Chapter 3 and 4; Deighan *et al.*, 2000).

5.1.1 In vivo-*induced genes*

Salmonella enterica serovar *typhimurium* (*S. typhimurium*) is a facultative intracellular pathogen that can infect a variety of hosts, causing gastroenteritis in humans and a typhoid fever-like disease in mice. These bacteria can survive and replicate within a vacuolar compartment in host cells including colonic epithelial cells at early stages of infection, and tissue macrophages during systemic infection (reviewed in Finlay and Falkow, 1997). During this voyage through an infected host the bacteria are subject to several, simultaneous environmental assaults including oxidative stress, acid stress, and osmotic stress, exposure to cationic peptides and starvation (reviewed in Foster and Spector, 1995). A great deal of work has been conducted on *S. typhimurium* and other pathogens grown within the host to identify the genes required by the bacteria for survival and establishment of infection (reviewed in Chiang *et al.*, 1999). DNA topology, which can globally influence gene expression

(Dorman, 1995), was also shown to undergo significant changes during adaptation to the intracellular environment (Marshall *et al.*, 2000). Indeed, transcription from the *ihfA*, *ihfB*, *gyrB* and *hns* genes, all of which code for determinants of DNA topology, were induced when Salmonellae were grown inside macrophage-like cells (Marshall *et al.*, 2000).

The results presented in this chapter show that expression of the StpA protein is subject to growth-phase regulation, and is induced by thermal, ethanol and salt stress. In addition, StpA and H-NS protein levels are induced in macrophage-engulfed *S. typhimurium* cells. Furthermore, evidence is presented to show that the StpA protein is involved in the modulation of cellular σ^s levels. Taken in combination, these results suggest that the StpA protein has an important role to play in bacterial physiology even in an *hns*$^+$ strain.

5.2 *Results*

5.2.1 *StpA antiserum*

Three injections, each of 300 μg His-tag-purified StpA (Fig. 4.2), diluted in either Freund's complete or incomplete adjuvant, were used to elicit an immune response in a New Zealand White rabbit. The resulting serum was absorbed against a CJD1600 (*E. coli* MC4100 *stpA*) cell lysate to remove cross-reacting antibodies. Western immunoblots performed with this antibody showed a specific interaction with the StpA protein (Fig. 5.1). Importantly, there was little evidence of cross-reaction with the StpA-homologue, H-NS. Indeed, faint cross-reaction to H-NS was only detected if the blots were exposed for longer than 90 min (data not shown). Typically blots were exposed from 45 sec to 10 min.

The anti-H-NS antibody used in this study was obtained from E. Bremer and is described in Dersch *et al.* (1993). This antibody gives a weak reaction against the StpA protein in an *hns* mutant (data not shown). However, in this study H-NS content was only monitored in a wild-type background, and as the level of StpA expressed in a *hns*$^+$ background is low, the cross-reaction of the H-NS antiserum with the StpA protein is negligible. The anti-σ^s antibody was a gift from R. Hengge-Aronis and specifically recognises σ^s.

Unless otherwise stated, wild-type *E. coli* strain MC4100 was grown overnight in LB broth or minimal broth, diluted into 200 ml fresh broth in a 2-L flask at an OD_{600} of 0.005, and grown at 37°C with vigorous aeration. It is important to note that samples for Western immunoblot analyses were prepared by directly lysing an equal number of cells, based on OD_{600} measurements, in SDS-sample buffer. Therefore, it should be noted that a direct comparison of either StpA, H-NS or σ^s content between the early exponential and stationary phases will be slightly overestimated as it is known that cell size shrinks in stationary phase (Åkerlund *et al.*, 1995). Thus, the sample will contain more cells, and therefore the total extract will

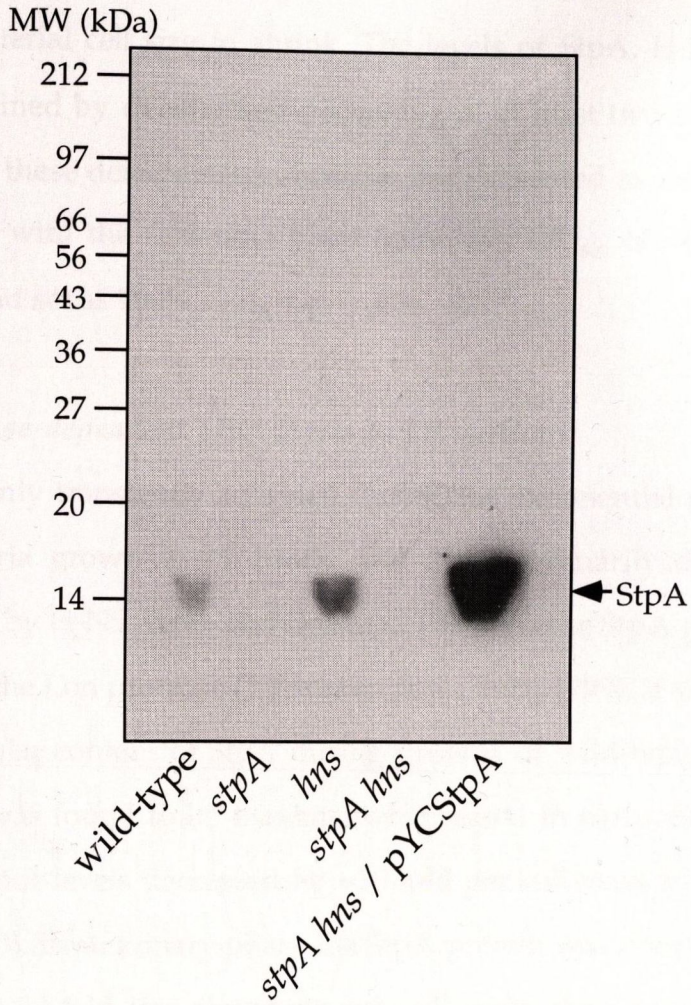

Fig. 5.1. Western immunoblot showing the specific reaction of the anti-StpA antibody

Total cell extracts were prepared from stationary phase cultures of wild-type strain MC4100, CJD1600 (*stpA*), PD32 (*hns*), CJD1601 (*stpA hns*), CJD1616 (*stpA hns*/pACYC184) and CJD1617 (*stpA hns*/pYCStpA). The extracts (normalised to OD_{600} values) were separated by SDS-12%-PAGE, transferred to nitrocellulose membrane, and incubated with a 1:1000 dilution of the StpA anti-serum. The autoradiograph shown was exposed to film for 1 min. Strain genotype is indicated below each lane and the position of migration of StpA is shown.

contain more protein. Additionally, exposure of bacteria to environmental stresses may cause the bacterial cell size to shrink. The levels of StpA, H-NS or σ^s per cell mass were determined by densitometric scanning of at least two exposures of each blot. The results of these densitometric analyses are presented as relative percentage StpA, H-NS or σ^s, with the first time point (generally OD_{600} of ~0.3) or the most intense protein band set as 100%.

5.2.2 *Growth-phase-dependent StpA levels in LB medium*

The *stpA* gene is only transiently activated during the exponential phase of growth in wild-type bacteria grown in LB broth, and this is primarily due to promoter silencing mediated by H-NS (Free and Dorman, 1997). As the StpA protein is subject to degradation by the Lon protease (Johansson and Uhlin, 1999), it was of interest to determine the cellular content of StpA during growth of wild-type *E. coli* MC4100. The StpA protein was found to be maximally expressed in early exponential phase (OD_{600} of 0.2–0.4), but levels decreased by ~10-fold per cell mass in late exponential phase (OD_{600} of ~1.3). In stationary phase the StpA protein was poorly expressed and was approximately 20-fold less abundant per cell mass than in early exponential phase (Fig. 5.2). This trend of expression is in good agreement with the detected level of the *stpA* message in the same background (Free and Dorman, 1997). In another analysis StpA protein levels in *E. coli* strain W3110 were also revealed to be higher in early exponential phase than at other stages of the growth phase (Talukder *et al.*, 1999). However, the difference in the quantity of StpA molecules per cell between the early exponential and stationary phases was only 3-fold, compared to a difference of ~20-fold (normalised to OD_{600} values) in this study. The authors noted that their StpA antiserum was cross-reactive with H-NS (Talukder *et al.*, 1999). This, coupled with the use of different strain backgrounds and a different means of expressing the results complicates a direct comparison of the data.

Fig. 5.2. Growth-phase-dependent StpA levels in rich broth

A. Western blot analysis of StpA content from wild-type *E. coli* MC4100 grown in LB broth at various time points throughout the growth curve. Total cell extracts (normalised to OD_{600} values) were separated by SDS-12%-PAGE, transferred to nitrocellulose membrane, and incubated with a 1:1000 dilution of the StpA antiserum. The labelling below each lane refers to the stage of the growth curve when the samples were harvested as depicted in (**B**). The position of migration of StpA is indicated.

B. Growth curve (open rectangles) of MC4100 in LB broth as monitored by measuring cellular density at OD_{600} and densitometric analysis (closed rectangles) of the bands in (**A**). The mean generation time during the exponential phase of growth was 29 min. The amounts of StpA are expressed as a relative percentage of that detected for the most intense band shown, i.e., MC4100 cells at OD_{600} = 0.2, the value of which was taken as 100%. The data shown for the relative % StpA expression are the average of two independent experiments, and a representative gel is shown.

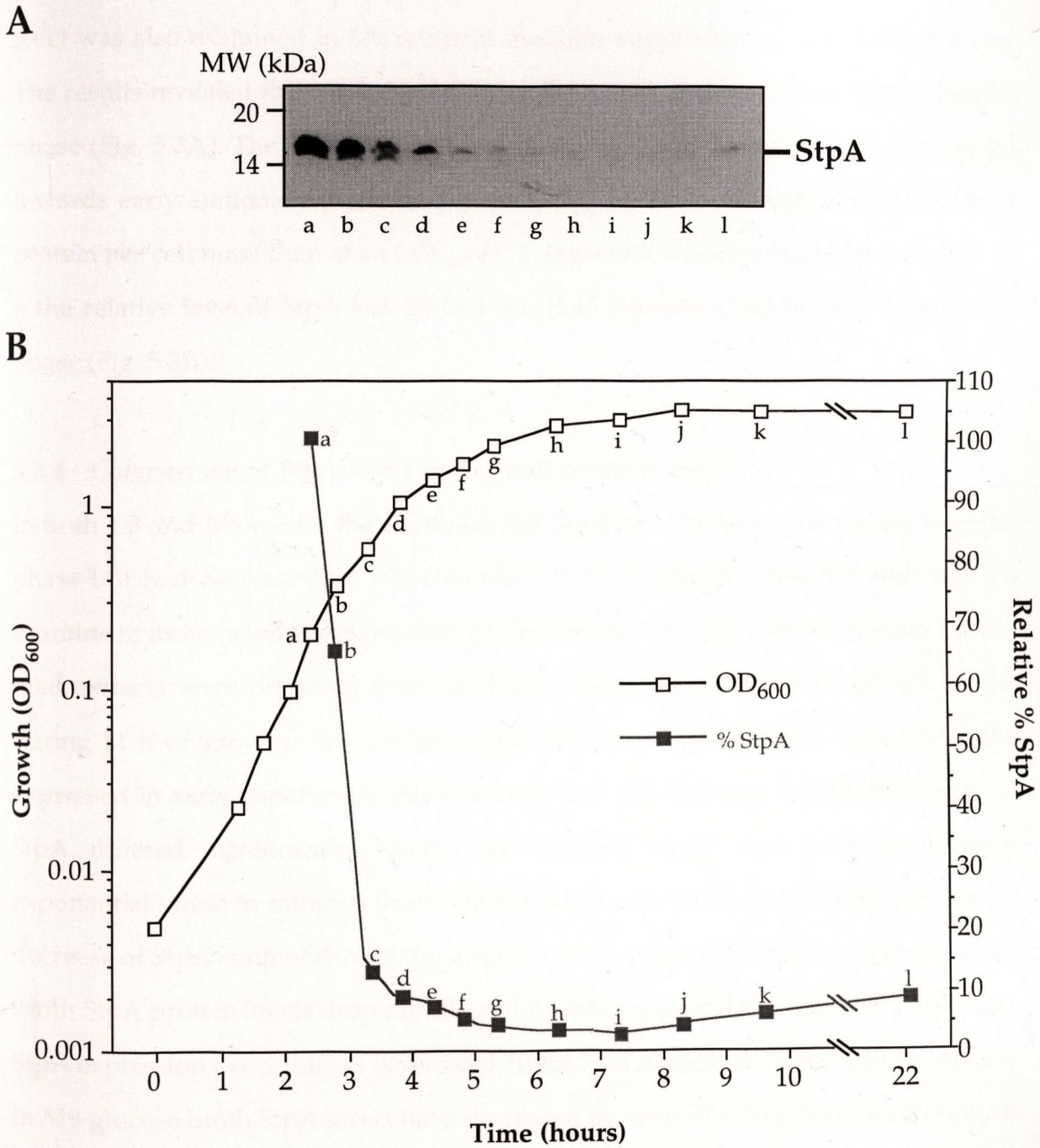
A
MW (kDa)
20
14
StpA
a b c d e f g h i j k l
B
Growth (OD600)
Relative % StpA
OD600
% StpA
Time (hours)
0.001
0.01
0.1
1
0 1 2 3 4 5 6 7 8 9 10 22
0 10 20 30 40 50 60 70 80 90 100 110

5.2.3 *Growth-phase-dependent StpA levels in M9 minimal medium*

The *stpA* mRNA was previously shown to be expressed at a higher and more sustained level during exponential growth in M9 minimal medium compared to growth in LB broth (Free and Dorman, 1997). In this study the cellular StpA protein level was also examined in M9 minimal medium supplemented with 0.4% glucose. The results revealed that peak expression of StpA was observed in early exponential phase (Fig. 5.3A). The StpA protein level slowly declined as the bacteria progressed towards early stationary phase and at an OD_{600} of 2.4 there was 10-fold less StpA protein per cell mass than at an OD_{600} of 0.2. If growth was continued for a further 12 h the relative level of StpA was 20-fold less than that observed in early exponential phase (Fig. 5.3B).

5.2.4 *Comparison of StpA levels in rich and minimal media*

In both LB and M9 media the expression of StpA was highest in early exponential phase but had decreased by ~20-fold after 22 h of growth (Figs. 5.2 and 5.3). To examine in more detail the expression profiles of StpA in rich versus minimal media, total extracts were prepared from MC4100 cells grown in either LB or M9 broths during 11 h of growth. The results confirmed that, although StpA was maximally expressed in early exponential phase in both rich and minimal media, the levels of StpA differed significantly. There was ~10-fold more StpA present in early exponential phase in minimal broth compared to rich broth. In addition, the rate of decrease of StpA content during the growth curves was considerably different. In LB broth StpA protein levels drop rapidly and by late exponential phase (OD_{600} of ~1.3), StpA expression per cell mass is reduced 10-fold. At a corresponding culture density in M9-glucose broth StpA levels have decreased by only 50% (Fig. 5.4). In addition, at comparable stages throughout the growth curves there was ~10–15-fold more StpA protein expressed in minimal medium than was expressed in rich medium.

One important difference between growth in minimal medium and growth in rich medium is the presence of elevated Lrp expression in the former case (Lin *et al.*,

Fig. 5.3. Growth-phase-dependent StpA levels in minimal broth

A. Western blot analysis of StpA content from wild-type *E. coli* MC4100 grown in M9-glucose minimal medium at various time points throughout the growth curve. Total cell extracts (normalised to OD_{600} values) were separated by SDS-12%-PAGE, transferred to nitrocellulose membrane, and incubated with a 1:1000 dilution of the StpA antiserum. The labelling below each lane refers to the stages of the growth curve when the samples were harvested as depicted in (**B**). The position of StpA is indicated.

B. Growth curve (open rectangles) of MC4100 in M9-glucose minimal medium as monitored by measuring cellular density at OD_{600}, and densitometric analysis (closed rectangles) of the bands in (**A**). The mean generation time during the exponential phase of growth was 41 min. The amounts of StpA are expressed as a relative percentage of that detected for the most intense band shown, i.e., MC4100 cells at OD_{600} of 0.2, the value of which was taken as 100%. The data shown for the relative % StpA expression are the average of two independent experiments, and a representative gel is shown.

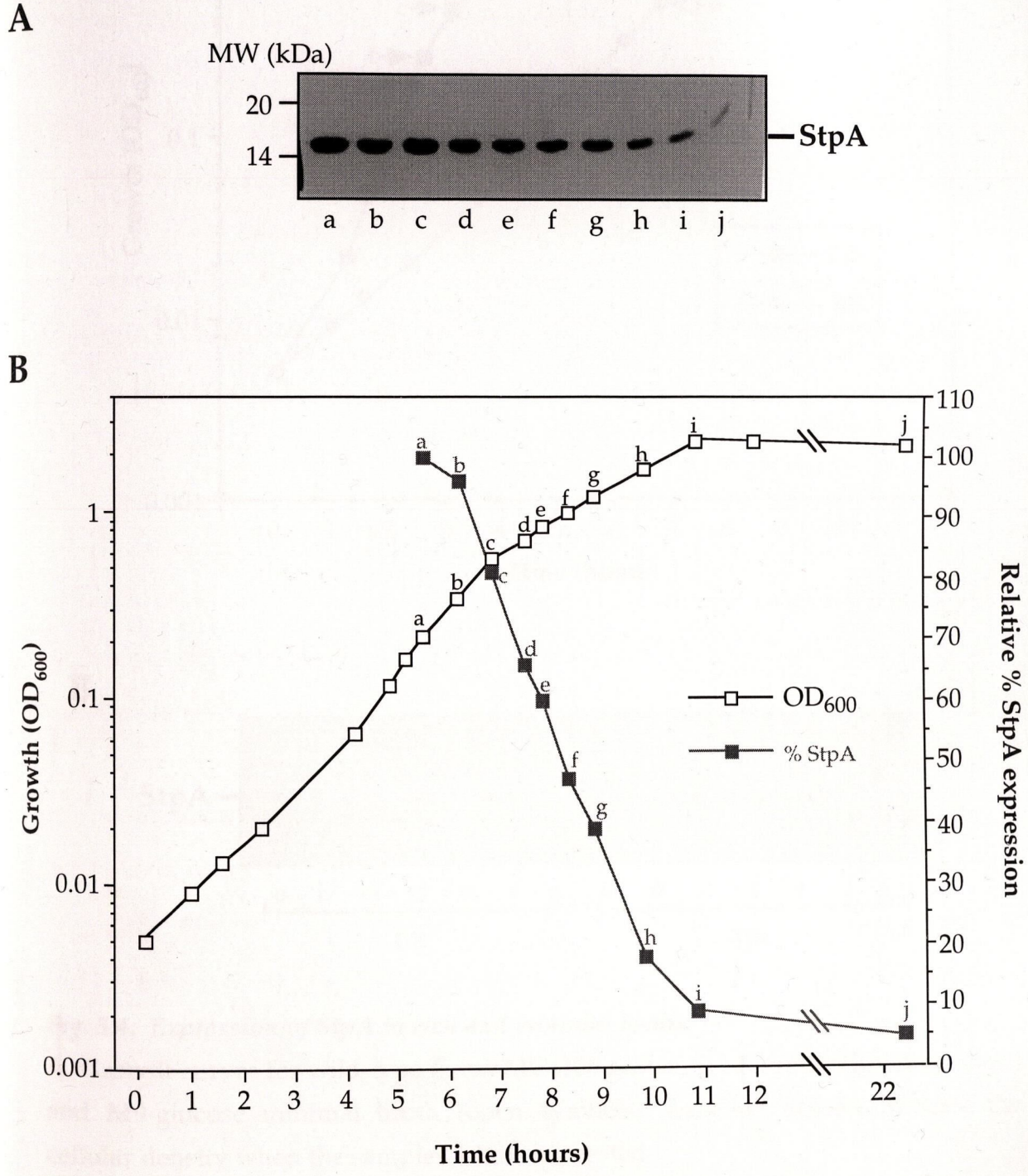
A
MW (kDa)
20
14
StpA
a b c d e f g h i j
B
Growth (OD_{600})
Relative % StpA expression
Time (hours)
OD_{600}
% StpA
0.001
0.01
0.1
1
0 1 2 3 4 5 6 7 8 9 10 11 12 22
0 10 20 30 40 50 60 70 80 90 100 110

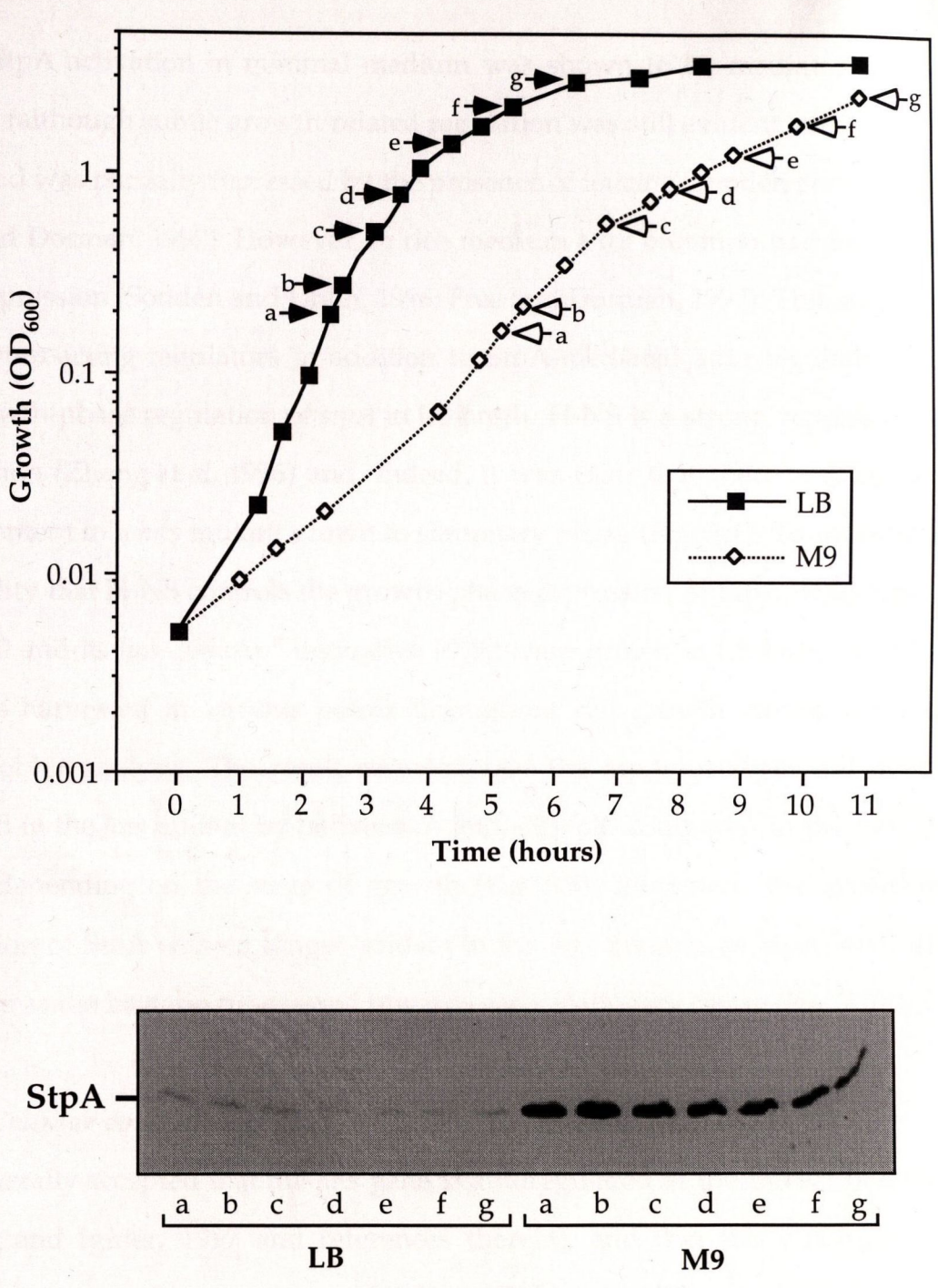

Fig. 5.4. Expression of StpA in rich and minimal media

A. Growth curves for wild-type *E. coli* MC4100 grown in LB broth (closed symbols) and M9-glucose minimal broth (open symbols). Labelled arrows indicate the cellular density when the samples where harvested.

B. Western blot analysis of StpA content from wild-type *E. coli* MC4100 grown in M9-glucose minimal broth and LB broth. Total cell protein samples (normalised to OD_{600} values) were separated by SDS-12%-PAGE, transferred to nitrocellulose membrane and incubated with a 1:1000 dilution of the StpA antiserum. The labelling below each lane refers to the stages of the growth curves when the samples were harvested as depicted in (**A**). The position of StpA is indicated.

1992). StpA activation in minimal medium was shown to be mediated by the Lrp protein (although subtle growth-related regulation was still evident in the absence of Lrp), and was partially repressed by the presence of leucine (Sondén and Uhlin, 1996; Free and Dorman, 1997). However, in rich medium a *lrp* mutation had little effect on *stpA* expression (Sondén and Uhlin, 1996; Free and Dorman, 1997). This suggests that other *trans*-acting regulators in addition to StpA-mediated auto-regulation, control the growth-phase regulation of *stpA* in LB broth. H-NS is a strong repressor of *stpA* expression (Zhang *et al*, 1996) and, indeed, it was clear that there was an elevated StpA content in a *hns* mutant grown to stationary phase (Fig. 5.1). To investigate the possibility that H-NS controls the growth-phase expression of StpA, wild-type strain MC4100 and its *hns-206*::Ap^R derivative PD32 were grown in LB broth at 37°C and samples harvested at various points throughout the growth curves for Western immunoblot analysis. The result revealed that the StpA level per cell mass was elevated in the *hns* mutant by between 7- and ~35-fold compared to the *hns*$^+$ parent strain, depending on the stage of growth (Fig. 5.5). Moreover, the growth-phase regulation of StpA was no longer evident in the *hns* mutant, as StpA level did not decrease as the bacteria progressed towards early stationary phase (Fig. 5.5B).

5.2.5 Cellular content of H-NS

It is generally accepted that the *hns* gene is autoregulated at the transcriptional level (Atlung and Igmer, 1997 and references therein), and that this autoregulation is important in coupling a constant H-NS to DNA ratio (Free and Dorman, 1995). However, the question of H-NS protein level as a function of growth-phase has been the subject of some dispute. Indeed, H-NS protein content has variously been reported to be ~3-fold more abundant in stationary phase cells (Spassky *et al.*, 1984; Dersch *et al.*, 1993; Ueguchi and Mizuno, 1993), to be relatively constant throughout the growth-phase (Hinton *et al.*, 1992; Free and Dorman, 1995; Sonnenfield *et al.*, 2001), or to be expressed at a lower level in stationary phase (Talukder *et al.*, 1999). To clarify this issue and to determine if the expression profile of H-NS differed from its homologue StpA, the cellular content of H-NS was examined from wild-type

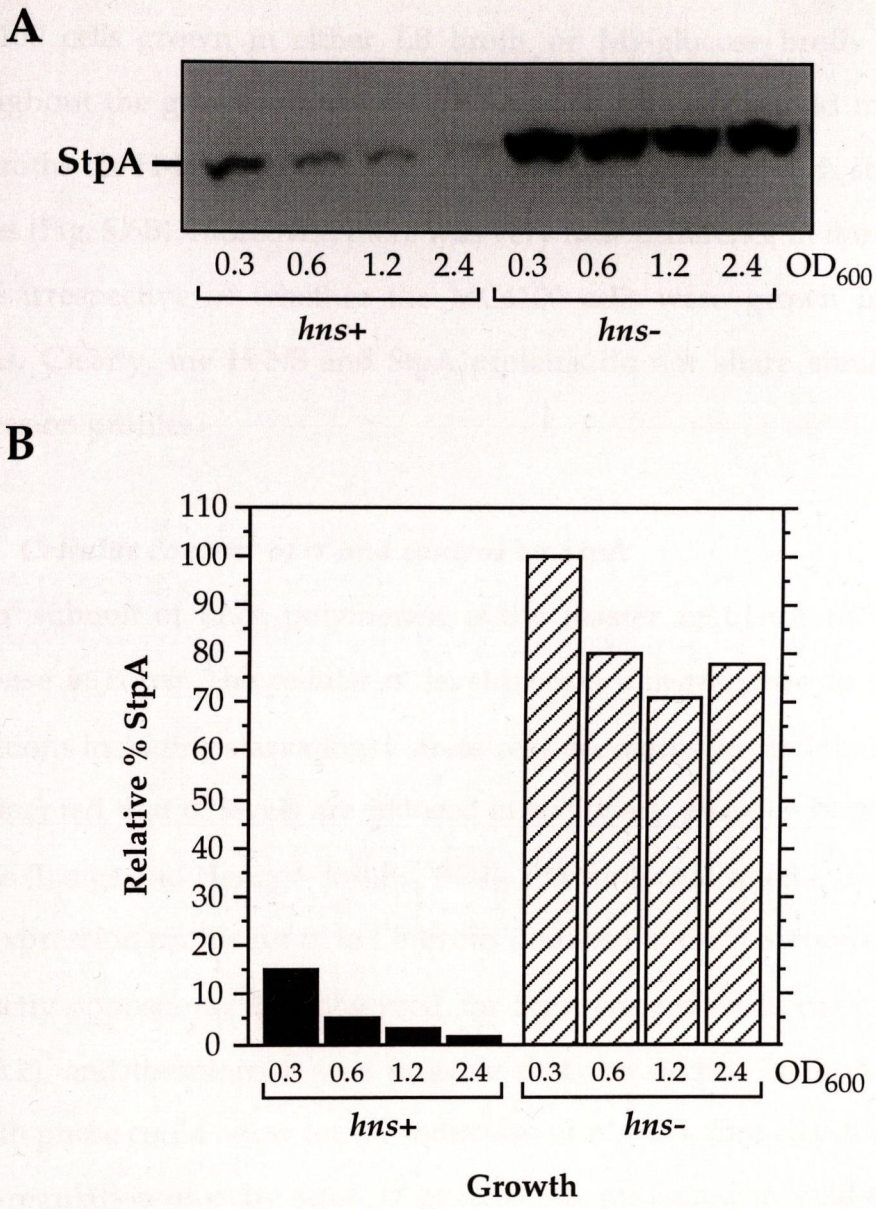

Fig. 5.5. H-NS mediates the growth-phase regulation of StpA in LB broth

A. The effect of *hns* on expression of StpA was monitored by Western blot analysis. Total cell extracts from strains MC4100 and PD32 (MC4100 *hns-206*::Ap^R) at four stages of the growth phase in LB medium were Western blotted (normalised to the indicated OD_{600} values) with anti-StpA antibodies. The position of migration of StpA is indicated.

B. Densitometric analysis of the data in (**A**), expressed as a relative percentage of that detected for the most intense band shown, i.e., PD32 cells at OD_{600} = 0.3, the value of which was taken as 100%. The data shown are an average of two independent experiments, and a representative gel is shown.

MC4100 cells grown in either LB broth or M9-glucose broth at various points throughout the growth curves (Fig. 5.6A). The results revealed that in both LB and M9 broths the H-NS levels were approximately constant at each stage of the growth curves (Fig. 5.6B). Moreover, there was very little difference in the cellular content of H-NS irrespective of whether the MC4100 cells were grown in rich or minimal broths. Clearly, the H-NS and StpA proteins do not share similar growth-related expression profiles.

5.2.6 Cellular content of σ^s and control by StpA

The σ^s subunit of RNA polymerase is the master regulator of the general stress response in *E. coli*. The cellular σ^s level increases in response to a variety of stress conditions including starvation, a stress cells encounter in stationary phase. It is well documented that σ^s levels are induced in stationary phase in both rich and minimal broths (Lange and Hengge-Aronis, 1994), a finding confirmed in this study (Fig. 5.7). The expression profile for σ^s in LB broth (induced in early stationary phase; Fig. 5.7) is exactly opposite to that observed for StpA (repressed in early stationary phase; Fig. 5.2), and therefore it was possible that the decline in StpA as a function of growth phase could allow for the induction of σ^s. As a first step to investigating any cross-regulation of σ^s by StpA, σ^s content was measured in wild-type MC4100 cells and its Δ*stpA*::Tc^R derivative CJD1600 at various points throughout the growth curves by Western immunoblotting. It should be noted that the *stpA* mutant CJD1600 grows at an identical rate to wild-type MC4100 strain (Fig. 5.8B). The results revealed that, as expected, σ^s expression was induced in stationary phase in the wild-type strain (Fig. 5.8A). Interestingly, σ^s was also growth-phase regulated in the *stpA* mutant. However, the level of σ^s attained was ~2-fold less than the *stpA*$^+$ wild-type strain at most stages during the growth curve (Fig. 5.8B).

The *stpA* gene is located at 60.27 min on the physical map of *E. coli* and the *rpoS* gene is located at 61.7 min (Rudd, 1998). Therefore, these genes are separated by ~69-kb. It was possible that, when constructing strain CJD1600 (MC4100 Δ*stpA*::Tc^R) by P1-

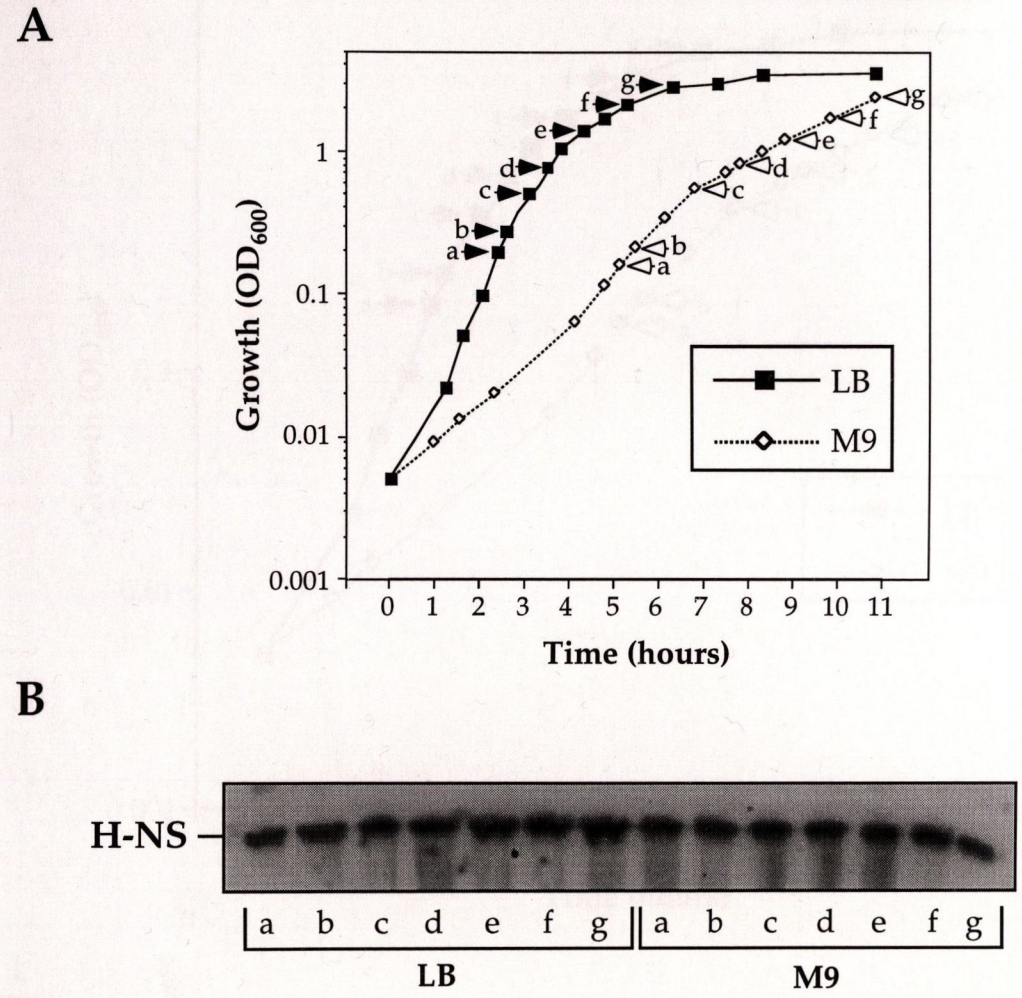

Fig. 5.6. Expression of H-NS in rich and minimal media

A. Growth curves for wild-type *E. coli* MC4100 grown in LB broth (closed symbols) and M9-glucose minimal broth (open symbols). Labelled arrows indicate the cellular density when the samples where harvested.

B. Western blot analysis of H-NS content from wild-type *E. coli* MC4100 grown in M9-glucose minimal broth and LB broth. Total cell extracts (normalised to OD_{600} values) were separated by SDS-12%-PAGE, transferred to nitrocellulose membrane and incubated with a 1:1000 dilution of the H-NS antiserum. The labelling below each lane refers to the stages of the growth curves when the samples were harvested as depicted in (**A**). The position of H-NS is indicated.

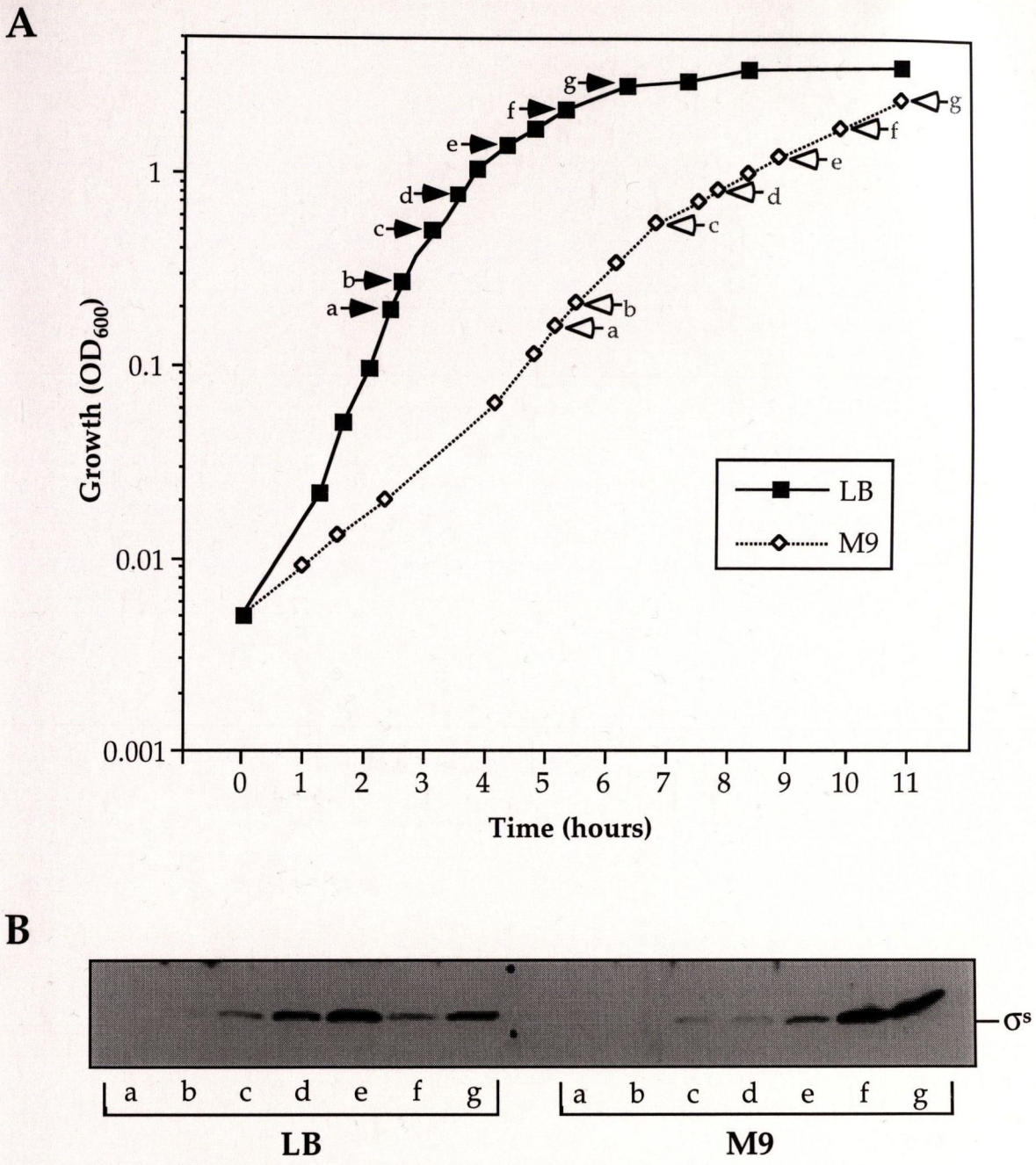

Fig. 5.7. Expression of σ^s in rich and minimal media

A. Growth curves for wild-type *E. coli* MC4100 grown in LB broth (closed symbols) and M9-glucose minimal broth (open symbols). Labelled arrows indicate the cellular density when the samples where harvested.

B. Western blot analysis of σ^s content from wild-type *E. coli* MC4100 grown in M9-minimal broth and LB broth. Total cell extracts (normalised to OD_{600} values) were separated by SDS-12%-PAGE, transferred to nitrocellulose membrane and incubated with a 1:1000 dilution of the σ^s antiserum. The labelling below each lane refers to the stage of the growth curve when the samples were harvested as depicted in (**A**). The position of σ^s is indicated.

Fig. 5.8. StpA is required for full expression of σ^s

A. Wild-type strain MC4100 and its *stpA* mutant derivative CJD1600 were grown in 200-ml LB broth with vigorous aeration. Total cell extracts (normalised to OD_{600} values) were separated by SDS-12%-PAGE, transferred to nitrocellulose membrane, and incubated with a 1:1000 dilution of the σ^s antiserum. The cellular densities at which the samples were extracted are shown below each lane and depicted by arrows in (**B**). The position of migration of σ^s is indicated.

B. Growth curve of MC4100 (open symbols, full line) and CJD1600 (closed symbols, full line) as monitored by measuring cellular density at OD_{600}, and densitometric analyses of the bands in (**A**), MC4100 (open symbols, dashed line) and CJD1600 (closed symbols, dashed line). The amounts of σ^s are expressed as a relative percentage of that detected for the most intense band shown, i.e., MC4100 cells at OD_{600} = 2.0, the value of which was taken as 100%. The position of migration of StpA is indicated. The data shown are an average of two independent experiments, and representative gels are shown.

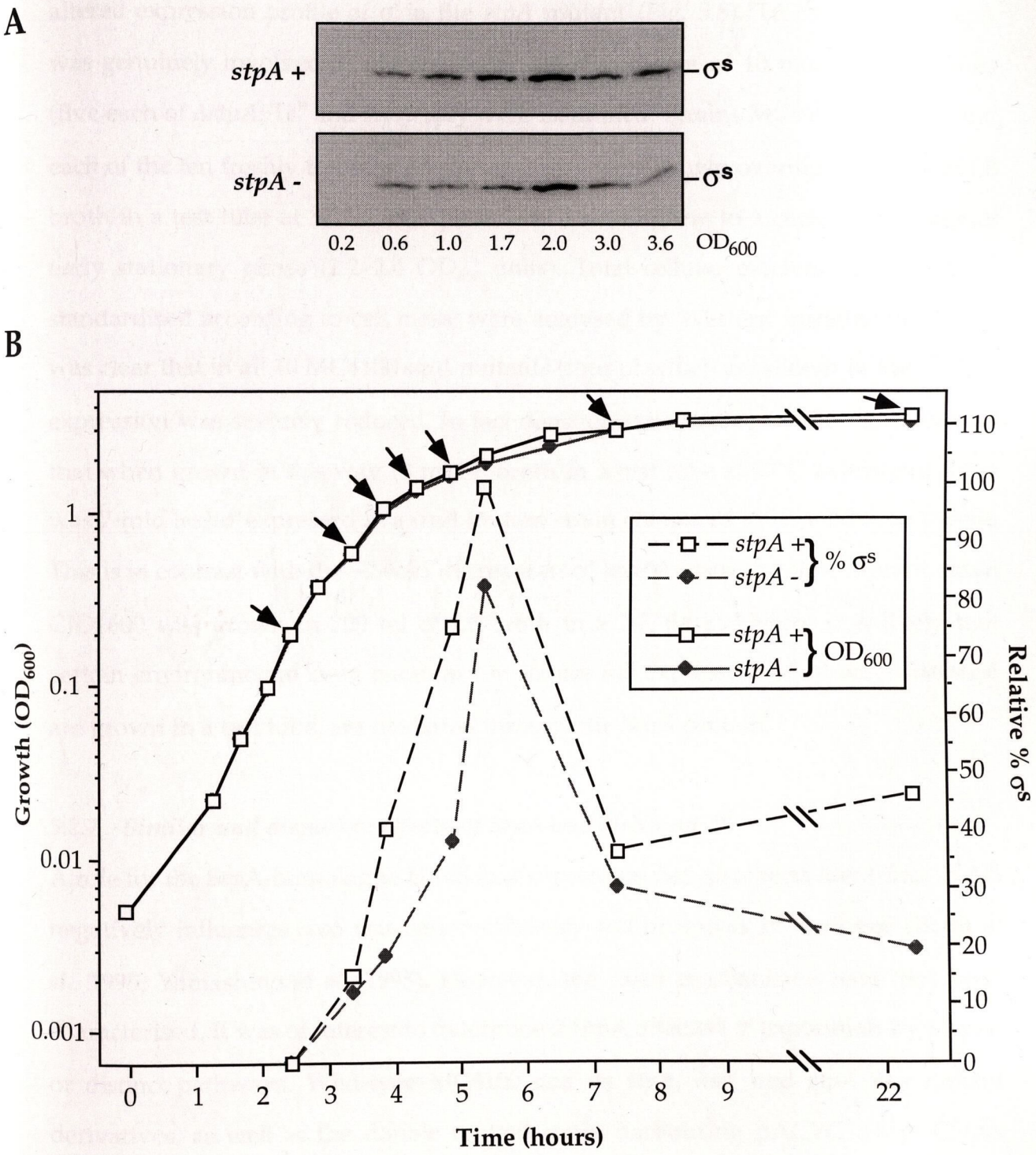
A
stpA +
σs
stpA -
σs
0.2 0.6 1.0 1.7 2.0 3.0 3.6 OD600
B
Growth (OD600)
1
0.1
0.01
0.001
stpA +
stpA -
% σs
stpA +
stpA -
OD600
Relative % σs
110
100
90
80
70
60
50
40
30
20
10
0
0 1 2 3 4 5 6 7 8 9 22
Time (hours)

mediated transduction (P1*cml* used in this study can efficiently package up to 100-kb) the region around the *rpoS* gene was disrupted and that this brought about the altered expression profile of σ^s in the *stpA* mutant (Fig. 5.8). To confirm that StpA was genuinely involved in σ^s expression, the σ^s contents of 10 more *stpA* mutants (five each of Δ*stpA*::Tc^R and *stpA*::*spc*) were examined. Strains MC4100, CJD1600 and each of the ten freshly transduced *stpA* mutants were grown overnight in 3 ml of LB broth in a test tube at 37°C. As expected each strain grew to a comparable stage of early stationary phase (2.2–2.4 OD_{600} units). Total cellular extracts of each strain, standardised according to cell mass, were analysed by Western immunoblotting. It was clear that in all 10 MC4100 *stpA* mutants (four of which are shown in Fig. 5.9), σ^s expression was severely reduced. In fact densitometric tracing of the blots showed that when grown in this way (3 ml LB broth in a test tube at 37°C overnight) there was 7-fold less σ^s expressed in a *stpA* mutant strain compared to its wild-type parent. This is in contrast with the ~2-fold decrease in σ^s levels when the *stpA* mutant strain CJD1600 was grown in 200 ml of LB broth in a 2-L flask. Hence, it is likely that certain environmental cues, necessary to induce full expression of σ^s when bacteria are grown in a test tube, are mediated through the StpA protein.

5.2.7 *Similar and disparate effects of StpA and H-NS on* σ^s

A role for the StpA-homologue H-NS in σ^s expression has also been identified. H-NS negatively influences *rpoS* translation efficiency and promotes σ^s turnover (Barth *et al.*, 1995; Yamashino *et al.*, 1995). However, the exact mechanisms have not been characterised. It was of interest to determine if StpA affected σ^s expression by similar or distinct pathways. Wild-type MC4100 and its *stpA*, *hns*, and *stpA hns* mutant derivatives, as well as the double mutant strain harbouring pACYC184, pYCStpA (functional StpA), or pAF201 (functional H-NS) were grown overnight to an OD_{600} of 1.6–2.2 depending on strain, and samples extracted for Western immunoblot analysis. The cultures were then diluted into fresh LB broth and grown to mid-exponential phase (OD_{600} of 0.6), and again samples were harvested for Western immunoblot analysis. The results revealed that, as expected, σ^s content was very low

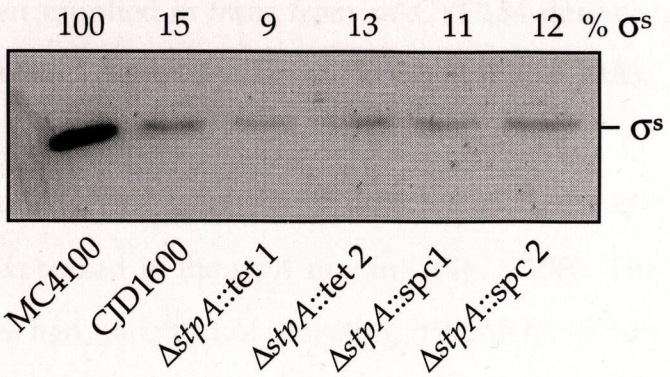

Fig. 5.9. Under-expression of σ^s in the absence of StpA

Western blot analysis of σ^s content from wild-type *E. coli* MC4100 and its Δ*stpA*::Tc^R mutant derivative CJD1600. The level of σ^s expressed in four other freshly transduced MC4100 *stpA* mutants (two each of Δ*stpA*::Tc^R and *stpA*::Sm^R) are also shown. All strains were grown overnight in 3 ml LB broth in a test tube to an OD_{600} of ~2.2. The relative percentage of σ^s in each strain as determined by densitometric analysis of the bands is indicated above the blot, expressed as a percentage of the σ^s content observed in the wild-type strain, which was set as 100%.

in exponential phase in the wild-type and *stpA* mutant strains, but was significantly elevated (>10-fold) in the *hns* mutant, consistent with a role for H-NS in negatively influencing *rpoS* translation and σ^s protein stability (Fig. 5.10A; Barth *et al.*, 1995; Yamashino *et al.*, 1995). When the *stpA* and *hns* alleles were combined, σ^s content was 2-fold further elevated when compared to the *hns* single mutant. Additionally, either StpA or H-NS when supplied in *trans* from pACYC184-derived plasmids in the *stpA hns* mutant background down-regulated σ^s content (Fig. 5.10A).

In stationary phase σ^s levels were easily detected in the wild-type strain but there was ~7-fold less expressed in the *stpA* mutant (Fig. 5.10B). The combination of the *stpA* and *hns* alleles had the effect of elevating σ^s content slightly over the *hns* single mutant and wild-type strains. Intriguingly, however, the effect of complementing the *stpA hns* mutations with plasmids over-expressing either StpA or H-NS was very different. Complementing with H-NS in stationary phase had little effect on σ^s content compared to the strong negative effect of over-expressed H-NS on σ^s content observed in exponential phase. However, when StpA was supplied *in trans*, σ^s was severely under-expressed, an effect also detected in exponentially growing cultures. Therefore, it is clear that the level of StpA in the cell is crucial for modulation of σ^s expression, as an under- or over-representation of StpA negatively influences σ^s content. Moreover, the data from the complementation study would suggest that at least in stationary phase StpA and H-NS modulate σ^s levels by different pathways.

5.2.8 *Control of* rpoS *transcript levels*

StpA can regulate gene expression at both the transcriptional level and at the post-transcriptional level via modulation of RNA stability (Deighan *et al.*, 2000). Thus, as a first step to defining the mechanism(s) of StpA-dependent control of σ^s, the steady state level of the *rpoS* message was measured in the presence and absence of StpA. Strain MC4100 and its *stpA* mutant derivative CJD1600 were grown in 200 ml LB broth in a 2-L flask (both strains grow at an identical rate), and samples harvested at

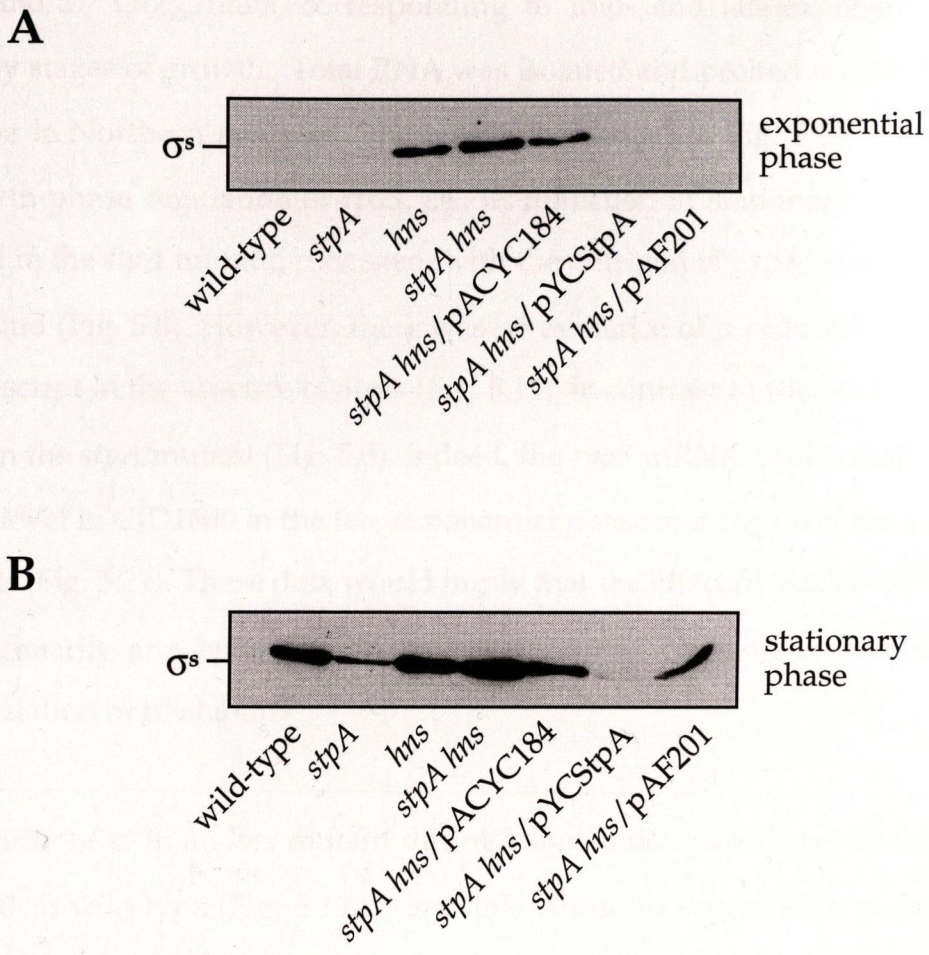

Fig. 5.10. Similar and disparate effects of StpA and H-NS on σ^s

Analysis of σ^s content from wild-type *E. coli* MC4100, CJD1600 (*stpA*), PD32 (*hns*), CJD1601 (*stpA hns*), CJD1616 (*stpA hns*/pACYC184), CJD1617 (*stpA hns*/pYCStpA) and CJD1618 (*stpA hns*/pAF201). All strains were grown overnight in 3 ml LB broth to stationary phase, and samples harvested. Strains were then diluted into fresh LB broth and cultured to mid-exponential phase (OD_{600} = 0.6), and samples again harvested. Total cell protein extracts from the mid-exponential phase samples (**A**), or stationary phase samples (**B**), (normalised to OD_{600} value) were subject to Western blot analysis. Strain genotype is indicated below each lane and the position of migration of σ^s is indicated.

0.6, 1.3 and 2.7 OD_{600} units, corresponding to mid- and late-exponential, and the stationary stages of growth. Total RNA was isolated and probed with a *rpoS*-specific riboprobe in Northern analysis. The results, presented in Fig. 5.11, confirmed that the growth-phase regulation of *rpoS*, i.e., its induction in stationary phase, was not impaired in the *stpA* mutant, consistent with the detected σ^s expression profile in this background (Fig. 5.8). However, there was no evidence of a reduced quantity of the *rpoS* transcript in the absence of StpA (Fig. 5.11), in contrast to the ~2-fold reduced σ^s content in the *stpA* mutant (Fig. 5.8). Indeed, the *rpoS* mRNA was actually present at a higher level in CJD1600 in the late exponential phase and the early stationary phase of growth (Fig. 5.11). These data would imply that the effect of StpA on σ^s expression occurs primarily at a level beyond transcription and could involve modulation of *rpoS* translation or σ^s-stability.

The quantity of σ^s in an *hns* mutant during exponential growth is >10-fold elevated compared to wild-type (Fig. 5.10A), and this is due to enhanced translation of the *rpoS* transcript and increased stability of the product (Barth *et al.*, 1995; Yamashino *et al.*, 1995). Furthermore, σ^s-content is further elevated in the *stpA hns* mutant background (Fig. 5.10). It was of interest to determine if the *rpoS* transcript was similarly expressed. Therefore, wild-type MC4100 and its *stpA*, *hns*, and *stpA hns* derivatives were grown to mid-exponential phase, total RNA extracted, and probed with a *rpoS*-specific riboprobe in Northern analysis. Here, the *rpoS* mRNA was equally abundant in the wild-type and *stpA* mutant strains, but was 2.5-fold and ~6-fold under-expressed in the *hns* and *stpA hns* derivatives, respectively (Fig. 5.12). A plasmid encoding functional StpA in the *stpA hns* background had the effect of restoring *rpoS* transcript levels to 62% of that detected in the wild-type strain. Therefore, the mechanisms of σ^s accumulation in an *hns* mutant, via enhanced translational efficiency and increased stability of the product (Yamashino *et al.*, 1995), are also operating in the *stpA hns* background (compare σ^s levels in Fig. 5.10A with *rpoS* transcript levels in Fig. 5.12). However, the effect of over-expressing StpA in the *stpA hns* background is more complex as, although the *rpoS* transcript is relatively

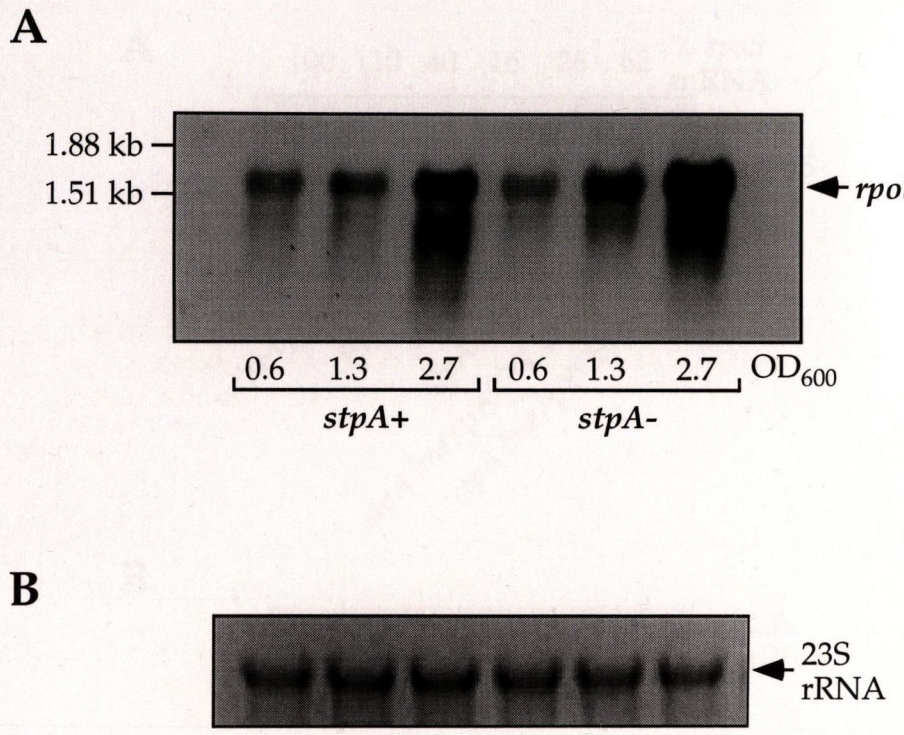

Fig. 5.11. Effect of a **stpA** *mutation on* **rpoS** *mRNA levels*

A. Total RNA was extracted from wild-type strain MC4100 and its *stpA* mutant derivative CJD1600 grown in LB broth to mid-exponential phase (OD_{600} = 0.6), transition to stationary phase (OD_{600} = 1.7), and early stationary phase (OD_{600} = 2.3) as indicated below each lane. Steady-state *rpoS* transcript levels were detected from 5 μg of total RNA with a *rpoS*-specific riboprobe in Northern analysis. The migrations of DNA molecular size markers are indicated as is the position of migration of the primary *rpoS* transcript.

B. Loading control. Following detection, the membrane used in (**A**) was stained, and the 23S rRNA bands are shown.

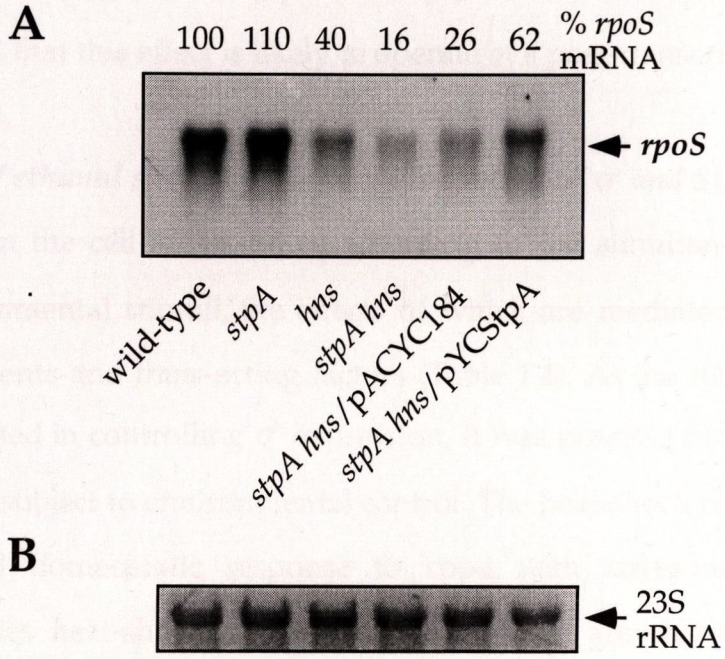

Fig. 5.12. Effect of StpA and H-NS on **rpoS** *mRNA levels*

A. Northern blot showing *rpoS* mRNA levels from *E. coli* strains grown to mid-exponential phase in LB medium. Total RNA (5 μg) was electrophoresed through a 1.25% agarose gel, electro-blotted to nylon membrane, and probed with a *rpoS*-specific riboprobe. The relevant strain genotypes are indicated below each lane. pACYC184 is vector control and pYCStpA is derived from pACYC184 and encodes wild-type StpA. Densitometric analysis of the bands is indicated above the blot, expressed as a relative percentage of the *rpoS* mRNA level observed in the wild-type strain, which was set as 100%. The data are the average of two experiments.

B. Loading control. Following detection the membrane used in (**A**) was stained, and the 23S rRNA bands are shown.

abundant, σ^s-content is barely detectable (Figs. 5.10A and 5.12). In any case it is clear that the RNA-binding protein StpA is deeply involved in the modulation of σ^s expression and that this effect is likely to operate at a post-transcriptional level.

5.2.9 Effect of ethanol shock on the cellular content of σ^s and StpA

σ^s expression in the cell is fine-tuned according to the simultaneous integration of several environmental stimuli, the effects of which are mediated through different *cis*-acting elements and *trans*-acting factors (Table 1.4). As the RNA-binding protein StpA is implicated in controlling σ^s expression, it was possible that the expression of StpA was also subject to environmental control. The heat-shock response is a cellular protective and homeostatic response to cope with stress-induced damage in proteins. Besides heat-shock, several forms of stress are channelled through the heat-shock response, which can result in the induction of more than 20 heat-shock proteins (HSPs) (Yuru and Nakahigashi, 1999). Different stress effectors can induce different subsets of HSPs. However, exposure to ethanol and thermal stress elicit the whole set of HSPs (Ramos *et al.*, 2001). It was of interest to investigate if the expression of σ^s or StpA was altered by treatment with ethanol. Strain MC4100 was grown in LB broth to OD_{600} of 0.32. The culture was then split into four aliquots, and to three of the aliquots ethanol was added to a final concentration of 2%, 4% or 8%. The remaining sample contained no ethanol and served as the control. All cultures were incubated at 37°C and samples harvested for 90 min. Total cell protein extracts were separated by SDS-PAGE and incubated with anti-StpA or anti-σ^s antibodies in Western immunoblot analyses (Fig. 5.13). It should be noted that an increasing concentration of ethanol in the medium had an inhibitory effect on cell growth (Fig. 5.13A). Nevertheless, it was clear that the expression of σ^s was markedly affected by ethanol treatment, and to a lesser extent the profile for StpA differed when compared to the control culture (Fig. 5.13B).

As expected StpA level in the untreated sample decreased as the culture progressed towards early stationary phase. However, the StpA content of the cells treated with

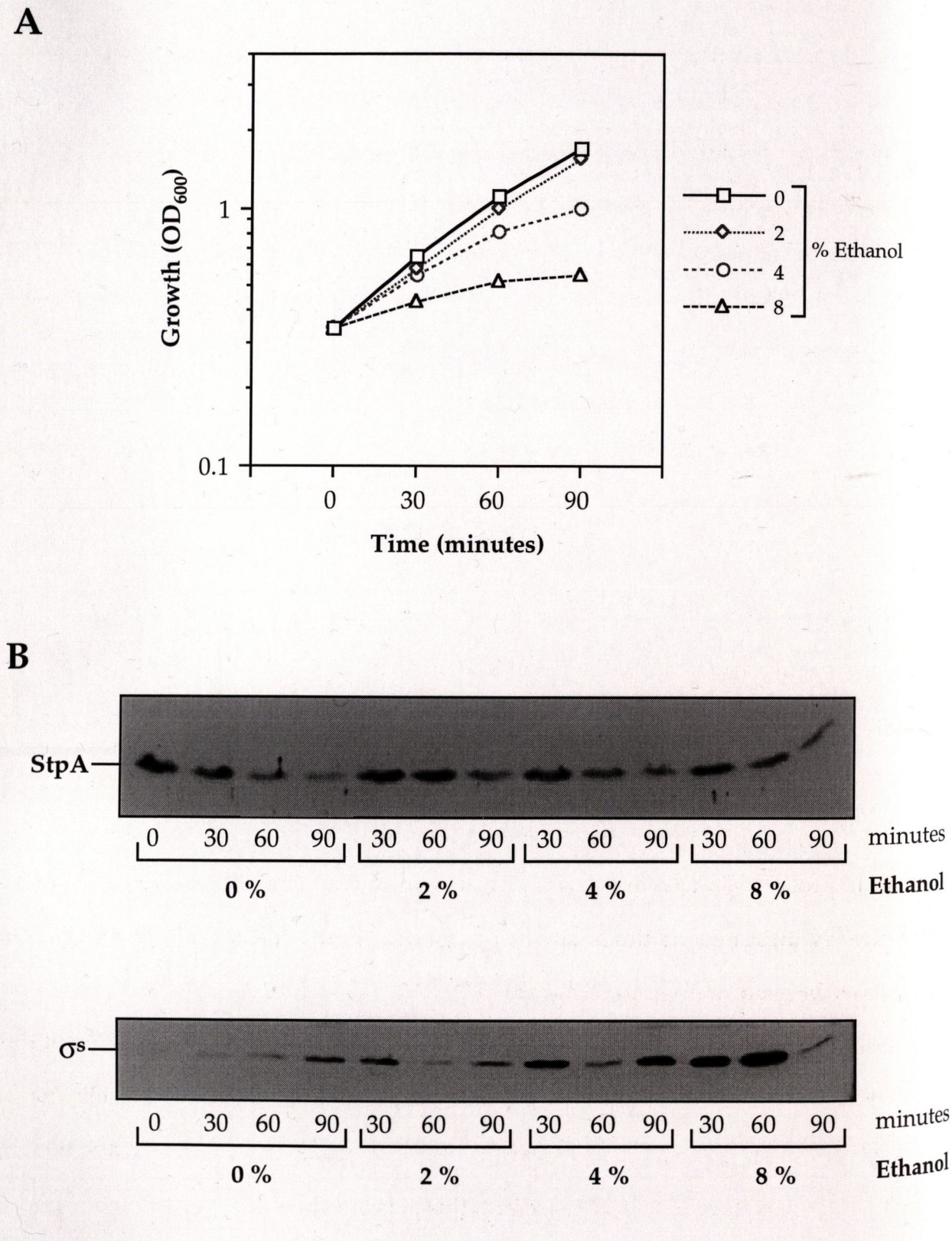
A
Growth (OD_{600})
1
0.1
0
30
60
90
Time (minutes)
0
2
4
8
% Ethanol
B
StpA
0 30 60 90 30 60 90 30 60 90 30 60 90
minutes
0 %
2 %
4 %
8 %
Ethanol
σ^s
0 30 60 90 30 60 90 30 60 90 30 60 90
minutes
0 %
2 %
4 %
8 %
Ethanol

C

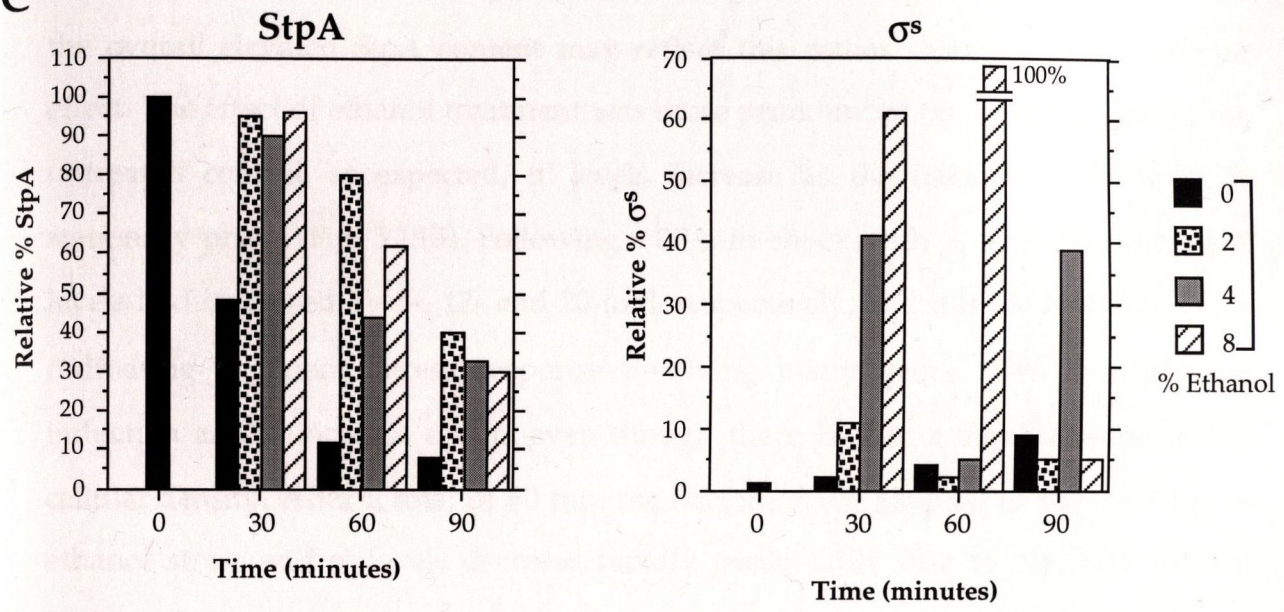

Fig. 5.13. Effect of ethanol shock on the cellular content of StpA and σ^s

A. Wild-type strain MC4100 was grown for several generations to OD_{600} = 0.3 in LB broth, the culture was then split into 4 aliquots, and each aliquot was treated with a final concentration of either 2, 4, or 8% ethanol. The control culture contained no ethanol. Bacterial growth was monitored for 90 min and is indicated (OD_{600} values).

B. Western immunoblot analyses with StpA and σ^s antisera were performed on total cellular proteins that were extracted from the ethanol-treated cultures and the control culture as indicated at time-point 0 (pre-shock) and 30, 60, and 90 min post-shock. Samples were normalised to OD_{600} values.

C. Densitometric analyses of the data in (**B**) expressed as a relative percentage of the most intense band shown (cells pre-shock at OD_{600} = 0.3 in the case of StpA; cells exposed to 8% ethanol for 60 min in the case of σ^s). The data shown are an average of two independent experiments, and representative gels are shown.

2% ethanol was 2- to 7-fold higher per cell mass than the control culture depending on the time point monitored (Fig. 5.13C). It is more difficult to interpret the effect of 4% and 8% ethanol shock on StpA levels as the growth rate is severely affected, and the overall elevated StpA content may reflect this rather than a genuine ethanol effect. The effect of ethanol treatment was more pronounced on σ^s expression. In the untreated control, as expected, σ^s levels increase as the bacteria grow towards stationary phase (Fig. 5.13B). Following a 30-min shock with 2, 4 or 8% ethanol σ^s levels had increased by 5-, 12- and 20-fold, respectively, and it is likely that σ^s is co-ordinating a general stress response involving many genes. This is a genuine induction as the increase occurs even though there is only a small change in the cellular density. After a total of 60 min the bacteria have adapted to the 2% and 4% ethanol stress and σ^s levels decrease rapidly presumably due to elevated protein turnover. However, σ^s levels continue to rise in the culture treated with 8% ethanol shock. Following 90 min of ethanol exposure σ^s level is fine-tuned to reflect the stage of growth and the presence of the stress.

5.2.10 Thermal shock and StpA levels

Bacteria exposed to ethanol had an elevated StpA content suggesting that StpA was induced by the heat-shock response (Fig. 5.13). Furthermore, previous studies showed that the *stpA* transcript was more abundant in cells grown at 37°C compared to 26°C (Sondén and Uhlin, 1996), and that *stpA* mRNA levels were induced 4-fold by a thermal shock from 30°C to 37°C (Free and Dorman, 1997).

The effect of thermal stress on StpA protein level was examined in more detail in this study. *E. coli* strain MC4100 was grown for several generations at 33°C to an OD_{600} of 0.5. The culture was then split into five aliquots which were incubated at 25°C, 29°C, 37°C or 42°C and bacterial growth was monitored (Fig. 5.14A). This covers a range of increases and decreases in the temperature of the growth medium (hereafter referred to as thermal up-shock and thermal down-shock). The control culture was left at 33°C. Samples for Western immunoblotting were harvested during a 90-min

Fig. 5.14. Effect of thermal shock on the cellular content of StpA

A. Wild-type strain MC4100 was grown for several generations to OD_{600} = 0.5 in LB broth at 33°C. The culture was then split into 5 aliquots, which were incubated at 25°C, 29°C, 33°C, 37°C, or 42°C covering a range of temperature up- and down-shifts. Bacterial growth was monitored for 90 min and is indicated (OD_{600} values).

B. Western immunoblot analysis was performed on total cell extracts (normalised to OD_{600} values) that were extracted from bacteria grown at the different growth temperatures as indicated, at time-point 0 (pre-shock) and 30, 60, and 90 min post-shock with anti-StpA antibodies. The position of migration of StpA is indicated. The experiment was repeated twice and a representative gel is shown.

C. MC4100 cells were grown to mid-exponential phase (OD_{600} = 0.6) at 25°C, 29°C, 33°C and 37°C as indicated, and total cell protein extracts were separated by SDS-12%-PAGE, transferred to nitrocellulose membrane and incubated with anti-StpA antibodies in Western immunoblot analysis.

A

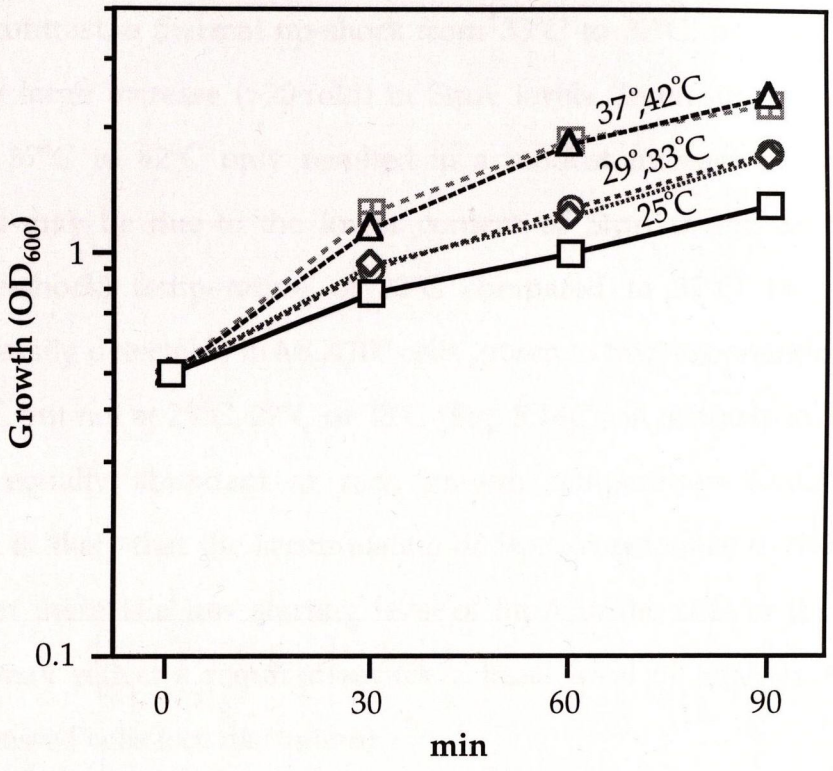
37°,42°C
29°,33°C
25°C
Growth (OD600)
1
0.1
0
30
60
90
min

B

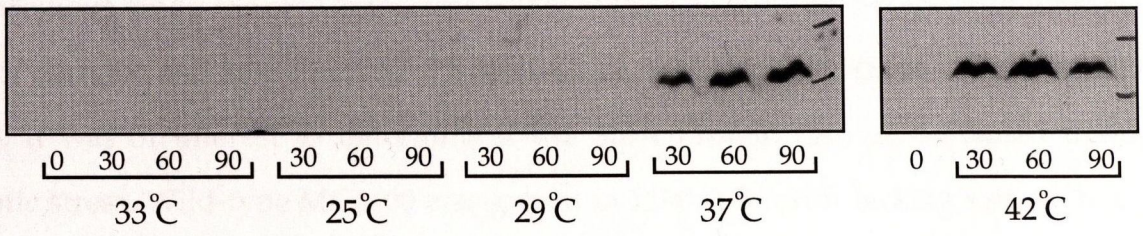
0 30 60 90
30 60 90
30 60 90
30 60 90
0 30 60 90
33°C
25°C
29°C
37°C
42°C

C

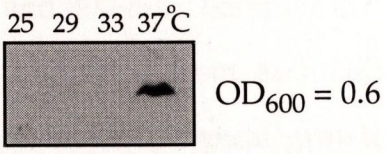
25 29 33 37°C
OD600 = 0.6

experiment. The results are presented in Figure 5.14B and C. The level of StpA was barely detectable at the control temperature of 33°C at any stage of the growth cycle, and no induction of StpA was revealed by a down-shift in temperature to 29°C or 25°C. In contrast, a thermal up-shock from 33°C to 37°C, or from 33°C to 42°C resulted in a large increase (>20-fold) in StpA levels. Interestingly, a thermal up-shock from 37°C to 42°C only resulted in a modest increase in StpA (data not shown). This may be due to the lower content of StpA in the cells at the initial starting (pre-shock) temperature of 33°C compared to 37°C. Indeed, the StpA protein was easily detectable in MC4100 cells grown to mid-exponential phase (OD_{600} = 0.6) at 37°C but not at 25°C, 29°C or 33°C (Fig. 5.14C), in contrast to H-NS content, which was equally abundant at each growth temperature (data not shown). Therefore, it is likely that the accumulation of StpA in response to thermal shock is greater when there is a low starting level of StpA in the cells at the onset of the stress. This may reflect a requirement for a basal level of StpA to be present in thermally stressed cells (see discussion).

5.2.11 Osmotic shock and StpA levels

In a previous study the *stpA* transcript was shown to be induced by ≈50-fold after 60 min of osmotic shock with either 0.4 M NaCl or 0.6 M sucrose (Free and Dorman, 1997). It was of interest to determine if the StpA protein also accumulated upon osmotic stress. Wild-type MC4100 was grown in LB-0 (LB broth lacking salt) at 37°C to an OD_{600} of 0.3. The culture was split into four aliquots; the control culture contained only LB-0, while NaCl was added to the other three aliquots to final concentrations of 100-mM, 200-mM and 300-mM. Samples for Western immunoblot analysis with StpA antiserum were harvested from each culture for 120 min (Fig. 5.15A). In the starting culture grown in LB-0, typical growth-phase regulation of StpA was observed (Fig. 5.15B), and after 120 min the StpA level had declined by 10-fold per cell mass (Fig. 5.15C). A mild osmotic up-shock with 100-mM NaCl had little effect on StpA expression. However, with a moderate shock of 200-mM or a more severe shock of 300-mM NaCl StpA level was elevated by between ~2- and 6-fold

Fig. 5.15. Effect of salt up-shock on the cellular content of StpA

A. Wild-type strain MC4100 was grown for several generations to OD_{600} = 0.3 in LB-0 broth (LB broth without NaCl). The culture was then split into four aliquots, and NaCl added to three of the aliquots to a final concentration of 100, 200 or 300 mM. The remaining sample served as the control. Bacterial growth was monitored for 120 min and is indicated (OD_{600} values).

B. Western immunoblot analysis was performed on total cell extracts that were prepared from the osmotically shocked cultures and the control culture (LB-0) as indicated at time-point 0 (pre-shock) and 30, 60, 90 and 120 min post-shock with anti-StpA antibodies. Total cell extracts were normalised to the OD_{600} values. The position of migration of StpA is indicated.

C. Densitometric analysis of the data in (**B**) expressed as a relative percentage of the most intense band shown (cells pre-shock at an OD_{600} = 0.3). The data shown are an average of two independent experiments, and a representative gel is shown.

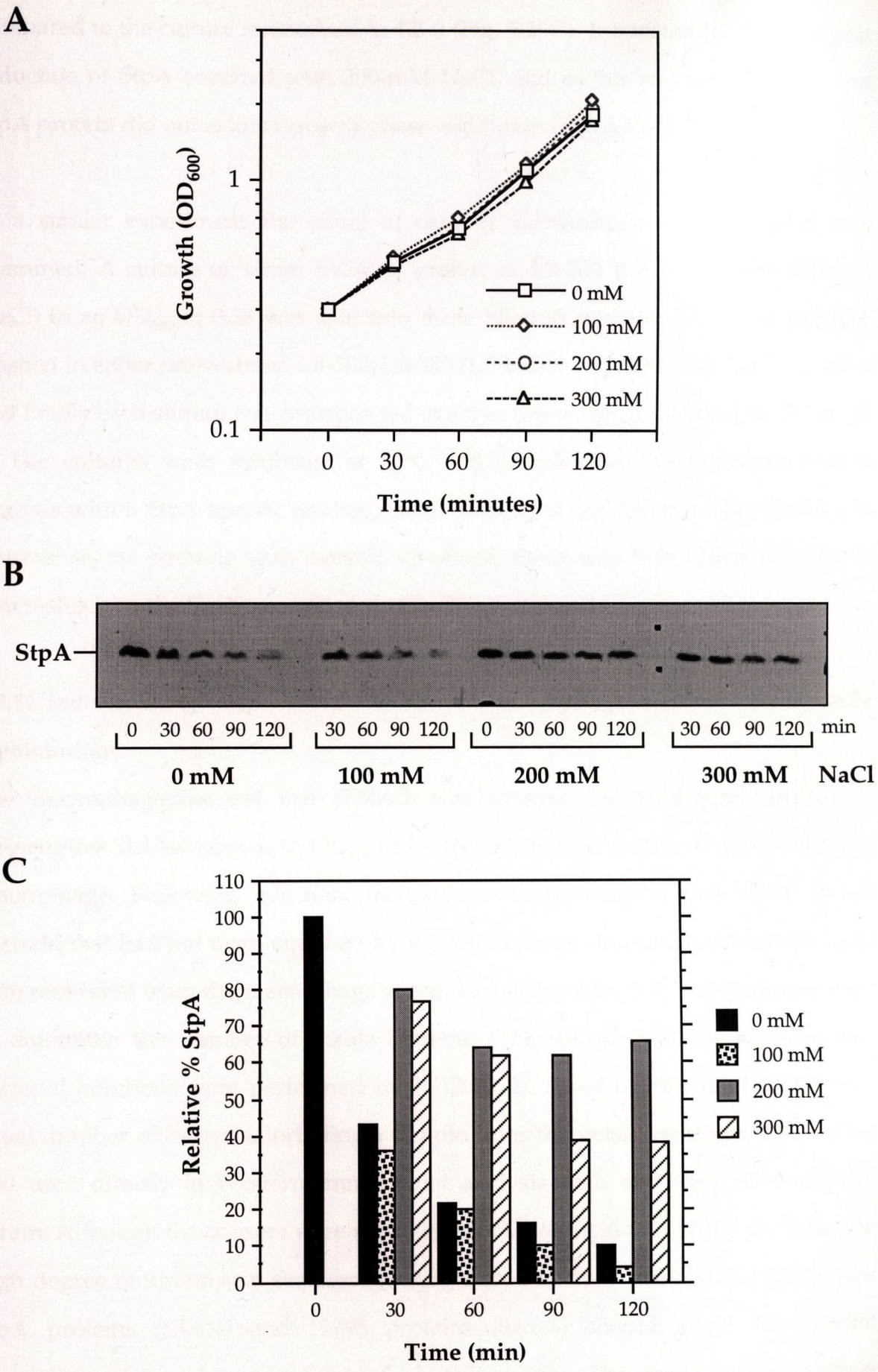
A
Growth (OD_{600})
1
0.1
0 mM
100 mM
200 mM
300 mM
0
30
60
90
120
Time (minutes)
B
StpA
0 30 60 90 120
30 60 90 120
0 30 60 90 120
30 60 90 120
min
0 mM
100 mM
200 mM
300 mM
NaCl
C
Relative % StpA
110
100
90
80
70
60
50
40
30
20
10
0
0 mM
100 mM
200 mM
300 mM
0
30
60
90
120
Time (min)

compared to the culture maintained in LB-0 (Fig. 5.15C). Interestingly, the strongest induction of StpA occurred with 200-mM NaCl, and at this salt concentration the StpA protein did not exhibit growth-phase regulation (Fig. 5.15C).

In a similar experiment the effect of osmotic down-shock on StpA level was examined. A culture of strain MC4100 grown in LB-300 (LB broth with 300-mM NaCl) to an OD_{600} of 0.33 was split into three aliquots and the cells were pelleted, washed in either pre-warmed LB-300, LB-150 (LB broth with 150-mM NaCl) or LB-0, and finally each aliquot was resuspended in either pre-warmed LB-300, LB-150 or LB-0. The cultures were incubated at 37°C and samples for Western immunoblot analysis with a StpA-specific antibody were harvested for 120 min (Fig. 5.16A). In contrast to the scenario with osmotic up-shock, there was little effect of osmotic down-shock on the StpA expression profile (Fig. 5.16B and C).

5.2.12 *Induction of StpA and H-NS in macrophage-engulfed* Salmonella typhimurium

The macrophage-like cell line J774A.1 was infected by wild-type virulent *S. typhimurium* SL1344 (grown to OD_{600} of 1.0 in LB broth) at a ratio of 10 bacteria per macrophage. Following infection, treatment with gentamycin was used to kill bacteria that had not been engulfed by the macrophage. Internalised bacteria were then recovered from the macrophage at regular intervals for 5 h, and a sample used to determine the number of viable bacteria. (The culturing of macrophage and bacterial infections were performed by R. Carroll). Based on this enumeration, an equal number of bacteria, including a sample from the initial inoculum, were lysed and used directly in Western immunoblot analysis with anti-StpA or anti-H-NS serum. Although the antisera were raised against *E. coli* StpA and H-NS proteins, the high degree of amino acid sequence identity between the *E. coli* and *S. typhimurium* StpA proteins (83.6%) and H-NS proteins (94.2%) should allow for specific recognition of *S. typhimurium* StpA and H-NS proteins. The results of this analysis are presented in Fig. 5.17.

Fig. 5.16. Effect of salt down-shock on the cellular content of StpA

A. Wild-type strain MC4100 was grown for several generations to OD_{600} of 0.3 in LB-300 broth (LB broth with 300-mM NaCl). The culture was then split into 3 aliquots, which were pelleted, washed, and resuspended in pre-warmed LB-300, LB-150 (LB broth with 150-mM NaCl) or LB-0 (LB broth without NaCl). Bacterial growth was monitored for 120 min and is indicated (OD_{600} values).

B. Western immunoblot analysis was performed on total cell extracts (normalised to OD_{600} values) that were prepared from the osmotically shocked cultures and the control culture (LB-300) as indicated at time-point 0 (pre-shock) and 30, 60, 90 and 120 min post-shock with anti-StpA antibodies. The position of migration of StpA is indicated.

C. Densitometric analysis of the data in (**B**) expressed as a relative percentage of the most intense band shown (cells pre-shock at an OD_{600} of 0.3). The data shown are an average of two independent experiments, and a representative gel is shown.

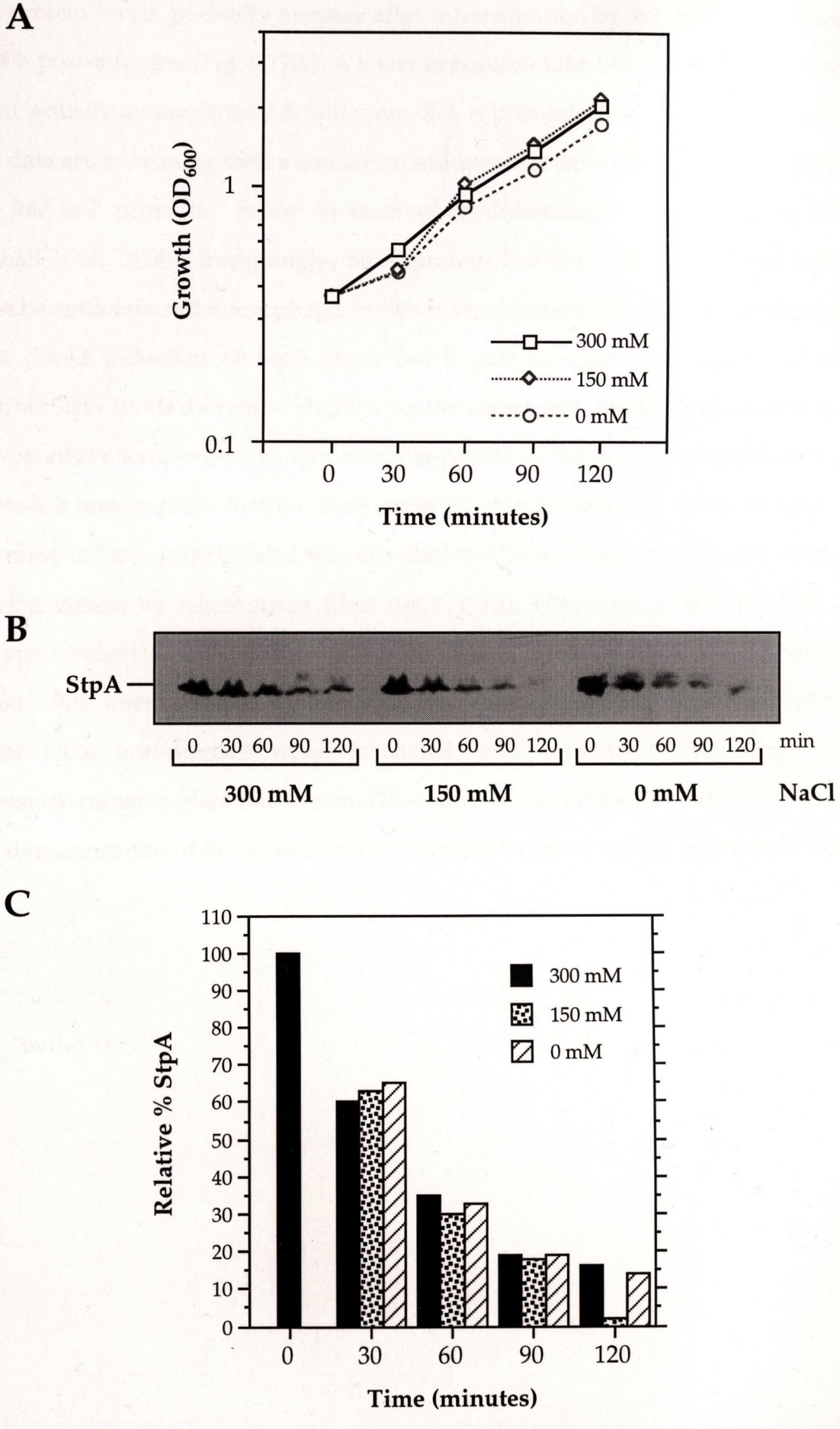
A
Growth (OD600)
1
0.1
0
30
60
90
120
Time (minutes)
300 mM
150 mM
0 mM
B
StpA
0 30 60 90 120
0 30 60 90 120
0 30 60 90 120
min
300 mM
150 mM
0 mM
NaCl
C
Relative % StpA
110
100
90
80
70
60
50
40
30
20
10
0
0
30
60
90
120
Time (minutes)
300 mM
150 mM
0 mM

H-NS protein levels gradually increase after internalisation by the macrophage and peak 4 h post-infection (Fig. 5.17A). A lower exposure of the blot revealed that H-NS content actually accumulated 6.5-fold from 3–4 h post-infection (Fig. 5.17B and C). These data are in keeping with a similar experiment that detected a ~7-fold induction of an *hns–lacZ* promoter fusion in macrophage-internalised *S. typhimurium* cells (Marshall *et al.*, 2000). Intriguingly, StpA protein content also accumulated when SL1344 bacteria infected macrophage. In this case, although overall StpA levels were low, a 5-fold induction of StpA from 2–4 h post-infection was observed, and thereafter StpA levels decreased slightly. As the signal with the StpA antiserum was low even after a long exposure, and a similar profile to the anti-H-NS antibody was observed, it was possible that the StpA antibody was recognising H-NS. However, an increase in StpA protein level was also detected in a *S. typhimurium hns* mutant following uptake by macrophage (data not shown). Therefore, it is likely that in wild-type virulent *S. typhimurium* both homologous proteins StpA and H-NS are induced after internalisation by macrophage. Importantly the StpA and H-NS antisera were non-reactive when incubated with an extract containing only macrophage proteins (data not shown). Therefore, these preliminary data represent a first demonstration of the actual level of bacterial proteins during invasion of host cells.

***Fig. 5.17. Induction of StpA and H-NS in macrophage-internalised* S. typhimurium**

Western immunoblot analysis of the StpA and H-NS content of *S. typhimurium* SL1344 cells recovered from the macrophage-like cell line J774A.1 in a time-course experiment. Bacterial samples at time point P (the initial inoculum of bacteria grown to OD_{600} = 1.0 in LB broth), at time-point 0 (only macrophage-internalised bacteria remain) and at 1, 2, 3, 4 and 5 h post-engulfment were harvested. Total cellular extracts were prepared by lysing an equal number of bacteria, as determined by counting the number of viable bacteria. Duplicate gels were probed with either anti-StpA or anti-H-NS antibodies. The resulting blots were exposed to film for 10 min (**B**) or 45 min (**A** and **C**). The positions of migration of StpA and H-NS are indicated. Densitometric analyses were performed on the bands in (**B**) and (**C**) and are indicated by the graphs below the respective blots, expressed as the fold induction of H-NS or StpA relative to the 3 or 2 h time points, respectively.

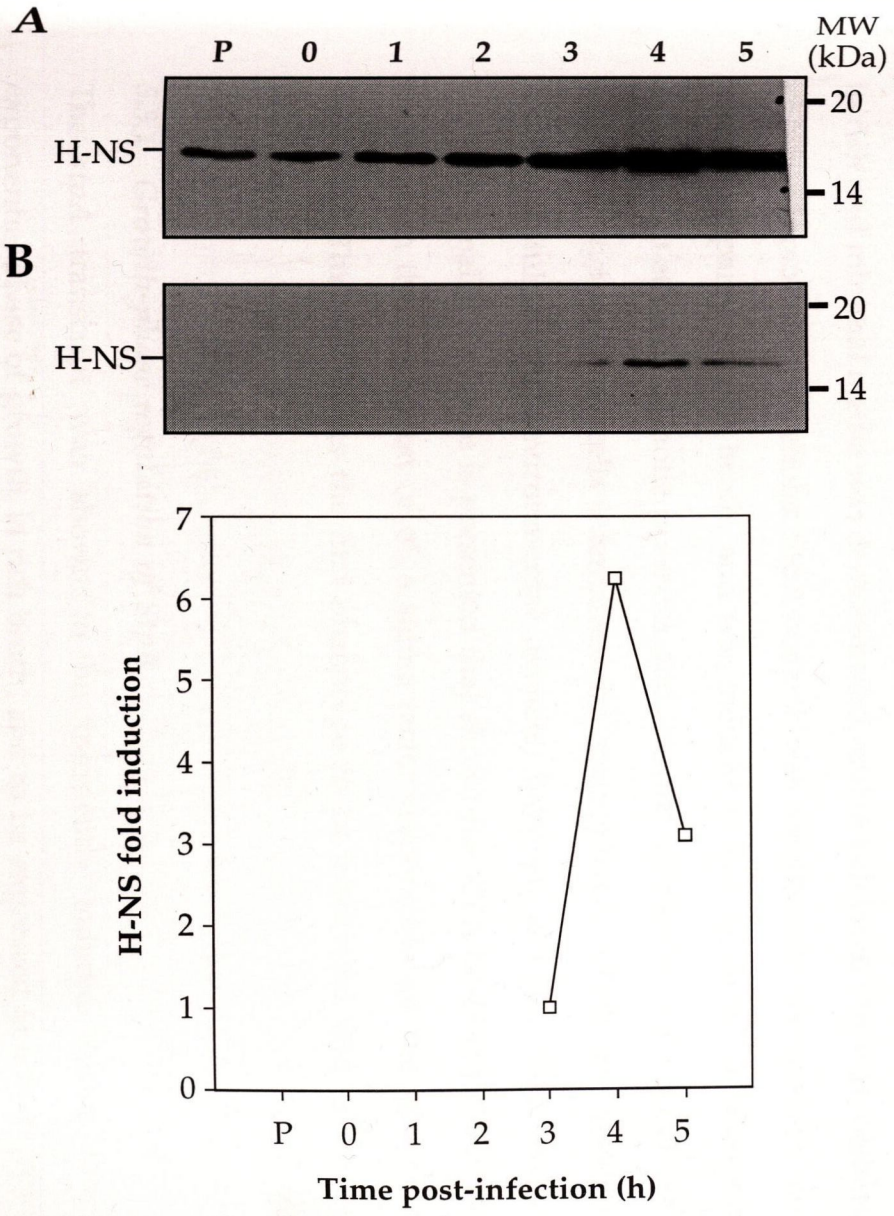
A
P 0 1 2 3 4 5
MW (kDa)
H-NS
20
14
B
H-NS
20
14
H-NS fold induction
0 1 2 3 4 5 6 7
P 0 1 2 3 4 5
Time post-infection (h)
C
P 0 1 2 3 4 5
MW (kDa)
StpA
20
14
StpA fold induction
0 1 2 3 4 5 6 7
P 0 1 2 3 4 5
Time post-infection (h)

5.3 *Discussion*

Expression of the *Escherichia coli stpA* gene has previously been shown to be silenced by the homologous protein H-NS with the result that *stpA* expression is low in a wild-type strain (Sondén and Uhlin, 1996; Zhang *et al.*, 1996). Therefore, it was postulated that *stpA* might function as a molecular back-up for H-NS. Indeed, the lack of any phenotype associated with a *stpA* single mutation and the fact that StpA and H-NS proteins are structurally similar, and functionally similar with respect to many activities supported this view (Bertin *et al.*, 1999). However, StpA also has properties different from those of H-NS particularly with respect to effects on RNA transactions (discussed in Chapters 3 and 4; Zhang *et al.*, 1996; Cusick and Belfort, 1998; Deighan *et al.*, 2000). Furthermore, the *stpA* transcript rather than being completely silent in wild-type *hns*$^+$ cells is in fact modulated by several environmental cues (Free and Dorman, 1997), and might thus have a more independent role. The results presented in this chapter are consistent with this. Using an antibody that recognises only the StpA protein, growth-phase regulation of StpA in rich and minimal media was demonstrated, and in rich broth this was mediated by H-NS. Moreover, the cellular StpA-content was significantly elevated in minimal broth compared to rich broth, and was induced in rich broth by stresses such as exposure to ethanol, osmotic up-shock and thermal up-shock. Additionally, virulent *Salmonella typhimurium* cells internalised by macrophage, which are subjected to several simultaneous environmental assaults, have an elevated StpA and H-NS content. Finally, evidence is presented that shows the RNA-binding protein StpA is involved in the regulation of σ^s, a sigma factor responsible for the general stress response. This represents the first phenotype to be associated with a *stpA* single mutation.

5.3.1 *Growth-phase regulation of StpA*

The *stpA* transcript was shown to be transiently induced during the early exponential phase of growth in rich broth, and to be expressed at a more sustained

level in minimal broth (Free and Dorman, 1997). Using a StpA-specific antibody (Fig. 5.1), the effect of growth-phase on StpA expression was monitored in more detail by Western immunoblot analyses. In rich broth the StpA protein content in wild-type strain MC4100 was highest in the early exponential phase consistent with the detected trend of the *stpA* transcript (Free and Dorman, 1997). However, the StpA level rapidly decreased inversely with an increase in the cellular density of the culture (Fig. 5.2). In fact the StpA content per cell mass was 10-fold reduced in late exponential phase (OD_{600} = 1.3) compared to the early exponential phase (OD_{600} = 0.2) and was further reduced in stationary phase (Fig. 5.2B). A similar trend was observed when strain MC4100 was grown in minimal broth, in that StpA levels decline as the bacteria progress towards stationary phase (Fig. 5.3). However, the rate at which this happens is markedly different. While StpA levels have decreased 10-fold by late exponential phase in LB broth, at a similar cellular density in M9 broth StpA content is reduced by only 50% (Fig. 5.4). Furthermore, there was 10–15-fold more StpA expressed at each stage of growth in minimal medium compared to rich medium (Fig. 5.4). This difference in expression is probably due to the requirement for Lrp in activating *stpA* expression in minimal broth, but not in rich broth (Free and Dorman, 1997), which correlates with the elevated level of Lrp in minimal broth (Calvo and Matthews, 1994).

Although *stpA* expression is autoregulated (Zhang *et al.*, 1996), it was possible that other *trans*-acting factors were responsible for this growth-phase regulation of *stpA* in LB broth. Results from this study and others have shown that H-NS is a dominant repressor of *stpA* expression (Fig. 5.1; Zhang *et al.*, 1996; Free and Dorman, 1997; Sonnenfield *et al.*, 2001), and thus it was possible that the observed growth-phase regulation of StpA was mediated through H-NS. Indeed, in the *hns* mutant strain Western immunoblot analysis revealed that StpA level was derepressed at each stage of the growth curve, and importantly, the ~10-fold decrease in StpA level as bacteria progressed to stationary phase was not evident in an *hns*$^-$ strain (Fig. 5.5). It is intriguing that StpA accumulates to such a degree in the absence of H-NS (up to

35-fold more than in the *hns*$^+$ strain), given that recent reports showed that in an *hns* mutant background the StpA protein is subject to Lon-protease-mediated degradation (Johansson and Uhlin, 1999). Moreover, a heteromeric interaction between H-NS and StpA was necessary to stabilise the StpA protein and protect it from degradation (Johansson *et al.*, 2001).

Therefore, in an attempt to understand how StpA protein level accumulates in an *hns* strain, it is necessary to take into account the change in the H-NS content of cells during the growth curve. However, there is the matter of disagreement in the literature and H-NS protein levels which have variously been reported to be ~3-fold more abundant in stationary phase cells (Spassky *et al.*, 1984; Dersch *et al.*, 1993; Ueguch and Mizuno, 1993), to be relatively constant throughout the growth-phase (Hinton *et al.*, 1992; Free and Dorman, 1995; Sonnenfield *et al.*, 2001), or to be expressed at a lower level in stationary phase (Talukder *et al.*, 1999). In this study the cellular content of H-NS was shown to be approximately constant at each stage of the growth curve in both rich and minimal broths (Fig. 5.6). So given that H-NS expression is more or less constant, how could H-NS modulate the growth-phase regulation of StpA in wild-type cells? It may not be the level of the H-NS protein that is important, but its repressive ability. H-NS can form heterodimers with StpA (Williams *et al.*, 1996; Free *et al.*, 1998; Johansson *et al.*, 2001) and interact with at least two other proteins in *E. coli*, namely Hfq (Kajitani and Ishihama, 1991) and Hha (Nieto *et al.*, 2000). It is possible that any of these interactions could alter the repressive ability of H-NS at the *stpA* promoter. Alternatively, in an *hns* mutant other *trans*-acting factors could modulate the growth-phase regulation of *stpA* expression in LB broth. An obvious candidate for this is Lrp, which is necessary for StpA activation in minimal broth, and *lrp* expression is induced 30-fold in an *hns* mutant (Hommais *et al.*, 2001). More experiments will be required to decipher the mechanism of growth-phase regulation of StpA expression in LB broth, as it is likely to be governed by both synthesis and degradation, and involve autoregulation and cross-talk regulation by H-NS.

5.3.2 *Influence of environmental stress conditions on StpA levels*

The *stpA* and *hns* genes not only differ markedly in the details of their expression profiles in rich and minimal medium as discussed above, but also respond differently to *trans*-acting factors and environmental cues. The FIS protein is a positive regulator of *hns* but has no effect on *stpA* (Falconi *et al.*, 1996; Free and Dorman, 1997). Translation of *hns* mRNA is blocked by the DsrA antisense RNA, but this antisense RNA has no effect on *stpA* expression (Lease *et al.*, 1998). Osmotic stress, temperature increases, carbon starvation, and DNA relaxation all fail to influence *hns* expression, whereas each alters the level of *stpA* mRNA (Dorman *et al.*, 1999). *stpA* expression is also SOS inducible (Benson *et al.*, 2000). Importantly, in this study, the effects of osmotic stress and heat-shock were also shown to affect StpA protein levels. In addition exposure of cells to ethanol up-regulated StpA expression but had no effect on H-NS. However, both StpA and H-NS were induced 4 h post-internalisation by macrophage.

Expression of StpA was elevated by a thermal up-shock from 33°C to 37°C or from 33°C to 42°C, but there was no detectable induction by a down-shift (33°C to 29°C or 33°C to 25°C) in temperature (Fig. 5.14B). Furthermore, considerably more StpA was expressed in mid-exponential phase cells grown at 37°C than at lower temperatures (Fig. 5.14C). How this thermal regulation is achieved is not clear, but it is likely to be H-NS-independent as there was less *stpA* transcript in cells grown at 26°C than at 37°C in both *hns*$^+$ and *hns*$^-$ strains (Sondén and Uhlin, 1996). This presence of StpA at higher temperatures may correlate with the cellular role of the protein. It is plausible to envisage that StpA and other RNA-chaperones may be required to prevent or resolve misfolded RNA molecules that could accumulate at elevated temperatures, analogous to the role of protein chaperones. Consistent with this, the fold-induction in StpA when exposed to a thermal up-shift from 37°C to 42°C was less than the induction of StpA with an up-shift from 33°C to 42°C (data not shown and Fig. 5.14). It is possible that the extent of StpA induction will be governed by the amount of StpA present in the cells at the onset of the shock, i.e., a greater induction occurs

from 33°C when StpA level is low. This may reflect a requirement for a nominal amount of StpA to be present in thermally stressed bacteria.

Treatment of cells with ethanol elicits a response similar to the heat-shock response. Cells treated with ethanol had an elevated StpA and σ^s content (Fig. 5.13), whereas H-NS levels were relatively unaffected (data not shown). Hence, ethanol stress represents another environmental stimulus that differentially modulates the homologous proteins StpA and H-NS. The induction of σ^s (up to 20-fold) in response to the ethanol shock and the rapid fine-tuning of the σ^s level (presumably by proteolysis) to integrate the stage of growth with the presence of the stress was particularly notable (Fig. 5.13). This is a first demonstration that ethanol shock modulates σ^s expression. Given the input of StpA in σ^s regulation (see below), and that StpA is itself induced by ethanol stress, it will be of interest to determine the σ^s content of CJD1600 (MC4100 *stpA*) cells exposed to ethanol.

The level of StpA was markedly induced when MC4100 cells were exposed to a salt up-shock of 200-mM or 300-mM NaCl (Fig. 5.15), but there was no discernable effect on StpA levels by a down-shift in the osmolarity of the medium (Fig. 5.16). The strongest induction occurred with 200-mM NaCl. It is intriguing that the induction of StpA upon salt shock (6-fold with 200-mM NaCl; 2-fold with 300-mM) is much less than the observed increase in *stpA* transcript levels (50-fold with 400-mM NaCl; Free and Dorman, 1997). It is, therefore, possible that *stpA* expression is subject to post-transcriptional control. Indeed, results of a preliminary experiment whereby StpA protein content and *stpA* mRNA levels were monitored from the same culture after osmotic shock with 300-mM NaCl revealed that the *stpA* transcript was elevated by ~7-fold, whereas the StpA protein only accumulated 2-fold (data not shown). It is an exciting possibility that the StpA protein, which can modulate gene expression at a post-transcriptional level (Deighan *et al.*, 2000) is itself subject to post-transcriptional control following osmotic shock.

Possibly the most difficult environmental stresses that bacteria must endure could be envisaged to occur during infection of host cells. Here, unlike the scenario of studying environmental regulation of gene expression in a test tube where generally the effect of one stimulus is monitored at a time, the bacteria are subject to multiple simultaneous assaults. Therefore, although helpful, it is difficult to make a direct correlation between the response of bacteria to stress in a test tube, and to the situation inside host cells (tissue culture) or living animals. Determining the response of *S. typhimurium* and other pathogens to the stressful intracellular environment has been the subject of intense research. Indeed, recently several methods have been developed to identify genes that are specifically activated in the host (reviewed in Chiang *et al.*, 1999). These include promoter-trap strategies using sensitive reporter fusions to genes whose products are necessary to complement auxotrophic mutations, encode antibiotic resistance determinants, or encode the γδ resolvase, which when expressed leads to a loss of antibiotic resistance (*In vivo* expression technology). Genes essential for pathogenicity can also be determined by signature-tagged mutagenesis (Hensel *et al.*, 1995), which relies on comparative hybridisation to identify mutants unable to survive in the host. Furthermore, the expression of genes post-infection can be followed by promoter fusions to *lacZ* or *gfp*. The induction of *gfp* in *S. typhimurium* within host cells can be monitored by differential fluorescence induction, and bacteria within the host cells that contain active *gfp* fusions can be sorted by fluorescence-activated cell sorting (Valdivia and Falkow, 1997). Each of these techniques has significantly accelerated our understanding of the adaptation and survival of bacteria to the stressful intracellular environment.

In this study the change in the H-NS and StpA content of *S. typhimurium* cells following up-take by macrophage was monitored directly by Western immunoblot analyses. Intriguingly, both StpA and H-NS were induced by ~6-fold beginning ~2 h post-internalisation by macrophage (Fig. 5.17). In fact, the overall fold-induction if taken from the moment only intracellular bacteria remain (time point = 0, compared to time point = 4 in Fig. 5.17A and C), is likely to be much greater than this. After 4 h

post-infection the levels of both StpA and H-NS drop slightly. This observed increase in H-NS is in keeping with a similar experiment where a ~7-fold induction of *hns* transcription 2 h post-uptake by macrophage was observed (Marshall *et al.*, 2000). These data implicate a role for H-NS in intracellular survival and/or virulence. Consistent with this, *S. typhimurium hns* mutants are attenuated for mouse virulence (Harrison *et al.*, 1994) and are not cytotoxic for macrophage (cytotoxicity is bacterial induced apoptosis of the host cell that results in a visible disruption of the monolayer; R. Carroll and C. J. Dorman, unpublished data). The induction of StpA in macrophage-engulfed *S. typhimurium* cells would also implicate a role for StpA in adaptation to this stressful environment. It will be of great interest to determine the response of other nucleoid-associated proteins to internalisation by macrophage. Importantly, these preliminary data represent a first demonstration of the actual level of bacterial proteins during invasion of host cells.

A summary of *trans*-acting factors and environmental signals currently implicated in the modulation of the cellular content of StpA is presented in Fig. 5.18. Intriguingly, many of these effectors do not contribute to the regulation of H-NS (see above and Dorman *et al.*, 1999) which would imply that the RNA-binding protein StpA has a unique role to play in bacterial physiology independent from its homologue. However, the mechanistic details of how these signals and regulatory proteins govern *stpA* expression have yet to be elucidated. Increases in the osmolarity or growth temperature of the medium are known to correlate with alterations in DNA topology (Goldstein and Drlica, 1984; Higgins *et al.*, 1988), as is adaptation to the intracellular environment (Marshall *et al.*, 2000). A response of the *stpA* promoter to DNA topology (Free and Dorman, 1997) could at least contribute to some of these effects.

5.3.3 *StpA modulates σ^s expression*

The master regulator of the general stress response, σ^s, is regulated at the level of transcription, translation and protein stability (reviewed in Nogueira and Springer,

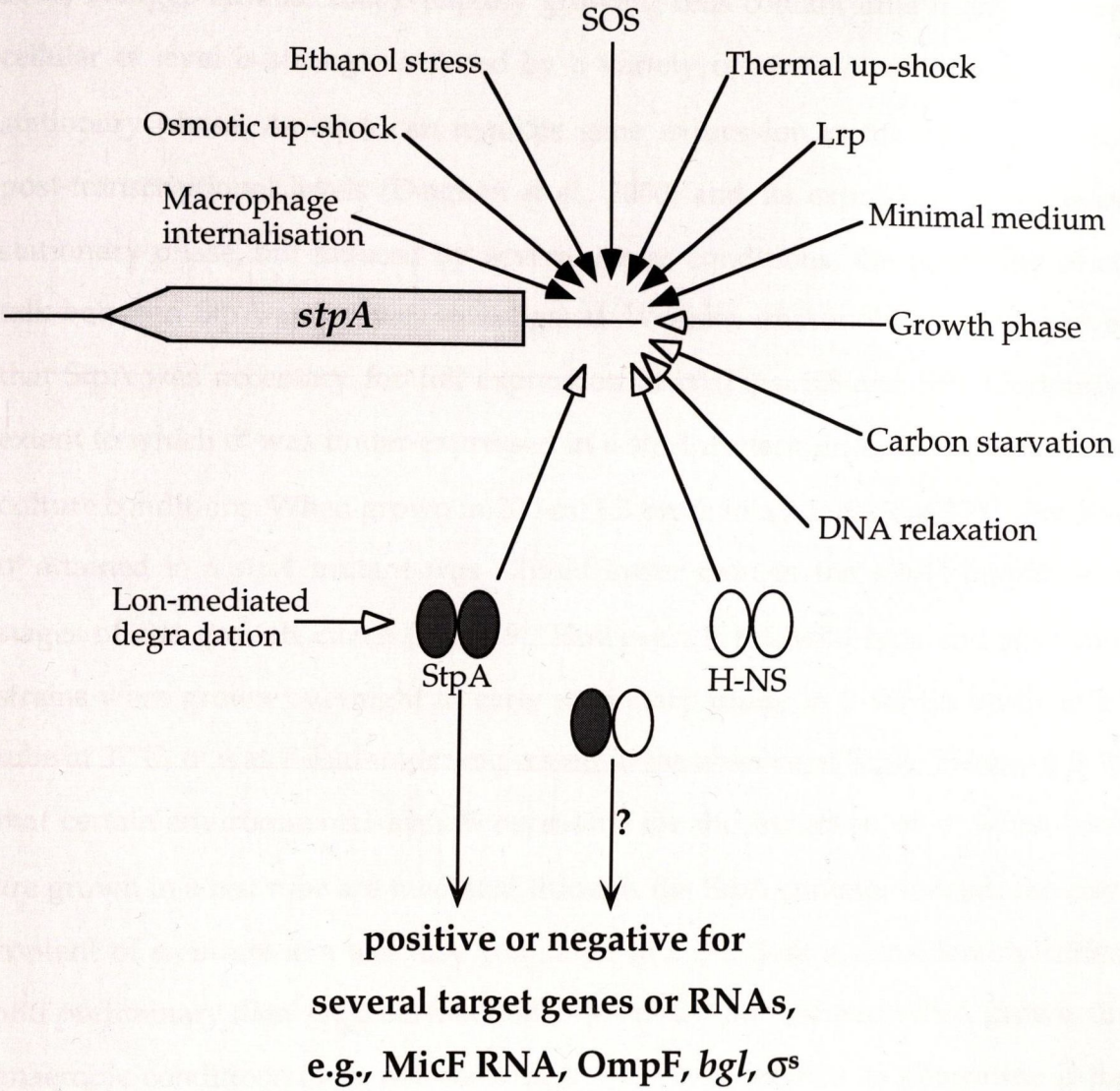

Fig. 5.18. **Trans-*acting factors and environmental conditions affecting expression of the* stpA *gene***

Open arrows refer to effectors that negatively influence *stpA* expression and closed arrows are effectors that positively influence *stpA* expression. For simplicity the effectors are shown to modulate transcription of *stpA*. However, post-transcriptional control of *stpA* is also possible, as is the case for the Lon-protease. The cellular content of StpA that results can, as homomultimers or perhaps as heteromultimers with H-NS, modulate gene expression at the transcriptional and post-transcriptional levels.

2000; Hengge-Aronis, 2000). Rapidly growing cells contain little if any σ^s, but the cellular σ^s level is strongly induced by a variety of stress conditions including the stationary phase. As StpA can regulate gene expression at the transcriptional and post-transcriptional levels (Deighan *et al.*, 2000) and its expression is repressed in stationary phase, but induced by several stress conditions, the possibility of cross-talk between StpA and σ^s was investigated. Western immunoblot analysis revealed that StpA was necessary for full expression of σ^s (Figs. 5.8 and 5.9). Curiously the extent to which σ^s was under-expressed in a *stpA* mutant differed depending on the culture conditions. When grown in 200-ml LB broth in a 2-L flask at 37°C, the level of σ^s attained in a *stpA* mutant was ~2-fold lower than in the *stpA*$^+$ parent at most stages of the growth curve (Fig. 5.9). However, if the wild-type and *stpA* mutant strains were grown overnight to early stationary phase in 3 ml LB broth in a test tube at 37°C, σ^s was 7-fold under-expressed in the absence of StpA. Hence, it is likely that certain environmental signals necessary for the induction of σ^s when bacteria are grown in a test tube are mediated through the StpA protein. Indeed, the oxygen content of a culture in a test tube compared to a 2-L flask is considerably different, and preliminary data suggests that both StpA and σ^s are induced when grown under anaerobic conditions (data not shown). It will be of interest to determine if the σ^s level is increased under anaerobic conditions in the absence of StpA.

The regulation of *rpoS* transcription and mRNA stability have not been studied in detail probably because most environmental signals that induce σ^s do not affect steady-state *rpoS* transcript levels. Nevertheless, the effect of a *stpA* mutation on *rpoS* transcript levels was investigated. It was revealed that the *rpoS* mRNA was expressed at a ~2-fold higher level in the absence of StpA in the late exponential phase and early stationary phase (Fig. 5.11). This is in contrast to the 2-fold reduction in σ^s level in a *stpA* mutant grown under similar conditions. Thus, StpA somehow influences the cellular σ^s content at a post-transcriptional level.

The StpA homologue H-NS also controls expression of σ^s at a level beyond transcription, and in an *hns* mutant the σ^s level is elevated due to enhanced translation and increased stability of the product (Barth *et al.*, 1995; Yamashino *et al.*, 1995). It was possible that the effect of a *stpA* mutation on σ^s content was mediated through increased H-NS protein content, and the opposite may also be true. In an attempt to clarify the pathways of StpA- and H-NS-dependent σ^s control, levels of the *rpoS* mRNA (Fig. 5.11) and protein product (Fig. 5.12) were measured in strains expressing only StpA, H-NS or neither of the homologues. In the *hns* and *stpA hns* mutants the *rpoS* mRNA was 2.5- and 6-fold less abundant than the wild-type and *stpA* single mutant strains, which express a similar amount of the transcript (Fig. 5.12). Nonetheless, the level of σ^s was ~10- and ~20-fold increased in the *hns* and *stpA hns* backgrounds respectively, compared to the wild-type or *stpA* mutant (Fig. 5.10A). This confirms that in the *hns* background σ^s levels are increased due to enhanced translation and/or increased stability of σ^s (Yamashino *et al.*, 1995) and this is also true in the *stpA hns* background. However, as the effects of the *stpA* and *hns* lesions on *rpoS* mRNA and σ^s levels were additive, this would suggest that the precise mechanisms of StpA- and H-NS-dependent control over σ^s are operating by different means. Consistent with this, plasmids over-expressing StpA or H-NS in the *stpA hns* background had differential effects on σ^s content in stationary phase cells (Fig. 5.10).

It is clear the StpA is involved in the modulation of σ^s expression at a level beyond transcription, a first phenotype to be associated with a *stpA* single mutation. Not only is the RNA-binding protein StpA necessary for full expression of σ^s during growth in batch culture, but StpA could also be the mediator of certain stress signals. It is intriguing to speculate that StpA could interact with any of the three untranslated RNAs (DsrA RNA, OxyS RNA or RprA RNA; Table 1.4) implicated in controlling σ^s, a mechanism that would be analogous to StpA-dependent OmpF expression which primarily involves the MicF antisense RNA. Defining the precise mechanism of StpA-dependent σ^s expression awaits further experimentation.

Chapter 6

General Discussion

During the past decade, genetic and biochemical studies on H-NS, an abundant protein associated with the bacterial chromosome, have considerably advanced our understanding of its structure and function in *E. coli* and other enterobacteria. Nowadays, with the availability of sequence data from the numerous microbial genome sequencing projects (37 genomes sequenced, 142 in progress; http://www.tigr.org/tdb/mdb/mdb.html), it is clear that the H-NS-like proteins constitute a large family of proteins in Gram-negative bacteria (42 identified members up to December 2000; Fig. 1.5). In some cases the role of these H-NS-related proteins has been identified. For example, HrvA in *Rhodobacter capsulatus* and SPB in *Rhodobacter sphaeroides* have been demonstrated to control photosystem gene expression (Buggy *et al.*, 1994; Shimada *et al.*, 1996, respectively), VicH has a pleiotropic role in gene expression in *Vibrio cholerae* (Tendeng *et al.*, 2000), and H-NS in *Erwinia chrysanthemi* is crucial for expression of the virulence genes of this plant pathogen (Nasser *et al.*, 2000). H-NS homologues are also often associated with pathogenicity islands or virulence-associated plasmids of bacterial pathogens. In the case of the locus of enterocyte effacement (LEE) pathogenicity island of EPEC, a role for the H-NS-like Ler protein in activating LEE transcription by disrupting H-NS-dependent repression has been demonstrated (Bustamante *et al.*, 2001; Sánchez-SanMartín *et al.*, 2001). However, in the majority of cases a physiological role for the H-NS-like proteins has not been assigned.

The StpA protein shares 58% amino acid sequence identity with H-NS, and both proteins are proposed to adopt a two-domain structure (Fig. 1.4). The coiled-coil N-terminal oligomerisation domain is separated by a linker region to the C-terminal nucleic acid-binding domain (Cusick and Belfort, 1998; Dorman *et al.*, 1999). This strong degree of structural similarity allows the formation of StpA–H-NS heteromers *in vitro* (Williams *et al.*, 1996) and *in vivo* (Johansson *et al.*, 2001), which potentially could modulate gene expression *in vivo* (Dorman *et al.*, 1999; Johansson and Uhlin, 1999). The H-NS and StpA proteins have both similar and diverse functional properties. Each protein can inhibit both its own gene promoter and that

of the other, constrain DNA supercoils *in vitro*, and repress transcription *in vivo* and *in vitro* (Zhang *et al.*, 1996). However, the StpA protein was shown to be superior to H-NS in RNA-related activities *in vitro* (Zhang *et al.*, 1996; Cusick and Belfort, 1998).

Under standard laboratory conditions there was no detectable change in the proteomic profile of an *E. coli stpA* mutant compared to its *stpA*$^+$ parent, as monitored by two-dimensional gel electrophoresis (Zhang *et al.*, 1996; Free and Dorman, 1997a). However, in a *stpA hns* double mutant, the proteomic profile is considerably different when compared to an *hns* single mutant or a wild-type strain (Zhang *et al.*, 1996; Deighan *et al.*, 2000). Thus, StpA makes a significant contribution to gene expression in the absence of H-NS, when StpA protein levels are elevated. *stpA* expression is also induced in response to various environmental cues (Free and Dorman, 1997). Hence, it was possible that the cellular role of StpA may be exploited under specific conditions to modulate gene expression, perhaps via RNA interactions. The purpose of the work described in this study was to define a more independent role for the H-NS homologue StpA.

The outer membrane porin protein, OmpF, was shown by two-dimensional gel electrophoresis to be strongly down-regulated in the absence of the nucleoid-associated proteins H-NS and StpA, (Fig. 3.1). In a previous study the OmpF level was shown to be under-expressed in a *hns* mutant, and this was mediated by a transcriptional effect at the promoter of the antisense MicF RNA (Suzuki *et al.*, 1996). However, an analysis of outer membrane proteins by one-dimensional gel electrophoresis revealed that there was a very strong negative effect of the *stpA* mutation on OmpF level, on top of an effect caused by mutating *hns* (Fig. 3.5). The synthesis of OmpF is controlled in response to a variety of environmental parameters and *trans*-acting factors, and additionally its expression is influenced by an RNA-component, the MicF antisense RNA (Pratt *et al.*, 1996). As StpA was proposed to have RNA-chaperone activity, and its expression also influenced by environmental cues, the influence of StpA on *ompF* gene expression seemed

particularly suited as a model system with which to study the activity of the StpA protein in gene regulation.

A series of *in vivo* genetic and biochemical analyses revealed that the StpA and H-NS proteins both modulated OmpF porin expression predominantly at a post-transcriptional level. The reduced stability of the *ompF* message in the *stpA hns* background explained the under-representation of OmpF in the outer membrane of the double mutant. The 93-nt MicF RNA is a determinant of *ompF* mRNA stability, and a requirement for the *micF* locus was shown for StpA- and H-NS-dependent OmpF control. Intriguingly, however, the effects of StpA and H-NS on *micF* expression were different. Whereas H-NS was shown to repress *micF* promoter activity as previously reported (Suzuki *et al.*, 1996), there was no evidence of transcriptional repression of *micF* by StpA. Instead, StpA was shown to modulate MicF RNA stability. Hence, the MicF RNA, which is proposed to fine-tune the amount of OmpF porin expressed in the bacterial outer membrane in response to environmental cues (Pratt *et al.*, 1996), is itself subject to post-transcriptional regulation, and this is mediated by the StpA protein. This represents a novel regulatory mechanism in the network controlling porin synthesis. Furthermore, this works highlights the first functional *in vivo* role for StpA that is different to that of its paralogue H-NS (Chapter 3; Deighan *et al.*, 2000).

MicF antisense RNA represses *ompF* translation by forming an RNA–RNA duplex with the 5′-UTR of the *ompF* message due to complementary sequences, and this results in a poorly translated complex. To investigate the post-transcriptional mechanism of StpA-dependent OmpF control via MicF RNA, StpA–RNA interactions were analysed *in vitro*. The His-tag recombinant StpA protein, purified by affinity chromatography, was shown to be proficient for oligomerisation, DNA and RNA associations, and modulated *proU* transcription when expressed *in vivo*. Therefore, both the purified StpA and H-NS proteins (a gift from S. Rimsky) were suitable for RNA gel-shift assays. The affinity of StpA for the *ompF-213*, *ompC-268* and the 93-nt

MicF RNA probes was on average 2-fold greater than that of H-NS under identical conditions. This result is in keeping with the proposed superior RNA-binding activity of StpA (Cusick and Belfort, 1998). However, the affinity of StpA for the MicF and *ompF-213* RNA transcripts was the same as for the control *ompC-268* probe. This suggests that StpA might function directly at the level of the MicF RNA–*ompF* mRNA interaction *in vivo*, rather than through prolonged stable association with either one of these RNA components. Therefore, the MicF RNA and the *ompF-213* RNAs were annealed *in vitro*. This slower-moving MicF RNA–*ompF-213* mRNA complex was not present if the sample was heated to 70°C prior to electrophoresis, consistent with an annealed RNA–RNA duplex spanning a region of 25-nt. Additionally, the MicF RNA–*ompF-213* RNA duplex did not form in the presence of StpA. This verifies the proposed model based on data obtained *in vivo*, and further suggests that the effect of StpA on *micF* expression is direct (Chapter 4).

A model summarising the proposed mechanism(s) of StpA-dependent OmpF control via MicF RNA collated from data obtained *in vivo* (Chapter 3) and *in vitro* (Chapter 4), is presented in Fig. 6.1. In wild-type cells MicF RNA level is low as H-NS represses *micF* transcription. However, *micF* expression may be induced by certain environmental parameters, or in an *hns* mutant. An elevated MicF RNA level leads to the formation of the MicF RNA–*ompF* mRNA duplex as shown in (**A**) which is non-proficient for translation and is degraded by cellular RNases (illustrated by scissors). The RNA-binding protein StpA is proposed to inhibit the formation of this RNA–RNA duplex by two possible mechanisms. In (**B**) StpA is shown to prevent the formation of the MicF RNA–*ompF* mRNA complex by directly associating with MicF RNA. This interaction is probably transient and could involve an RNA-chaperone activity whereby StpA resolves or prevents denaturation of stem-loop I of MicF RNA (mis folding), which is necessary for duplex formation. The MicF RNA may also be destabilised/targeted for degradation by this StpA–RNA association. It is also possible that StpA could interact with the *ompF* mRNA directly and thus provide a steric barrier to an interaction with the antisense RNA. In (**C**) the effect of StpA

Fig. 6.1. Model summarising StpA-dependent regulation of* ompF *translation via MicF antisense RNA

In wild-type cells, H-NS (illustrated by squares) represses transcription of the *micF* gene leading to low levels of the MicF antisense RNA in the cell. However, *micF* expression may be induced by certain environmental parameters or in an *hns* mutant, and an elevated MicF RNA level leads to the formation of the MicF RNA–*ompF* mRNA duplex as shown in (**A**). When complexed with the MicF RNA, the *ompF* message is inefficiently translated and is degraded by cellular RNases (illustrated by scissors). The RNA-binding protein StpA is proposed to prevent the stable formation of the MicF RNA–*ompF* mRNA duplex by two possible mechanisms. In (**B**) StpA is shown to directly inhibit formation of the duplex through an interaction with the MicF RNA. This interaction could involve an RNA chaperone activity whereby StpA resolves or prevents denaturation of stem-loop I of MicF RNA (mis folding) which is necessary for duplex formation. StpA could also associate directly with the *ompF* mRNA and thereby hinder its interactions with the MicF antisense RNA. In (**C**) the inhibitory effect of StpA operates after annealing of the MicF RNA–*ompF* mRNA duplex. The structural changes (mis folding) in the MicF and *ompF* RNAs upon formation of the duplex may be recognised by the StpA protein that could then actively destabilise and dissociate the MicF RNA–*ompF* mRNA duplex. Whichever of these mechanisms operates (**B** or **C** above) it is clear that StpA impedes the stable formation of the RNA–RNA duplex between the MicF RNA and the *ompF* mRNA and consequently the *ompF* mRNA is freely available for ribosome loading and translation (**D**).

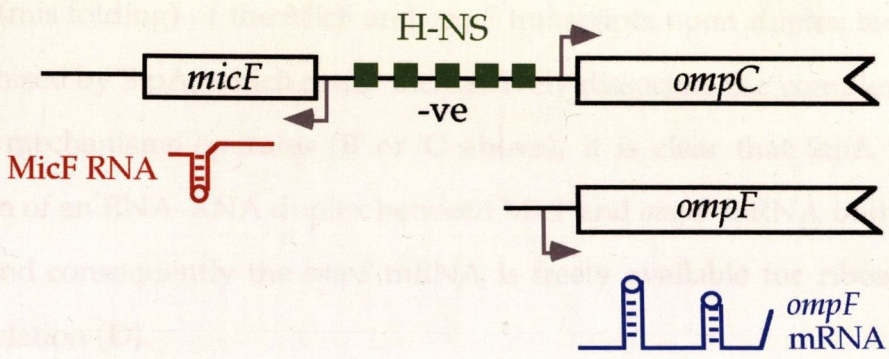
H-NS
micF
ompC
-ve
MicF RNA
ompF
ompF
mRNA

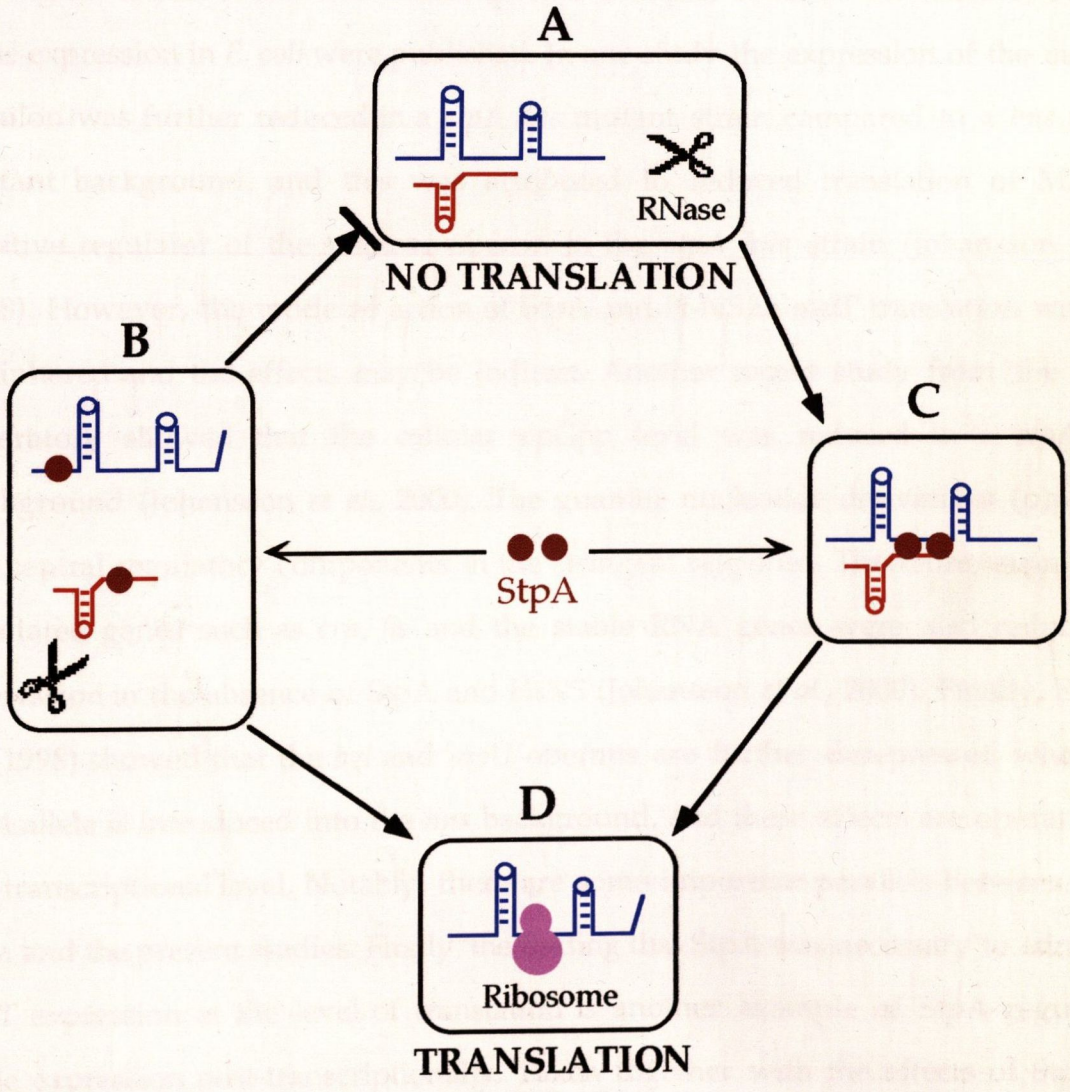
A
RNase
NO TRANSLATION
B
C
StpA
D
Ribosome
TRANSLATION

operates after annealing of the MicF RNA–*ompF* mRNA duplex. The structural changes (mis folding) of the MicF and *ompF* transcripts upon duplex formation may be recognised by StpA, which could then actively dissociate the complex. Whichever of these mechanisms operates (**B** or **C** above), it is clear that StpA impedes the formation of an RNA–RNA duplex between MicF and *ompF* mRNA both *in vitro* and *in vivo*, and consequently the *ompF* mRNA is freely available for ribosome loading and translation (**D**).

During the course of this work other specific examples of an involvement of StpA in gene expression in *E. coli* were published. In one study the expression of the maltose regulon was further reduced in a *stpA hns* mutant strain compared to a *hns* single mutant background, and this was attributed to reduced translation of MalT, a positive regulator of the maltose operon in the *stpA hns* strain (Johansson *et al.*, 1998). However, the mode of action of StpA and H-NS in *malT* translation was not deciphered and the effects may be indirect. Another recent study from the same laboratory showed that the cellular ppGpp level was reduced in a *stpA hns* background (Johansson *et al.*, 2000). The guanine nucleotide derivatives (p)ppGpp are central regulatory components in the stringent response. Therefore, stringently regulated genes such as *crp*, *fis* and the stable RNA genes were also reduced in expression in the absence of StpA and H-NS (Johansson *et al.*, 2000). Finally, Free *et al.* (1998) showed that the *bgl* and *proU* operons are further derepressed when the *stpA* allele is introduced into the *hns* background, and these effects are operating at the transcriptional level. Notably, there are some important parallels between these data and the present studies. Firstly, the finding that StpA was necessary to stimulate *malT* expression at the level of translation is another example of StpA regulating gene expression post-transcriptionally. Taken together with the effects of StpA on *ompF* and *rpoS* expression as identified in this study, this suggests that the cellular role of StpA may primarily involve RNA–interactions, rather than the regulation at the level of transcription generally associated with its paralogue H-NS. Secondly, there was little or no effect of a *stpA* single mutation on expression of the target

genes discussed above (except σ^s, see below). In all cases an effect of a *stpA* lesion was only seen in the absence of H-NS. Similarly, there was no noticeable difference in the proteomic profiles of *stpA*$^+$ and *stpA*$^-$ strains when analysed by two-dimensional electrophoresis (Zhang *et al.*, 1996; Free and Dorman, 1997a). What, therefore, is the physiological relevance of StpA?

The *stpA* message, unlike the *hns* mRNA, accumulates in response to osmotic stress and with increases in temperature (Free and Dorman, 1997). It is possible that, if the StpA protein was similarly expressed it could play a role in modulating gene expression in response to environmental signals. Therefore, using a specific anti-StpA antibody, the StpA-content of wild-type *E. coli* MC4100 cells was monitored during growth in rich and minimal broths, and in response to different environmental cues by Western immunoblot analyses. The results demonstrated that the cellular content of StpA is maximal in early exponential phase in both rich and minimal broths, and that *stpA* expression is growth-phase regulated. Significantly, the level of StpA was ~12-fold higher in minimal broth than in rich broth at each stage of growth. In LB-broth, the H-NS protein mediates the growth-phase regulation of StpA. However, the StpA protein accumulates in response to thermal up-shock, salt up-shock, exposure to ethanol (Chapter 5) and when grown under anaerobic conditions (data not shown) even in an *hns*$^+$ strain. Bacteria grown under some of these conditions do not exhibit growth-phase regulation of *stpA* expression. Additionally, the H-NS and StpA cellular content of macrophage-engulfed *S. typhimurium* cells is markedly increased 4 h post-infection, a first demonstration of the actual level of bacterial regulatory proteins within host cells. It will be of great interest to monitor the expression of OmpF and other StpA-dependent genes in cells grown under *stpA*-inducing conditions like those described above, experiments which would further confirm the physiological relevance of StpA in wild-type bacteria.

All in all, these data may help explain the lack of a detectable phenotype associated with a *stpA* mutation. In studies monitoring StpA-dependent regulation, the expression of various target genes (e.g., *ompF*, *micF*, *malT*, *proU*, *bgl*, *crp*) or the whole proteome was monitored in *stpA*$^+$ and *stpA*$^-$ backgrounds that were grown in rich broth to either mid-exponential phase or stationary phase. However, at these stages of growth there is little expression of StpA (Fig. 5.2) and, consequently, little effect on target-gene expression in a *stpA* strain. In contrast, in an *hns* mutant StpA levels are elevated up to 35-fold compared to a wild-type strain (Fig. 5.5). Thus, there is a noticeable difference in expression of the target gene in an *hns* mutant when compared to a strain also lacking StpA.

σ^s is responsible for co-ordinating the general stress response in *E. coli* and other bacteria, and its expression is consequently induced in response to various stressful conditions including the stationary phase and ethanol stress as shown in this study. Modulation of cellular σ^s content is complex and involves control at the level of transcription, translation and σ^s stability (reviewed in Hengge-Aronis, 2000). As the expression profile for StpA (repressed in stationary phase) is reciprocal to that of σ^s, and given that StpA is induced by certain stresses and can modulate gene expression at a post-transcriptional level, the potential for cross-talk regulation between StpA and σ^s was investigated. Surprisingly, a 'normal amount' of StpA was required for full expression of σ^s. In a *stpA* mutant σ^s content was reduced by~2-fold at most stages during growth in a vigorously aerated flask. However, when grown in a test tube σ^s was ~7-fold under-expressed. Furthermore, a strain over-expressing StpA *in trans* also had a reduced level of σ^s. Taken in combination these data suggest that σ^s expression is particularly sensitive to StpA protein levels, and this may explain why (unlike other genes) σ^s expression is altered in a *stpA* single-mutant background. These effects are likely to be mediated at a post-transcriptional level as the expression of the *rpoS* mRNA in a *stpA* mutant and a *stpA* over-expressing strain did not correlate with the observed cellular σ^s content. Moreover, the results of epistatic and complementation experiments suggest that StpA- and H-NS-dependent control

of σ^s operates by different mechanisms. Further careful experiments will need to be performed to precisely define the role for StpA in modulating cellular σ^s levels.

In conclusion, this work has contributed to the understanding of the differential roles of the paralogous proteins H-NS and StpA in *E. coli*, using regulation of *ompF* porin gene expression as a model system. The regulation of σ^s is a second example where H-NS and StpA have functionally distinct roles to play. The future will likely reveal many more specific examples of target genes that require StpA and/or H-NS for controlled expression. Indeed, recently it was shown that ~250 genes (5% of the *E. coli* genome) in an *hns* mutant are differentially expressed compared to a wild-type strain under standard growth conditions, and many of these genes have no known function (Hommais *et al.*, 2001). The transcriptomic profile for *E. coli stpA* and *stpA hns* strains has also already been done (P. Bertin, personal communication). These data will provide a valuable catalogue of genes controlled by StpA and H-NS, but will tell us nothing about the manner in which this genetic expression is controlled. mRNA is only one intermediate between DNA and protein. Results from this study highlight the importance of small RNAs for StpA-dependent regulation and these are not represented in standard 'DNA arrays'. More traditional molecular biological and proteomic approaches are still required to gain a more integrated view of bacterial gene regulatory circuits.

Bibliography

Åkerlund, T., K. Nordstrom, and R. Bernander. 1995. Analysis of cell size and DNA content in exponentially growing and stationary-phase batch cultures of *Escherichia coli*. J. Bacteriol. **177**:6791-6797.

Altschul, S. F., W. Gish, W. Miller, E. W. Myers, and D. J. Lipman. 1990. Basic local alignment search tool. J. Mol. Biol. **215**:403-410.

Altuvia, S., D. Weinstein-FIScher, A. Zhang, L. Postow, and G. Storz. 1997. A small, stable RNA induced by oxidative stress: role as a pleiotropic regulator and antimutator. Cell. **90**:43-53.

Altuvia, S., A. Zhang, L. Argaman, A. Tiwari and G. Storz. 1998. The *Escherichia coli* OxyS RNA represses *fhlA* translation by blocking ribosome binding. **17**:6069-6075

Andersen, J., N. Delihas, K. Ikenaka, P. J. Green, O. Pines, O. Ilercil, and M. Inouye. 1987. The isolation and characterization of RNA coded by the *micF* gene in *Escherichia coli*. Nucleic Acids Res. **15**:2089-2101.

Andersen, J., S. A. Forst, K. Zhao, M. Inouye, and N. Delihas. 1989. The function of *micF* RNA. J. Biol. Chem. **264**:17961-17970.

Andersen, J., and N. Delihas. 1990. *micF* RNA binds to the 5'-end of *ompF* mRNA and to a protein from *Escherichia coli*. Biochemistry. **29**:9249-9256.

Argaman, L., R. Hershberg, J. Vogel, G. Bejerano, E. G. Wagner, H. Margalit and S. Altuvia. 2001. Novel small RNA-encoding genes in the intergenic regions of *Escherichia coli*. Curr. Biol. **26**:941-950

Ariza, R. R., Z. Li, N. Ringstad, and B. Demple. 1995. Activation of multiple antibiotic resistance and binding of stress-inducible promoters by *Escherichia coli* Rob protein. J. Bacteriol. **177**:1655-1661.

Atlung, T., and H. Ingmar. 1997. H-NS: a modulator of environmental regulated gene expression. Mol. Microbiol. **24**:7-17.

Ausubel, F. M., R. Brent, R. E. Kingston, D. D. Moore, J. G. Seidman, J. A. Smith, and K. Struhl. 1990. Current protocols in molecular biology, Vol. 1. John Wiley & Sons, New York.

Bachellier, S., J. M. Clement, and M. Hofnung. 1999. Short palindromic repetitive DNA elements in enterobacteria: a survey. Res Microbiol. **150**:627-639.

Balandina, A., L. Claret, R. Hengge-Aronis, and J. Rouviere-Yaniv. 2001. The *Escherichia coli* histone-like protein HU regulates *rpoS* translation. Mol. Microbiol. **39**:1069-1079

Barth, M., C. Marschall, A. Muffler, D. FIScher, and R. Hengge-Aronis. 1995. Role for the histone-like protein H-NS in growth-phase-dependent and osmotic regulation of σ^S and many σ^S-dependent genes in *Escherichia coli*. J. Bacteriol. **177**:3455-3464.

Becker, G., E. Klauck, and R. Hengge-Aronis. 1999. Regulation of RpoS proteolysis in *Escherichia coli*: the response regulator RssB is a recognition factor that interacts with the turnover element in RpoS. Proc. Natl. Acad. Sci. U S A. **96**:6439-6444.

Becker, G., and R. Hengge-Aronis. 2001. What makes an *Escherichia coli* promoter σ^s dependent? Role of the -13/-14 nucleotide promoter positions and region 2.5 of σ^s. Mol. Microbiol. **39**:1153-1165

Bendich, A. J., and K. Drlica. 2000. Prokaryotic and eukaryotic chromosomes: what's the difference? Bioessays. **22**:481-486.

Bendich, A. J. 2001. The form of chromosomal DNA molecules in bacterial cells. Biochimie. **83**:177-186.

Bennik, M. H., P. J. Pomposiello, D. F. Thorne, and B. Demple. 2000. Defining a *rob* regulon in *Escherichia coli* by using transposon mutagenesis. J. Bacteriol. **182**:3794-3801.

Benson, N. R., R. M. Wong, M. McClelland. 2000. Analysis of the SOS response in *Salmonella enterica* serovar *typhimurium* using RNA fingerprinting by arbitrarily primed PCR. J. Bacteriol. 182:3490-3497

Bergström, L. C., L. Qin, S. L. Harlocker, L. A. Egger, and M. Inouye. 1998. Hierarchical and co-operative binding of OmpR to a fusion construct containing the *ompC* and *ompF* upstream regulatory sequences of *Escherichia coli.* Genes Cells. **3**:777-788.

Bernardini, M. L., M. G. Sanna, A. Fontaine, and P. J. Sansonetti. 1993. OmpC is involved in invasion of epithelial cells by **Shigella flexneri**. Infect. Immun. **61**:3625-3635.

Bernstein, H. D. 2000. The biogenesis and assembly of bacterial membrane proteins. Curr. Opin. Microbiol. **3**:203-209.

Bertin, P., N. Benhabiles, E. Krin, C. Laurent-Winter, C. Tendeng, E. Turlin, A. Thomas, A. Danchin, and R. Brasseur. 1999. The structural and functional organisation of H-NS-like proteins is evolutionarily conserved in Gram-negative bacteria. Mol. Microbiol. **31**:319-329

Bertin, P., F. Hommais, E. Krin, O. Soutourina, C. Tendeng, S. Derzelle, and A. Danchin. 2001. H-NS and H-NS-like proteins in Gram-negative bacteria and their multiple role in the regulation of bacterial metabolism. Biochimie. **83**:235-241.

Blattner, F. R., G. Plunkett, C. A. Bloch, N. T. Perna, V. Burland, M. Riley, J. Collado-Vides, J. D. Glasner, C. K. Rode, G. F. Mayhew, J. Gregor, N. W. Davis, H. A. Kirkpatrick, M. A. Goeden, D. J. Rose, B. Mau, and Y. Shao. 1997. The complete genome sequence of *Escherichia coli* K-12. Science. **277**:1453-1474.

Blum, G., I. Muhldorfer, P. Kuhnert, J. Frey, and J. Hacker. 1996. Comparative methodology to investigate the presence of *Escherichia coli* K-12 strains in environmental and human stool samples. FEMS Microbiol. Lett. **143**:77-82.

Böhringer, J. D., G. FIScher, G. Mosler, and R. Hengge-Aronis. 1995. UDP-glucose is a potential intracellular signal molecule in the control of expression of σ^s and σ^s-dependent genes in *Escherichia coli.* J. Bacteriol. **172**:3450-3461.

Bradford, M. M. 1976. A rapid and sensitive method for the quantification of microgram quantities of protein utilizing the principle of protein-dye binding. Anal. Biochem. **72**:248-254.

Braun, V., C. Bos, M. Braun, and H. Killmann. 2001. Outer membrane channels and active transporters for the uptake of antibiotics. J. Infect. Dis. **183**:S12-S16.

Browning, D. F., J. A. Cole, and S. J. Busby. 2000. Suppression of FNR-dependent transcription activation at the *Escherichia coli nir* promoter by FIS, IHF and H-NS: modulation of transcription initiation by a complex nucleo-protein assembly. Mol. Microbiol. **37**:1258-1269.

Brukner, I., R. Sanchez, D. Suck, and S. Pongor. 1995. Sequence-dependent bending propensity of DNA as revealed by DNase I: parameters for trinucleotides. EMBO J. **14**:1812-1818.

Buckler, D. R., G. S. Anand, and A. M. Stock. 2000. Response-regulator phosphorylation and activation: a two-way street? Trends Microbiol. **8**:153-156.

Buggy, J. J., M. W. Sganga, and C. E. Bauer. 1994. Characterization of a light-responding trans-activator responsible for differentially controlling reaction center and light-harvesting-I gene expression in *Rhodobacter capsulatus*. J. Bacteriol. **176**:6936-6943.

Busby, S., A. Kolb, and H. Buc. 1979. Isolation of plasmid-protein complexes from *Escherichia coli*. Eur. J. Biochem. **99**:105-111.

Bustamante, V., F. Santana, E. Calva, and J. Puente. 2001. Transcriptional regulation of type III secretion genes in enteropathogenic *Escherichia coli*: Ler antagonizes H-NS-dependent repression. Mol. Microbiol. **39**:664-678.

Casadaban, M. J. 1976. Transposition and fusion of the *lac* genes to selected promoters in *Escherichia coli* using bacteriophage lambda and Mu. J. Mol. Biol. **104**:541-555

Calvo, J.M. and R.G. Matthews. (1994) The leucine-responsive regulatory protein, a global regulator of metabolism in *Escherichia coli*. Microbiol. Rev. **58**:466-490.

Carpousis, A. J., G. Van Houwe, C. Ehretsmann, and H. M. Krisch. 1994. Copurification of *Escherichia coli* RNAase E and PNPase: evidence for a specific association between two enzymes important in RNA processing and degradation. Cell. **76**:889-900.

Ceschini, S., G. Lupidi, M. Coletta, C. L. Pon, E. Fioretti, and M. Angeletti. 2000. Multimeric self-assembly equilibria involving the histone-like protein H-NS. A thermodynamic study. J. Biol. Chem. **275**:729-734.

Chatfield, S. N., C. J. Dorman, C. Hayward, and G. Dougan. 1991. Role of OmpR-dependent genes in *Salmonella typhimurium* virulence: mutants deficient in both *ompC* and *ompF* are attenuated *in vivo*. Infect. Immun. **59**:449-452.

Chiang, S. L., J. J. Mekalanos, and D. W. Holden. 1999. *In vivo* genetic analysis of bacterial virulence. Annu. Rev. Microbiol. 53:129-154.

Chou, J. H., J. T. Greenberg, and B. Demple. 1993. Post-transcriptional repression of *Escherichia coli* OmpF protein in response to redox stress: positive control of the *micF* antisense RNA by the *soxRS* locus. J. Bacteriol. **175**:1026-1031.

Clodi, E., K. Semrad, and R. Schroeder. 1999. Assaying RNA chaperone activity *in vivo* using a novel RNA folding trap. EMBO J. **18**:3776-3782.

Cogoni, C., and G. Macino. 2000. Post-transcriptional gene silencing across kingdoms. Curr. Opin. Genet. Dev. **10**:638-643.

Cohen, S. P., L. M. McMurry, and S. B. Levy. 1988. *marA* locus causes decreased expression of OmpF porin in multiple-antibiotic-resistant (Mar) mutants of *Escherichia coli*. J. Bacteriol. **170**:5416-5422.

Cohen, S. P., S. B. Levy, J. Foulds, and J. L. Rosner. 1993. Salicylate induction of antibiotic resistance in *Escherichia coli*: activation of the *mar* operon and a *mar*-independent pathway. J. Bacteriol. **175**:7856-7862.

Collier, D. N., V. A. Bankaitis, J. B. Weiss, and P. J. Bassford. 1988. The antifolding activity of SecB promotes the export of the *E. coli* maltose-binding protein. Cell. **53**:273-283.

Conn, G. L., and D. E. Draper. 1998. RNA structure. Curr. Opin. Struct. Biol. **8**:278-285.

Cowan, S. W., T. Schirmer, G. Rummel, M. Steiert, R. Ghosh, R. A. Pauptit, J. N. Jansonius, and J. P. Rosenbusch. 1992. Crystal structures explain functional properties of two *Escherichia coli* porins. Nature. **358**:727-733.

Cozzarelli, N. R. 1980. DNA gyrase and the supercoiling of DNA. Science. **207**:953-960.

Cunha, S., T. Odijk, E. Suleymanoglu, and C. L. Woldringh. 2001. Isolation of the *Escherichia coli* nucleoid. Biochimie. **83**:149-154.

Cunning, C., L. Brown, and T. Elliott. 1998. Promoter substitution and deletion analysis of upstream region required for *rpoS* translational regulation. J. Bacteriol. **180**:4564-4570.

Cusack, S. 1999. RNA-protein complexes. Curr. Opin. Struct. Biol. **9**:66-73.

Cusick, M. E., and M. Belfort. 1998. Domain Structure and RNA annealing activity of the *Escherichia coli* regulatory protein StpA. Mol. Microbiol. **28**:847-857.

Dame, R. T., C. Wyman, and N. Goosen. 2000. H-NS mediated compaction of DNA visualised by atomic force microscopy. Nucleic Acids Res. **28**:3504-3510.

Dame, R., C. Wyman, and N. Goosen. 2001. Structural basis for preferential binding of H-NS to curved DNA. Biochimie. **83**:231-234.

Darveau, R. P. 1998. Lipid A diversity and the innate host response to bacterial infection. Curr. Opin. Microbiol. **1**:36-42.

de Biase, D., A. Tramonti, F. Bossa, and P. Visca. 1999. The response to stationary-phase stress conditions in *Escherichia coli*: role and regulation of the glutamic acid decarboxylase system. Mol. Microbiol. **32**:1198-1211.

Deighan, P., A. Free, and C. J. Dorman. 2000. A role for the *Escherichia coli* H-NS-like protein StpA in OmpF porin expression through modulation of *micF* RNA stability. Mol. Microbiol. **38**:126-139.

Delihas, N., S. E. Rokita, and P. Zheng. 1997. Natural antisense RNA/target RNA interactions: possible models for antisense oligonucleotide drug design. Nat. Biotechnol. **15**:751-753.

Dersch, P., K. Schmidt, and E. Bremer. 1993. Synthesis of the *Escherichia coli* K-12 nucleoid-associated DNA-binding protein H-NS is subjected to growth-phase control and autoregulation. Mol. Microbiol. **8**:875-889.

Dorman, C. J., N. N. Bhriain, and C. F. Higgins. 1990. DNA supercoiling and environmental regulation of virulence gene expression in *Shigella flexneri*. Nature. **344**:789-792.

Dorman, C. J. 1995. DNA topology and the global control of bacterial gene expression: implications for the regulation of virulence gene expression. Microbiology. **141**:1271-1280.

Dorman, C. J., J. C. D. Hindon, and A. Free. 1999. Domain organization and oligomerization amoung H-NS-like nucleoid-associated proteins in bacteria. Trends Microbiol. 7:124-128.

Dorman, C. J., S. Mc Kenna, and C. Beloin. 2001. Regulation of virulence gene expression in *Shigella flexneri*, a facultative intracellular pathogen. Int. J. Med. Microbiol. **291**:89-96.

Draper, D. E. 1996. Strategies for RNA folding. Trends Biochem Sci. **21**:145-149.

Draper, D. E. 1999. Themes in RNA-protein recognition. J. Mol. Biol. **295**:255-270

Drlica, K. 1990. Bacterial topoisomerases and the control of DNA supercoiling. Trends Genet. **6**:433-437.

Esterling, L., and N. Delihas. 1994. The regulatory RNA gene *micF* is present in several species of Gram-negative bacteria and is phylogenetically conserved Mol. Microbiol. **12**:639-646

Ellis, R. J. 2001. Macromolecular crowding: an important but neglected aspect of the intracellular environment. Curr. Opin. Struct. Biol. **11**:114-119.

Falconi, M., M. T. Gualtieri, A. La Teana, M. A. Losso, and C. L. Pon. 1988. Proteins from the prokaryotic nucleoid: primary and quaternary structure of the 15-kDa *Escherichia coli* DNA binding protein H-NS. Mol. Microbiol. **2**:323-329.

Falconi, M., A. Brandi, A. La Teana, C. O. Gualerzi, and C. L. Pon. 1996. Antagonistic involvement of FIS and H-NS proteins in the transcriptional control of *hns* expression. Mol. Microbiol. **19**:965-75.

Falconi, M., B. Colonna, G. Prosseda, G. Micheli, and C. O. Gualerzi. 1998. Thermoregulation of Shigella and *Escherichia coli* EIEC pathogenicity. A temperature-dependent structural transition of DNA modulates accessibility of *virF* promoter to transcriptional repressor H-NS. EMBO J. **17**:7033-7043.

Farinha, M. A., and A. M. Kropinski. 1990. Construction of broad-host-range plasmid vectors for easy visible selection and analysis of promoters. J. Bacteriol. **172**:3496-3499.

Ferrario, M., B. R. Ernsting, D. W. Borst, D. E. N. Wiese, R. M. Blumenthal, and R. G. Matthews. 1995. The leucine-responsive regulatory protein of *Escherichia coli* negatively regulates transcription of *ompC* and *micF* and positively regulates translation of *ompF*. J. Bacteriol. 177:103-113.

Finkel, S. E., and R. C. Johnson. 1993. The FIS protein: it's not just for DNA inversion anymore. Mol. Microbiol. **6**:3257-3265.

Finlay, B. B., and S. Falkow. 1997. Common themes in microbial pathogenicity revisited. Microbiol. Mol. Biol. Rev. **61**:136-169.

Foster, J. W., and M. P. Spector. 1995. How Salmonella survive against the odds. Annu. Rev. Microbiol. **49**:145-174.

Franch, T., M. Petersen, E. G. Wagner, J. P. Jacobsen, and K. Gerdes. 1999. Antisense RNA regulation in prokaryotes: rapid RNA/RNA interaction facilitated by a general U-turn loop structure. J. Mol. Biol. **294**:1115-1125.

Franch, T., and K. Gerdes. 2000. U-turns and regulatory RNAs. Curr. Opin. Microbiol. **3**:159-164.

Frankel, A. D. 2000. Fitting peptides into the RNA world. Curr. Opin. Struct. Biol. **10**:332-340.

Free, A., and C. J. Dorman. 1995. Coupling of *Escherichia coli hns* mRNA levels to DNA synthesis by autoregulation: implications for growth-phase control. Mol. Microbiol. **18**:101-113.

Free, A., and C. J. Dorman. 1997. The *Escherichia coli stpA* gene is transiently expressed during growth in rich medium and is induced in minimal medium and by stress conditions. J. Bacteriol. **179**:909-918.

Free, A., and C. J. Dorman. 1997a. Unpublished data.

Free, A., R. M. Williams, and C. J. Dorman. 1998. The StpA protein functions as a molecular adapter to mediate repression of the *bgl* operon by truncated H-NS in *Escherichia coli*. J. Bacteriol. **180**:994-997.

Gaillard, C., and F. Strauss. 1990. Ethanol precipitation of DNA with linear polyacrylamide as carrier. Nucleic Acids Res. **18**:378.

Giangrossi, M., C. O. Gualerzi, and C. L. Pon. 2001. Mutagenesis of the downstream region of the Escherichia coli hns promoter. Biochemie. **83**:251-259

Gibson, K. E., and T. J. Silhavy. 1999. The LysR homolog LrhA promotes RpoS degradation by modulating activity of the response regulator SprE. J. Bacteriol. **181**:563-571.

Goldstein, E., and K. Drlica. 1984. Regulation of bacterial DNA supercoiling: plasmid linking numbers vary with growth temperature. Proc. Natl. Acad. Sci. U S A. **81**:4046-4050.

Goosen, N., and P. van de Putte. 1995. The regulation of transcription initiation by integration host factor. Mol. Microbiol. **16**:1-7.

Göransson, M., B. Sondén, P. Nilsson, B. Dagberg, K. Forsman, K. Emanuelsson, and B-E. Uhlin. 1990. Transcriptional silencing and thermoregulation of gene expression in *Escherichia coli*. Nature **344**:682-685.

Grabarek, Z., and J. Gergely. 1990. Zero-length crosslinking procedure with the use of active esters. Anal. Biochem. **185**:131-135.

Graeme-Cook, K. A., G. May, E. Bremer, and C. F. Higgins. 1989. Osmotic regulation of porin expression: A role for DNA supercoiling. Mol. Microbiol. **3**:1287-1294.

Guzman, L. M., D. Belin, M. J. Carson, J. Beckwith. 1995. Tight regulation, modulation, and high-level expression by vectors containing the arabinose pBAD promoter. J. Bacteriol. **177**:4121-4130

Hall, M. N., and T. J. Silhavy. 1979. Transcriptional regulation of *Escherichia coli* K-12 major outer membrane protein 1b. J. Bacteriol. **140**:342-350

Hall, M. N., and T. J. Silhavy. 1981. The *ompB* locus and the regulation of the major outer membrane porin proteins of *Escherichia coli* K-12. J. Mol. Biol. **146**:23-43

Harrison, J. A., D. Pickard, C. F. Higgins, A. Khan, S. N. Chatfield, T. Ali, C. J. Dorman, C. E. Hormaeche, and G. Dougan. 1994. Role of *hns* in the virulence phenotype of pathogenic Salmonellae. Mol. Microbiol. **13**:133-140.

Head, C. G., A. Tardy, and L. J. Kenney. 1998. Relative binding affinities of OmpR and OmpR-phosphate at the *ompF* and *ompC* regulatory sites. J. Mol. Biol. **281**:857-870.

Hengge-Aronis, R. 1996. Regulation of gene expression during entry into stationary phase, p. 1497-1512. *In Escherichia coli and Salmonella typhimurium*, Cellular and Molecular Biology. Neidhardt, F. C., Curtiss III, R., Ingraham, J. L., Lin, C. C., Low, K. B., Magasanuk, B., Reznikoff, W. S., Riley, M., Schaechter, M., and Umbarger, H. E. (eds). Washington, DC: Americian Society for Microbiology Press.

Hengge-Aronis, R. 2000. The general stress response in *Escherichia coli*, p. 161-178. *In* Bacterial Stress Responses. G. Storz, G., and Hengge-Aronis, R. (eds). Washington, DC: Americian Society for Microbiology Press.

Hensel, M., J. E. Shea, C. Gleeson, M. D. Jones, E. Dalton, and D. W. Holden. 1995. Simultaneous identification of bacterial virulence genes by negative selection. Science. **269**:400-403.

Herschlag, D. 1995. RNA chaperones and the RNA folding problem. J. Biol. Chem. **270**:20871-20874.

Higgins, C. F., C. J. Dorman, D. A. Stirling, L. Waddell, I. R. Booth, G. May, and E. Bremer. 1988. A physiological role for DNA supercoiling in the osmotic regulation of gene expression in *Salmonella. typhimurium* and *Escherichia coli*. Cell. **52**:569-584.

Higgins, C. F., J. C. Hinton, C. S. Hulton, T. Owen-Hughes, G. D. Pavitt, and A. Seirafi. 1990. Protein H1: a role for chromatin structure in the regulation of bacterial gene expression and virulence? Mol. Microbiol. **4**:2007-12.

Hinnebusch, B. J., and A. J. Bendich. 1997. The bacterial nucleoid visualised by fluorescence microscopy of cells lysed within agarose: comparison of *Escherichia coli* and spirochetes of the genus Borrelia. J. Bacteriol. **179**:2228-2237.

Hinton, J. C., D. S. Santos, A. Seirafi, C. S. Hulton, G. D. Pavitt, and C. F. Higgins. 1992. Expression and mutational analysis of the nucleoid-associated protein H-NS of *Salmonella typhimurium*. Mol. Microbiol. **6**:2327-2337.

Hoch, J. A. 2000. Two-component and phosphorelay signal transduction. Curr. Opin. Microbiol. **3**:165-170.

Hommais, F., E. Krin, C. Laurent-Winter, O. Soutourina, A. Malpertuy, J. P. Le Caer, A. Danchin, and P. Bertin. 2001. Large-scale monitoring of pleiotropic regulation of gene expression by the prokaryotic nucleoid-associated protein, H-NS. Mol. Microbiol. **40**:20-36.

Huang, L., P. Tsui, and M. Freundlich. 1990. Integration Host Factor is a negative effector of *in vivo* and *in vitro* expression of *ompC* in *Escherichia coli*. J. Bacteriol. **172**:5293-5298.

Huisman, G. W., and R. Kolter. 1994. Sensing starvation: a homoserine lactone-dependent signaling pathway in *Escherichia coli*. Science. **265**:537-539.

Hulton, C. S., A. Seirafi, J. C. Hinton, J. M. Sidebotham, L. Waddell, G. D. Pavitt, T. Owen-Hughes, A. Spassky, H. Buc, and C. F. Higgins. 1990. Histone-like protein H1 (H-NS), DNA supercoiling, and gene expression in bacteria. Cell. 63:631-642.

Ibanez-Ruiz, M., V. Robbe-Saule, D. Hermant, S. Labrude, and F. Norel. 2000. Identification of RpoS (σ^s)-regulated genes in *Salmonella enterica* serovar *typhimurium*. J. Bacteriol. **182**:5749-5756.

Inoue, K., H. Matsuzaki, K. Matsumoto, and I. Shibuya. 1997. Unbalanced membrane phospholipid compositions affect transcriptional expression of certain regulatory genes in *Escherichia coli*. J. Bacteriol. **179**:2872-2878.

Ishihama, A. 1999. Modulation of the nucleoid, the transcription apparatus, and the translation machinery in bacteria for stationary phase survival. Genes Cells. **4**:135-143.

Jacquet, M., R. Cukier-Kahn, J. Pla, and F. Gros. 1971. A thermostable protein factor acting on *in vitro* DNA transcription. Biochem. Biophys. Res. Commun. **45**:1597-1607.

Jair, K-W., R. G. Martin, J. L. Rosner, N. Fujita, A. Ishihama, and R. E. Wolf, Jr. 1995. Purification and regulatory properties of MarA protein, a transcriptional activator of *Escherichia coli* multiple antibiotic and superoxide resistance promoters. J. Bacteriol. **177**:7100-7104.

Jair, K-W., X. Yu, K. Skarstad, B. Thöny, N. Fujita, A. Ishihama and R. E. Wolfe, Jr. 1996. Transcriptional activation of promoters of the superoxide and multiple antibiotic resistance regulons by Rob, a binding protein of the *Escherichia coli* origin of chromosomal replication. J. Bacteriol. **178**:2507-2513

Johansson, J., B. Dagberg, E. Richet, and B. E. Uhlin. 1998. H-NS and StpA proteins stimulate expression of the maltose regulon in *Escherichia coli*. J. Bacteriol. **180**:6117-6125.

Johansson, J., and B. E. Uhlin. 1999. Differential protease-mediated turnover of H-NS and StpA revealed by a mutation altering protein stability and stationary-phase survival of *Escherichia coli*. Proc. Natl. Acad. Sci. U S A. **96**:10776-10781.

Johansson, J., C. Balsalobre, S. Y. Wang, J. Urbonaviciene, D. J. Jin, B. Sonden, and B. E. Uhlin. 2000. Nucleoid proteins stimulate stringently controlled bacterial promoters: a link between the cAMP-CRP and the (p)ppGpp regulons in *Escherichia coli*. Cell. 102:475-485.

Johansson, J., S. Eriksson, B. Sonden, S. N. Wai, and B. E. Uhlin. 2001. Heteromeric interactions among nucleoid-associated bacterial proteins: localization of StpA-stabilising regions in H-NS of *Escherichia coli*. J. Bacteriol. **183**:2343-2347.

Jordi, B. J., A. E. Fielder, C. M. Burns, J. C. Hinton, N. Dover, D. W. Ussery, and C. F. Higgins. 1997. DNA binding is not sufficient for H-NS-mediated repression of *proU* expression. J. Biol. Chem. **272**:12083-12090.

Jordi, B. J., and C. F. Higgins. 2000. The downstream regulatory element of the *proU* operon of *Salmonella typhimurium* inhibits open complex formation by RNA polymerase at a distance. J. Biol. Chem. **275**:12123-12128.

Kaidow, A., M. Wachi, J. Nakamura, J. Magae, and K. Nagai. 1995. Anucleate cell production by *Escherichia coli* Δ*hns* mutant lacking a histone-like protein, H-NS. J. Bacteriol. **177**:3589-3592.

Kajitani, M., and A. Ishihama. 1991. Identification and sequence determination of the host factor gene for bacteriophage Q_{β}. Nucleic Acids Res. **19**:1063-1066.

Karzai, A. W., E. D. Roche, and R. T. Sauer. 2000. The SsrA-SmpB system for protein tagging, directed degradation and ribosome rescue. Nat. Struct. Biol. **7**:449-455

Kellenberger, E. 1990. Intracellular organisation of the bacterial genome, p173-186. *In* the Bacterial chromosome. Drlica, K., and M. Riley (eds)Washington, DC: American Society for Microbiology Press.

Kim, D.-J., and S. Forst. 2001. Genomic analysis of the histidine kinase family in bacteria and archaea. Microbiology. **147**:1197-1212.

Klauck, E., J. Böhringer, and R. Hengge-Aronis. 1997. The LysR-like regulator LeuO in *Escherichia coli* is involved in the translational regulation of *rpoS* by affecting the expression of the small regulatory DsrA RNA. Mol. Microbiol. **25**:559-569.

Klebba, P. E., and S. M. Newton. 1998. Mechanisms of solute transport through outer membrane porins: burning down the house. Curr. Opin. Microbiol. **1**:238-247.

Koebnik, R., K. P. Locher, and P. Van Gelder. 2000. Structure and function of bacterial outer membrane proteins: barrels in a nutshell. Mol. Microbiol. **37**:239-253.

Koronakis, V., A. Sharff, E. Koronakis, B. Luisi, and C. Hughes. 2000. Crystal structure of the bacterial membrane protein TolC central to multidrug efflux and protein export. Nature. **405**:914-919.

Krieg, P. A. 1996. A Laboratory Guide to RNA: Isolation, Analysis and Synthesis. New York: Wiley-Liss Press.

Kuhnert, P., P. Boerlin, and J. Frey. 2000. Target genes for virulence assessment of *Escherichia coli* isolates from water, food and the environment. FEMS Microbiol. Rev. **24**:107-117.

Kushner, S. R. 1996. mRNA decay, p. 849-860. *In Escherichia coli and Salmonella typhimurium*, Cellular and Molecular Biology. Neidhardt, F. C., Curtiss III, R., Ingraham, J. L., Lin, C. C., Low, K. B., Magasanuk, B., Reznikoff, W. S., Riley, M., Schaechter, M., and Umbarger, H. E. (eds). Washington, DC: Americian Society for Microbiology Press.

Kyrpides, N. C., and C. A. Ouzounis. 1999. Whole-genome sequence annotation: 'Going wrong with confidence'. Mol. Microbiol. **32**:886-887.

La Teana, A., A. Brandi, M. Falconi, R. Spurio, C. L. Pon, and C. O. Gualerzi. 1991. Identification of a cold shock transcriptional enhancer of the *Escherichia coli* gene encoding nucleoid protein H-NS. Proc. Natl. Acad. Sci. U S A. **88**:10907-10911.

Lange, R., and R. Hengge-Aronis. 1994. The cellular concentration of the σ^s subunit of RNA polymerase in *Escherichia coli* is controlled at the levels of transcription, translation, and protein stability. Genes Dev. **8**:1600-1612.

Lange, R., D. FIScher, and R. Hengge-Aronis. 1995. Identification of transcriptional start sites and the role of ppGpp in the expression of *rpoS*, the structural gene for the σ^s subunit of RNA polymerase in *Escherichia coli*. J. Bacteriol. **177**:4676-4680.

Laurent-Winter, C., S. Ngo, A. Danchin, and P. Bertin. 1997. Role of *Escherichia coli* histone-like nucleoid-structuring protein in bacterial metabolism and stress response-identification of targets by two-dimensional electrophoresis. Eur. J. Biochem. **244**:767-773.

Lease, R. A., M. E. Cusick, and M. Belfort. 1998. Riboregulation in *Escherichia coli*: DsrA RNA acts by RNA:RNA interactions at multiple loci. Proc. Natl. Acad. Sci. U S A. **95**:12456-61

Lease, R. A., and M. Belfort. 2000a. A trans-acting RNA as a control switch in *Escherichia coli*: DsrA modulates function by forming alternative structures. Proc. Natl. Acad. Sci. U S A. **97**:9919-9924.

Lease, R. A., and M. Belfort. 2000b. Riboregulation by DsrA RNA: trans-actions for global economy. Mol Microbiol. **38**:667-672.

Li, Z., and B. Demple. Sequence specificity for DNA binding by *Escherichia coli* SoxS and Rob proteins. Mol. Microbiol. **20**:937-945

Lin, R., R. D'Ari, and E. B. Newman. 1992. λ *plac*Mu insertions in genes of the leucine regulon: extension of the regulon to genes not regulated by leucine. J. Bacteriol. **174**:1948-1955.

Loewen, P. C., B. Hu, J. Strutinsky, and R. Sparling. 1998. Regulation in the *rpoS* regulon of *Escherichia coli*. Can. J. Microbiol. **44**:707-717.

Lucht, J. M., P. Dersch, B. Kempf, and E. Bremer. 1994. Interaction of the nucleoid-associated DNA-binding protein H-NS with the regulatory region of the osmotically controlled *proU* operon of *Escherichia coli*. J. Biol. Chem. **269**:6578-6586.

Majdalani, N., S. Chen, J. Murrow, K. St John, S. Gottesman. 2001. Regulation of RpoS by a novel small RNA: the characterisation of RprA. Mol. Microbiol. **39**:1382-1394.

Marshall, D. G., F. Bowe, C. Hale, G. Dougan, and C. J. Dorman. 2000. DNA topology and adaptation of *Salmonella typhimurium* to an intracellular environment. Philos. Trans R. Soc. Lond. Biol. Sci. **355**:565-574.

Martin, R. G., W. K. Gillette, S. Rhee, and J. L. Rosner. 1999. Structural requirements for marbox function in transcriptional activation of *mar/sox/rob* regulon promoters in *Escherichia coli*: sequence, orientation and spatial relationship to the core promoter. Mol. Microbiol. **34**:431-441.

Matsubara, M., S. Kitaoka, S. Takeda and T. Mizuno. 2000. Tuning of the porin expression under anaerobic growth conditions by His-to-Asp cross-phosphorelay through both the EnvZ-osmosensor and ArcB-anaerosensor in *Escherichia coli*. Genes Cells. **5**:555-569

Matsuyama, S.-I., and S. Mizushima. 1985. Construction and characterization of a deletion mutant lacking *micF*, a proposed regulatory gene for OmpF synthesis in *Escherichia coli*. J. Bacteriol. **162**:1196-1202.

May, G., P. Dersch, M. Haardt, A. Middendorf, and E. Bremer. 1990. The *osmZ* (*bglY*) gene encodes the DNA-binding protein H-NS (H1a), a component of the *Escherichia coli* K12 nucleoid. Mol. Gen. Genet. **224**:81-90.

McCleary, W. R., and J. B. Stock. 1994. Acetyl phosphate and the activation of two-component response regulators. J. Biol. Chem. **269**:31567-31572.

McLeod, S. M., and R. C. Johnson. 2001. Control of transcription by nucleoid proteins. Curr. Opin. Microbiol. **4**:152-159.

Medeiros, A. A., T. F. O'Brien, E. Y. Rosenberg, and H. Nikaido. 1987. Loss of OmpC porin in a strain of *Salmonella typhimurium* causes increased resistance to cephalosporins during therapy. J. Infect. Dis. **156**:751-757.

Miller, J. H. 1992. A short course in bacterial genetics. New York: Cold Spring Harbour Laboratory Press.

Misra, R., and P. R. Reeves. 1987. Role of *micF* in the TolC-mediated regulation of OmpF, a major outer membrane protein of *Escherichia coli* K-12. J. Bacteriol. **169**:4722-4730.

Mizuno, T., M.-Y. Chou, and M. Inouye. 1984. A unique mechanism regulating gene expression: Translational inhibition by a complementary RNA transcript (micRNA). Proc. Natl. Acad. Sci. U S A. **81**:1966-1970.

Mizuno, T. 1987. Static bend of DNA helix at the activator recognition site of the *ompF* promoter in *Escherichia coli*. Gene. **54**:57-64.

Mizuno, T., and S. Mizushima. 1990. Signal transduction and gene regulation through the phosphorylation of two regulatory components: The molecular basis for the osmotic regulation of the porin genes. Mol. Microbiol. **4**:1077-1082.

Mojica, F. J., and C. F. Higgins. 1997. *In vivo* supercoiling of plasmid and chromosomal DNA in an *Escherichia coli hns* mutant. J. Bacteriol. **179**:3528-3533.

Muffler, A., D. FIScher, and R. Hengge-Aronis. 1996. The RNA-binding protein HF-I, known as a host factor for phage Q_β RNA replication, is essential for *rpoS* translation in *Escherichia coli*. Genes Dev. **10**:1143-1151.

Muffler, A., M. Barth, C. Marschall, and R. Hengge-Aronis. 1997. Heat-shock regulation of σ^s turnover: a role for DnaK and relationship between stress responses mediated by σ^s and σ^{32} in *Escherichia coli*. J. Bacteriol. **179**:445-452.

Mukhopadhyay, S., J. P. Audia, R. N. Roy, and H. E. Schellhorn. 2000. Transcriptional induction of the conserved alternative sigma factor RpoS in *Escherichia coli* is dependent on BarA, a probable two-component regulator. Mol. Microbiol. **37**:371-381.

Nasser, W., M. Faelen, N. Hugouvieux-Cotte-Pattat, and S. Reverchon. 2001. Role of the nucleoid-associated protein H-NS in the synthesis of virulence factors in the phytopathogenic bacterium *Erwinia chrysanthemi*. Mol. Plant Microbe Interact. **14**:10-20.

Neidhardt, F. C. 1996. *Escherichia coli* and *Salmonella typhimurium*, Cellular and Molecular Biology. Washington, DC: Americian Society for Microbiology Press.

Nieto, J. M., C. Madrid, A. Prenafeta, E. Miquelay, C. Balsalobre, M. Carrascal, and A. Juarez. 2000. Expression of the hemolysin operon in *Escherichia coli* is modulated by a nucleoid-protein complex that includes the proteins Hha and H-NS. Mol Gen Genet. **263**:349-358.

Nikaido, H. 1992. Porins and specific channels of bacterial outer membranes. Mol. Microbiol. **6**:435-442.

Nikaido, H., and M. H. Saier. 1992. Transport proteins in bacteria: common themes in their design. Science. **258**:936-942.

Nikaido, H. 1994. Isolation of outer membranes. Methods Enzymol. **235**:225-234.

Nikaido, H. 1996. Outer membrane, p. 29-47. *In Escherichia coli and Salmonella typhimurium*, Cellular and Molecular Biology. Neidhardt, F. C., Curtiss III, R., Ingraham, J. L., Lin, C. C., Low, K. B., Magasanuk, B., Reznikoff, W. S., Riley, M., Schaechter, M., and Umbarger, H. E. (eds). Washington, DC: Americian Society for Microbiology Press.

Nogueira, T., and M. Springer. 2000. Post-transcriptional control by global regulators of gene expression in bacteria. Curr. Opin. Microbiol. **3**:154-158.

Oh, J. T., Y. Cajal, E. M. Skowronska, S. Belkin, J. Chen, T. K. Van Dyk, M. Sasser, and M. K. Jain. 2000. Cationic peptide antimicrobials induce selective transcription of *micF* and *osmY* in *Escherichia coli*. Biochim. Biophys. Acta. **1463**:43-54.

Ohta, T., C. Ueguchi, and T. Mizuno. 1999. *rpoS* function is essential for *bgl* silencing caused by C-terminally truncated H-NS in *Escherichia coli*. J. Bacteriol. **181**:6278-6283

Owen-Hughes, T. A., G. D. Pavitt, D. S. Santos, J. M. Sidebotham, C. S. Hulton, J. C. Hinton, and C. F. Higgins. 1992. The chromatin-associated protein H-NS interacts with curved DNA to influence DNA topology and gene expression. Cell. **71**:255-265.

Painbeni, E., M. Caroff, and J. Rouviere-Yaniv. 1997. Alterations of the outer membrane composition in *Escherichia coli* lacking the histone-like protein HU. Proc. Natl. Acad. Sci. U S A. **94**:6712-6717.

Pettijohn, D. E. 1996. The nucleoid, p. 158-166. *In Escherichia coli and Salmonella typhimurium*, Cellular and Molecular Biology. Neidhardt, F. C., Curtiss III, R., Ingraham, J. L., Lin, C. C., Low, K. B., Magasanuk, B., Reznikoff, W. S., Riley, M., Schaechter, M., and Umbarger, H. E. (eds). Washington, DC: Americian Society for Microbiology Press.

Phadtare, S., and M. Inouye. 2001. Role of CspC and CspE in regulation of expression of RpoS and UspA, the stress response proteins in *Escherichia coli*. J. Bacteriol. **183**:1205-1214.

Phale, P. S., A. Philippsen, T. Kiefhaber, R. Koebnik, V. P. Phale, T. Schirmer, and J. P. Rosenbusch. 1998. Stability of trimeric OmpF porin: the contributions of the latching loop L2. Biochemistry. **37**:15663-15670.

Pomposiello, P. J., and B. Demple. 2000. Identification of SoxS-regulated genes in *Salmonella enterica* serovar *typhimurium*. J. Bacteriol. 182:23-29.

Pratt, L. A., and T. J. Silhavy. 1995. Identification of base pairs important for OmpR-DNA interaction. Mol. Microbiol. **17**:565-573.

Pratt, L. A., W. Hsing, K. E. Gibson, and T. J. Silhavy. 1996. From acids to *osmZ*: multiple factors influence synthesis of the OmpF and OmpC porins in *Escherichia coli*. Mol. Microbiol. 20:911-917.

Prentki, P., and H. M. Krisch. 1984. *In vitro* insertional mutagenesis with a selectable DNA fragment. Gene. **29**:303-313.

Puente, J. L., and B. B. Finlay. 2001. Pathogenic *Escherichia coli*, p. 387-456. *In* E. A. Groisman (ed.), Principles of Bacterial Pathogenesis. San Diego: Academic Press.

Qin, L., T. Yoshida, and M. Inouye. 2001. The critical role of DNA in the equilibrium between OmpR and phosphorylated OmpR mediated by EnvZ in *Escherichia coli.* Proc Natl Acad Sci U S A. **98**:908-913.

Ramani, N., L. Huang, and M. Freundlich. 1992. *In vitro* interactions of integration host factor with the *ompF* promoter-regulatory region of *Escherichia coli.* Mol. Gen. Genet. **231**:248-255.

Ramos, J. L., M. Gallegos, S. Marques, M. Ramos-Gonzalez, M. Espinosa-Urgel, and A. Segura. 2001. Responses of Gram-negative bacteria to certain environmental stressors. Curr. Opin. Microbiol. **4**:166-171.

Rauhut, R., and G. Klug. 1999. mRNA degradation in bacteria. FEMS Microbiol. Rev. **23**:353-370.

Renzoni, D., D. Esposito, M. Pfuhl, J. C. Hinton, C. F. Higgins, P. C. Driscoll, and J. E. Ladbury. 2001. Structural characterization of the N-terminal oligomerization domain of the bacterial chromatin-structuring protein, H-NS. J. Mol. Biol. **306**:1127-1137.

Romeo, T. 1998. Global regulation by the small RNA-binding protein CsrA and the non-coding RNA molecule CsrB. Mol. Microbiol. **29**:1321-1330

Rosner, J. L., T. J. Chai, and J. Foulds. 1991. Regulation of *ompF* porin expression by salicylate in *Escherichia coli.* J Bacteriol. **173**:5631-5638.

Rudd, K. E. 1998. Linkage map of *Escherichia coli* K-12, edition 10: the physical map. Microbiol. Mol. Biol. Rev. **62**:985-1019.

Saiki, R. K., D. H. Gelfand, S. Stoffel, S. J. Scharf, R. Higuchi, G. T. Horn, K. B. Mullis, and H. A. Erlich. 1988. Primer-directed enzymic amplification of DNA with a thermostable DNA polymerase. Science. **239**:487-491.

Sambrook, J., E. F. Fritsch, and T. Maniatis. 1989. Molecular cloning: a laboratory manual. New York: Cold Spring Habour Laboratory Press.

Sánchez-SanMartín, C., V. H. Bustamante, E. Calva, and J. L. Puente. 2001. Transcriptional Regulation of the *orf19* Gene and the *tir-cesT-eae* operon of enteropathogenic *Escherichia coli.* J. Bacteriol. **183**:2823-2833.

Sanger, F., S. Nicklen, and A. R. Coulson. 1977. DNA sequencing with chain-terminating inhibitors. . Proc. Natl. Acad. Sci. U S A. **74**:5463-5467.

Schirmer, T., and P. S. Phale. 1999. Brownian dynamics simulation of ion flow through porin channels. J. Mol. Biol. **294**:1159-1167.

Schmidt, M., and N. Delihas. 1995. MicF RNA is a substrate for RNase E. FEMS Microbiol. Lett. **133**:209-213.

Schmidt, M., P. Zheng, and N. Delihas. 1995. Secondary structures of *Escherichia coli* antisense MicF RNA, the 5'-end of the target *ompF* mRNA, and the RNA/RNA duplex. Biochemistry. 34:3621-3631.

Sondén, B., and B. E. Uhlin. 1996. Co-ordinated and differential expression of histone-like proteins in *Escherichia coli*: regulation and function of the H-NS analog StpA. EMBO J. **15**:4970-4980.

Sonnenfield, J. M., C. M. Burns, C. F. Higgins, J. C. D. Hinton. 2001. The nucleoid-associated protein StpA binds curved DNA, has a greater DNA-binding affinity than H-NS and is present in significant levels in *hns* mutants. Biochemie. **83**:243-249.

Southern, E. M. 1975. Detection of specific sequences among DNA fragments separated by gel electrophoresis. J. Mol Biol. **98**:503-517.

Soutourina, O., A. Kolb, E. Krin, C. Laurent-Winter, S. Rimsky, A. Danchin, and P. Bertin. 1999. Multiple control of flagellum biosynthesis in *Escherichia coli*: role of H-NS protein and the cyclic AMP-catabolite activator protein complex in transcription of the *flhDC* master operon. J. Bacteriol. **181**:7500-7508.

Spassky, A., S. Rimsky, H. Garreau, and H. Buc. 1984. H1a, an *Escherichia coli* DNA-binding protein which accumulates in stationary phase, strongly compacts DNA *in vitro*. Nucleic Acids Res. **12**:5321-5340.

Spurio, R., M. Durrenberger, M. Falconi, A. La Teana, C. L. Pon, and C. O. Gualerzi. 1992. Lethal overproduction of the *Escherichia coli* nucleoid protein H-NS: ultramicroscopic and molecular autopsy. Mol. Gen. Genet. **231**:201-211.

Spurio, R., M. Falconi, A. Brandi, C. L. Pon, and C. O. Gualerzi. 1997. The oligomeric structure of nucleoid protein H-NS is necessary for recognition of intrinsically curved DNA and for DNA bending. EMBO J. **16**:1795-1805.

Sternberg, N. L., and R. Maurer. 1991. Bacteriophage-mediated generalised transduction in *Escherichia coli* and *Salmonella typhimurium*. Methods Enzymol. **204**:18-43.

Studier, F. W., B. A. Moffatt. 1986. Use of bacteriophage T7 RNA polymerase to direct selective high-level expression of cloned genes. J. Mol. Biol. **189**:113-30

Suzuki, T., C. Ueguchi, and T. Mizuno. 1996. H-NS Regulates OmpF Expression through *micF* Antisense RNA in *Escherichia coli*. J Bacteriol. **178**:3650-3653.

Talukder, A. A., and A. Ishihama. 1999. Twelve species of the nucleoid-associated protein from *Escherichia coli*. Sequence recognition specificity and DNA binding affinity. J Biol. Chem. **274**:33105-33113.

Taludker, A. A., A. Iwata, A. Nishimura, S. Ueda, and A. Ishihama. 1999. Growth-phase-dependent variation in protein composition of the *Escherichia coli* nucleoid. J. Bacteriol. **181**:6361-6370.

Talukder, A. A., S. Hiraga, and A. Ishihama. 2000. Two types of localization of the DNA-binding proteins within the *Escherichia coli* nucleoid. Genes Cells. **5**:613-626.

Tendeng, C., C. Badaut, E. Krin, P. Gounon, S. Ngo, A. Danchin, S. Rimsky, and P. Bertin. 2000. Isolation and characterization of *vicH*, encoding a new pleiotropic regulator in *Vibrio cholerae*. J. Bacteriol. **182**:2026-2032.

Trun, N. J., Marko, and J. F. 1998. Architecture of a bacterial chromosome. ASM News. **64**:276-283.

Tupper, A. E., T. A. Owen-Hughes, D. W. Ussery, D. S. Santos, D. J. Ferguson, J. M. Sidebotham, J. C. Hinton, and C. F. Higgins. 1994. The chromatin-associated protein H-NS alters DNA topology *in vitro*. EMBO J. 13:258-268.

Ueguchi, C., and T. Mizuno. 1993. The *Escherichia coli* nucleoid protein H-NS functions directly as a transcriptional repressor. EMBO J. **12**:1039-1046.

Ueguchi, C., C. Seto, T. Suzuki, and T. Mizuno. 1997. Clarification of the dimerisation domain and its functional significance for the *Escherichia coli* nucleoid protein H-NS. J Mol. Biol. **274**:145-151.

Ueguchi, C., N. Misonou, and T. Mizuno. 2001. Negative control of *rpoS* expression by phosphoenolpyruvate: carbohydrate phosphotransferase system in *Escherichia coli*. J. Bacteriol. **183**:520-527.

Urbanowski, M. L., L. T. Stauffer, and G. V. Stauffer. 2000. The *gcvB* gene encodes a small untranslated RNA invovled in expression of the dipeptide and oligopeptide transport systems in *Escherichia coli*. Mol. Microbiol. **37**:856-868

Ussery, D. W., J. C. Hinton, B. J. Jordi, P. E. Granum, A. Seirafi, R. J. Stephen, A. E. Tupper, G. Berridge, J. M. Sidebotham, and C. F. Higgins. 1994 The chromatin-associated protein H-NS. Biochimie **76**:968-980.

Ussery, D., T. Schou Larsen, K. Trevor Wilkes, C. Friis, P. Worning, A. Krogh, and S. Brunak. 2001. Genome organisation and chromatin structure in *Escherichia coli*. Biochimie. 83:201-212.

Vaara, M. 1993. Antibiotic-supersusceptible mutants of *Escherichia coli* and *Salmonella typhimurium*. Antimicrob. Agents Chemother. **37**:2255-2260.

Valdivia, R. H., and S. Falkow. 1997. Fluorescence-based isolation of bacterial genes expressed within host cells. Science. **277**:2007-2011.

Van Bogelen, R. A., E. R. Olsen, B. L. Wanner, and F. C. Neidhardt. 1996. Global analysis of proteins synthesised during phosphorus restriction in *Escherichia coli*. J. Bacteriol. **178**:4344-4366.

Van Wye, J. D., E. C. Bronson, and J. N. Anderson. 1991. Species-specific patterns of DNA bending and sequence. Nucleic Acids Res. **19**:5253-5261.

Varshavsky, A. J., S. A. Nedospasov, V. V. Bakayev, T. G. Bakayeva, and G. P. Georgiev. 1977. Histone-like proteins in the purified *Escherichia coli* deoxyribonucleoprotein. Nucleic Acids Res. **4**:2725-2745.

Wagner, E. G., and R. W. Simons. 1994. Antisense RNA control in bacteria, phages, and plasmids. Annu. Rev. Microbiol. **48**:713-42.

Wagner, E. G., and S. Brantl. 1998. Kissing and RNA stability in antisense control of plasmid replication. Trends Biol. Sci. **23**:451-454

Wassarman, K. M., A. Zhang, and G. Storz. 1999. Small RNAs in *Escherichia coli.* Trends Microbiol. **7**:37-45.

Wassarman, K. M., and G. Storz. 2000. 6S RNA regulates *Escherichia coli* RNA polymerase activity. Cell. **6**:613-624

Wassarman, K. M., F. Repoila, C. Rosenow, G. Storz, and S. Gottesman. 2001. Identification of novel small RNAs using comparative genomics and microarrays. Genes Dev. **15**:1637-1651

Wery, M., C. L. Woldringh, and J. Rouviere-Yaniv. 2001. HU-GFP and DAPI co-localise on the *Escherichia coli* nucleoid. Biochimie. **83**:193-200.

Whitfield, C., and I. S. Roberts. 1999. Structure, assembly and regulation of expression of capsules in *Escherichia coli.* Mol. Microbiol. **31**:1307-1319.

Williams, R. M., S. Rimsky, and H. Buc. 1996. Probing the structure, function, and interactions of the *Escherichia coli* H-NS and StpA proteins by using dominant negative derivatives. J Bacteriol. **178**:4335-4343.

Williams, R. M., and S. Rimsky. 1997. Molecular aspects of the *Eshcerichia coli* nucleoid protein, H-NS: a central controller of gene regulatory networks. FEMS Microbiol. Lett. **156**:175-185.

Wolf, S. G., D. Frenkiel, T. Arad, S. E. Finkel, R. Kolter, and A. Minsky. 1999. DNA protection by stress-induced biocrystallisation. Nature. **400**:83-85.

Wu, J., and M. Grunstein. 2000. 25 years after the nucleosome model: chromatin modifications. Trends Biochem. Sci. **25**:619-623.

Yamada, H., T. Yoshida, K. Tanaka, C. Sasakawa, and T. Mizuno. 1991. Molecular analysis of the *Escherichia coli hns* gene encoding a DNA-binding protein, which preferentially recognises curved DNA sequences. Mol. Gen. Genet. **230**:332-336.

Yamashino, T., C. Ueguchi, and T. Mizuno. 1995. Quantitative control of the stationary phase-specific sigma factor, σ^s, in *Escherichia coli*: involvement of the nucleoid protein H-NS. EMBO J. **14**:594-602.

Yarmolinsky, M. 2000. Transcriptional silencing in bacteria. Curr. Opin. Microbiol. **3**:138-143.

Yoshida, T., C. Ueguchi, H. Yamada, and T. Mizuno. 1993. Function of the *Escherichia coli* nucleoid protein, H-NS: molecular analysis of a subset of proteins whose expression is enhanced in a *hns* deletion mutant. Mol. Gen. Genet. **237**:113-122.

Yura, T., and K. Nakahigashi. 1999. Regulation of the heat-shock response. Curr. Opin. Microbiol. **2**:153-158.

Zhang, A., and M. Belfort. 1992. Nucleotide sequence of a newly-identified *Escherichia coli* gene, *stpA*, encoding an H-NS-like protein. Nucleic Acids Res. **20**:6735.

Zhang, A., V. Derbyshire, J. L. G. Salvo, and M. Belfort. 1995. *Escherichia coli* protein StpA stimulates self-splicing by promoting RNA assembly *in vitro*. RNA. **1**:783-793.

Zhang, A., S. Rimsky, M. E. Reaban, H. Buc, and M. Belfort. 1996. *Escherichia coli* protein analogs StpA and H-NS: regulatory loops, similar and disparate effects on nucleic acid dynamics. EMBO J. **15**:1340-1349.

Zhang, A., S. Altuvia, A. Tiwari, L. Argaman, R. Hengge-Aronis, and G. Storz. 1998. The OxyS regulatory RNA represses *rpoS* translation and binds the Hfq (HF-I) protein. EMBO J. **17**:6061-6068.

Zhou, Y., S. Gottesman, J. R. Hoskins, M. R. Maurizi, and S. Wickner. 2001. The RssB response regulator directly targets σ^s for degradation by ClpXP. Genes Dev. **15**:627-637.

Zuber, F., D. Kotlarz, S. Rimsky, and H. Buc. 1994. Modulated expression of promoters containing upstream curved DNA sequences by the *Escherichia coli* nucleoid protein H-NS. Mol Microbiol. **12**:231-240.